

AD-A060 339

BOEING AEROSPACE CO SEATTLE WASH
CAST ALUMINUM STRUCTURES TECHNOLOGY (CAST) MANUFACTURING METHOD--ETC(U)
MAY 78 R G CHRISTNER, D D GOEHLER

F/G 11/6

F33615-76-C-3111

UNCLASSIFIED

D180-24610-1

AFFDL-TR-78-62

NL

1 OF 4
AD
A060339



AD A060339

DDC FILE COPY

AFFDL-TR-78-62

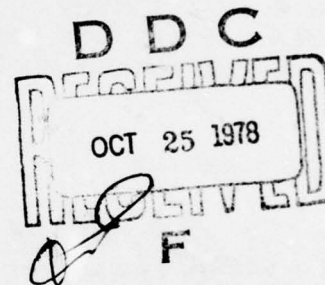
LEVEL II

2

CAST ALUMINUM STRUCTURES TECHNOLOGY (CAST) MANUFACTURING METHODS — PHASE II

THE BOEING COMPANY
SEATTLE, WASHINGTON 98124

MAY 1978



TECHNICAL REPORT AFFDL-TR-78-62
Final Report for Period August 1976 — March 1978

Approved for public release; distribution unlimited.

AIR FORCE FLIGHT DYNAMICS LABORATORY
AIR FORCE WRIGHT AERONAUTICAL LABORATORIES
AIR FORCE SYSTEMS COMMAND
WRIGHT-PATTERSON AIR FORCE BASE, OHIO 45433

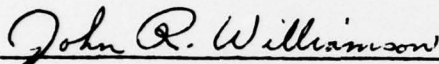
78 10 12 031

NOTICE

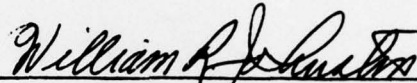
When Government drawings, specifications, or other data are used for any purpose other than in connection with a definitely related Government procurement operation, the United States Government thereby incurs no responsibility nor any obligation whatsoever; and the fact that the government may have formulated, furnished, or in any way supplied the said drawings, specifications, or other data, is not to be regarded by implication or otherwise as in any manner licensing the holder or any other person or corporation, or conveying any rights or permission to manufacture, use, or sell any patented invention that may in any way be related thereto.

This report has been reviewed by the Information Office (OI) and is releasable to the National Technical Information Service (NTIS). At NTIS, it will be available to the general public, including foreign nations.

This technical report has been reviewed and is approved for publication.

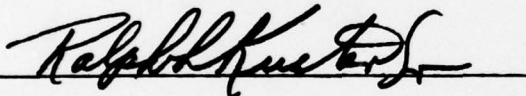


JOHN R. WILLIAMSON
Deputy Program Mgr, AMS Program Off
Structural Mechanics Division



WILLIAM R. JOHNSTON
Actg Prog Mgr, AMS Program Off
Structural Mechanics Division

FOR THE COMMANDER



RALPH L. KUSTER, JR., Col, USAF
Chief, Structural Mechanics Division

"If your address has changed, if you wish to be removed from our mailing list, or if the addressee is no longer employed by your organization please notify AFFDL/FBA, W-PAFB, OH 45433 to help us maintain a current mailing list".

Copies of this report should not be returned unless return is required by security considerations, contractual obligations, or notice on a specific document.

1. REPORT DOCUMENTATION PAGE		READ INSTRUCTIONS BEFORE COMPLETING FORM	
1. REPORT NUMBER AFFDL-TR-78-62	2. GOVT ACCESSION NO.	3. RECIPIENT'S CATALOG NUMBER	
4. TITLE (and Subtitle) CAST ALUMINUM STRUCTURES TECHNOLOGY (CAST) MANUFACTURING METHODS--PHASE II	5. TYPE OF REPORT & PERIOD COVERED Final report August 1976-March 1978	6. PERFORMING ORG. REPORT NUMBER D180-24610-1	
7. AUTHOR(s) Richard G. Christner Donald D. Goehler	8. CONTRACT OR GRANT NUMBER(s) F33615-76-C-3111		
9. PERFORMING ORGANIZATION NAME AND ADDRESS The Boeing Company Boeing Aerospace Company Seattle, Washington 98124	10. PROGRAM ELEMENT, PROJECT, TASK AREA & WORK UNIT NUMBERS Project No. 486U Work Unit 485U		
11. CONTROLLING OFFICE NAME AND ADDRESS Air Force Flight Dynamics Laboratory (FBA) Air Force Wright Aeronautical Laboratories AFSC, Wright-Patterson AFB, Ohio 45433	12. REPORT DATE May 1978	13. NUMBER OF PAGES 293	
14. MONITORING AGENCY NAME & ADDRESS (if different from Controlling Office) 12 316 p.	15. SECURITY CLASS. (of this report) Unclassified	15a. DECLASSIFICATION/DOWNGRADING SCHEDULE	
16. DISTRIBUTION STATEMENT (of this Report) Approved for public release, distribution unlimited.			
17. DISTRIBUTION STATEMENT (of the abstract entered in Block 20, if different from Report) Approved for public release, distribution unlimited.			
18. SUPPLEMENTARY NOTES			
19. KEY WORDS (Continue on reverse side if necessary and identify by block number) CAST, aluminum castings, YC-14 bulkhead, A357 aluminum alloy, allowables, sand casting			
20. ABSTRACT (Continue on reverse side if necessary and identify by block number) The objective of CAST is to establish the necessary structural and manufacturing technologies and to demonstrate and validate the integrity, producibility, and viability of cast aluminum primary airframe structures. The necessary casting foundry practices and related manufacturing technologies needed to cast aluminum primary structural components are discussed in this report. This effort involved extensive characterization of each step of the casting process to define acceptable limits of the process parameters.			

DD FORM 1 JAN 73 1473

EDITION OF 1 NOV 65 IS OBSOLETE

Unclassified

SECURITY CLASSIFICATION OF THIS PAGE (When Data Entered)

78 10 12 031

FOREWORD

This report was prepared by the Boeing Military Airplane Development Division of the Boeing Aerospace Company, Seattle, Washington under USAF Contract No. F33615-76-C-3111. The contract work was performed under project 486U under the direction of the Air Force Flight Dynamics Laboratory, Advanced Metallic Structures/Advanced Development Program Office, Wright-Patterson AFB, Ohio. A significant portion of the contract, including all effort discussed in this report, is being funded by the Metals Branch of the Manufacturing Technology Division of the Air Force Materials Laboratory. The Air Force Project Engineer is John R. Williamson of the AMS Program Office, Structural Mechanics Division, Air Force Flight Dynamics Laboratories (AFFDL/FBA).

The Boeing Aerospace Company, Boeing Military Airplane Development, is the contractor, with Donald E. Strand as Program Manager and Donald D. Goehler as Technical Leader. This phase of the program was conducted by Richard G. Christner assisted by Calvin R. Belden, James W. Faber, Jerry E. Ginn, L. Arne Logan, Robert C. McField, Howard L. Southworth, and Andrew S. Tam.

The contractor's report number is D180-24610-1. This report covers work from June 1976 through March 1978.

Other work in the CAST program is reported in:

- o AFFDL-TR-77-36, Final Report, Phase I, June 1976-February 1977
- o AFFDL-TR-78-7, Final Report, Phase III, August 1976-March 1978

DDC SE	W FOR				
PLAS	White Section	<input checked="" type="checkbox"/>			
ODC	Buff Section	<input type="checkbox"/>	<input type="checkbox"/>		
MANNOV/D F S L H A I O V					
AS					
DIC	DISCRETIONARY AMT COTS				
	SF DIAL				
A					

CONTENTS

<u>Section</u>	<u>Page</u>
I. INTRODUCTION	1
II. ALLOY SELECTION	3
III. METAL MELTING AND POURING TECHNIQUES	7
1. Baseline Data for Spectrographic Analysis	7
2. Fluidity Test	7
3. Holding Temperature	21
4. Pouring Temperature	28
5. Melting and Pouring Techniques	34
a. Material Control	35
b. Metal Handling	36
c. Process Controls	36
d. Pouring Techniques	38
e. Screening	39
f. Summary	40
6. Degassing	40
a. Analyzing Equipment	42
b. Degassing Media	47
7. Grain Refining and Modification	59
IV. MOLD AND CORE MAKING	62
1. Sand Types	62
2. Binder Types and Properties	67
3. Venting	96
4. Parting Agents	98
5. Mold Leveling	100

<u>Section</u>	<u>Page</u>
6. Shake-Out	100
7. Summary	102
V. CHILLING AND/OR INSULATION REQUIREMENTS	104
1. Chill Material, Size, and Location	104
2. Insulation Material, Size, and Location	111
VI. GATING AND RISERING TECHNIQUES	124
1. Gating Techniques	124
a. Pouring Position	124
b. Gating Ratio	125
c. Sprue Design	130
d. Runner and Ingate Configuration	134
2. Straining Materials	136
3. Riserling Techniques	138
VII. CROSS SECTION, OVERALL DIMENSIONAL TOLERANCES, AND STRAIGHTENING REQUIREMENTS	147
1. Dimensional Requirements	147
2. Straightening Requirements	150
3. Summary	152
VIII. DISTORTION	154
1. Design-Related Distortion	154
2. Heat-Treat Distortion	155
3. Summary	163
IX. NDE PROCEDURES AND VERIFICATION OF RESULTS	164
1. Surface Inspection Methods	165
2. Determination of Dendrite Arm Spacing (DAS)	169
3. Casting Soundness	170

<u>Section</u>	<u>Page</u>
X. WELD CORRECTION OF CAST IMPERFECTIONS	174
1. Welding Process Selection	174
2. Weld Tests	175
3. Welding Equipment	175
4. Mechanical Properties	177
5. Weld Correction Procedures	184
XI. SURFACE FINISHING	185
XII. PRELIMINARY MATERIAL AND PROCESS SPECIFICATION	186
XIII. ALLOWABLES TEST CASTINGS DATA	187
1. Test Configurations and Test Plan	187
2. Test Castings	187
3. Test Data	196
a. Tensile Ultimate Strength versus Dendrite Arm Spacing	196
b. Tensile Yield Strength versus Dendrite Arm Spacing . .	212
c. Elongation versus Dendrite Arm Spacing	212
d. Tensile Ultimate Strength versus Elongation	212
e. Tensile Yield Strength versus Elongation	212
f. Tensile Ultimate Strength versus Porosity	222
g. Elongation versus Porosity	222
h. Integrally Cast Test Bars	222
4. Discussion of Data	227
XIV. METALLURGICAL STUDIES	228
1. Boeing Allowables Part B -- Casting S/N 369	228
a. Integral Cast Fitting	228
b. Fitting No. 2	231

<u>Section</u>	<u>Page</u>
2. Hitchcock Allowables Part A -- Casting S/N 9	236
a. Integral Cast Lug	236
b. Lug B	236
3. Boeing Allowables Part A -- Casting S/N 578	242
4. Summary of Findings	254
XV. MANUFACTURING PLAN	256
XVI. FOUNDRY CONTROL PROCEDURES	257
1. Personnel Qualifications and Critical Skills	257
2. Critical Operations	260
3. Process Plans	261
4. Record Keeping	262
APPENDIX A WELD CORRECTION OF IMPERFECTIONS; PROCEDURES FOR STRUCTURAL A357 ALUMINUM SAND CASTINGS	273
1. Application Note	273
2. Typical Casting Imperfections	275
a. Surface Imperfections	275
b. Internal Imperfections	275
c. Misruns	276
d. Cracks	276
3. Preweld Preparation	276
a. Equipment	276
b. Cutters	277
c. Groove Preparation	277
4. Preweld Cleaning	278

Section

Page

5. Welding Considerations	280
a. Welding Process Selection	280
b. Welding Equipment	281
c. Preheating	281
d. Shielding Gases	282
e. Tungsten Electrodes	283
f. Filler Material	283
g. Edge Wetting and Laps	284
h. Interpass Cleaning	284
i. Tailouts	285
6. Weld Bead Reinforcement Removal	286
a. Weld Bead Shaving	286
b. Bead Shaving Equipment	286
c. Bead Shaving Techniques	286
7. Weld Correction Procedures	289
a. Weld Correction of Surface Imperfections	289
b. Weld Correction of Internal Imperfections	290
c. Weld Correction of Misruns	291
d. Weld Correction of Cracks	293

ILLUSTRATIONS

<u>No.</u>		<u>Page</u>
1	Typical Microstructure of A357-T6	6
2	Pouring a Sample of Aluminum for Spectrographic Analysis .	8
3	Spiral Casting for Fluidity Testing of A357	9
4	Double Spiral Casting for Fluidity Testing	10
5	Effect of Temperature on Fluidity of A357 When Cast with Different Silica Sand Finenesses	13
6	Typical Double Fluidity Spirals Used for the Determination of the Fluidity of A357	14
7	Effect of Temperature on Fluidity of A357 When Cast with Different Sand Types	15
8	Test Plate Configuration	16
9	Applying Amorphous Carbon Mold Coating to the Surface of a Mold	17
10	Comparison of the Effects of Mold Coatings on the Fluidity of A357 in Thin Wall Castings	18
11	Effect of Temperature on Fluidity of A357 When Cast with Double Spiral Molds Coated and Uncoated	20
12	Alloy Stability of A357 When Melt Held at 1250°F	23
13	Alloy Stability of A357 When Melt Held at 1300°F	24
14	Alloy Stability of A357 When Melt Held at 1350°F	25
15	Alloy Stability of A357 When Melt Held at 1450°F	26
16	Effect of Holding Temperature at 1300°F on Hydrogen Content of A357	27

<u>No.</u>		<u>Page</u>
17	Effect of Pouring Temperature on Mechanical Properties of A357	31
18	Part A Test Section of YC-14 Station 170 Body Bulkhead . .	32
19	Part B Test Section of YC-14 Station 170 Body Bulkhead . .	33
20	Solubility of Hydrogen in Aluminum at One Atmosphere Hydrogen Pressure	41
21	Observing the Solidification of a Vacuum Freeze Sample for Evidence of Hydrogen in the Melt	43
22	Measurement of the Hydrogen Content of a Melt with an Alcoa Telegas Hydrogen Analyzer	45
23	Calibration Chart for Pure Aluminum for Telegas Hydrogen Determination Equipment	46
24	Decreasing Rate of Hydrogen Content in A357 After Degassing with N_2 at 1300°F	49
25	Deviation of A357 Alloy Chemistry After Degassing with N_2 at 1300°F	50
26	A357 Alloy Chemistry After Degassing with Hexachloroethane at 1300-1350°F	52
27	Decreasing Rate of Hydrogen Content in A357 After Degassing with 95% N_2 /5% Cl_2 at Various Temperatures . .	54
28	A357 Alloy Chemistry After Degassing with 95% N_2 /5% Cl_2 at 1250°F	55
29	A357 Alloy Chemistry After Degassing with 95% N_2 /5% Cl_2 at 1300°F	56
30	A357 Alloy Chemistry After Degassing with 95% N_2 /5% Cl_2 at 1400°F	57

<u>No.</u>		<u>Page</u>
31	Effect of Storage Time on Mold Tensile Strength of Various Sand Types with Synthetic Resin Binder Stored at Room Temperature	64
32	Effect of Storage Time on the Permeability of Various Sand Types	65
33	Effect of Storage Time on Mold Compressive Strength of Various Sand Types with Synthetic Resin Binder Stored at Room Temperature	66
34	Effect of Storage Time on Mold Tensile Strength with AFS 70 Silica Sand with Various Binders Stored at Room Temperature	71
35	Effect of Storage Time on Mold Tensile Strength with AFS 70 Silica Sand/Sodium Silicate Airset Binder Stored at Various Temperatures	72
36	Effect of Storage Time on Mold Tensile Strength with AFS 70 Silica Sand/Sodium Silicate Binder Stored at Various Temperatures	73
37	Effect of Storage Time on Mold Tensile Strength with AFS 70 Silica Sand and Synthetic Resin Binder Stored at Various Temperatures	74
38	Effect of Storage Time on Mold Mechanical Properties of Two Silica Sand Finenesses with 0.90% Linocure Binder . .	75
39	Effect of Storage Time on Mold Mechanical Properties of Two Silica Sand Finenesses with 1.0% Linocure Binder . .	76
40	Effect of Storage Time on Mold Mechanical Properties of Two Silica Sand Finenesses with 1.25% Linocure Binder . .	77

<u>No.</u>		<u>Page</u>
41	Effect of Storage Time on Mold Mechanical Properties of Two Silica Sand Finenesses with 1.5% Linocure Binder . .	78
42	Effect of Storage Time on Mold Compressive Strength of AFS 70 Silica Sand with Various Binder Types	80
43	Effect of Storage Time on Mold Permeability with Various Binders and Sand Types	83
44	Effect of Storage Time on Mold Permeability of AFS 70 Silica Sand with Various Binders	84
45	Effect of Storage Time on Mold Permeability of AFS 70 Silica Sand with Various Binders	85
46	Effect of Storage Time and Temperature on Permeability of Sand Bonded with 0.90% Linocure Binder	86
47	Effect of Storage Time and Temperature on Permeability of Sand Bonded with 1.0% Linocure Binder	87
48	Effect of Storage Time and Temperature on Permeability of Sand Bonded with 1.25% Linocure Binder	88
49	Effect of Storage Time and Temperature on Permeability of Sand Bonded with 1.5% Linocure Binder	89
50	Effect of Mulling Time on Mold Tensile Strength with AFS 70 Silica Sand and Various Binders	90
51	Effect of Mulling Time on Mold Permeability and Compressive Strength of AFS 70 Silica Sand with Various Binders . . .	91
52	Effect of CO ₂ Gassing Pressure on Mold Tensile Strength of AFS 70 Silica Sand at Various Gassing Times	93
53	Effect of Elevated Temperatures on Retained Compressive Strength of AFS 70 Silica Sand	94

<u>No.</u>		<u>Page</u>
54	Effect of Elevated Temperature on Retained Tensile Strength of AFS 70 Silica Sand	95
55	Effect of Chill Material on Mechanical Properties of A357	106
56	Effect of Chill Material on Mechanical Properties of A357	107
57	Effect of Chill Mass on Mechanical Properties of A357 . . .	108
58	Effect of Chill Configuration with Same Mass on Mechanical Properties of A357	109
59	Test Configuration for the Evaluation of Vertical Runner Insulation Material	113
60	Effect of Insulating Riser Material on the Solidification Rate of A357	114
61	Configuration of Test Plate for Insulation Tests	115
62	Effect of 0.50-inch-thick Plaster Insulation on Solidification Rate of 0.10-inch-thick Test Plate	116
63	Effect of 1-inch-thick Plaster Insulation on the Solidification Rate of 0.10-inch-thick Test Plate	117
64	Effect of 1-inch-thick Ceramic Insulation on the Solidification Rate of 0.10-inch-thick Test Plate	118
65	Effect of 0.50-inch-thick Ceramic Insulation on the Solidification Rate of 0.10-inch-thick Test Plate	119
66	Solidification of 0.10-inch-thick Test Plate	121
67	Part A Configuration with Gating System	127
68	Part B Configuration with Gating System	128

<u>No.</u>		<u>Page</u>
69	Part A Configuration Cast in Inverted Position with Gating System	131
70	Cascade Sprue System for Configuration "A"	133
71	Typical Runner, Pouring Well and Ingate Configuration . . .	135
72	Application for the Use of Screening Material in Vertical Gating Systems	137
73	Mechanical Properties of 0.10-inch-thick Plate at Various Distances from an Unchilled End	140
74	Mechanical Properties of 0.10-inch-thick Plate at Various Distances from a 6- x 2- x 2-inch Aluminum Chill	141
75	Mechanical Properties of 0.50-inch-thick Plate at Various Distances from a 6- x 2- x 2-inch Aluminum Chill	142
76	Mechanical Properties of 0.50-inch-thick Plate at Various Distances from a 6- x 3- x 3-inch Aluminum Chill	143
77	Effect of Natural Aging on the Mechanical Properties of A357	151
78	Heat Treat Fixture for Determining Effect of Age Straightening	153
79	Test Block Configuration	156
80	Resultant Distortion of Test Plates Quenched in Different Media	162
81	Penetrant Indications Obtained with Water Suspension Developer	167
82	Penetrant Indications Obtained with Dry Powder Developer .	167
83	Penetrant Inspection Results Before and After Etching . . .	168

<u>No.</u>		<u>Page</u>
84	Fluorescent Penetrant Indications with Ultrasonic Indications	172
85	Fluorescent Penetrant Indications with Ultrasonic Indications	173
86	Weld Test Panel Configuration	176
87	Allowables Test Part A	189
88	Allowables Test Part B	190
89	Details of Drag -- Hitchcock Allowables Part A Castings . .	191
90	Details of Cope -- Hitchcock Allowables Part A Castings . .	192
91	Details of Mold, Forward Side -- Boeing Allowables Part A Castings	193
92	Details of Mold, Aft Side -- Boeing Allowables Part A Castings	194
93	Details of Mold, Aft and Forward Sides -- Boeing Allowables Part B Castings	195
94	TUS versus DAS -- Hitchcock Allowables Part A Castings . .	209
95	TUS versus DAS -- Boeing Allowables Part A Castings	210
96	TUS versus DAS -- Boeing Allowables Part B Castings	211
97	Elongation versus DAS -- Hitchcock Allowables Part A Castings	213
98	Elongation versus DAS -- Boeing Allowables Part A Castings	214
99	Elongation versus DAS -- Boeing Allowables Part B Castings	215
100	TUS versus Elongation -- Hitchcock Allowables Part A Castings	216

<u>No.</u>		<u>Page</u>
101	TUS versus Elongation -- Boeing Allowables Part A	
	Castings	217
102	TUS versus Elongation -- Boeing Allowables Part B	
	Castings	218
103	TYS versus Elongation -- Hitchcock Allowables Part A	
	Castings	219
104	TYS versus Elongation -- Boeing Allowables Part A	
	Castings	220
105	TYS versus Elongation -- Boeing Allowables Part B	
	Castings	221
106	TUS versus Porosity Index -- Boeing Allowables Part A	
	Castings	223
107	TUS versus Porosity Index -- Boeing Allowables Part B	
	Castings	224
108	Elongation versus Porosity Index -- Boeing Allowables	
	Part A Castings	225
109	Elongation versus Porosity Index -- Boeing Allowables	
	Part B Castings	226
110	Boeing Allowables Part B, Showing Locations of Fittings,	
	Forward Side	228
111	Integral Cast Fitting from Boeing Allowables Preproduction	
	Part B Casting S/N 369	230
112	DAS Measurements Along Grid Lines A-A, B-B, C-C, and D-D;	
	Integral Cast Fitting, Piece B, from Boeing Casting	
	S/N 369	232

<u>No.</u>		<u>Page</u>
113	DAS Measurements Along Grid Lines X-X, Y-Y, and Z-Z; Integral Cast Fitting, Piece B, from Boeing Casting S/N 369	233
114	Lines of Constant Average DAS and Extent of Visual Porosity, Fittings from Boeing Casting S/N 369	234
115	Fitting No. 2 from Boeing Allowables Preproduction Part B Casting S/N 369	235
116	Hitchcock Allowables Part A, Aft/Cope Side, Showing Locations of Lugs and Chills	237
117	DAS Measurements Along Grid Lines 1-1, 2-2, and 3-3; Integral Cast Lug, Plane 1-2-3-4, from Hitchcock Casting S/N 9	238
118	DAS Measurements Along Grid Lines A-A, B-B, and C-C; Integral Cast Lug, Plane 1-2-3-4, from Hitchcock Casting S/N 9	239
119	Lines of Constant Average DAS in Plane 1-2-3-4; Integral Cast Lug from Hitchcock Casting S/N 9	240
120	Lug B from Hitchcock Casting S/N 9	241
121	Integral Cast Lug from Boeing Allowables Part A Casting S/N 578	243
122	DAS Measurements Along Grid Lines 1-1, 2-2, and 3-3; Integral Cast Lug, Plane B, from Boeing Casting S/N 578	244
123	DAS Measurements Along Grid Lines A-A, B-B, and C-C; Integral Cast Lug, Plane B, from Boeing Casting S/N 578	245

<u>No.</u>		<u>Page</u>
124	DAS Measurements Along Grid Lines 1-1, 2-2, and 3-3; Integral Cast Lug, Plane C, from Boeing Casting S/N 578	246
125	DAS Measurements Along Grid Lines A-A, B-B, and C-C; Integral Cast Lug, Plane C, from Boeing Casting S/N 578	247
126	DAS Measurements Along Grid Lines 1-1, 2-2, and 3-3; Integral Cast Lug, Plane D, from Boeing Casting S/N 578	248
127	DAS Measurements Along Grid Lines A-A, B-B, and C-C; Integral Cast Lug, Plane D, from Boeing Casting S/N 578	249
128	Lines of Constant Average DAS and Extent of Visual Porosity in Planes B, C, and D; Integral Cast Lug from Boeing Casting S/N 578	250
129	Lines of Constant Average DAS in Plane E; Integral Cast Lug from Boeing Casting S/N 578	251
130	Lines of Constant Average DAS in Plane F; Integral Cast Lug from Boeing Casting S/N 578	252
131	Maximum Pore Dimensions Along Grid Line 2-2 in Planes B, C, and D; Integral Cast Lug from Boeing Casting S/N 578	253
132	Average Maximum Pore Dimension versus Average DAS; Integral Cast Lug from Boeing Casting S/N 578	255
133	Typical Casting Record Form -- Parameters	264
134	Typical Casting Record Form -- Parameters	265

<u>No.</u>		<u>Page</u>
135	Typical Casting Record Form -- Parameters	266
136	Typical Casting Record Form -- Pouring System	267
137	Typical Casting Record Form -- Production Tests	268
138	Typical Casting Record Form -- Test Specimens	269
139	Typical Casting Record Form -- Approval	270
140	Typical Casting Record Form -- Furnace	271
141	Typical Casting Record Form -- Inspection	272
142	Weld Correction of Cast Test Part	274
143	Typical Groove Configuration for Weld Correction	279
144	Bead Shaving Equipment for Checking Corrected Area After Welding	287
145	Use of Fine Tooth Rotary File for Weld Bead Reinforcement Removal	288

TABLES

<u>No.</u>		<u>Page</u>
1	A357 Chemical Composition	4
2	A357 Heat Treatment	5
3	Thermal Expansion of Mold Sand at Elevated Temperatures . .	97
4	Gas Evolution of Mold Sand at Elevated Temperatures	99
5	Effect of Insulation on DAS Measurements at Various Locations of a 0.10-inch Test Plate	122
6	Dimensional Tolerances -- A357 Sand Castings	148
7	Effect of Various Quenching Media on the Mechanical Properties of A357	159
8	Mechanical Properties of Weld Test Specimens	178
9	Mechanical Properties of Weld Test Specimens	179
10	Mechanical Properties of Weld Test Specimens	180
11	Mechanical Properties of Weld Test Specimens	181
12	Mechanical Properties of Weld Test Specimens	182
13	Mechanical Properties of Weld Test Specimens	183
14	Static Mechanical Properties Data -- Hitchcock Allowables Part A Castings -- A357-T6	197
15	Static Mechanical Properties Data -- Boeing Allowables Part A Castings -- A357-T6	201
16	Static Mechanical Properties Data -- Boeing Allowables Part B Castings -- A357-T6	205

SECTION I

INTRODUCTION

The purpose of this program is to demonstrate that the use of castings in airframe construction can be extended to primary structural components. The program goal is to achieve the above with no weight penalty and with a minimum of 30% cost savings. Specific objectives of the program are to establish necessary structural and manufacturing technologies and to demonstrate improved integrity, reliability, and reproducibility of cast aluminum airframe components. The baseline component selected to demonstrate structural casting capability is the YC-14 body bulkhead at body station 170. This is the body nose bulkhead that provides forward support for the nose landing gear and nose gear door. The cast version of the bulkhead weighs 185 pounds and measures 90 x 53 inches. Much of it is only 0.10 inch thick.

The CAST program is a six-phase effort. The six phases include the following specific activities:

- Phase I: Preliminary Design
- Phase II: Manufacturing Methods
- Phase III: Detail Design
- Phase IV: Fabrication of Demonstration Component
- Phase V: Structural Test and Verification
- Phase VI: Technology Transfer

The objective of Phase II, Development of Manufacturing Methods, is to establish necessary casting foundry practices and related manufacturing technologies to support all design and fabrication efforts. In accomplishing this objective, the trial-and-error methods of casting were minimized and a more scientific approach was taken. This will ensure high and more consistent mechanical properties. This effort involved extensive characterization of each step of the casting process to define acceptable limits of process parameters. This technology will then be used during the fabrication of the demonstration component during Phase IV.

SECTION II

ALLOY SELECTION

The age-hardenable aluminum-silicon-magnesium alloy A357 was selected for the CAST program. This alloy is characterized by excellent castability, good response to heat treatment, high resistance to corrosion, and good weldability.

A357 is similar to A356, but has a slightly higher magnesium content and controlled amounts of titanium and beryllium added to increase the strength. Table 1 shows the chemical composition limits established by the preliminary material and process specification, M-XXXX, "Aluminum Alloy A357 Castings, Primary Aircraft Structure."

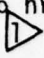
A357 is used in the solution-heat-treated and aged condition. Table 2 presents the nominal heat treatment specified in M-XXXX.


A typical microstructure of heat-treated A357 shows that solid solution dendrites of primary aluminum form the matrix, with an interdendritic eutectic network of alpha aluminum and silicon particles (Fig. 1). Extremely fine particles of the intermetallic phase, Mg_2Si , precipitate out of solid solution during aging; however, these are not visible at the magnification of Figure 1.

TABLE 1. A357 CHEMICAL COMPOSITION

Elements	Percent, Minimum	Percent, Maximum
Copper	--	0.20
Silicon	6.5	7.5
Iron	--	0.10
Manganese	--	0.10
Zinc	--	0.10
Magnesium	0.55	0.65
Titanium	0.10	0.20
Beryllium	0.04	0.07
Others, each	--	0.05
Others, total	--	0.15
Aluminum	Remainder	

TABLE 2. A357 HEAT TREATMENT

Solution Heat Treatment	Quench Delay	Quenchant	Natural Aging	Precipitation Heat Treatment (Aging)
1010°F \pm 10°F for 16 hrs. min. 	8 sec. max.	170°F \pm 30°F water	Room temp. for 16-24 hrs.	325°F \pm 10°F for 8 hrs. \pm 1 hr.

 For castings with 1 inch maximum thickness. Add 2 hours soak for each additional 1/2 inch thickness.

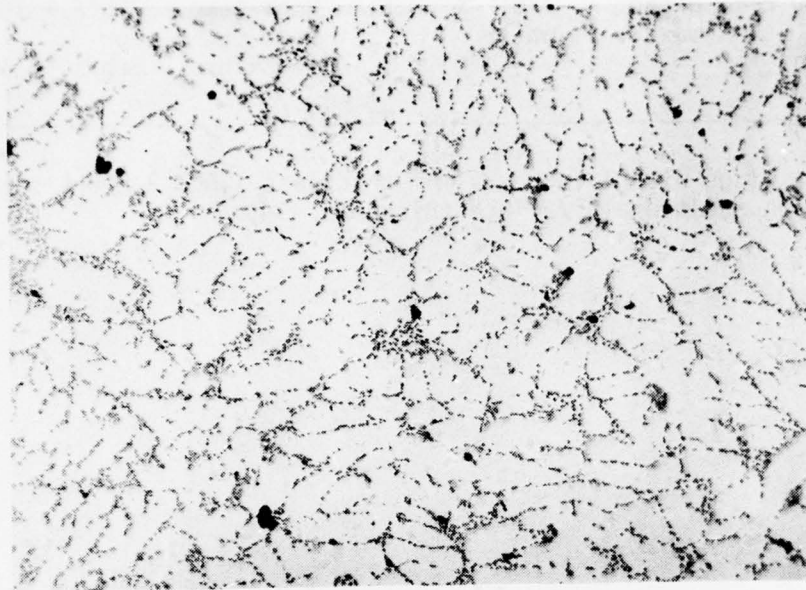


Figure 1. Typical Microstructure of A357-T6

Mag.: 100X

SECTION III

METAL MELTING AND POURING TECHNIQUES

1. BASELINE DATA FOR SPECTROGRAPHIC ANALYSIS

Close control of alloy composition throughout the casting process is critical if mechanical properties are to be optimized. This can be accomplished only if the means of determining alloy composition are reliable. During this program, vacuum emission spectrographic analysis was used for determining alloy composition. The removal of a spectrographic analysis sample from a melt is shown in Figure 2. This analysis method is fast, convenient, and can produce reliable results. Its accuracy was compared with the more accurate wet chemical analysis at the beginning of this program. The results of analyzing an A357 aluminum alloy sample by the two methods indicate that the silicon and magnesium content differed by only 3% and 7%, respectively. Based upon this comparison, it is concluded that vacuum spectrographic analysis does produce reliable results.

2. FLUIDITY TEST

Fluidity may be described as being the property of molten metal that allows it to flow through the mold gating system and ultimately fill the mold cavity to produce a casting. The amount of fluidity a given metal will display in casting operations is generally measured with standard fluidity test molds. Figures 3 and 4 show two configurations of the fluidity test molds used in this investigation. Figure 3 shows a single spiral-type fluidity test pattern in which the width of the part decreases as the length of the spiral increases. It was believed that this design would

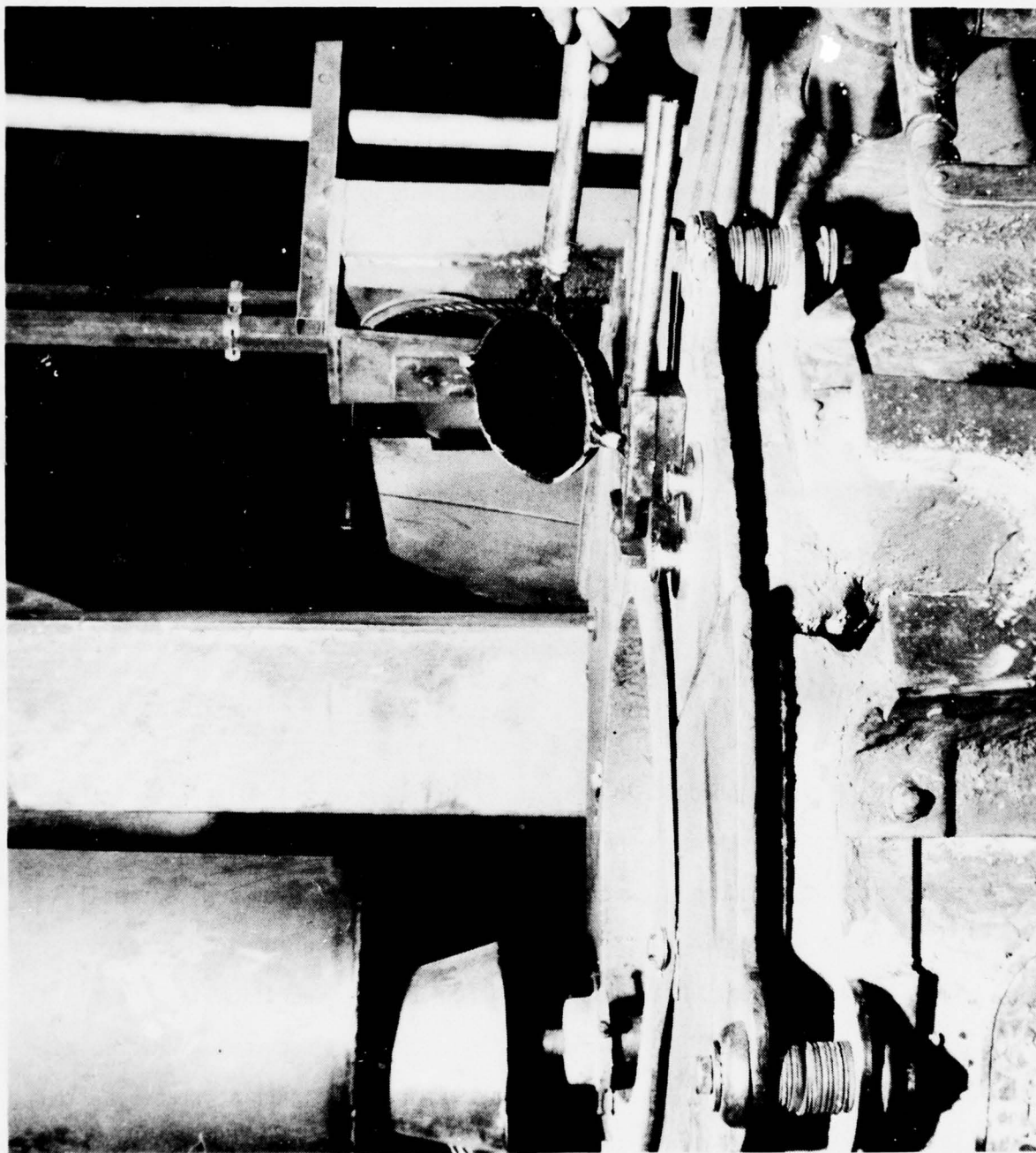


FIGURE 2 POURING A SAMPLE OF ALUMINUM FOR SPECTROGRAPHIC ANALYSIS

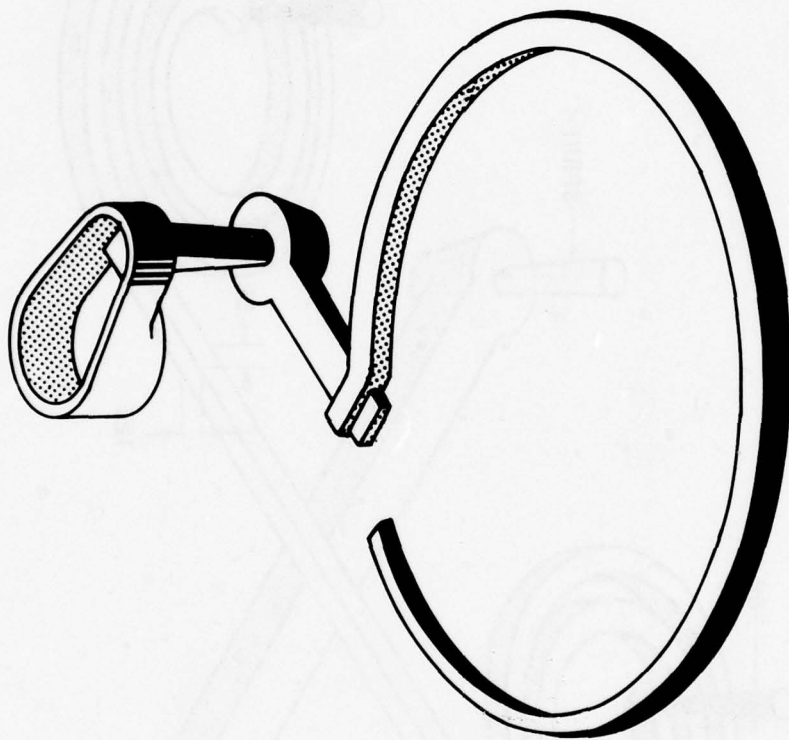
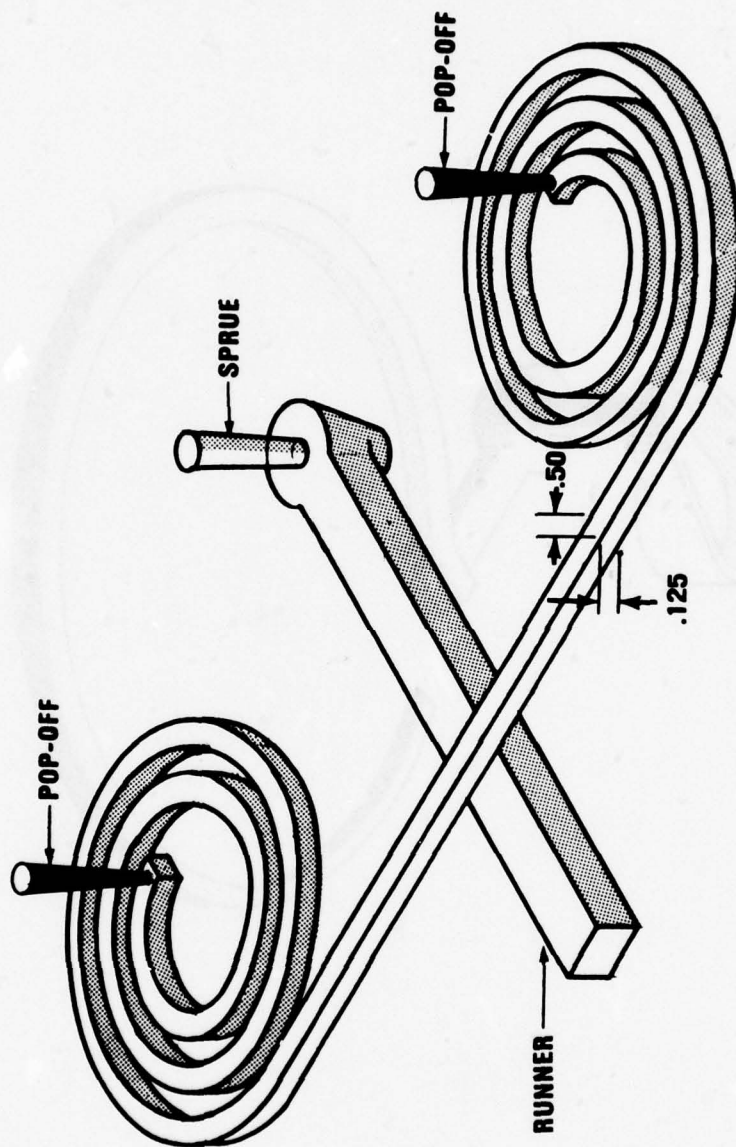


FIGURE 3 SPIRAL CASTING FOR FLUIDITY TESTING OF A357



TOTAL LENGTH ONE SIDE: 31.5 IN.

FIGURE 4 DOUBLE SPIRAL CASTING FOR FLUIDITY TESTING

display the fluidity characteristics of molten metal flowing from a thick to a thin section. Due to the constant velocity of the metal entering the mold through the sprue, the molten flow appeared to accelerate as the spiral section narrowed. Although this test significantly shows the effect of nonuniform section thickness in molds on the fluidity characteristics of the molten metal, it does not provide reliable data for estimating the fluidity of molten metal in a mold of uniform section thickness. The determination of the amount of fluidity obtained in molds of uniform section thickness was made by casting parts in the form of a double-spiral, as shown in Figure 4.

The double-spiral fluidity test pattern described above was evaluated in molds made with AFS 53, 70, and 140 silica sand. The molds made with AFS 53 and 70 silica sand were bonded with 4% sodium silicate- CO_2 , and those made with AFS 140 silica sand were bonded with 6% sodium silicate- CO_2 . The larger amount of binder required for AFS 140 silica sand was due to the greater total surface area of the finer sand grains with respect to the surface area displayed by the AFS 53 and 70 grains. In addition to the silica sand fluidity test molds, tests were also conducted with molds made of zircon and chromite sands bonded with 4% sodium silicate- CO_2 . Amorphous carbon and hexachloroethane mold coatings were tested to determine their effect on metal fluidity, and the effect of alloy composition on the fluidity characteristics of molten aluminum was also evaluated. Each of the test castings was poured with A357 at 1400°F at a height of 11 inches above the sprue. To eliminate problems resulting from pressure or gas generated in the molds, a 0.25-inch-diameter vent was placed at the end of each spiral. The amount of fluidity displayed by each condition using the spiral molds was determined by weighing and measuring each cast and trimmed spiral.

The results of fluidity tests using AFS 53, 70, and 140 silica sand are shown in Figure 5. These results indicate that the fluidity of AFS 70 sand was better than AFS 140 or 53. Visual examination of the spiral castings shows that the cast surface finish obtained with AFS 140 silica sand was better than AFS 70, which was superior to AFS 53. A typical example of a cast double spiral is shown in Figure 6.

The effect of zircon and chromite sand on the fluidity of molten A357 aluminum alloy is shown in Figure 7. These sands are typically used in molding and casting operations for their light chilling effect on the molten aluminum. This chilling effect is due to the higher thermal diffusivity of the two sands with respect to silica sand. These sands were tested with the double-spiral fluidity pattern. The results of these tests show that these sands reduce the fluidity by about 9% and 29%, respectively, when compared to AFS 70 silica sand.

The effect of amorphous carbon and hexachloroethane mold coatings was evaluated on parts cast in the configuration of Figure 8 ($T = 0.100$ inch). The amorphous carbon was applied with an acetylene flame torch (Fig. 9) to a thickness of 0.001-0.003 inch and the hexachloroethane was mixed with alcohol (1:1) and sprayed on the molds to a thickness of about 0.003 inch. The molds were made with AFS 70 silica sand bonded with 4% sodium silicate- CO_2 and poured at 1400°F. The results of this evaluation are shown in Figure 10. These results show the effect of mold coatings on metal fluidity with respect to uncoated molds. Examination of the parts cast in this evaluation show that significantly greater fluidity is obtained by coating the mold

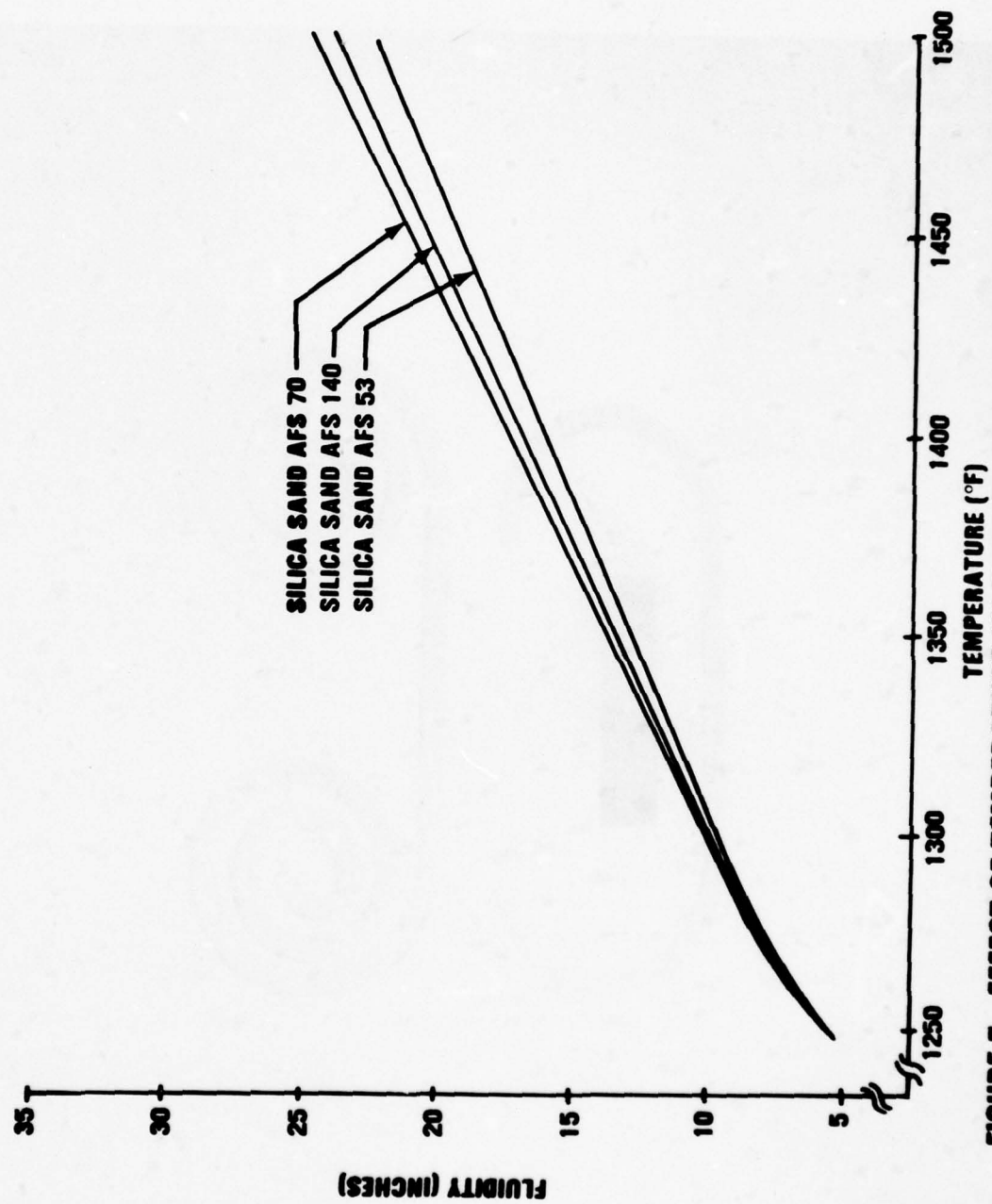


FIGURE 5 EFFECT OF TEMPERATURE ON FLUIDITY OF A357 WHEN CAST WITH DIFFERENT SILICA SAND FINENESSES



FIGURE 6 TYPICAL DOUBLE FLUIDITY SPIRALS USED FOR THE DETERMINATION OF THE FLUIDITY OF A357

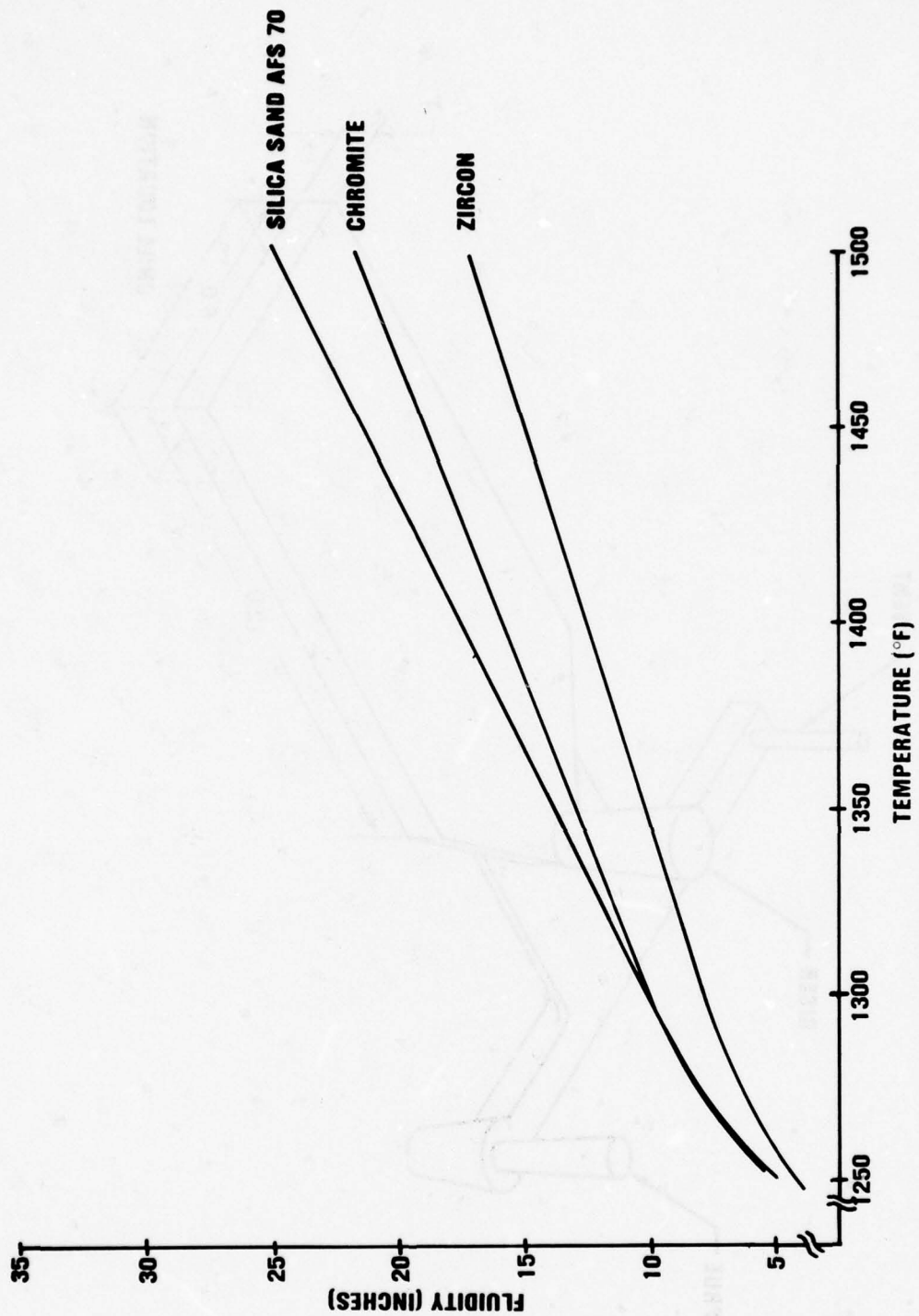


FIGURE 7 EFFECT OF TEMPERATURE ON FLUIDITY OF A 357 WHEN CAST WITH DIFFERENT SAND TYPES

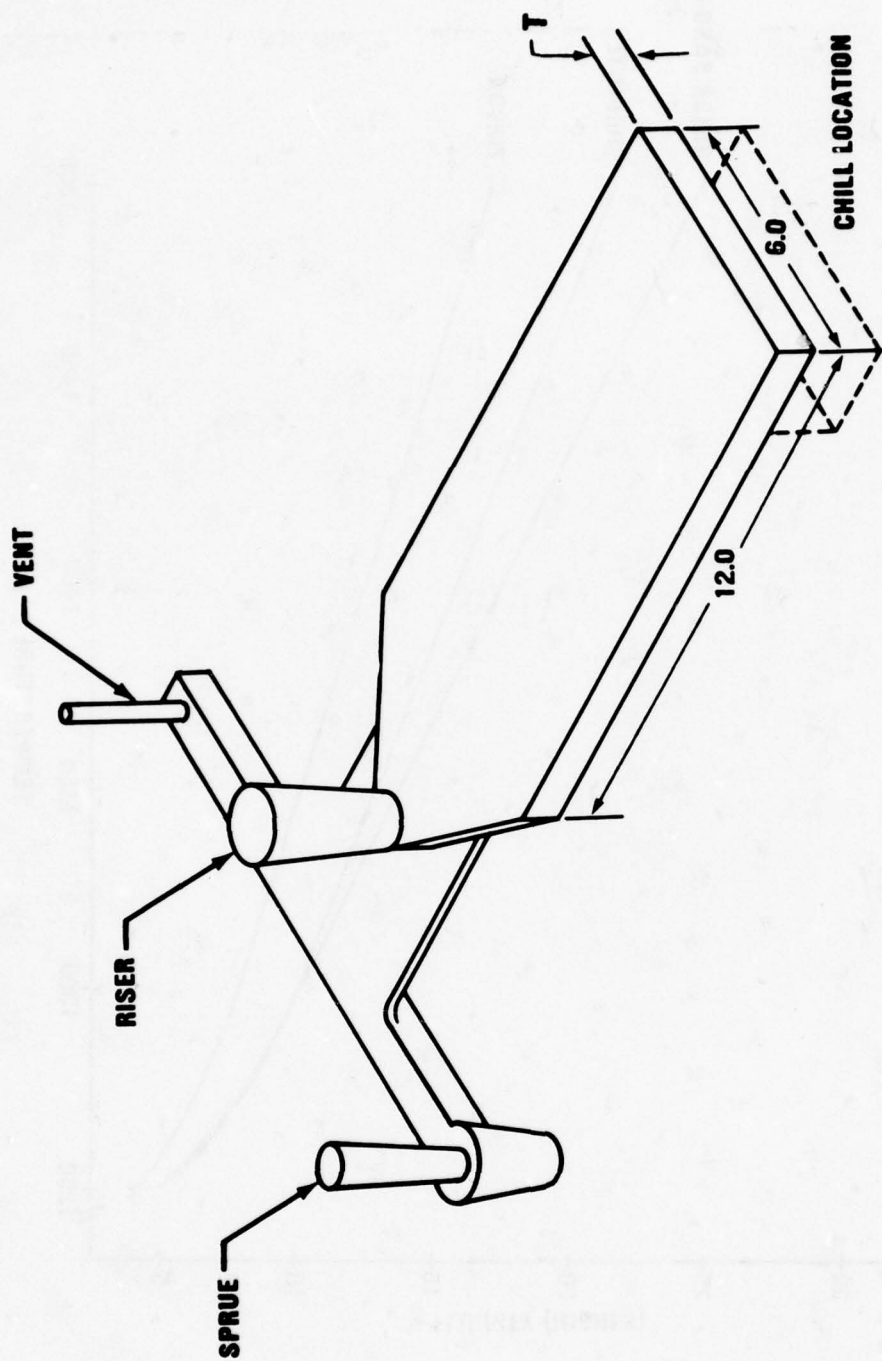


FIGURE 8 TEST PLATE CONFIGURATION



FIGURE 9 APPLYING AMORPHOUS CARBON MOLD COATING TO THE SURFACE OF A MOLD

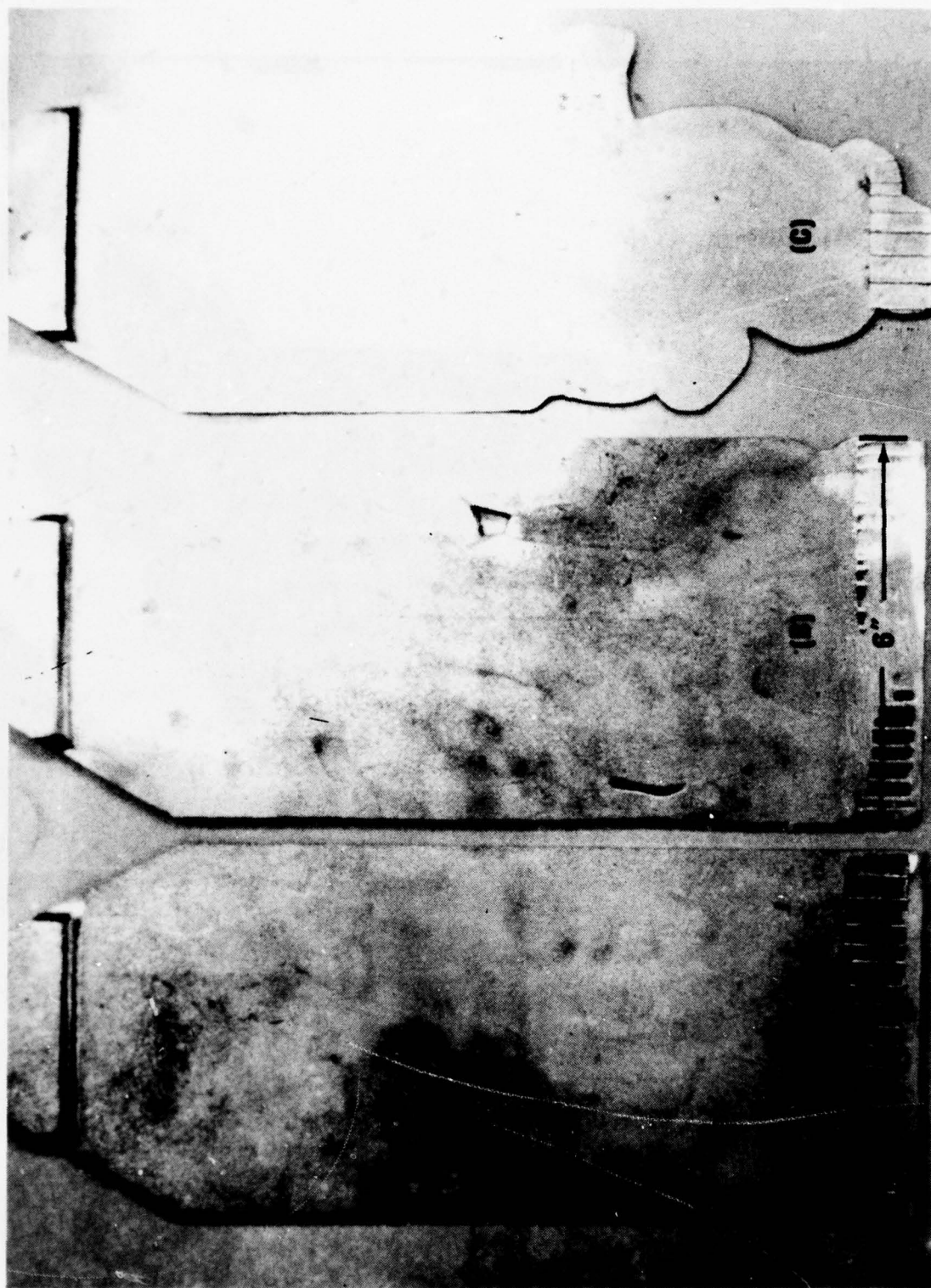


FIGURE 10 COMPARISON OF THE EFFECTS OF MOLD COATINGS ON THE FLUIDITY OF A367 IN THIN WALL (.100) CASTINGS. (A) AMORPHOUS CARBON; (B) HEXACHLOROETHANE; (C) NO COATING

with amorphous carbon than with hexachloroethane, and 40% more fluidity is obtained than with uncoated molds. In addition, the hexachloroethane presents a health hazard to the foundryman and requires special precautions for use as a molding material. Castings produced from molds coated with hexachloroethane also displayed surface discoloration. This discoloration is believed to be an aluminum-chloride oxide or residue that resulted from contact between the molten aluminum and the mold coating.

An additional test was conducted to compare the relative effects of amorphous carbon mold coating and no mold coating. Double fluidity spirals were coated with amorphous carbon or left uncoated, then poured at various temperatures. The results are shown in Figure 11. It is readily apparent that amorphous carbon does enhance the fluidity of A357.

The effect of alloy composition on the fluidity of molten aluminum was evaluated by modifying the silicon, magnesium, and beryllium contents of A357 within its given alloy range. The results of this evaluation displayed no significant difference in fluidity resulting from chemistry variation.

It is not practical to use the results of the fluidity tests to define the foundry variables necessary to cast a part. These data offer a comparison of the relative effects that some of the foundry parameters have on fluidity. However, some general conclusions can be drawn:

- o Amorphous carbon mold coating is needed to enhance the fluidity of thin-wall castings.
- o AFS 70 sand offers improved fluidity over AFS 53 sand.
- o Variation in the chemistry of A357 does not affect fluidity.

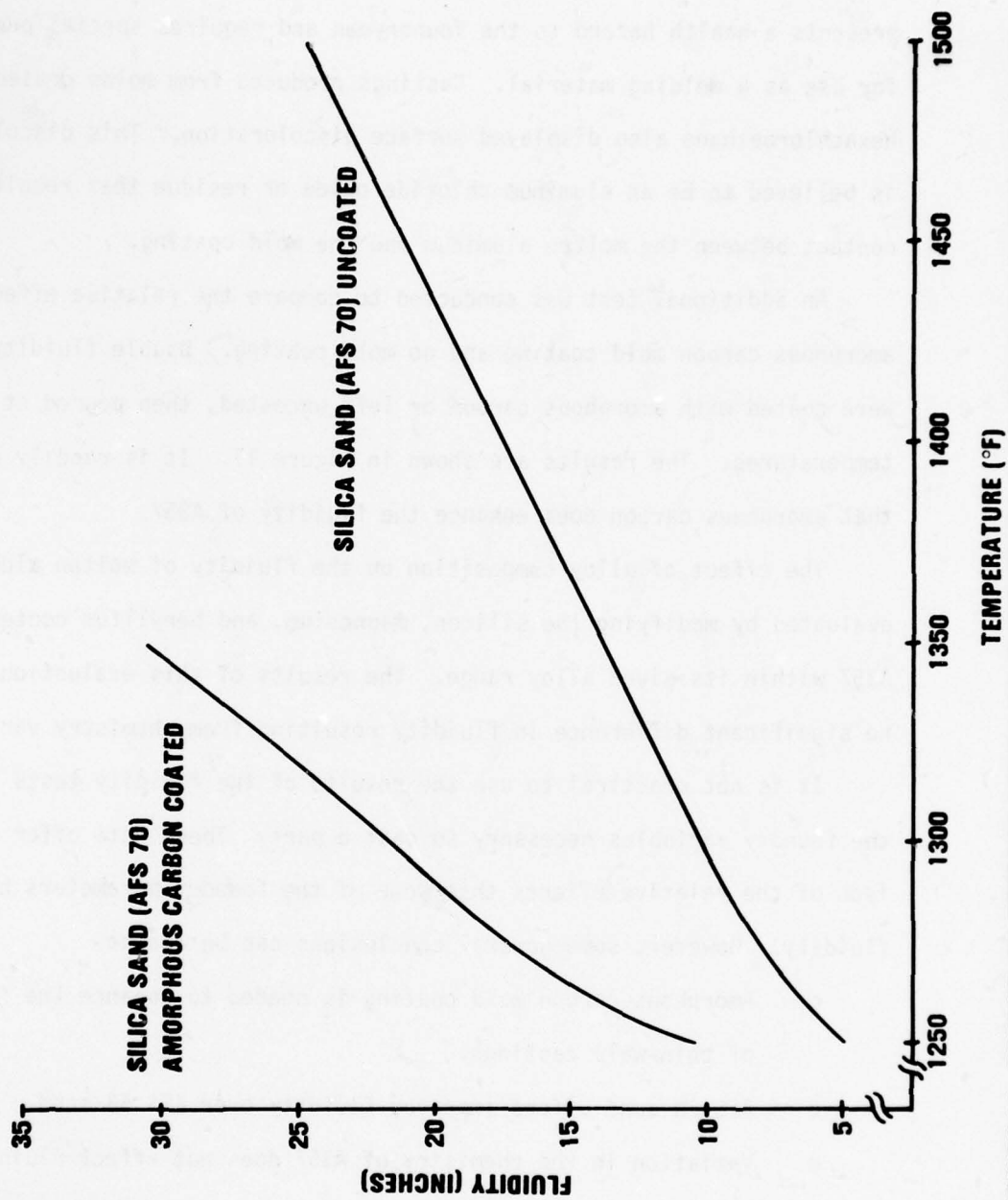


FIGURE 11 EFFECT OF TEMPERATURE ON FLUIDITY OF A357 WHEN CAST WITH DOUBLE SPIRAL MOLDS COATED & UNCOATED

3. HOLDING TEMPERATURE

When a charge of metal is completely molten, it is typically held at a temperature between the melting point and the pouring temperature until preparations for pouring and degassing operations are complete. For aluminum alloys, this temperature is generally between 1300 and 1400°F. The length of time that the metal remains at the holding temperature depends upon the time required for degassing operations and/or mold and pouring preparations.

The effect of melt holding temperature and time on the stability of A357 aluminum alloy was evaluated at 1250, 1300, 1350, and 1450°F for holding times ranging from 0 to 24 hours. At each of the prescribed test temperatures, the alloy composition (Si, Mg, and Be) was adjusted to the maximum allowable for the A357 alloy range (7.5, 0.70, and 0.070%, respectively). The charges were melted in production-type gas-fired furnaces equipped with 350-pound capacity silicon carbide crucibles. When the temperature of the melt had stabilized at the desired holding temperature and correct chemistry was obtained, metallurgical and gas test samples were taken at prescribed intervals up to and including 24 hours. The metallurgical samples were subjected to spectrographic analysis and the gas samples were evaluated by solidifying a molten specimen in a vacuum chamber, sectioning, and observing gas hole formation at the interior surfaces of each specimen.

The design of the melting furnace used in this evaluation was such that a minimum amount of surface area was exposed to the atmosphere at the top of the melt. It is believed that minimizing the molten surface area in contact with the air will reduce the amount of hydrogen contamination by this atmosphere.

The effect of holding temperature on alloy stability as a function of time is shown in Figures 12-15. The results show that the amount of time the melt is held at temperature has relatively little effect on the silicon, magnesium, and beryllium content.

Visual examination of the gas test specimens revealed that the amount of hydrogen gas present in the melt increased as the holding temperature was increased. This increase in hydrogen present at the higher holding temperature is due to the increased solubility of hydrogen at elevated temperatures.

The effect of holding time on the amount of hydrogen present in the melt at 1300°F is shown in Figure 16. In this evaluation, the charge was degassed with a 95% nitrogen/5% chlorine gas mixture at 1300°F for 20 minutes and then held for a period of 2 hours. Measurements of the hydrogen present in the melt after degassing were taken with an Alcoa "Telegas" hydrogen analyzer. The data show a constant decrease in the amount of hydrogen present in the melt from 0 to 60 minutes, and then an increase in gas content from 1 to 2 hours at the holding temperature. The initial decrease in hydrogen content is believed to be due to residual nitrogen-chlorine gas still in the melt, acting as a deoxidizing agent.

Based on the results of this investigation, the holding temperature for A357 aluminum prior to degassing operations may be considered arbitrary, but should be between 1250 and 1325°F. The holding temperature of the melt for degassing operations is discussed in Section III.6.

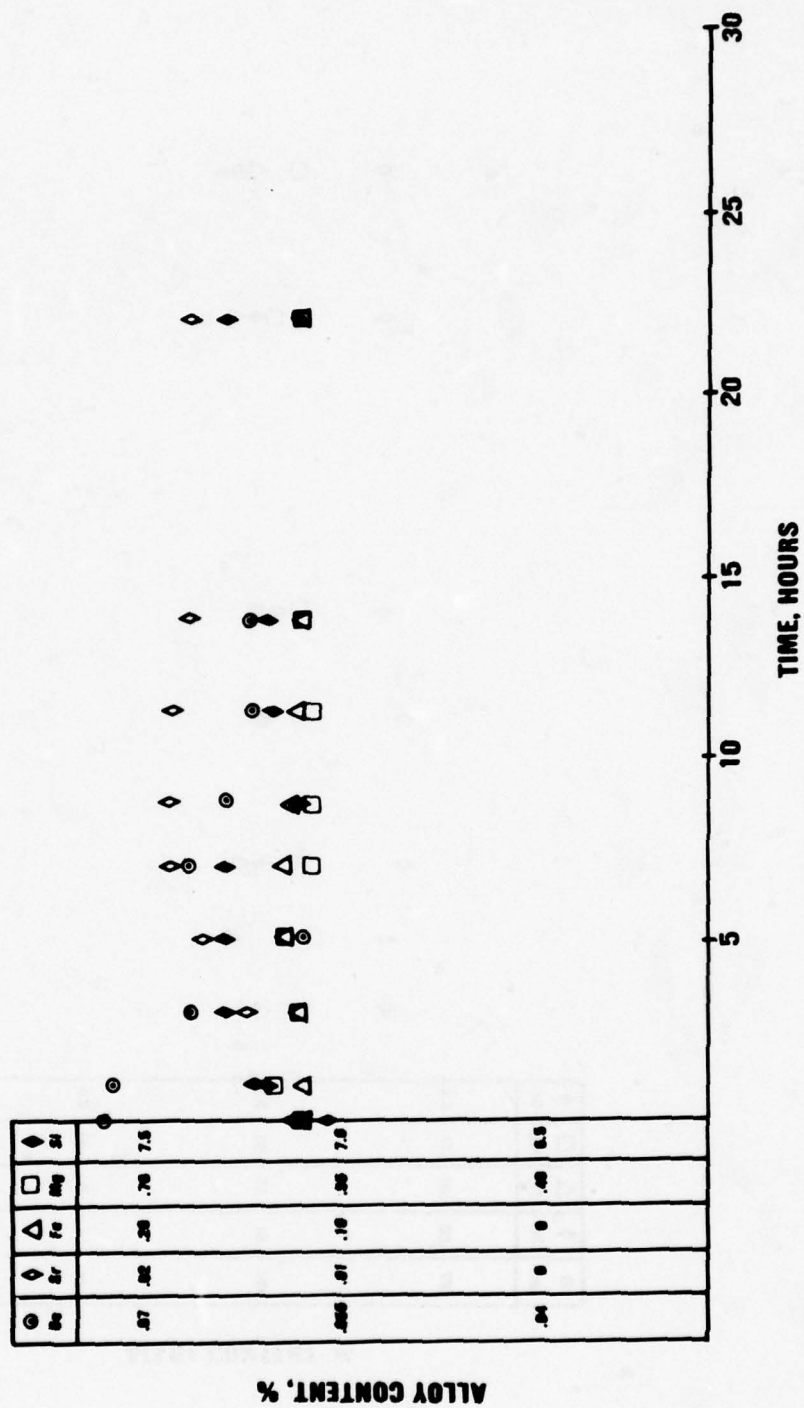


FIGURE 12 ALLOY STABILITY OF A357 WHEN MELT HELD AT 1250°F

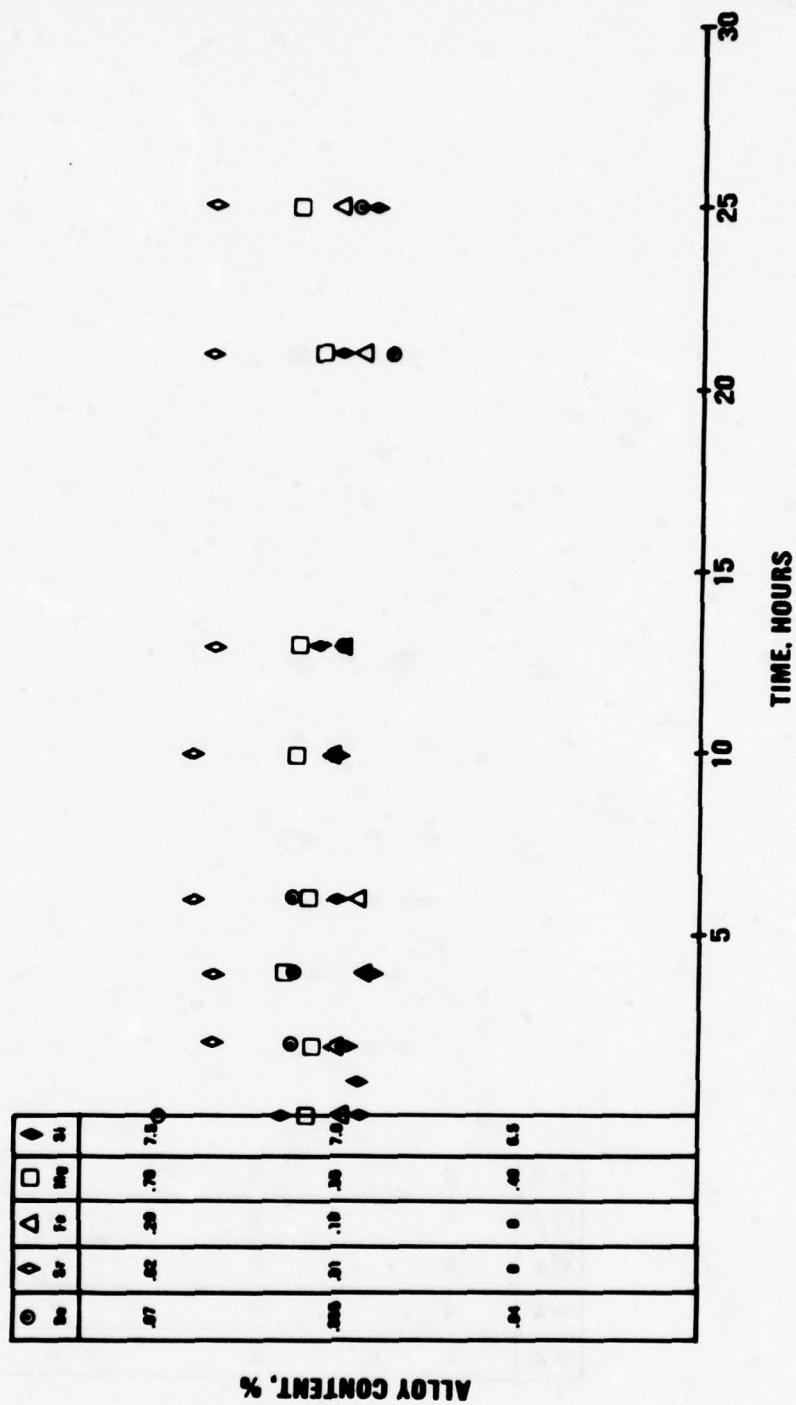


FIGURE 13 ALLOY STABILITY OF A357 WHEN MELT HELD AT 1300°F

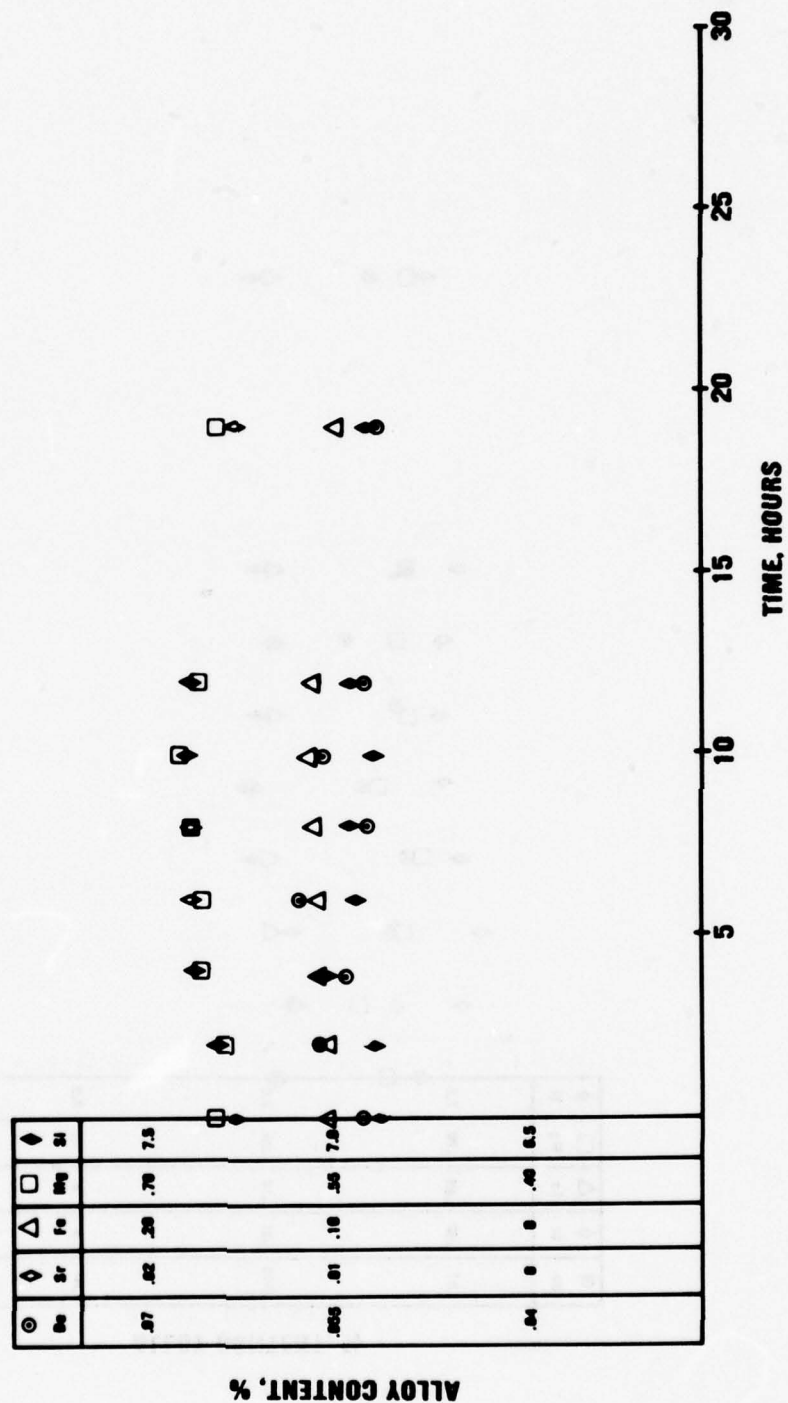


FIGURE 14 ALLOY STABILITY OF A357 WHEN MELT HELD AT 1350°F

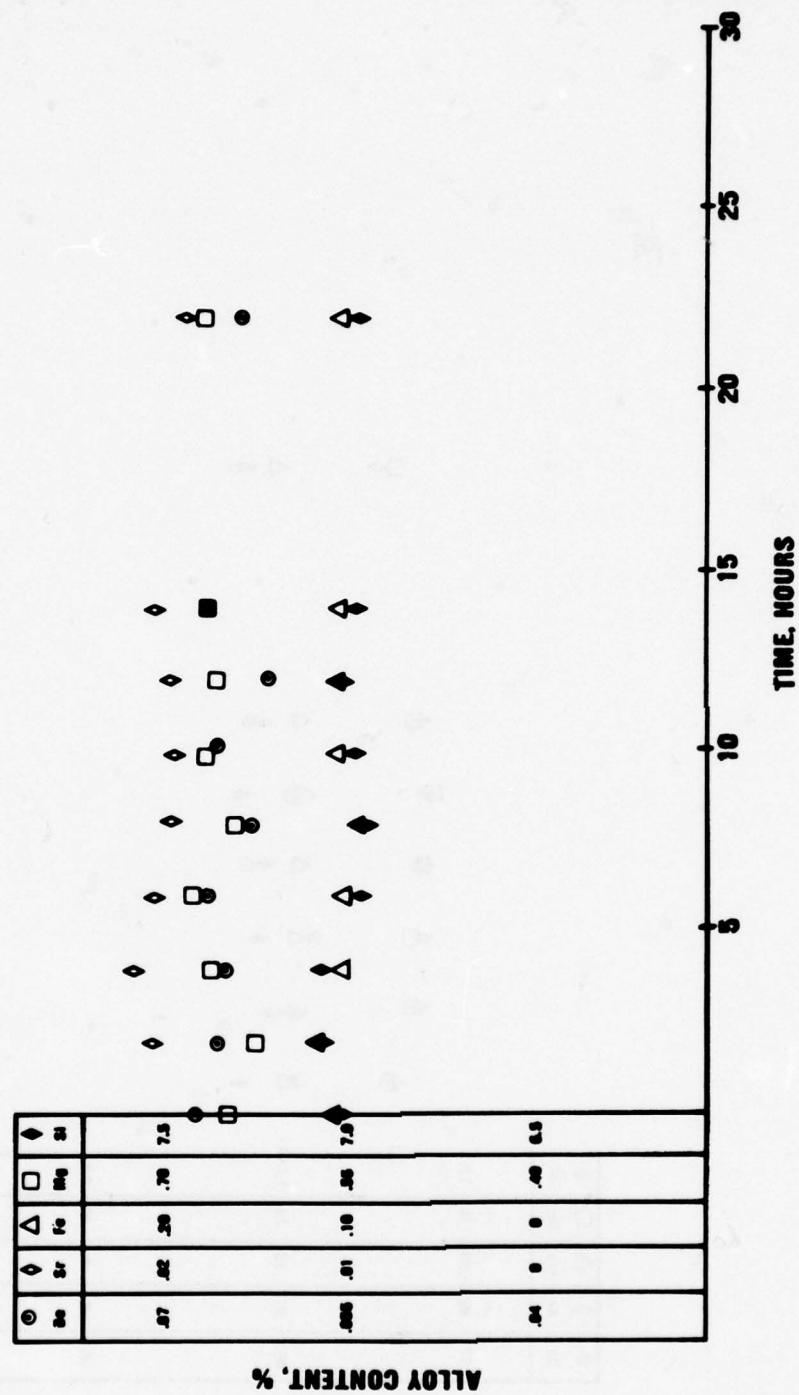


FIGURE 13 ALLOY STABILITY OF A357 WHEN MELT HELD AT 1450°F

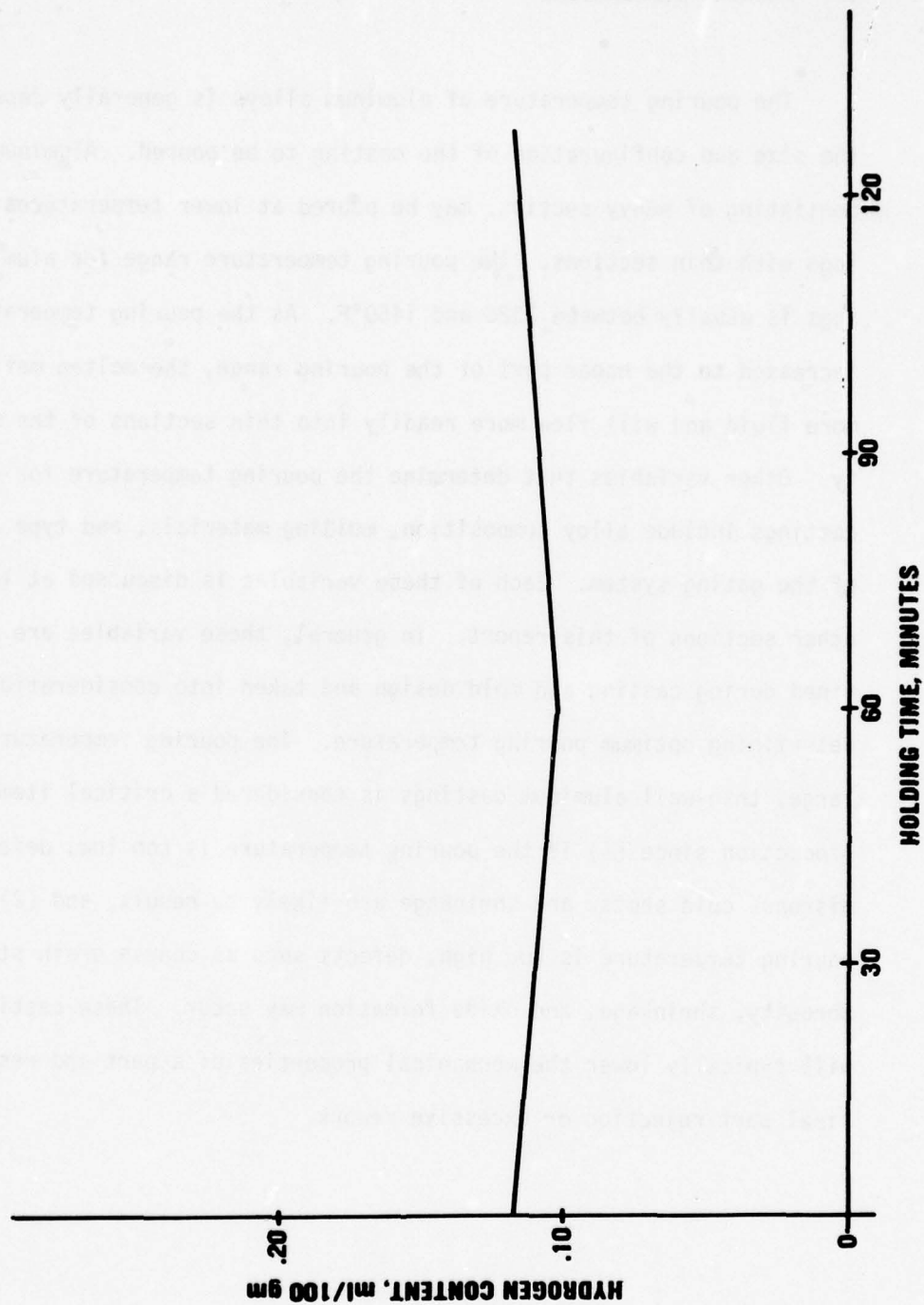


FIGURE 16 EFFECT OF HOLDING TEMPERATURE AT 1300°F ON HYDROGEN CONTENT OF A357

4. POURING TEMPERATURE

The pouring temperature of aluminum alloys is generally dependent upon the size and configuration of the casting to be poured. Aluminum castings consisting of heavy sections may be poured at lower temperatures than castings with thin sections. The pouring temperature range for aluminum castings is usually between 1325 and 1450°F. As the pouring temperature is increased to the upper part of the pouring range, the molten metal becomes more fluid and will flow more readily into thin sections of the mold cavity. Other variables that determine the pouring temperature for aluminum castings include alloy composition, molding materials, and type and ratio of the gating system. Each of these variables is discussed at length in other sections of this report. In general, these variables are predetermined during casting and mold design and taken into consideration when determining optimum pouring temperature. The pouring temperature for large, thin-wall aluminum castings is considered a critical item in casting production since (1) if the pouring temperature is too low, defects such as misruns, cold shuts, and shrinkage are likely to result, and (2) if the pouring temperature is too high, defects such as coarse grain structure, porosity, shrinkage, and oxide formation may occur. These casting defects will typically lower the mechanical properties of a part and result in final part rejection or excessive rework.

When the optimum pouring temperature for a casting is established, it is controlled by monitoring the molten bath with immersion-type pyrometers at frequent intervals. Pyrometric control of the molten aluminum is mandatory in the production of quality aluminum castings, since temperature determination by observation is considered no better than a guess. Temperature determination by methods such as observing bubbling action, oxide skim formation, or melt color are considered poor foundry practice.

In addition to the tests conducted to determine the effect of pouring temperature on metal fluidity discussed earlier in this section, parts were cast in the configuration of Figure 8 ($T = 0.500$ inch) and specimens were taken to evaluate the effect of pouring temperature on the mechanical properties of cast A357. A 6- x 3- x 3-inch aluminum chill was placed in the position shown in the figure and test panels were poured at 1350, 1400, and 1450°F. Tensile specimens were fabricated from the test panels at 1-, 4-, 8-, and 11-inch distances from the chilled end. Each of the test panels was subjected to radiographic inspection prior to specimen fabrication. This inspection revealed that sponge shrinkage occurred in most of the test panels about midway between the chill and riser ends of the panels. This shrinkage defect is due to the directional solidification that was promoted by the chill with respect to the maximum feeding distance of the riser during solidification. As the metal solidified from the chilled end toward the riser, it solidified faster than the riser could feed. This condition produced castings with sound metal at areas near the chill and near the riser, but unsound at the center.

Tests to determine the optimum pouring temperature range for large, thin-wall aluminum castings were also conducted on parts of the configuration shown in Figures 18 and 19. These test parts were evaluated by radiographic and penetrant techniques.

The results of tests performed on specimens described in the preceding paragraph are shown in Figure 17. The results show that highest mechanical properties in terms of ultimate tensile strength, yield strength, and percent elongation are developed at the chilled end by pouring at 1350°F. It is believed that the higher mechanical properties displayed by specimens poured at the lower pouring temperature are due to the length of time required for the molten metal to solidify. Specifically, it took less time for the metal to cool from 1350°F than from 1400 or 1450°F. This faster cooling rate resulted in a finer grain structure, and subsequent higher mechanical properties than obtained with the higher pouring temperatures. At the riser end of the casting, highest mechanical properties were obtained by pouring the metal at 1450°F. Since the higher pouring temperature provided more adequate riser feeding than at 1350 or 1400°F, a more equiaxed grain structure was obtained. In general, the pouring temperature of the metal should be kept as low as possible with respect to section thickness, alloy composition, required mechanical properties, and chill-to-riser distances. The optimum distance between chill and riser is discussed in section VI.

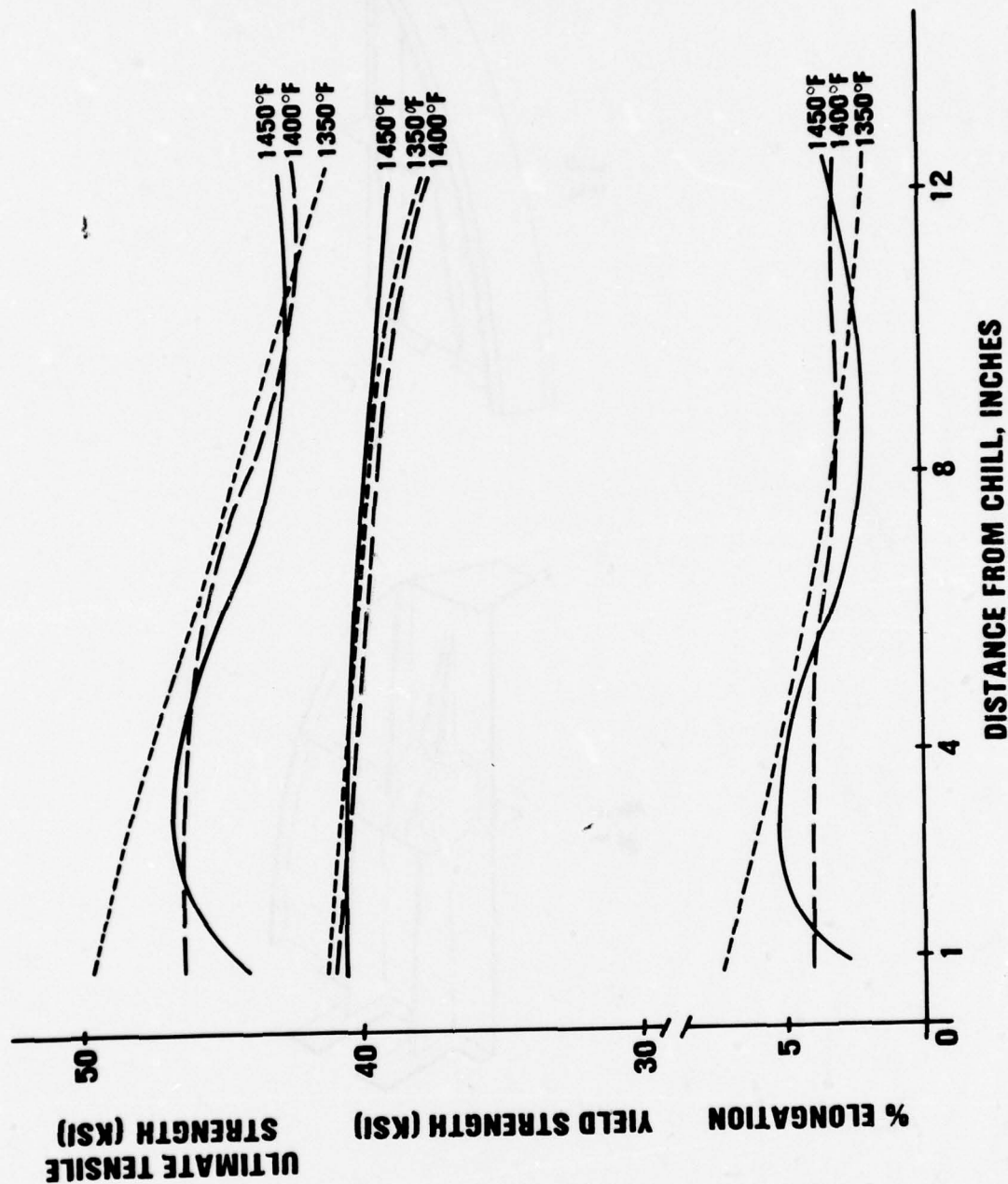


FIGURE 17 EFFECT OF POURING TEMPERATURE ON MECHANICAL PROPERTIES OF A357

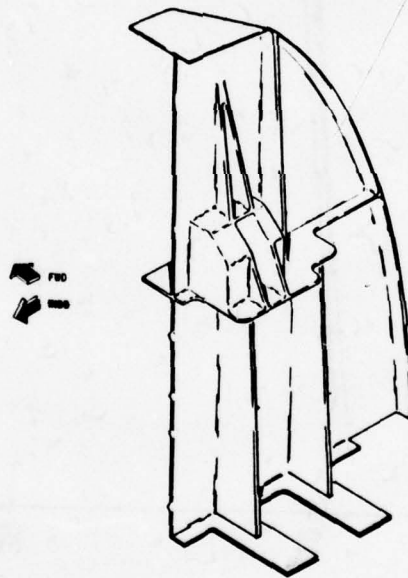
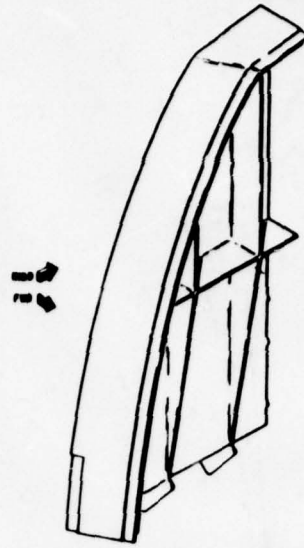


FIGURE 18 PART "A" TEST SECTION OF YC-14 STATION 170 BODY BULKHEAD

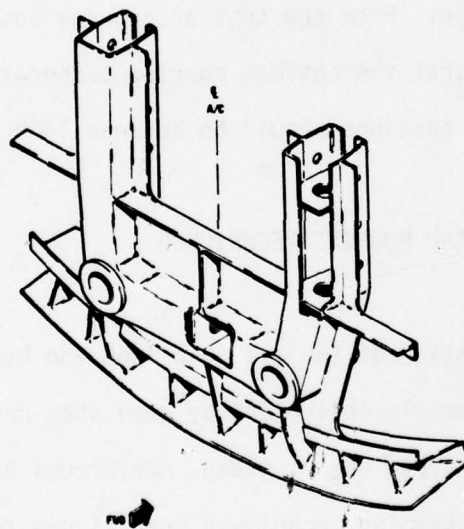
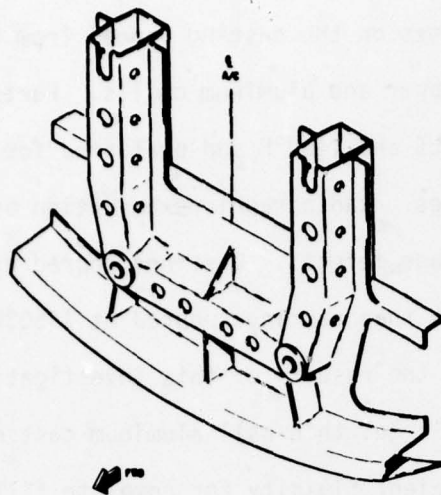


FIGURE 19 PART "B" TEST SECTION OF YC-14 STATION 170 BODY BULKHEAD

To determine the optimum pouring temperature for large, thin-wall aluminum castings, parts were cast of the configuration shown in Figure 18. Section thicknesses on the casting ranged from 0.100 to 1.500 inches and included both copper and aluminum chills. Parts were cast with A357 aluminum alloy at 1425 and 1450°F and evaluated for casting defects by radiographic techniques. Radiographic examination of test parts cast at 1450°F displayed shrinkage defects. Castings poured at 1425°F displayed fewer shrinkage defects than castings poured at 1450°F.

In summary, the results of this investigation show that the pouring temperature for large, thin-wall aluminum castings must be (1) high enough to provide sufficient fluidity for complete filling of the mold cavity and to avoid casting defects such as misruns, cold shuts, and shrinkage, and (2) low enough to minimize coarse grain structure, porosity, shrinkage, and oxide formation. From the test procedures described in this section, we can conclude that the optimum pouring temperature range for large, thin-wall aluminum castings should be between 1400 and 1450°F.

5. MELTING AND POURING TECHNIQUES

Contamination of the melt via iron and hydrogen pickup and oxide formation is generally controlled by good shop practices. Cleaning and preheating the charge, use of clean, nonferrous handling equipment, and proper stirring and skimming techniques are all considered standard foundry practice.

a. Material Control

Good shop practice begins with the control of materials to be used in the production of quality aluminum castings. Virgin materials should be stored under dry and clean conditions to minimize contamination by moisture or possible mixing of alloys. The latter item may be controlled by labeling each individual lot of material placed in storage. Areas in which virgin materials are stored should be separate from areas provided for remelted scrap storage, and records of the chemical composition for each lot of virgin or scrap should be maintained. Distinction between scrap and virgin lots should be maintained by labeling each lot of scrap with its respective heat number and alloy designation to maintain material traceability.

Preheating of a metal charge prior to melting is often necessary if the material has not been stored under dry conditions. Aluminum alloys are very susceptible to hydrogen contamination, and moisture on the material to be melted may result in contamination of the melt. If scrap material is to be remelted and cast, preheating of the scrap charge to 500°F for 2 to 4 hours should remove any oils or moisture present on the surface of the material. In general, preheating of the charge will shorten the amount of time required for melting in the furnace, and eliminate surface contaminants such as moisture or oils. Preheating operations were not evaluated in this investigation, due to lack of facilities.

b. Metal Handling

Use of clean, nonferrous handling equipment is essential in the melting of aluminum alloys to avoid contamination by iron, oxides, and hydrogen. If steel or iron tools are used to control the melt or contact the molten charge in any way, they must be coated with a protective material to insulate the melt from contamination. The protective coating used on ferrous equipment in this investigation is a water-based graphite solution. The coating was applied either by dipping or by brushing the solution onto the tool and then baking the coated tool at about 1700°F for 30 minutes (minimum). This baking operation removes moisture present on the tool, leaving the graphite coating. Direct contact of steel or iron handling equipment with the melt should be avoided in melting and pouring operations. Whenever possible, nonferrous equipment (such as graphite) should be used.

Oxides and slag, which tend to float to the top of the furnace charge or pouring ladle, are removed by skimming. The removal of impurities from the melt surface is mandatory, since they may cause inclusion, dross, or slag defects in the casting. Skimming operations were performed in this investigation with a graphite block suspended on a steel shaft. The graphite was located on the shaft so as to avoid contact between the steel shaft and the molten aluminum.

c. Process Controls

Prior to tapping the molten charge from the furnaces, the pouring ladles should be thoroughly cleaned and preheated. If metal ladles with refractory linings are used, the lining should be inspected and kept in

good repair. In addition to cleaning, the ladles should receive a coating of graphite wash to avoid contamination of the melt by ladle materials or refractories. The ladles should be preheated to a temperature above that at which the metal is to be poured and positioned so that easy travel between the ladles and the furnace is permitted. In this investigation, silicon carbide ladles were used to transport the molten metal. These ladles were coated with graphite wash and preheated to about 1700°F for about 2 hours prior to furnace tapping.

When the molten charge has been degassed, chemically balanced, and skimmed, the melt is transferred to the pouring ladle. This is accomplished by placing the preheated ladle approximately 4 inches below the pouring lip of the furnace and adjusting the angle of the ladle to match that of the metal flow. The angle of the metal flow into the pouring ladle is adjusted to minimize the turbulence of the molten metal as it fills the ladle. Dross or slag that forms on the surface of the metal in the ladle is removed by skimming.

Proper control of metal temperature in the furnace and in the pouring ladle is essential in the production of sound aluminum castings. Means of controlling the temperature of the melt was discussed in preceding sections. Typically, the temperature of the molten aluminum is controlled by taking frequent measurements of the melt temperature with an immersion-type pyrometer. When the pyrometer indicates that the pouring temperature has cooled from the furnace tapping temperature to the pouring temperature, the ladle is moved to the mold pouring basin.

d. Pouring Techniques

The mold pouring basin is described as being a cavity on top of the cope section of the mold into which metal is poured before it enters the sprue. The design of the pouring basin may range from a tapered, cone-shaped cavity located directly over the sprue to an offset basin with a dam or elevation between it and the sprue. Each pouring basin design offers distinct advantages. A tapered, cone-shaped pouring basin is easy to construct and is satisfactory for molds requiring relatively small amounts of metal. A dam-type pouring basin is preferred for molds that require large amounts of metal and is efficient in separating any slag that enters the pouring basin from entering the sprue. With any type of pouring basin, the most important factor is to keep the basin full of metal so that the slag or dross on the surface of the metal will not enter the sprue and contaminate the casting. The size of the pouring basin is typically regulated by the size of the sprue it must feed. In cases where the metal flows into the sprue faster than the pouring basin can fill, measures can be taken to restrict the flow into the sprue until filling of the basin is complete. A typical method of stopping off the flow into the sprue is by using a graphite or bonded sand plug at the sprue opening. When the level of the metal in the pouring basin has reached the desired height, the plug is removed and the metal is allowed to enter the sprue. The pouring of molten metal into the basin continues until the mold cavity and risers are full and then the pouring ladle is removed. During the transfer of metal from the ladle to the pouring basin, it is important that the height between the two be kept to a minimum to minimize turbulence.

e. Screening

Oxides, slag, dirt, or dross that enter the mold gating system may be kept from entering the mold cavity by using strainer screens at ingate and riser openings. Screening and filtering techniques were evaluated on parts cast in the configuration of Figures 18 and 19. Screening materials that were evaluated include perforated tin-plated steel, fiberglass cloth, and steel wool. Iron contamination of the molten aluminum by steel wool screening material is not considered to be a problem since (1) the mass of the steel wool with respect to the mass of molten aluminum is negligible, and (2) the steel wool is in contact with the molten aluminum for a short time. The tin-plated steel screens and the fiberglass cloth screens were positioned at the entrance of the mold runner and the steel wool was located in the pouring well. The positioning of the screens and the steel wool is depicted in Figure 7. The design of the screens was such that 50% of the metal flow was restricted. Parts were cast with and without screens and steel wool in the gating system and were inspected by radiographic techniques.

Inspection of the cast parts disclosed a reduction in oxide, slag, dirt, and dross inclusions in the molds using screens and steel wool. No significant difference was noted between the filtering effects of tin-plated steel screen and fiberglass cloth. However, due to the cost of material and ease of fabrication, the fiberglass cloth screens are preferred.

The effect of screening the molten metal prior to entering the mold cavity was also evaluated. Mechanical property specimens were made from the parts cast of the configurations shown in Figure 8 with various screening materials. However, because of shrinkage defects in the castings due to a large riser-to-chill distance, accurate mechanical property data could not be obtained.

f. Summary

In summary, we can conclude from this investigation that good melting and pouring techniques must include (1) good material control and storage procedures, (2) use of handling and skimming equipment that will not contaminate the melt, (3) proper control of metal temperature in the furnace and pouring ladle, (4) good pouring basin design to permit only clean metal to enter the sprue and mold gating system, (5) good pouring techniques, and (6) the use of screens and/or filters in the gating system to minimize dross or slag defects in the casting.

6. DEGASSING

Hydrogen dissolution and oxide formation in molten aluminum alloys can cause degradation of mechanical properties of the casting. As shown in Figure 20, temperature exerts a profound effect on the solubility of hydrogen in aluminum. When the melt cools to the melting point, a rapid decrease in solubility occurs that subsequently will cause porosity defects in the casting. It is therefore essential to have low hydrogen content metal before pouring to avoid an undesirable high casting rejection rate. Some foundries, however, deliberately leave some hydrogen in the metal to disperse shrinkage in the castings. This is not recommended because the best remedy for a shrinkage problem is a properly designed gating and risering system.

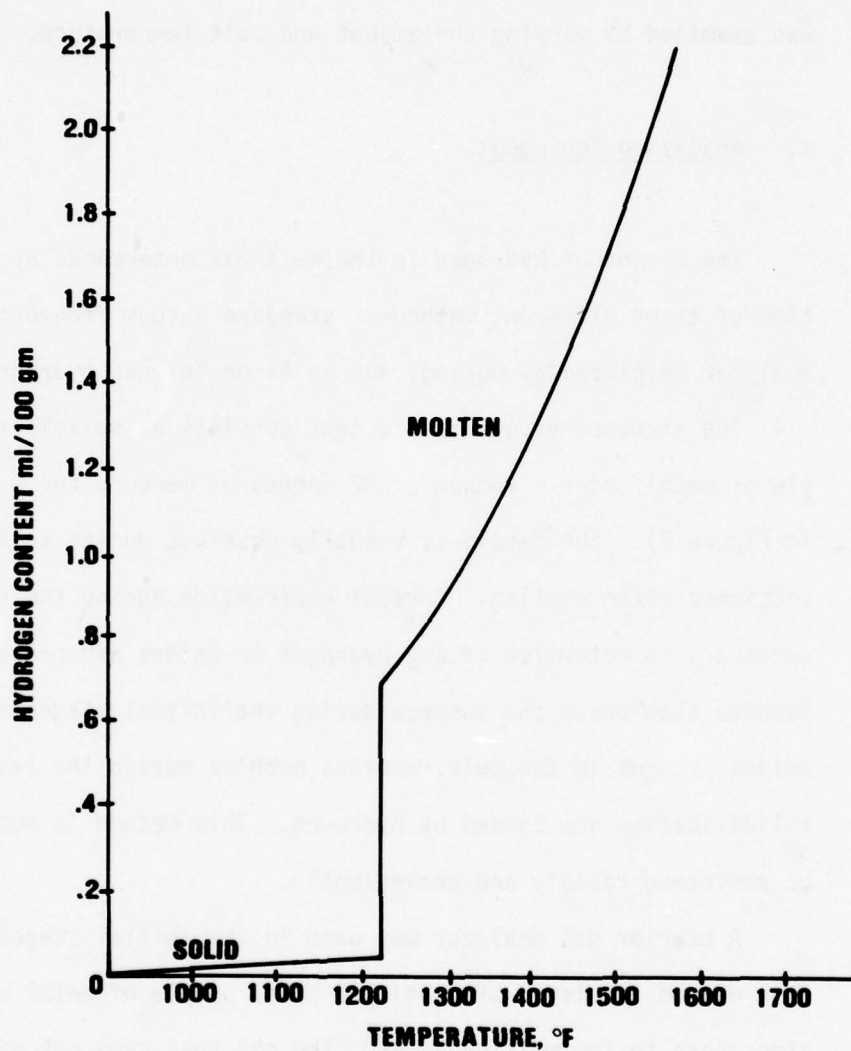


FIGURE 20 SOLUBILITY OF HYDROGEN IN ALUMINUM AT ONE ATMOSPHERE HYDROGEN PRESSURE

In this evaluation, three different degassing media, including nitrogen gas, 95% nitrogen/5% chlorine gas mixture, and solid hexachloroethane tablets (C_2Cl_6), were evaluated for their ability to remove hydrogen and oxides from molten aluminum. The gaseous media were examined by varying the flow rate, flow time, and melt temperature. The solid hexachloroethane was examined by varying the amount and melt temperature.

a. Analyzing Equipment

The amount of hydrogen in the melt was determined by one or a combination of three different methods: standard vacuum freeze test, carrier gas analyzer developed by Boeing, and an Alcoa Telegas hydrogen analyzer.

The standard vacuum freeze test consists of solidifying a molten sample of metal under a vacuum of 27 inches of mercury for 7 minutes as shown in Figure 21. The sample is visually observed during solidification and is sectioned after cooling. Careful observation during the solidification is necessary to determine if any hydrogen or oxides are present in the melt. Bubbles that break the surface during the initial stages are a result of oxides present in the melt, whereas bubbles during the latter stage of solidification are caused by hydrogen. This method is economical and can be performed rapidly and conveniently.

A carrier gas analyzer was used in the initial stages of the program. This method consisted of heating a solid sample of metal under an argon atmosphere to the melting point. The gas that came out of solution was then quantitatively analyzed. Due to its low sensitivity to dispersed hydrogen (1.0 ml/100 gm of aluminum), this method was determined to be inadequate for examining high-quality casting metal.

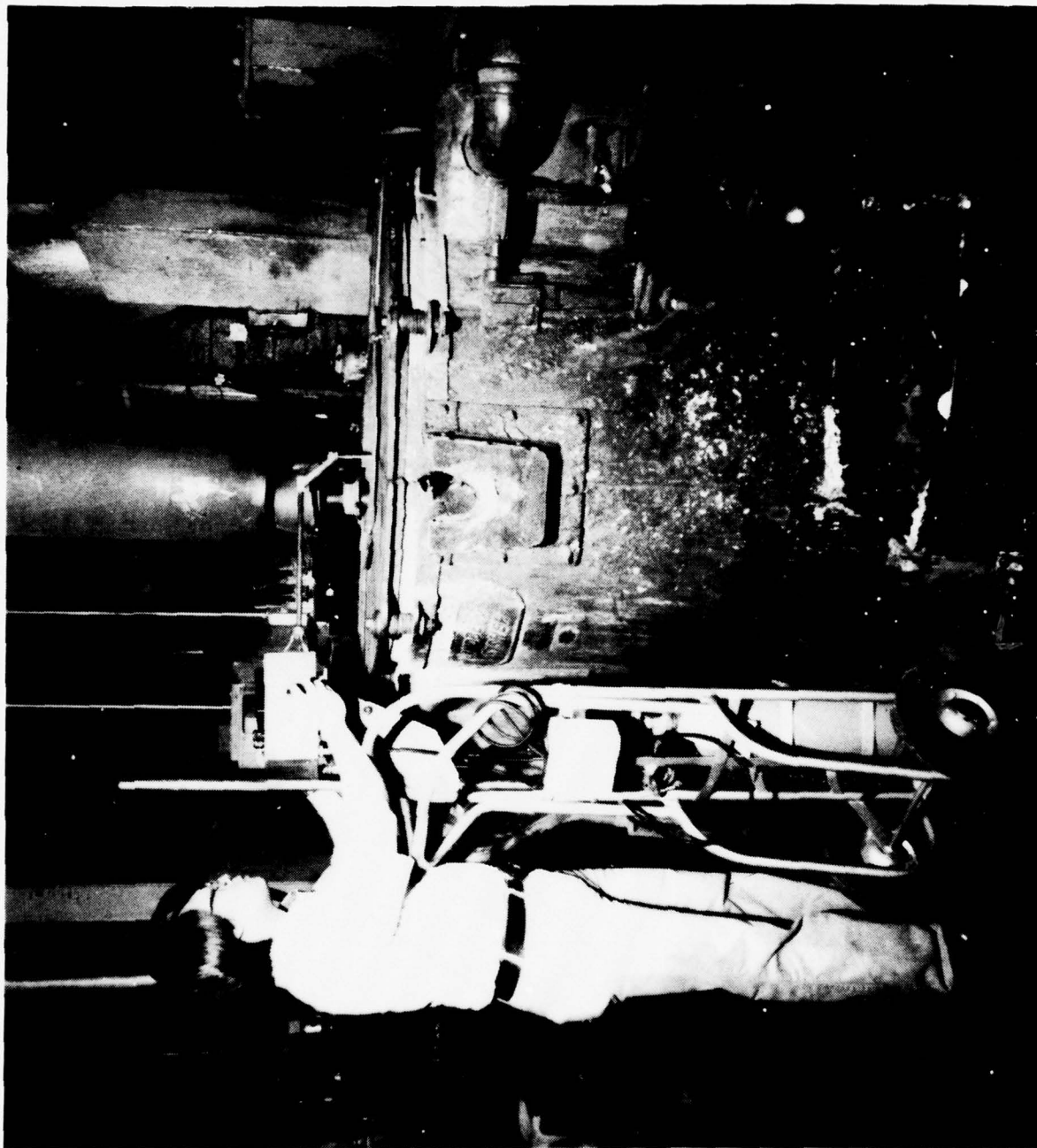


FIGURE 21 OBSERVING THE SOLIDIFICATION OF A VACUUM FREEZE GAS SAMPLE
FOR EVIDENCE OF HYDROGEN IN THE MELT

The third method, which employed the Alcoa Telegas hydrogen analyzer, proved to be very sensitive to foundry conditions. The operation of this equipment is illustrated in Figure 22. As described by the manufacturer, this analyzer consists of a millivolt meter, a 12-volt power supply, a cylinder of high-purity nitrogen, and a special probe. The principle behind the operation of this equipment is as follows.

The amount of dissolved hydrogen present in a melt at a known temperature can be determined by creating a free surface with the use of nitrogen. The equilibrium pressure of the hydrogen that collects at the free surface of the nitrogen can be measured. The amount of hydrogen in the melt is expressed as a millivolt reading. The actual amount, in milliliters/100 grams of aluminum, is found from the chart shown in Figure 23. This chart is based on pure aluminum only, since the partial pressure of gas in a melt is a function of the solubility of hydrogen, which varies with alloy. It is therefore necessary to apply a correction factor. The correction factor for A375 is 0.83, which is the ratio of the hydrogen solubility in A357 to that of pure aluminum.

Due to the sensitive nature of this instrument, frequent maintenance checks and calibration exercises are essential to ensure accurate results. If care is taken, this instrument provides useful quantitative data not otherwise obtainable. However, due to the inherent conditions in most foundries, it is our experience that equipment such as the Telegas hydrogen analyzer will not stand up in a production environment. However, we feel that the analyzer is useful as laboratory equipment.



**FIGURE 22 MEASUREMENT OF THE HYDROGEN CONTENT OF A MELT WITH
AN ALCOA HYDROGEN TELEGAAS ANALYZER**

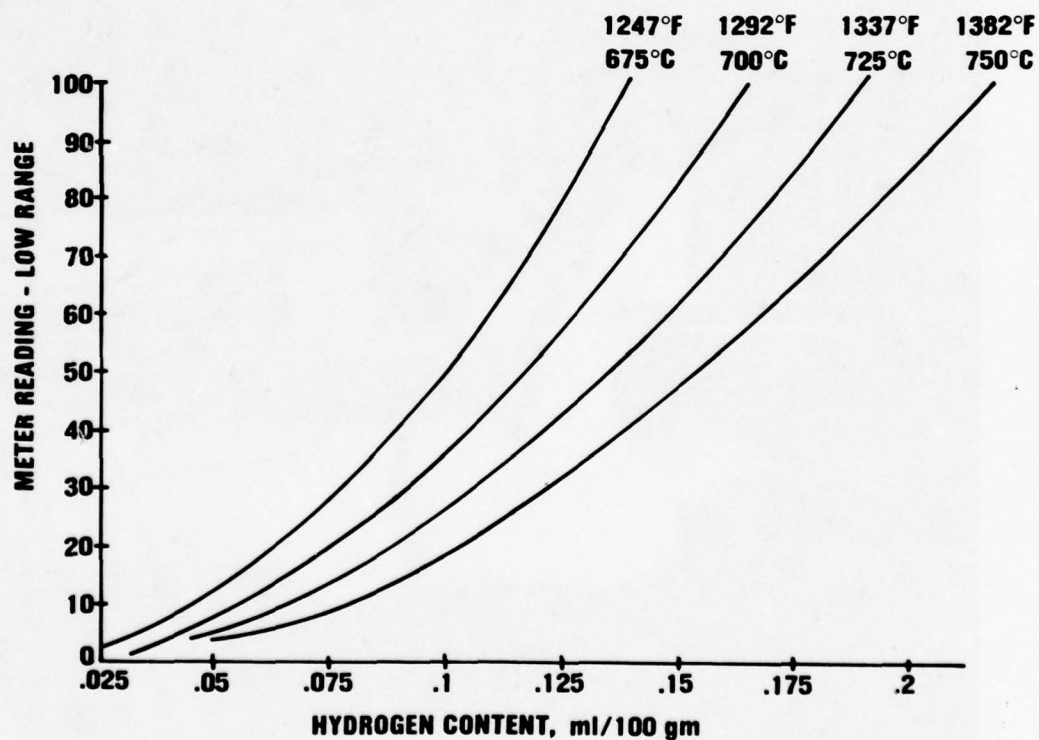
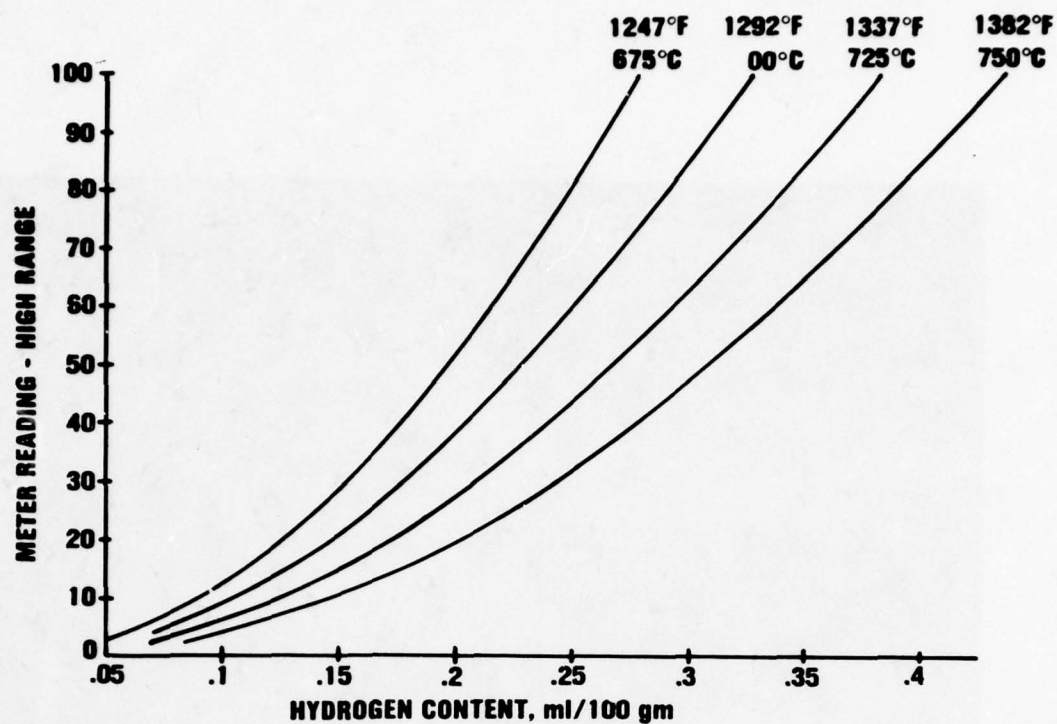


FIGURE 23 CALIBRATION CHART OF PURE ALUMINUM FOR TELE GAS HYDROGEN DETERMINATION EQUIPMENT

b. Degassing Media

Nitrogen gas, a commonly used degassing medium, was evaluated for its ability to remove hydrogen from the melt. Nitrogen, being relatively inert, acts only as a mechanical degassing agent. Nitrogen bubbles coming up through the melt bring with them hydrogen and oxides. These are removed from the surface by skimming.

The effect of nitrogen on the removal of hydrogen from A357 was examined by varying the flow rate, flow time, and melt temperature. The method of determining the hydrogen level was the standard vacuum freeze test, which implies that the results are quantitative.

In all degassing tests, except those noted, the gaseous media were introduced into the melt with a graphite degassing lance. This was a 2-inch O.D. graphite tube, with one end plugged. Several 1/16-inch holes were drilled at the plugged end to allow the gas to escape into the melt.

Tests were conducted varying the flow rate of nitrogen from 10 cfh to 30 cfh. The 10 cfh was equivalent to a gentle rolling action of the melt surface, and 30 cfh corresponded to a turbulent action of the melt surface. The results show that degassing at 1250°F and 10 cfh decreased the amount of bubbles and porosity in the vacuum gas samples, whereas at 30 cfh the amount of gas porosity increased. Since the actual flow rate depends on the degassing temperature and quantity of melt being degassed, it is not practical to specify an optimum flow rate. A general rule that should be followed is to maintain the flow of gas so that a gentle rolling action is observed at the melt surface. If the melt is violently agitated, the exposed metal surface will form oxides and hydrogen gas will go into solution.

The effect of nitrogen degassing temperatures was evaluated at 1200, 1250, 1300, and 1350°F with a flow rate of 10 cfh. Again, the relative hydrogen content was determined by the standard vacuum gas technique. The results indicate that degassing between 1250 and 1300°F was most effective. Representative test results from degassing at 1300°F are shown in Figure 24. These results were obtained with the Telegas hydrogen analyzer.

Spectrographic analysis was conducted on samples removed from the melt at the same time as the gas samples. Typical results are shown in Figure 25. There did not appear to be any appreciable variation in alloy content when degassing with nitrogen. The reason for the variation in beryllium content was attributed to the experimental error in the spectrographic analyzer.

The effect of a NaCl/KCl overflux was evaluated for the prevention of hydrogen absorption into the melt and the removal of oxides from the melt. This evaluation was conducted with a nitrogen degassing medium. The cover flux melts at 1280°F, so it was necessary to degas at 1300-1325°F. A 0.25-inch layer of flux was placed on the melt surface. Initially, the hydrogen content increased due to the hygroscopic nature of the cover flux. Subsequent degassing removed the hydrogen, but the end result was the same as degassing without a cover flux. The cover flux was preheated in an attempt to drive off the hydrogen, prior to placing in the melt surface. The results were the same: the flux caused an initial increase in hydrogen content. The use of a cover flux was discontinued.

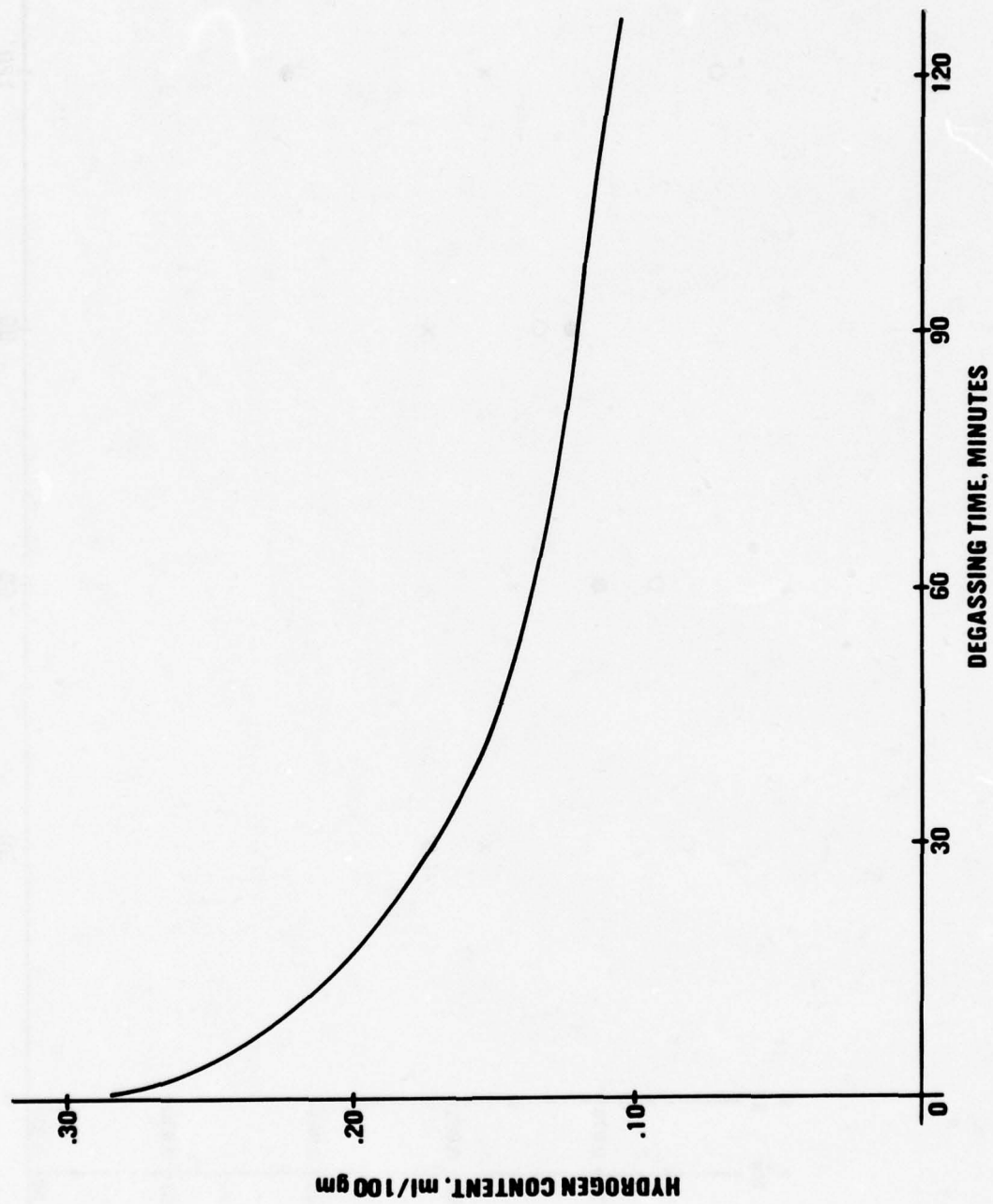


FIGURE 24 DECREASING RATE OF HYDROGEN CONTENT IN A357 AFTER DEGASSING WITH N₂ AT 1300°F

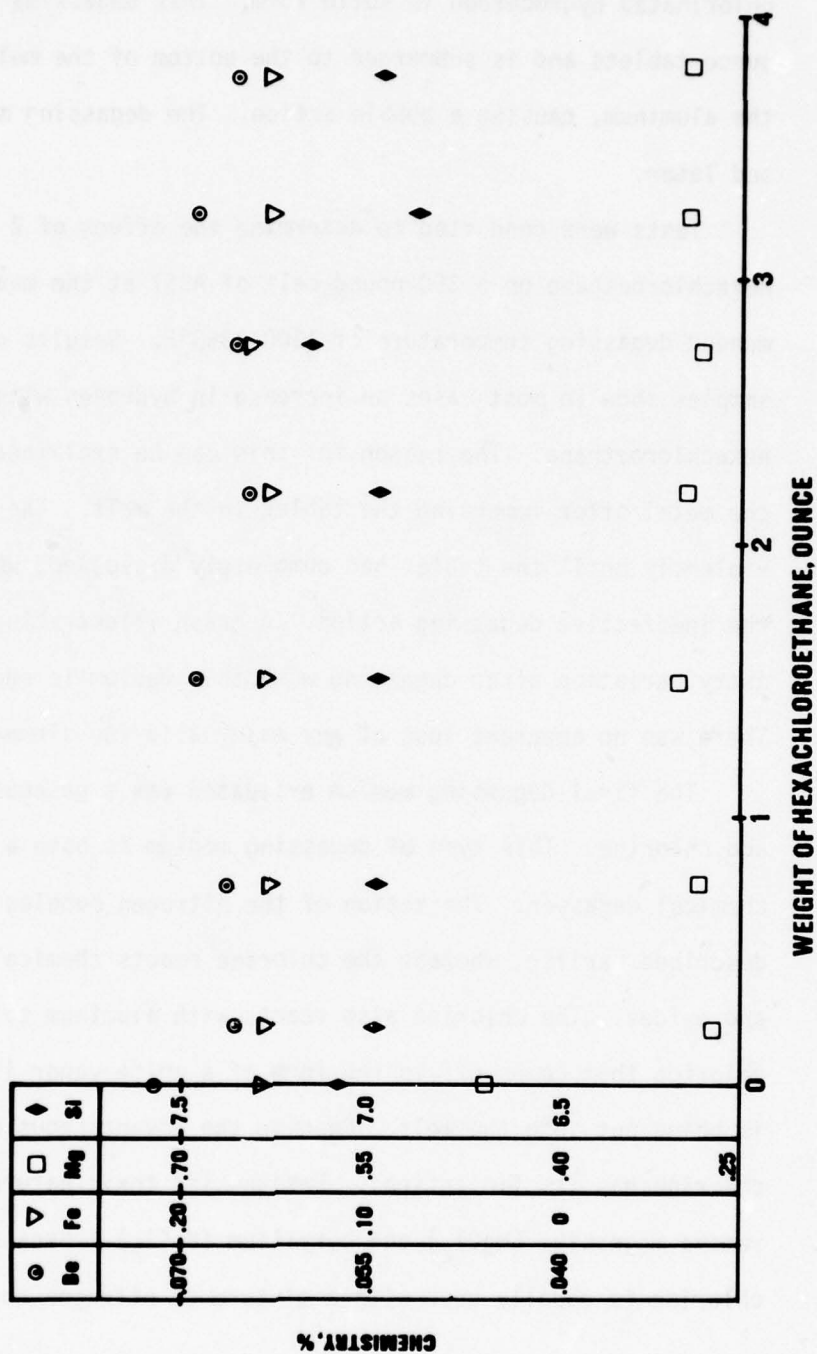


FIGURE 25 DEVIATION OF A357 ALLOY CHEMISTRY AFTER DEGASSING WITH N₂ AT 1300°F

The next degassing medium evaluated was hexachloroethane, which is a chlorinated hydrocarbon in solid form. This degassing agent comes in 4-ounce tablets and is submerged to the bottom of the melt. It reacts with the aluminum, causing a bubble action. The degassing mechanism is discussed later.

Tests were conducted to determine the effect of 2 and 4 ounces of hexachloroethane on a 350-pound melt of A357 at the manufacturer's recommended degassing temperature of 1300-1350°F. Results of the vacuum gas samples show in most cases an increase in hydrogen with either quantity of hexachloroethane. The reason for this can be explained by the action of the metal after immersing the tablet in the melt. The metal "boiled" violently until the tablet had completely dissolved, which contributed to the ineffective degassing action. A graph illustrating the effect of chemistry variation after degassing with this medium is shown in Figure 26. There was no apparent loss of any major alloying element.

The final degassing medium evaluated was a gaseous mixture of nitrogen and chlorine. This type of degassing medium is both a mechanical and a chemical degasser. The action of the nitrogen bubbles is the same as described earlier, whereas the chlorine reacts chemically with the hydrogen and oxides. The chlorine also reacts with aluminum to form an aluminum chloride that comes off in the form of a white vapor if too much chlorine is being put into the melt. Despite the advantageous chemical effect, chlorine has its limitations. Besides its toxic nature, it will chemically remove magnesium ($MgCl_2$) and beryllium ($BeCl_2$). Because of these reasons, chlorine is usually used with a mixture of nitrogen to reduce its toxicity.



**FIGURE 26 A357 ALLOY CHEMISTRY AFTER DEGASSING WITH HEXACHLOROETHANE
AT 1300 - 1350°F**

Degassing tests were conducted with a mixture of 95% nitrogen/10% chlorine at temperatures of 1250, 1300, and 1400°F. In each test, hydrogen was added to the melt in order to learn the relative effectiveness of the degassing medium. The melt was degassed at 30-minute intervals with a flow rate of 10 cfh. The amount of hydrogen was determined with the Telegas hydrogen analyzer. The results are shown in Figure 27. It is evident that a lower hydrogen content was obtained when degassing at 1300°F. When degassing at 1250°F, the hydrogen does not come out of the melt as readily, even though its solubility is lower relative to 1300°F. The reason is that the viscosity of the melt is much higher at reduced temperatures, which provides more resistance to the gas bubbles. On the other hand, degassing at a higher temperature introduces as much hydrogen as it removes because of the higher solubility of hydrogen in aluminum.

The results of the spectrographic chemical analysis of samples taken during the above degassing tests are shown in Figures 28-30. At degassing temperatures of 1250 and 1300°F, there was no apparent loss of major alloying constituents. When degassing at 1400°F, there was a loss of magnesium and beryllium. This trend for loss of magnesium and beryllium, as temperature increases, is a result of the increased reactivity of aluminum with increased temperature. The loss of chemistry during degassing can be predicted and a higher amount of magnesium and beryllium can be added to compensate for this alloy loss.

When degassing with chlorine in any form or mixture, it is very important to preheat all degassing tools (i.e., graphite lances, hoses, etc.) prior to immersing in the molten aluminum. It is speculated that chlorine at room temperature will form a hydride and when rapidly heated in the molten aluminum will dissociate into chlorine and water. From our experience, this can easily result in an explosion.

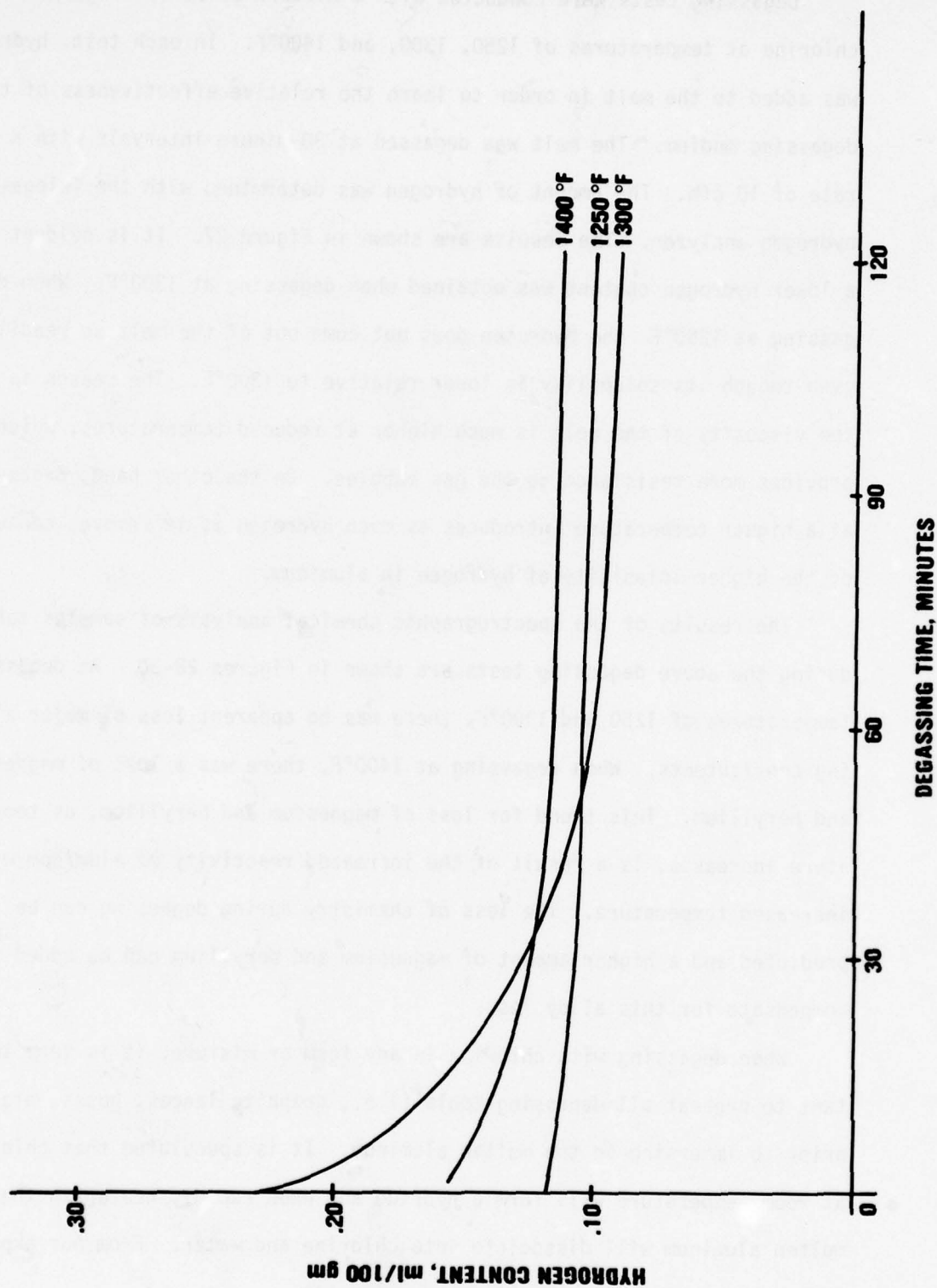


FIGURE 27 DECREASING RATE OF HYDROGEN CONTENT IN A357 AFTER DEGASSED WITH 95% N₂/5% Cl₂ AT VARIOUS TEMPERATURES

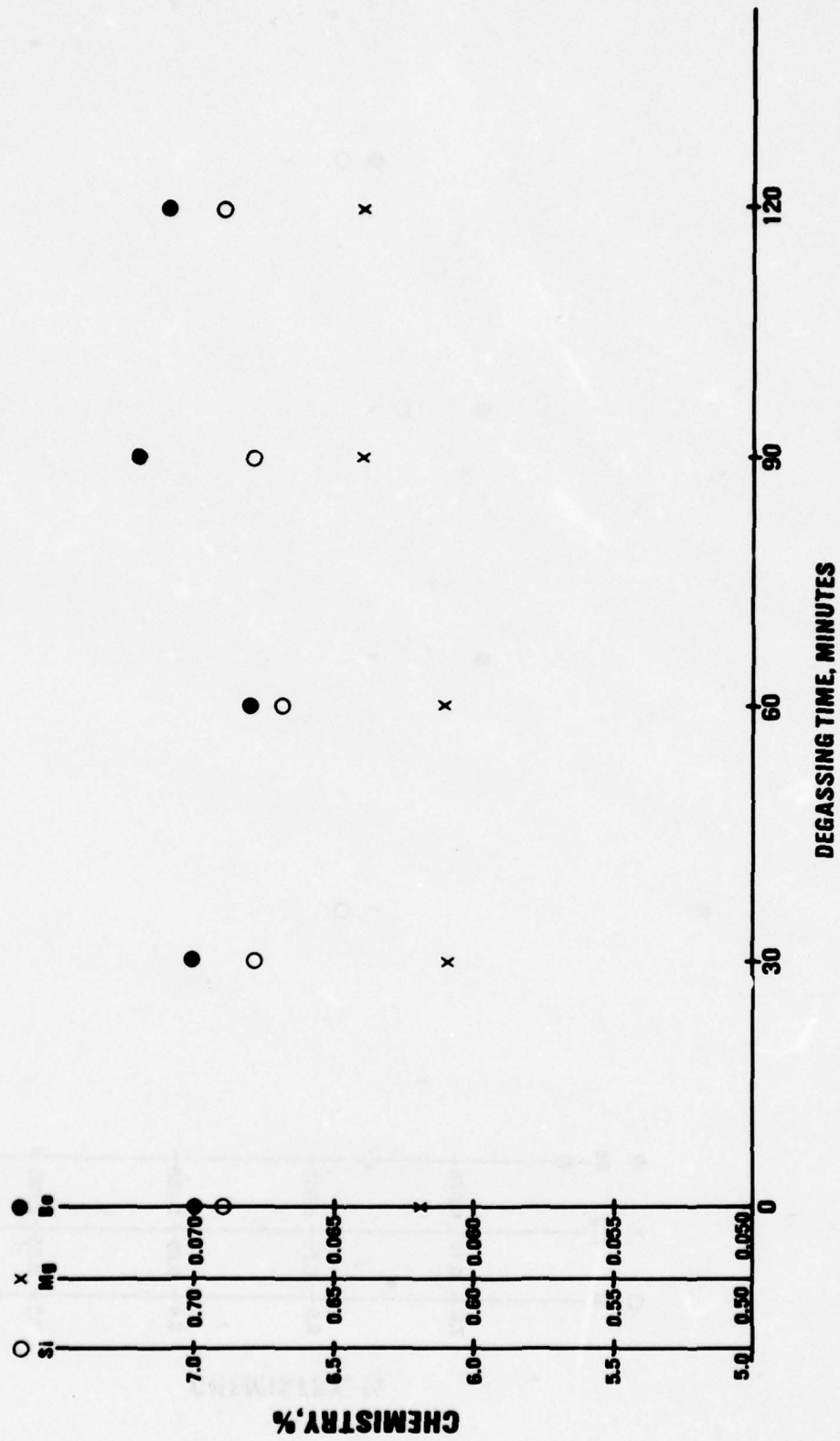


FIGURE 28 A357 ALLOY CHEMISTRY AFTER DEGASSING WITH 95% N₂/5% Cl₂ AT 1250°F

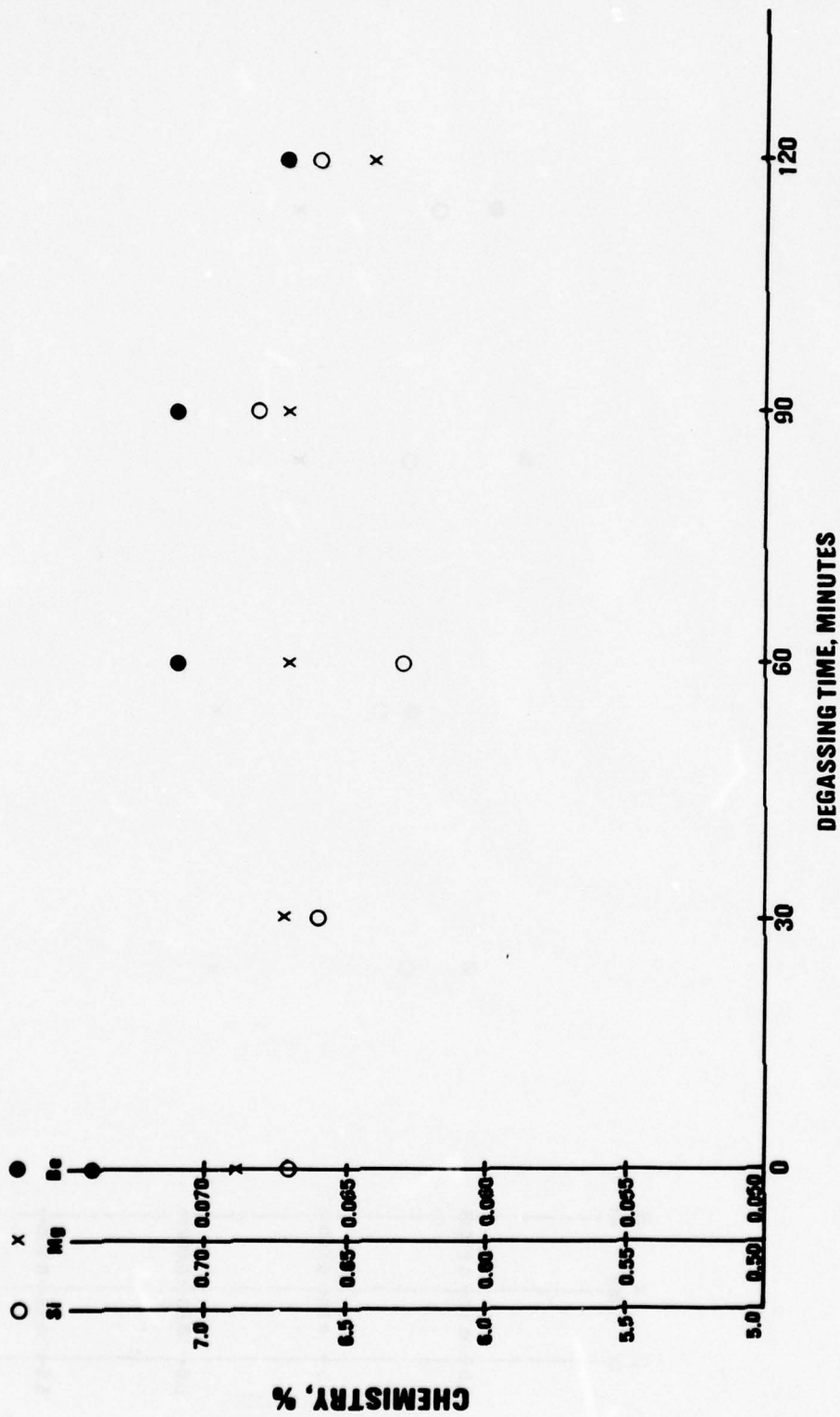


FIGURE 29 A357 ALLOY CHEMISTRY AFTER DEGASSING WITH 95% N₂ / 5% Cl₂ AT 1300°F

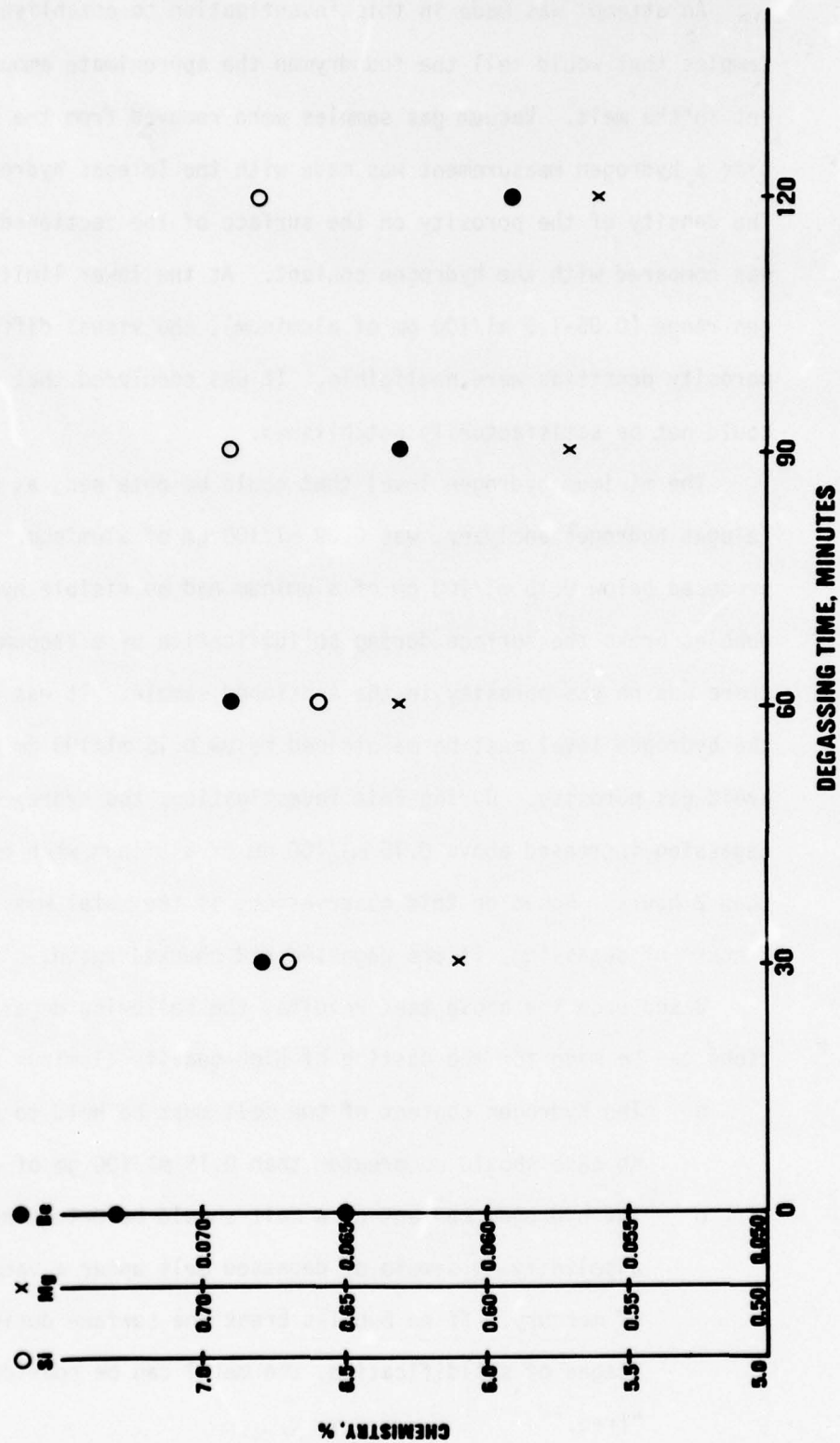


FIGURE 30 A357 ALLOY CHEMISTRY AFTER DEGASSING WITH 95% N₂ / 5% Cl₂ AT 1400°F

An attempt was made in this investigation to establish visual gas samples that would tell the foundryman the approximate amount of gas present in the melt. Vacuum gas samples were removed from the melt at the same time a hydrogen measurement was made with the Telegas hydrogen analyzer. The density of the porosity on the surface of the sectioned vacuum sample was compared with the hydrogen content. At the lower limits of the hydrogen range (0.05-1.5 ml/100 gm of aluminum), the visual differences between porosity densities were negligible. It was concluded that visual standards could not be satisfactorily established.

The minimum hydrogen level that could be obtained, as measured by the Telegas hydrogen analyzer, was 0.09 ml/100 gm of aluminum. However, samples produced below 0.15 ml/100 gm of aluminum had no visible hydrogen, i.e., no bubbles broke the surface during solidification of a vacuum gas sample and there was no gas porosity in the sectioned sample. It was concluded that the hydrogen level must be maintained below 0.15 ml/100 gm of aluminum to avoid gas porosity. During this investigation, the hydrogen content after degassing increased above 0.15 ml/100 gm of aluminum when held for more than 2 hours. Based on this observation, if the metal was not poured after 2 hours of degassing, it was degassed and checked again.

Based upon the above test results, the following degassing recommendations can be made for the casting of high-quality aluminum castings:

- o The hydrogen content of the melt must be held to a minimum and in no case should be greater than 0.15 ml/100 gm of aluminum.
- o The hydrogen content of a melt should be determined by observing a solidifying sample of degassed melt under a vacuum of 27 inches of mercury. If no bubbles break the surface during the latter stages of solidification, the metal can be considered hydrogen "free."

- o The maximum holding time between degassing and pouring should be 2 hours, after which the metal should be rechecked.
- o Of the gases analyzed, the optimum degassing conditions are a mixture of 90-95% nitrogen/5-10% chlorine at a melt temperature of 1300-1325°F. Degassing intervals should be at least 30 minutes apart.
- o A holding time of 15-20 minutes between degassing and taking a vacuum gas sample should be observed to be assured of an accurate determination.

7. GRAIN REFINING AND MODIFICATION

To achieve good mechanical properties in a casting, close control of the grain size and shape of the silicon constituents must be exercised. This is accomplished with the use of grain refiners, grain modifiers, and controlled solidification of the casting.

Grain size control of A357 castings is accomplished by the addition of titanium, a grain growth inhibitor, which is an alloying constituent of A357. Replenishment of the melt with titanium was done with an Al-5Ti-1Be master alloy. The effects of titanium on the resultant mechanical and metallurgical properties of A357 were not evaluated because, as shown in Table I, it is an element of A357 and its range is limited.

Modification of the silicon particles is necessary to achieve good mechanical strength and ductility. The two grain modifiers investigated were sodium and strontium. Sodium is the most commonly used modifier; however, recent literature indicates that strontium is as effective a modifier as sodium, but with some distinct advantages. The loss of strontium,

in molten aluminum, is much less than with sodium. The reactivity of sodium at molten aluminum temperatures is very high and will burn off when in contact with oxygen. Strontium, however, is a relatively stable element with a minimum loss on addition and subsequent melting. Another reported advantage of strontium is its ability to modify the iron-rich intermetallic compounds, which should reduce the detrimental effect iron has on the properties of A357.

The test procedure used for the evaluation of sodium grain modification involved the addition of pure sodium (0.02-0.05%), vacuum sealed in aluminum bags, into a 350-pound melt of A357. The sodium was submerged in the melt to prevent contact with oxygen. When the sodium came in contact with the molten metal, a reaction occurred, causing the molten aluminum to bubble. This resulted in an increase in the hydrogen gas content of the melt. Subsequent degassing removed the hydrogen gas. Atomic absorption analysis of the melt indicated that the sodium content had dropped from 0.043 to 0.003%, well below the range required for sodium modification. Additional tests yielded the same results: sodium modification introduced hydrogen into the melt. Degassing removed both the hydrogen and sodium.

The more stable strontium modifier was evaluated in a similar manner. Strontium in the form of an Al-15Si-10Sr master alloy was added to a 350-pound melt of A357 in a gas-fired crucible. The amount of strontium required for modification was 0.010%. There did not appear to be any reaction with the melt, but as with sodium, the hydrogen content of the melt increased with the addition of strontium. Degassing with a mixture of nitrogen/chlorine removed both the gas and strontium. Several approaches were taken to determine the cause for the increase in gas with the addition

of strontium. It was first thought that surface moisture on the strontium ingot may be a source of hydrogen. Preheated strontium ingot was added to several melts of A357. In most cases, the hydrogen content increased. The next approach was related to the quality of the master alloy. Metallurgical examination of the master ingot revealed a large amount of gas porosity. The ingot was melted under an argon atmosphere and solidified in a water-cooled copper mold to drive out any hydrogen. The strontium remelt was added to several melts of A357 with the same results as before.

After degassing the strontium-modified melt with nitrogen/chlorine, the slag on the surface of the melt was analyzed and showed a high concentration of strontium, whereas the strontium content of the melt was depleted. It appeared from these tests that the hygroscopic nature of strontium caused it to act as a hydrogen getter when added to the melt, forming a strontium hydride. This increased the hydrogen content. When degassed with nitrogen/chlorine, the chlorine reacted with the strontium hydride, thereby removing both the hydrogen and strontium. However, this does not mean that strontium does not make a good modifier. Some foundries have successfully developed techniques for strontium modification.

Test specimens for mechanical property evaluation of the modified material were tested. However, no conclusions could be made because of the excessive hydrogen content of the material.

Considering the problems experienced with sodium and strontium modification, the decision was made to use unmodified A357. When casting thin sections and heavily chilled sections, the solidification rate is fast enough that the silicon constituents showed good modification without the use of grain modifiers as illustrated in Figure 1.

SECTION IV

MOLD AND CORE MAKING

Boeing's experience in making molds for large, high-strength aluminum castings dictates that to consistently maintain close dimensional tolerances, sound castings, and good surface finishes, it is necessary to use a dry (moisture free), chemically bonded sand. In addition, close control over the design and fabrication of molds for large castings is essential if the aforementioned characteristics are to be achieved. Since all molding variables are interdependent, an extensive testing program was conducted. Variables that were investigated in this program include the effects of sand types and sizes, binder types, mixing times, and storage times and temperatures on the mechanical and physical properties of molding sand. AFS standard tensile and compression specimens were used in this investigation.

1. SAND TYPES

The sand types and sizes that were evaluated in this investigation were AFS numbers 70 and 53 silica sand, and AFS number 120 olivine sand. These sands were selected for evaluation because they are the most commonly used sands in the aluminum casting industry. Silica sands with AFS numbers greater than 70 were given a summary evaluation and considered to be too fine for the subject casting applications.

Silica sand grains may be round, angular, subangular, or compound. Olivine sand grains are typically angular in shape. Round sand grains are described as being fully spherical; angular sand grains are split particles with sharp edges and corners; subangular grains are a combination of round

and angular grains having somewhat rounded corners; and compound grains consist of two or more grains joined in such a way that binder removal or sieve analysis will not break them apart. Typically, angular grains will not compact or accept binder coating as readily as round grains. Angular grains have a greater amount of surface area in comparison to round grains and require more binder for complete coating of the grains. Also, due to the irregularity of angular grain surfaces, they will not compact as uniformly as round grains. As a result, compaction of angular grains provides high permeability values but less flowability (free movement of the sand during molding) and lower quality cast surface finish than is obtained with round grains. Based on this evaluation, silica sands having spherical (round) grains were chosen for use in this investigation.

The effects of sand type on mold properties are shown in Figures 31-33. These figures display the results of testing AFS 70 silica sand and AFS 120 olivine sand to determine sand tensile strength, compressive strength, and permeability after specified storage times. Delta 475-X Ester Set with Delta 217-6X co-reactant (synthetic resin binder) was chosen to bond the sand test specimens. The selection of binders to be used with olivine sand was based on vendor literature. According to the reviewed literature, the synthetic resin binder would provide the base bonding characteristics of the binders under evaluation. Due to the high acid demand of olivine, few binders are compatible. The binder quantity in the sands was 1.5% for the silica sand and 2.0% for the olivine sand.

Results of tests conducted on specimens made under the described conditions showed significantly higher strength and permeability values for specimens made with AFS 70 silica sand than with AFS 120 olivine sand. Although the olivine sand is composed of angular grains and would normally express higher permeability values than the round silica grains, the lower

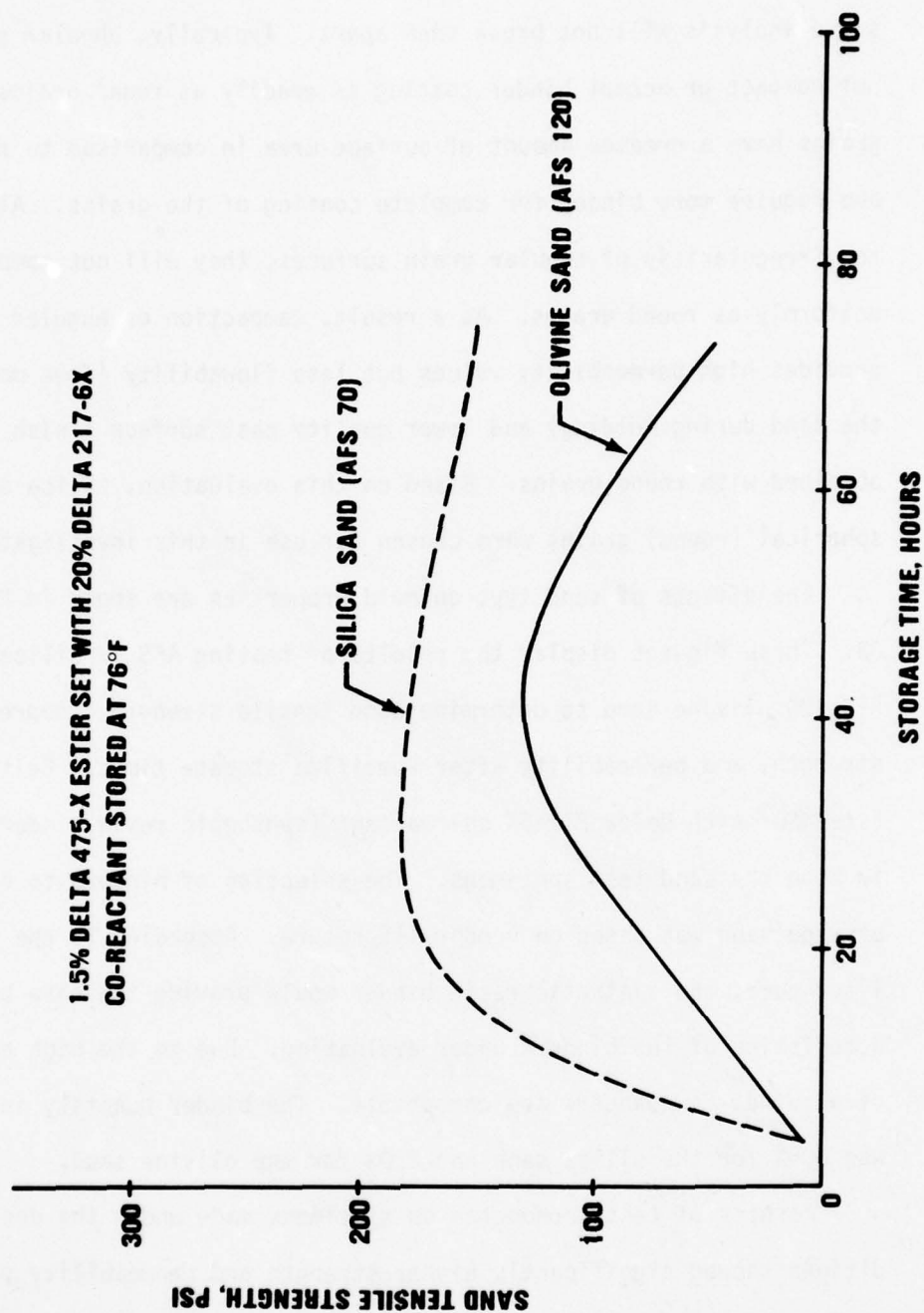


FIGURE 31 EFFECT OF STORAGE TIME ON MOLD TENSILE STRENGTH OF VARIOUS SAND TYPES
WITH SYNTHETIC RESIN BINDER STORED AT ROOM TEMPERATURE

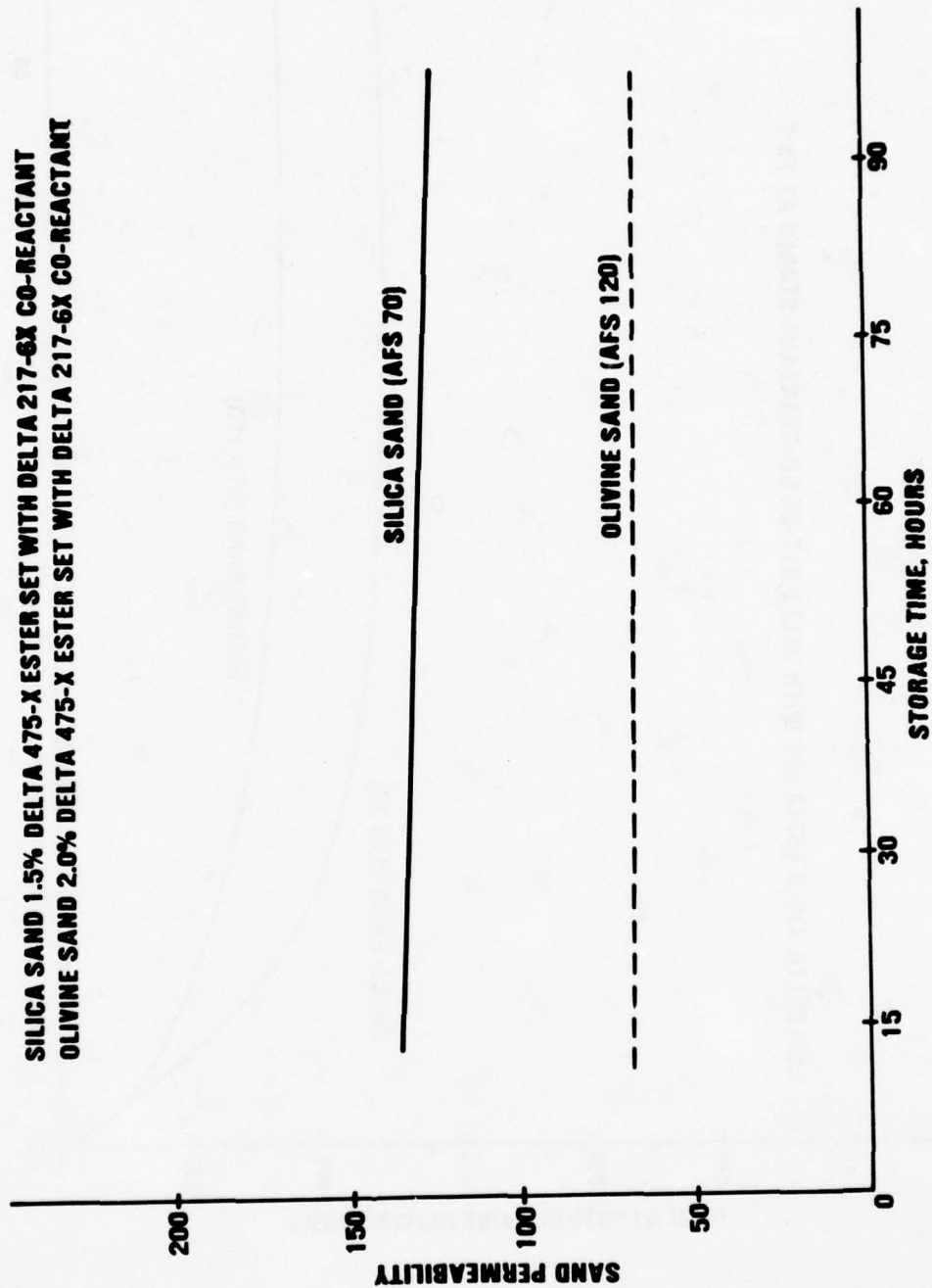
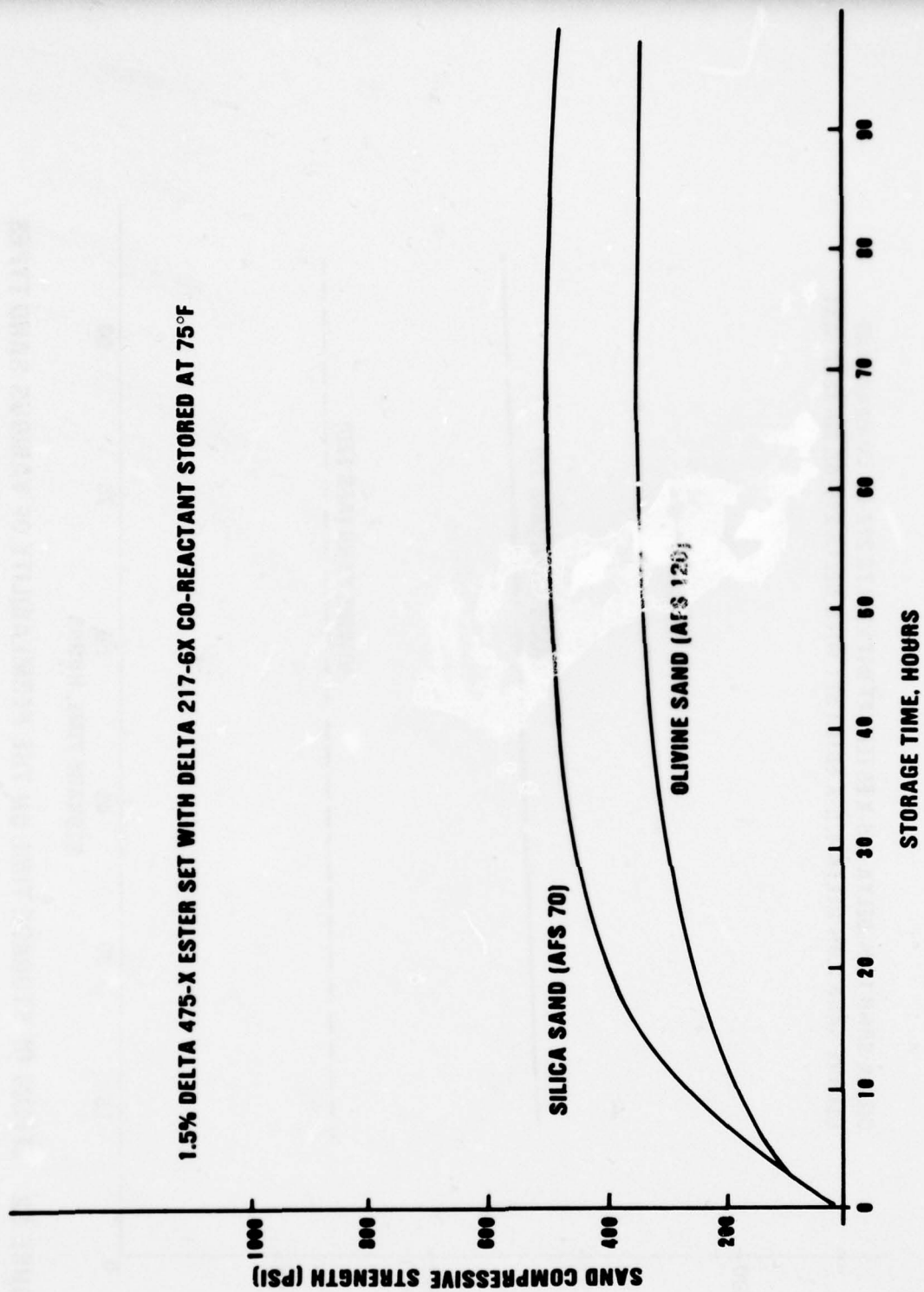


FIGURE 32 EFFECT OF STORAGE TIME ON THE PERMEABILITY OF VARIOUS SAND TYPES



**FIGURE 33 EFFECT OF STORAGE TIME ON MOLD COMPRESSIVE STRENGTH OF VARIOUS SAND TYPES
WITH SYNTHETIC RESIN BINDER STORED AT ROOM TEMPERATURE**

values displayed in these tests are attributed to the finer grain size of the olivine. The AFS 70 grains represent a greater proportion of large sand grains and larger voids between the grains than found with the AFS 120 grains. The presence of the larger voids between the grains in AFS 70 permits the passage of gas through the sand more readily than with AFS 120 sand.

2. BINDER TYPES AND PROPERTIES

In addition to the synthetic resin binder discussed in the preceding paragraphs, tests were also conducted with silica sand using (1) sodium silicate cured with CO_2 , (2) sodium silicate no-bake, and (3) oil-urethane no-bake systems. These binders were chosen for evaluation because they represent the spectrum of binder types currently in use in the aluminum casting industry. Cold box processes that involve the coating of sand with a phenolic resin and a urethane polymer and curing with a vaporized amine were not evaluated due to the facility requirements for using amine gases.

The Delta 475-X Ester Set binder noted in the preceding paragraphs is a synthetic resin binder that forms an insoluble polymer when reacted with polyisocyanate (Delta 217-6X). This type of binder system is relatively insensitive to sand chemistry, with respect to acid-catalyzed resins (phenolic resins, urea formaldehyde resins), and is compatible with silica, zircon, chromate, and olivine sands. Sands bonded with synthetic resin may be mixed in either conventional or continuous mixers. Although sand mixes using this type of binder are generally flowable, some form of compaction is usually necessary, as with most no-bake binder systems. The work time of sand bonded with synthetic resin is approximately one-half the strip time. The work and strip time for the Delta synthetic resin binders is

incorporated into the resin by the manufacturer. This is accomplished by adding specified quantities of catalyst to the resin to obtain a desired work and strip time. The synthetic resin (Delta 475-X) used in this investigation had a work time of 40 minutes and a strip time of 75 minutes. This particular combination of resin and catalyst was chosen because long work times are required when molding large complex castings.

Steinex "Super C" sodium silicate was used to evaluate sodium silicate- CO_2 bonded sand. This type of sand is made by mixing silica sand with sodium silicate and hardening the mixture by gassing it with carbon dioxide for a specified amount of time. When carbon dioxide is passed through the mixed sand under designated pressure, the sodium silicate binder thickens to such a degree that the sand grains are bound together, making the sand mass rigid. This results from the chemical reaction between the sodium silicate binder and the CO_2 gas which forms sodium carbonate and silica. Since both sodium carbonate and silica are solids, a part of the liquid binder is converted to a solid material that stiffens the binder and provides strength to the sand. Sodium silicate binder has a relatively low acid content (low pH) and will not bond with olivine sands due to its high acid demand. For this reason, olivine sand was not evaluated with the chemically basic sodium silicate binder.

Delta 241-7X with Delta 192-7X co-reactant was used to evaluate sodium silicate no-bake binders. Sodium silicate no-bake binder systems are basically sodium silicate binders that are catalyzed with proprietary materials to produce rigid bonds at room temperature. The catalyst used in these no-bake systems serves a dual purpose. The first purpose is to cause the silicate to form a rigid silica gel, and secondly, it controls the set time of the sand mix. As with sodium silicate- CO_2 sand mixes, these binders have insufficient acid content to be used with olivine sands.

To evaluate oil-urethane no-bake systems, the Ashland 3 part Linocure (AW, part C, BW-3) system was used. This binder system offers maximum flexibility in terms of work and strip times and obtainable mold properties. Oil-urethane binder systems may be mixed with sand in either conventional or continuous mixers, and are extremely flowable. This flowability allows the sand to compact uniformly around the contour of the part to be cast, which provides excellent dimensional control and surface finish characteristics of the casting. The properties of mold sand bonded with oil-urethane no-bake binders proved to be of special interest in this investigation, and are discussed at greater length later in this section.

Generally, when mold fabrication is complete, the mold is stored and/or allowed to set for a period of time before pouring. This storage interval may range from a few minutes to a number of hours, depending on several factors. These factors include mold temperature, production flow time, amount of time required for metal preparation, etc. In addition to storage time, the temperature at which molds are stored may also vary. To evaluate the effects of storage time and temperature on mold properties, tests were conducted using each of the aforementioned binder systems, after being held at various temperatures for predetermined periods of time. The storage temperatures used in this evaluation ranged from room temperature (70-78°F) to temperatures typical of dry-room conditions (about 98°F). Specimens were tested to determine the effect of these storage variables on mold tensile and compressive strengths and permeability. All tests were performed with AFS 70 silica sand.

The effects of storage temperatures and times on the tensile strength of molding sand bonded with 4% sodium silicate cured with CO₂, 4% Delta 241-7X sodium silicate airset, and 1.5% Delta 475-X Ester Set are shown in

Figures 34-37, respectively. Results of these tests show that higher tensile strengths are obtained from molding sand stored at room temperature than at 98°F, regardless of binder type. Maximum tensile strength was displayed from the sand bonded with sodium silicate airset after 48 hours at room temperature (357.5 psi average). Molding sands bonded with sodium silicate-CO₂ and synthetic resin displayed the same maximum tensile developments (160-180 psi). However, the sand bonded with 4% sodium silicate-CO₂ developed maximum tensile strength after only 8 hours in storage at room temperature, whereas the sand bonded with 1.5% ester set required 24 hours under the same conditions. It was noted from the test data that sands bonded with sodium silicate airset and synthetic resin displayed a gradual decrease in strength after reaching their maximum. Sand bonded with sodium silicate-CO₂ showed an abrupt decrease in strength after 8 hours in storage at room temperature.

The results of tensile tests performed on the oil-urethane no-bake binder (Linocure) are shown in Figures 38-41. Tests were conducted with sands bonded with 0.90, 1.00, 1.25, and 1.50% Linocure. In addition to the AFS 70 silica sand used in tests on the other binder systems, tests using AFS 53 silica sand were also performed. In contrast to tensile strengths developed by sands bonded with sodium silicate-CO₂, airset, or synthetic resin, sands bonded with Linocure developed maximum strengths when stored at 98°F rather than at room temperature. This reversal in tensile strength development characteristics is due to the effect of temperature on the chemical bonding reaction of oil-urethane binders. The bonding reaction of the Linocure binder is extremely temperature-sensitive. According to information obtained from vendors of oil-urethane binder systems, the temperature of sand used with this type of no-bake binder should never be below 65-70°F. As the temperature of the sand increases above 70°F, the speed

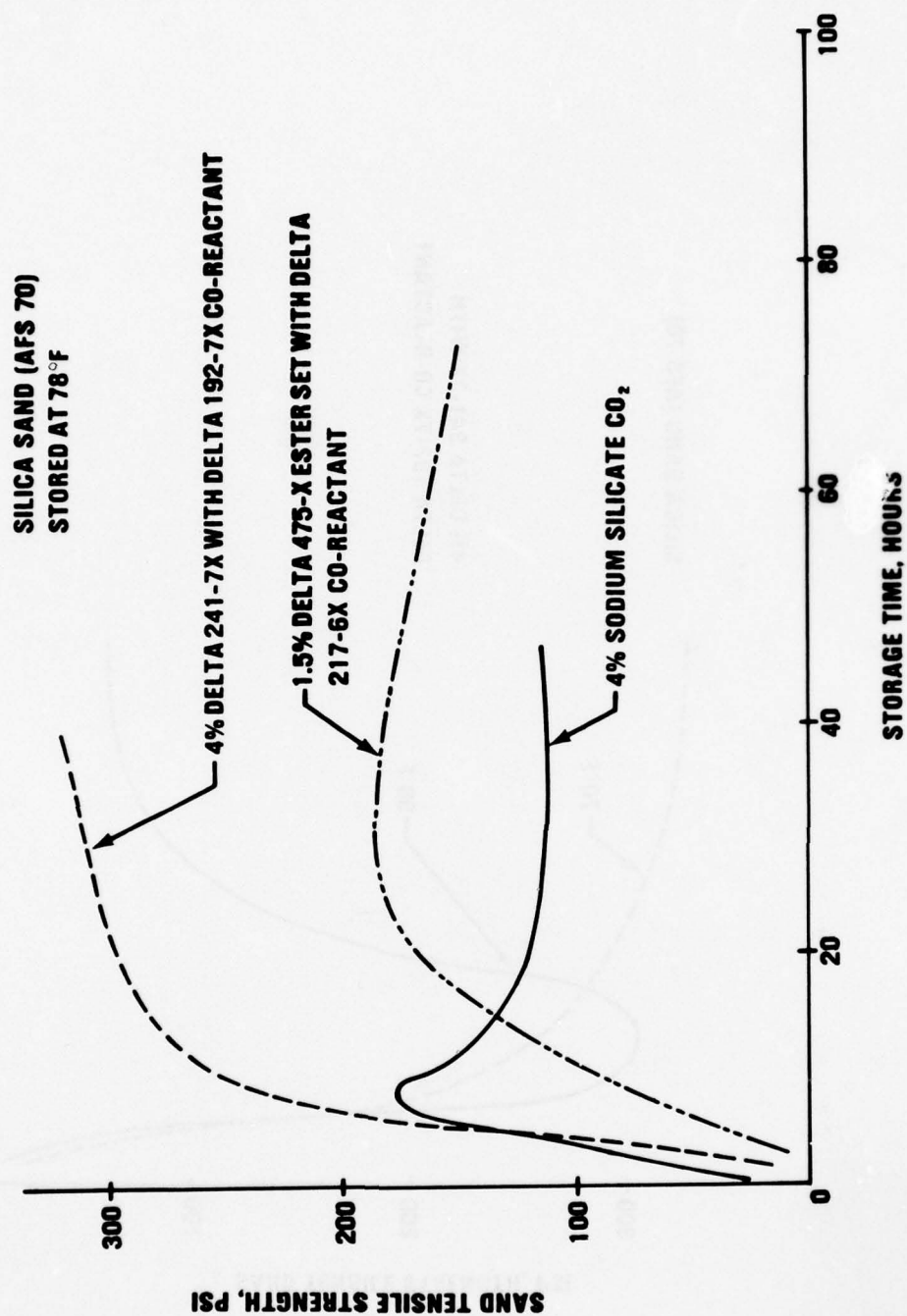


FIGURE 34 EFFECT OF STORAGE TIME ON MOLD TENSILE STRENGTH WITH AFS 70 SILICA SAND WITH VARIOUS BINDERS STORED AT ROOM TEMPERATURE

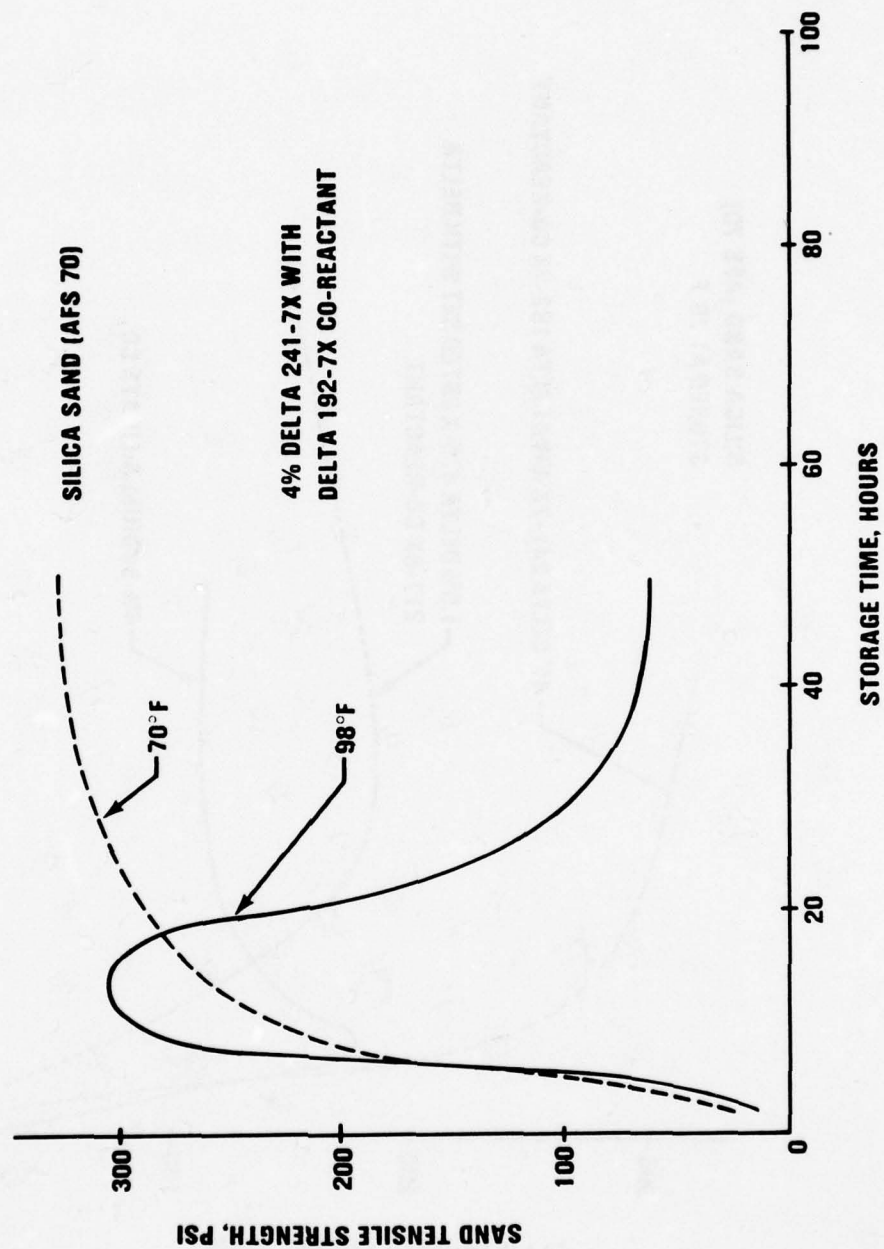
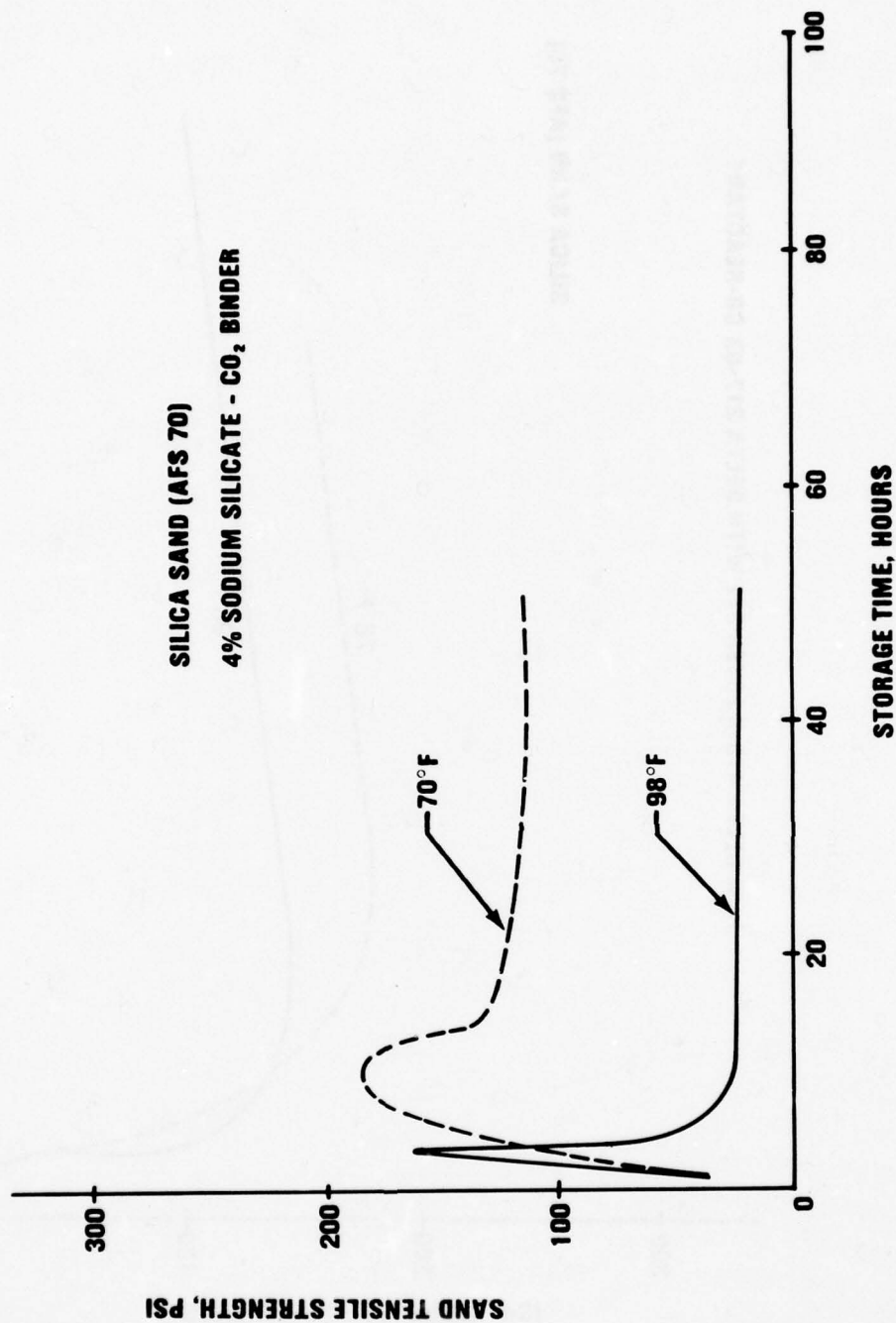


FIGURE 35 EFFECT OF STORAGE TIME ON MOLD TENSILE STRENGTH WITH AFS 70 SILICA SAND/SODIUM SILICATE AIRSET BINDER STORED AT VARIOUS TEMPERATURES



**FIGURE 36 EFFECT OF STORAGE TIME ON MOLD TENSILE STRENGTH WITH AFS 70
SILICA SAND/SODIUM SILICATE BINDER STORED AT VARIOUS TEMPERATURES**

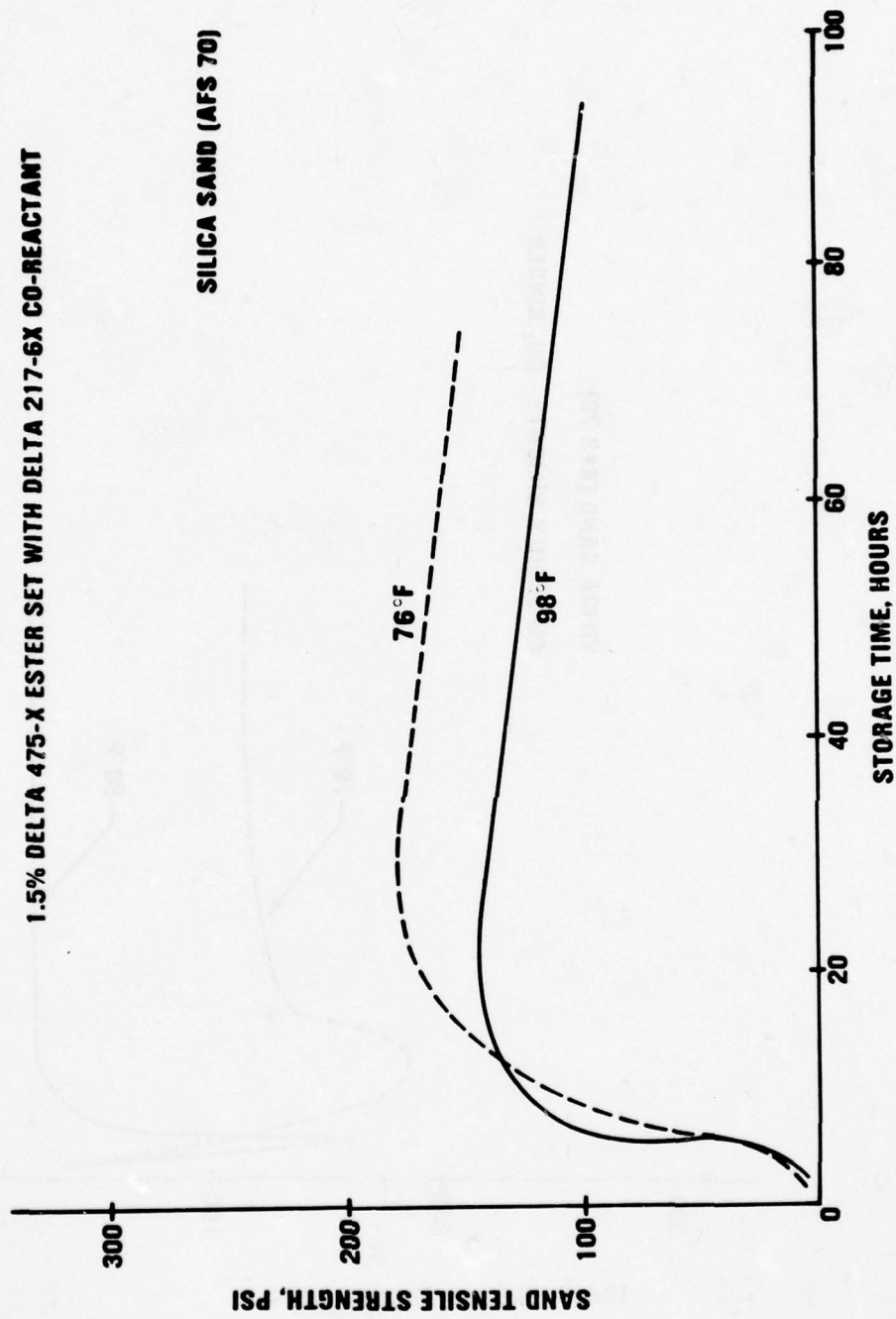


FIGURE 37 EFFECT OF STORAGE TIME ON MOLD TENSILE STRENGTH WITH AFS 70 SILICA SAND AND SYNTHETIC RESIN BINDER STORED AT VARIOUS TEMPERATURES

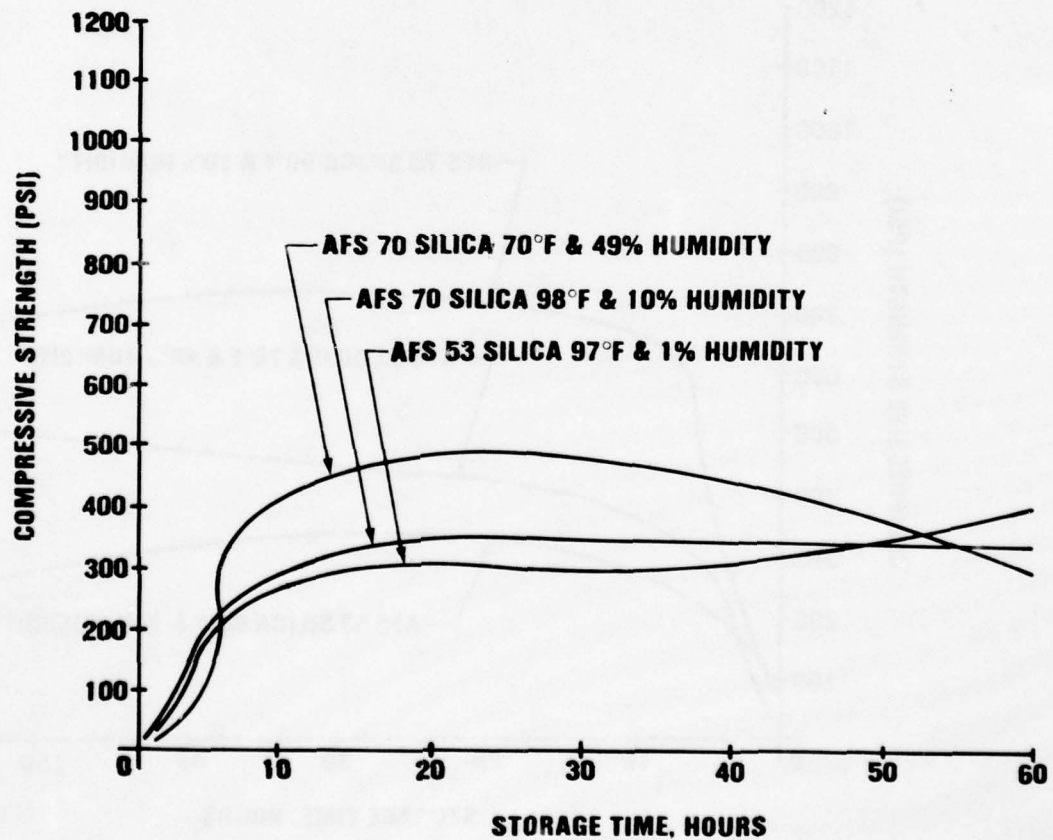
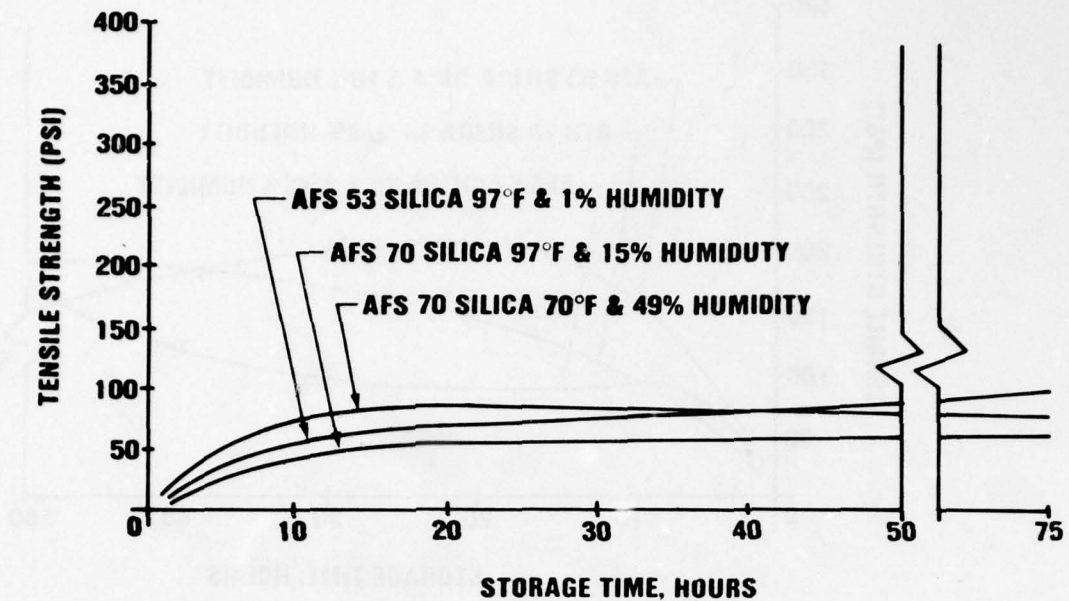


FIGURE 38 EFFECT OF STORAGE TIME ON MOLD MECHANICAL PROPERTIES OF TWO SILICA SAND FINENESSES WITH .90% LINOCURE BINDER STORED AT DRY ROOM TEMPERATURES & ROOM TEMPERATURE

AD-A060 339

BOEING AEROSPACE CO SEATTLE WASH
CAST ALUMINUM STRUCTURES TECHNOLOGY (CAST) MANUFACTURING METHOD--ETC(U)
MAY 78 R G CHRISTNER, D D GOEHLER

F/G 11/6

F33615-76-C-3111

UNCLASSIFIED

D180-24610-1

AFFDL-TR-78-62

NL

2 OF 4
AD
A060339



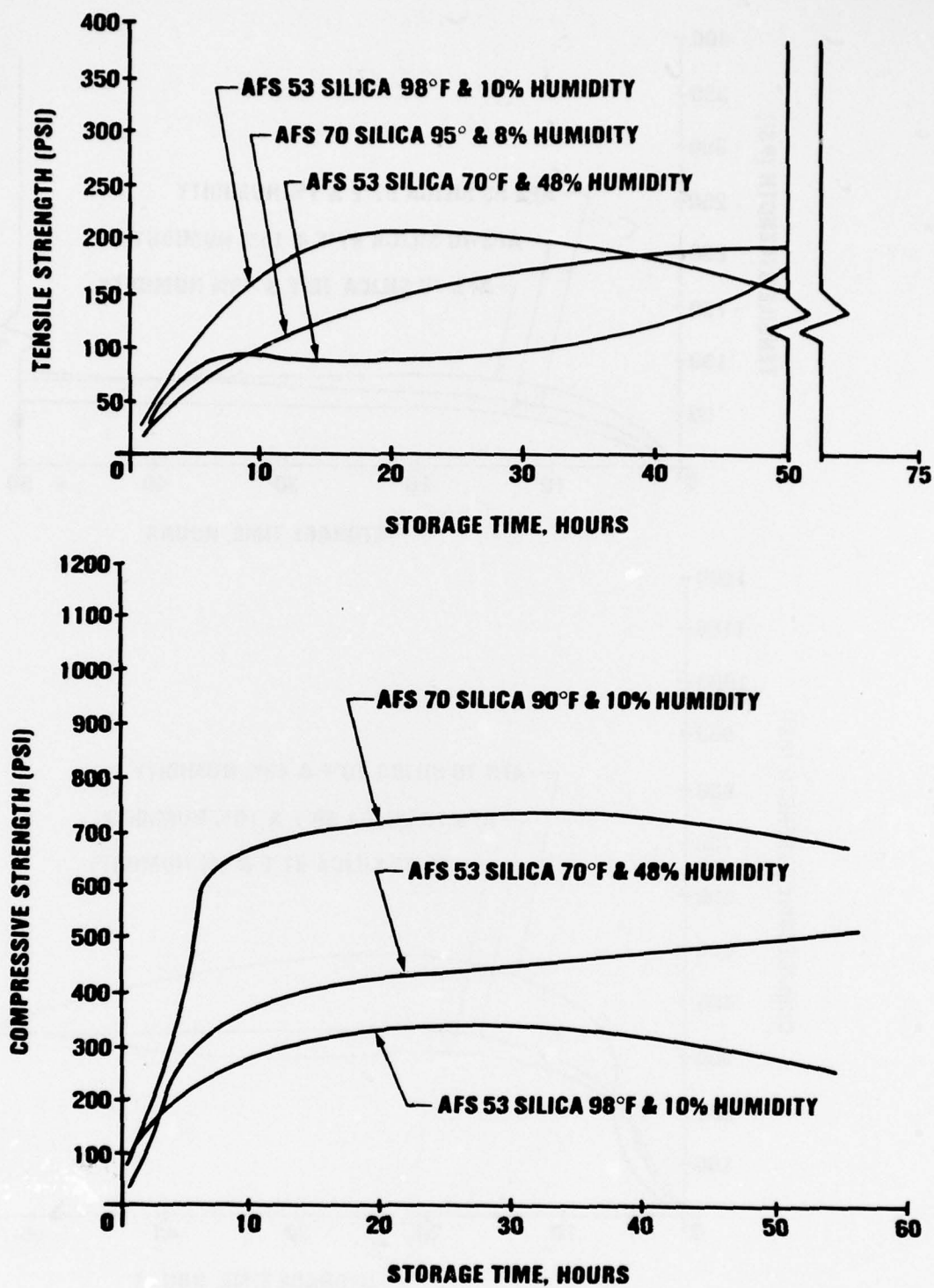


FIGURE 39 EFFECT OF STORAGE TIME ON MOLD MECHANICAL PROPERTIES OF TWO SILICA FINENESSES WITH 1.0% LINOCURE BINDER STORED AT DRY ROOM TEMPERATURES & ROOM TEMPERATURES

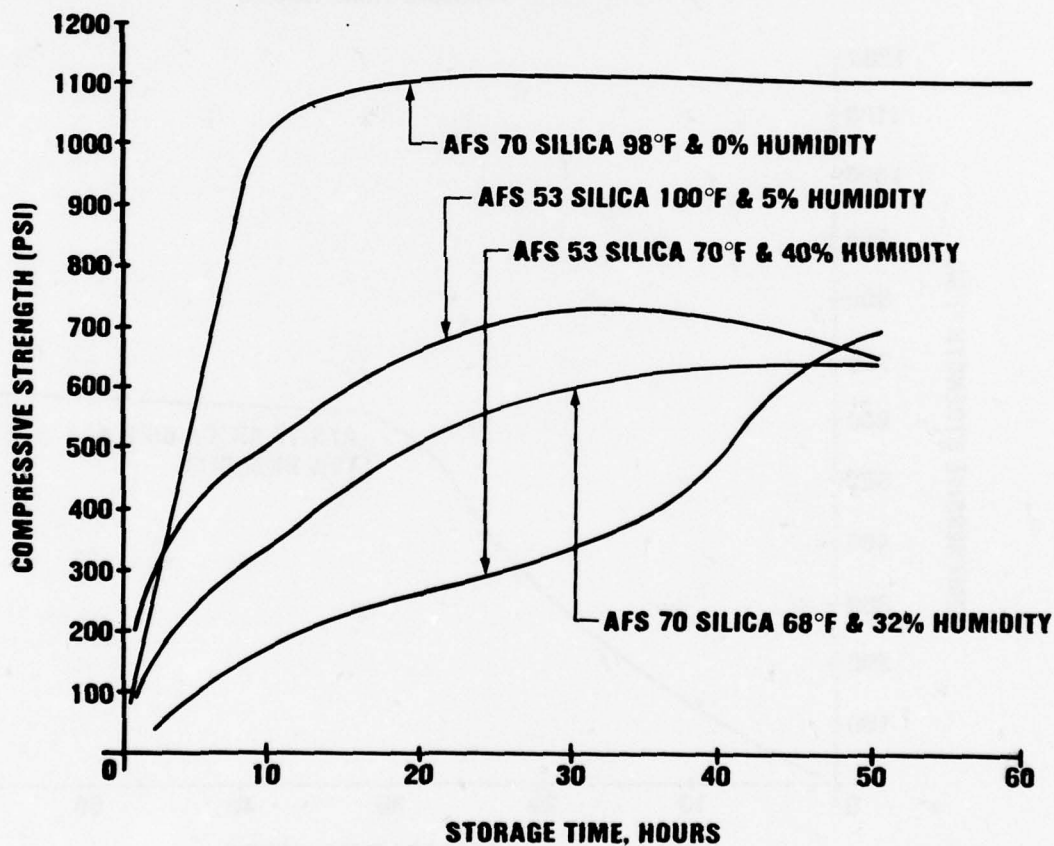
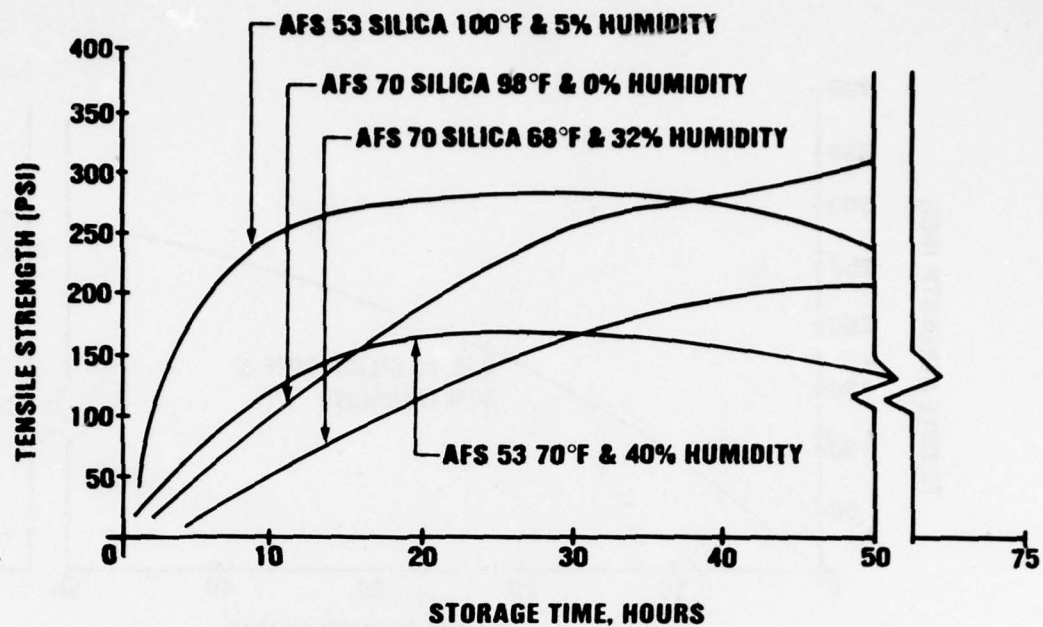


FIGURE 40 EFFECT OF STORAGE TIME ON MOLD MECHANICAL PROPERTIES OF TWO SILICA SAND FINENESSES WITH 1.25% LINCURE BINDER STORED AT DRY ROOM TEMPERATURES & ROOM TEMPERATURES

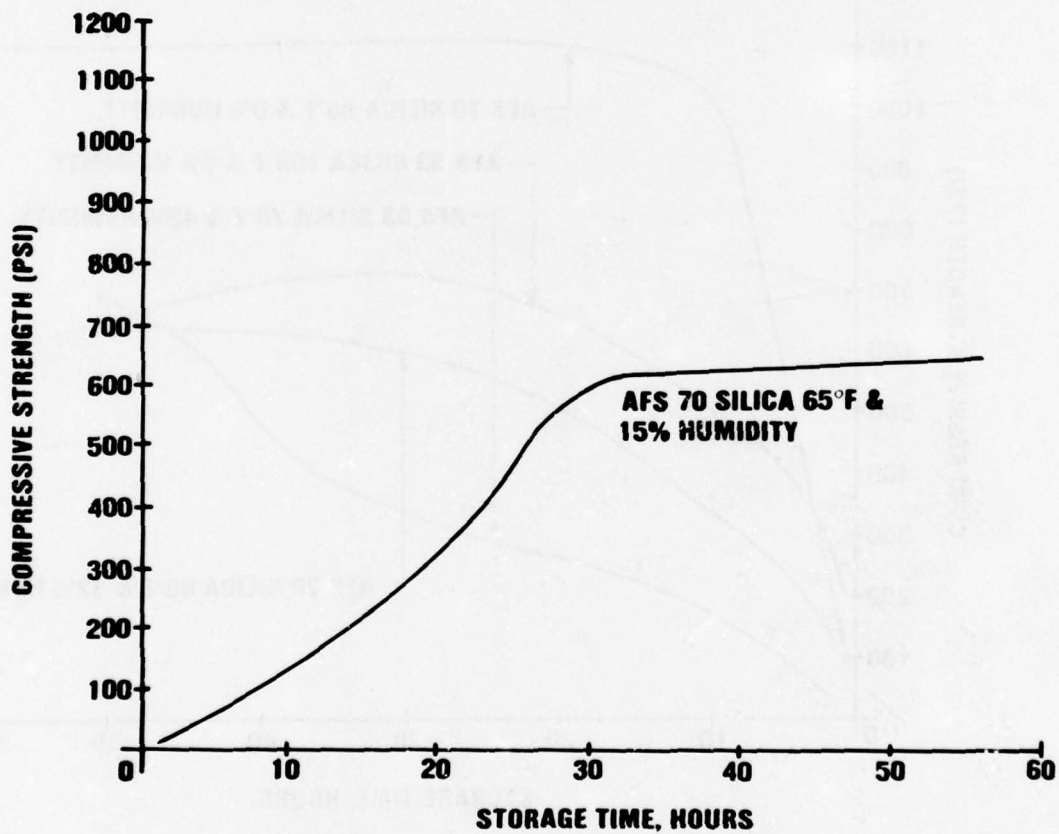
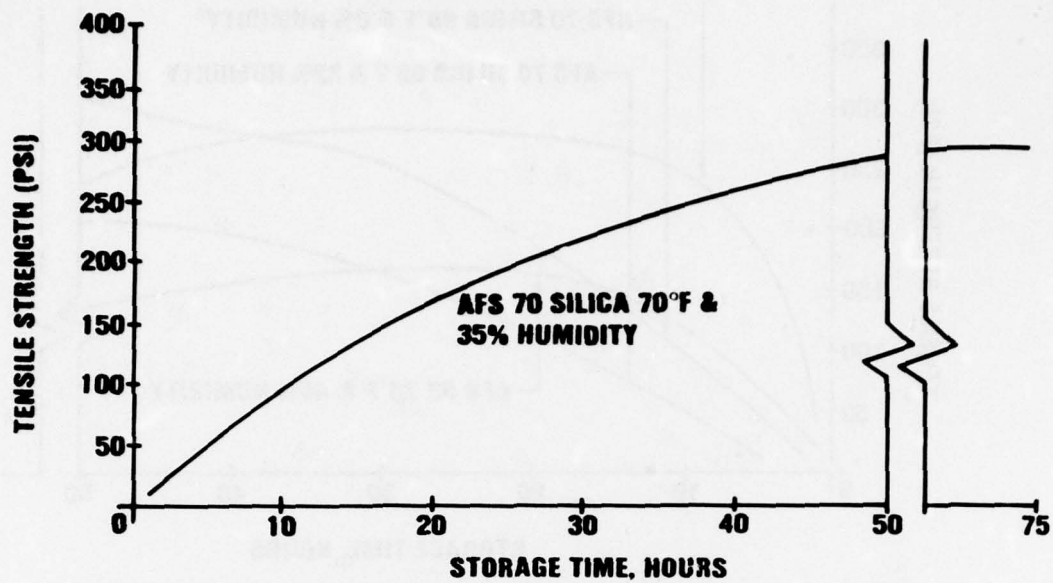
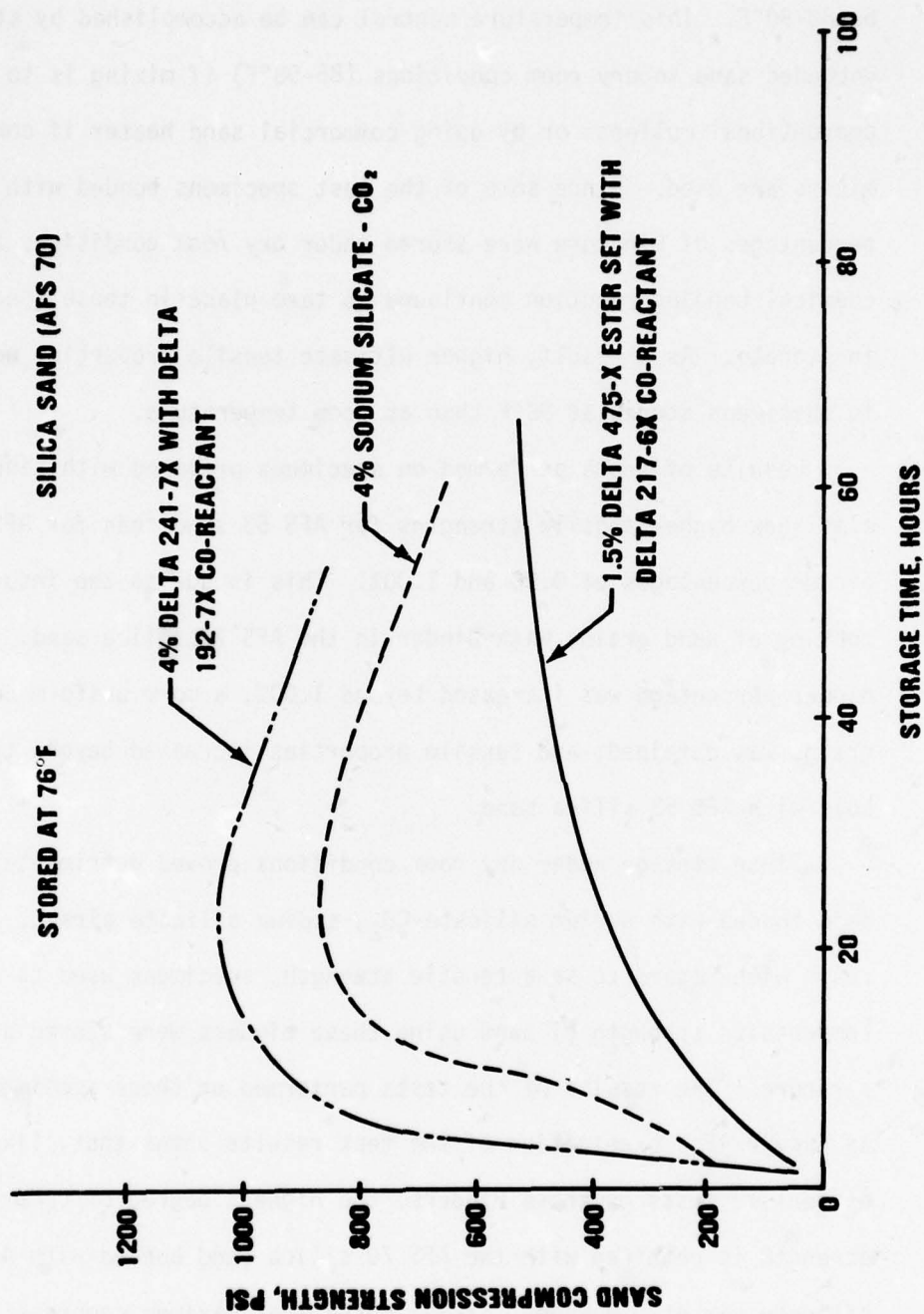


FIGURE 41 EFFECT OF STORAGE TIME ON MOLD MECHANICAL PROPERTIES OF TWO SILICA SAND FINENESSES WITH 1.5% LINCURE BINDER STORED AT ROOM TEMPERATURE

and efficiency of the bonding reaction increases proportionately. Optimum temperature for sand used with oil-urethane binders has been determined to be 80-90°F. This temperature control can be accomplished by storing the unbonded sand in dry room conditions (85-98°F) if mixing is to be done with conventional mullers, or by using commercial sand heater if continuous mixers are used. Since some of the test specimens bonded with various percentages of Linocure were stored under dry room conditions at 98°F, the chemical bonding reaction continued to take place in those specimens while in storage. As a result, higher ultimate tensile properties were developed in specimens stored at 98°F than at room temperature.

Results of tests performed on specimens prepared with Linocure binder also show higher tensile strengths for AFS 53 sand than for AFS 70 sand for binder percentages of 0.90 and 1.00%. This is due to the insufficient coating of sand grains with binder in the AFS 70 silica sand. As the binder percentage was increased beyond 1.00%, a more uniform coating of the grains was obtained, and tensile properties increased beyond those obtainable with AFS 53 silica sand.

Since storage under dry room conditions proved detrimental to molding sand bonded with sodium silicate- CO_2 , sodium silicate airset, or synthetic resin with regard to sand tensile strength, specimens used to determine the compressive strength of sand using these binders were stored at room temperature. The results of the tests performed on these specimens is shown in Figure 42. Examination of the test results shows that, like the results of tensile tests on these binders, the highest degree of compressive strength is obtained with the AFS 70 silica sand bonded with 4% sodium silicate airset. However, it was noted that maximum compressive strength was developed after 40 hours in storage in comparison to the 48-hour storage time required for maximum tensile development.



**FIGURE 42 EFFECT OF STORAGE TIME ON MOLD COMPRESSIVE STRENGTH OF AFS 70
SILICA SAND WITH VARIOUS BINDER TYPES STORED AT ROOM TEMPERATURE**

Compressive strength development for sands bonded with the previously mentioned percentages of Linocure as a function of storage time and temperature is shown in Figures 38-41. As in the results of the tensile tests performed on sands bonded with Linocure, the data from the compression tests show that the strength of AFS 53 bonded sand continues to surpass strengths obtained with AFS 70 bonded silica until the binder percentage increases beyond 1.00%. However, it was noted from the results of tests performed on sand bonded with 1.00% Linocure that the compressive strength of mixed sand stored at room temperature continued to increase steadily after 50 hours in storage, while sand with the same amount of binder (both AFS 70 and AFS 53) stored at 90-98°F displayed gradual decreases in strength after about 25 hours.

The permeability of molding sand depends upon four factors: shape of the sand grains, fineness of the sand grains, type and amount of binder, and moisture content. In this investigation, spherical grains of AFS 70 grain fineness were bonded with sodium silicate- CO_2 , sodium silicate air-set, and synthetic resin binders. For the evaluation of mold permeability for sands bonded with Linocure, spherical grains of AFS 53 and AFS 70 were used. The decision to evaluate both AFS 53 and AFS 70 silica sands was based on examinations of cast surface finishes obtained on parts cast in the configuration of Figure 18. Parts cast in molds made with AFS 53 silica sand displayed metal penetration defects in heavy sections and a generally rough surface finish. Identical parts cast in molds made in AFS 70 silica sand displayed greater resistance to metal penetration and a smoother surface finish. In essence, even though molds made with AFS 53 silica sand displayed higher permeability readings than found with AFS 70 silica sand, the AFS 70 silica sand produced castings with negligible metal penetration defects and good surface finish.

The effect of binder type and amount on mold permeability is shown in Figures 43-45 for sodium silicate- CO_2 , sodium silicate airset, and synthetic resin binder, and in Figures 46-49 for oil-urethane binder. As shown in these figures, highest permeability values were obtained from AFS 70 silica sand bonded with 4% sodium silicate airset (Delta 241-7X with Delta 192-7X co-reactant).

The effect of mulling (mixing) time on mold properties was evaluated with sand bonded with sodium silicate cured with CO_2 and sodium silicate airset. Molding sand was prepared using each of the binders in quantities of 4% with AFS 70 silica sand. Each sand mix was mulled from 1 to 6 minutes and tested for tensile and compressive strengths and mold permeability. The effect of mulling time on mold properties is significant only to sands mixed in batch-type mullers, since the mulling time in continuous mixers is automatically controlled.

The effect of mulling time on mold properties is shown in Figures 50 and 51. In general, the tensile and compressive strengths of sand bonded with sodium silicate and cured with CO_2 increased with increased mulling time. Permeability of sand bonded with sodium silicate- CO_2 decreased steadily for mulling times between 1 and 3 minutes, then increased for mulling times greater than 3 minutes. Sand bonded with sodium silicate airset showed increases in tensile and compressive strengths for mulling times between 1 and 3 minutes, then decreased gradually as mulling time increased. The permeability of sand bonded with this binder was relatively constant (80-85) for mulling times between 1 and 3 minutes, then increased gradually as mulling time increased.

In addition to mulling time, sodium silicate- CO_2 molding sand is affected by the pressure and length of time with which the CO_2 is passed through the sand mass. Tests were conducted to illustrate the effect of

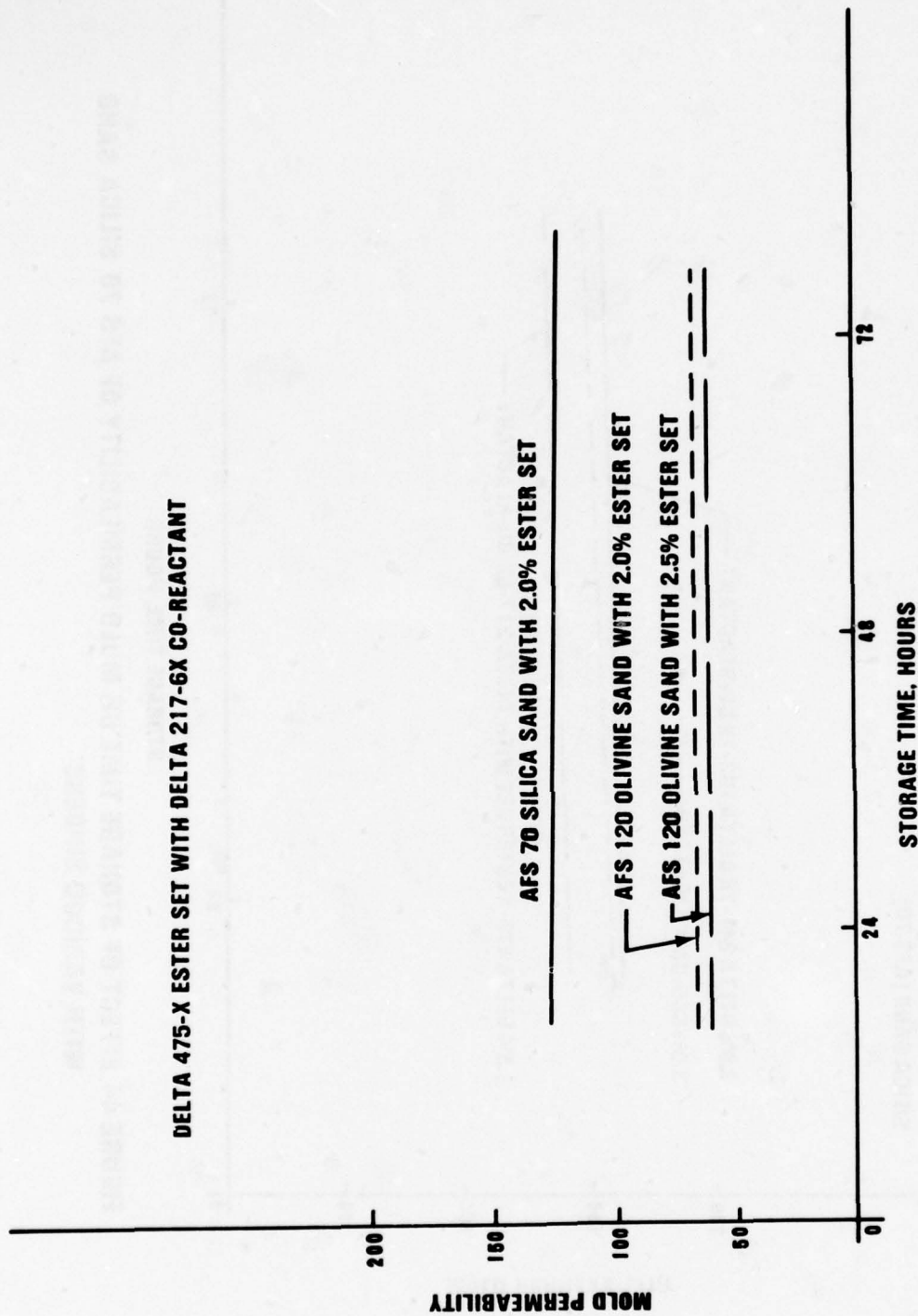


FIGURE 43 EFFECT OF STORAGE TIME ON MOLD PERMEABILITY WITH VARIOUS BINDERS & SAND TYPES

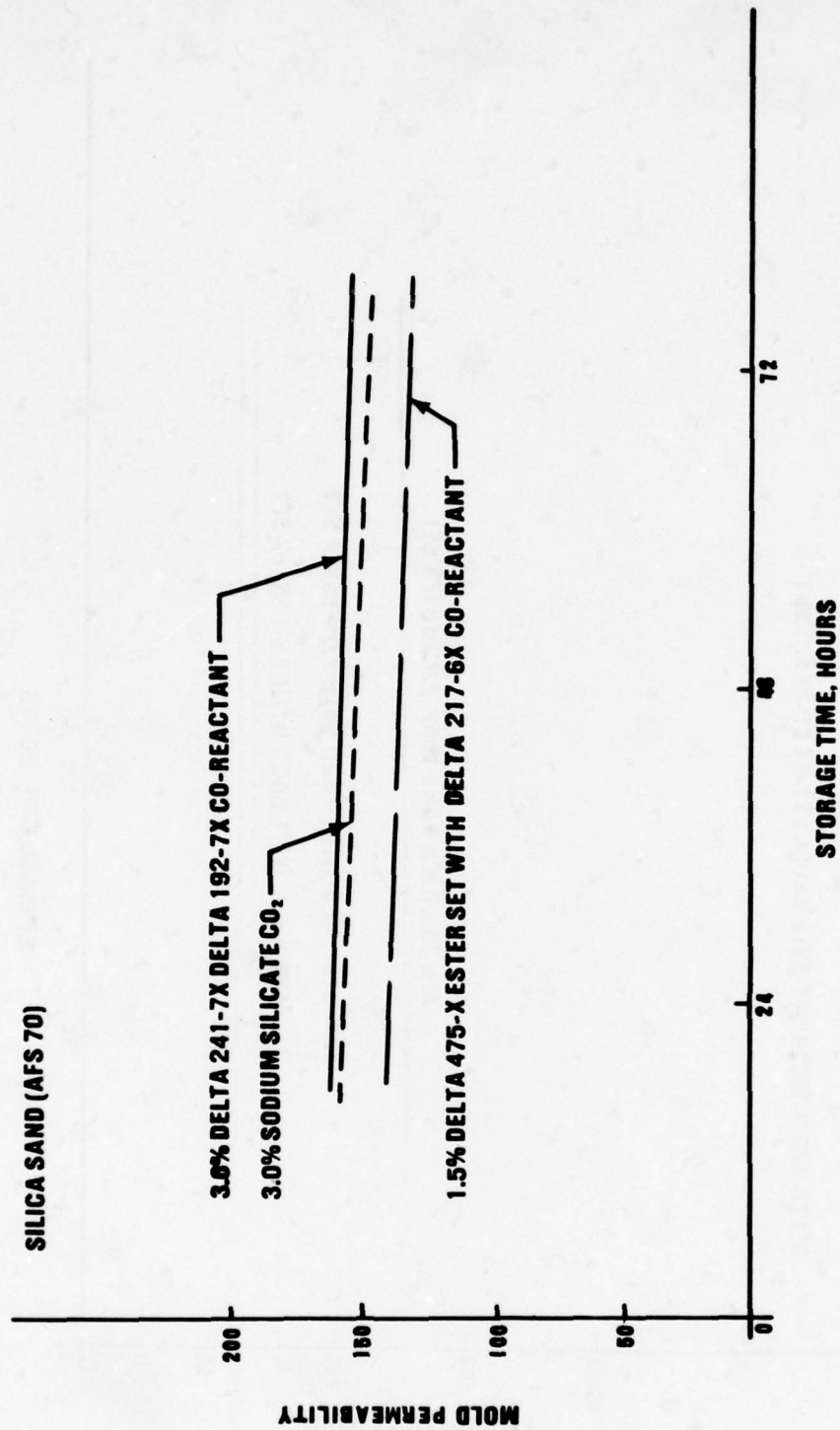


FIGURE 44 EFFECT OF STORAGE TIME ON MOLD PERMEABILITY OF AFS 70 SILICA SAND WITH VARIOUS BINDERS

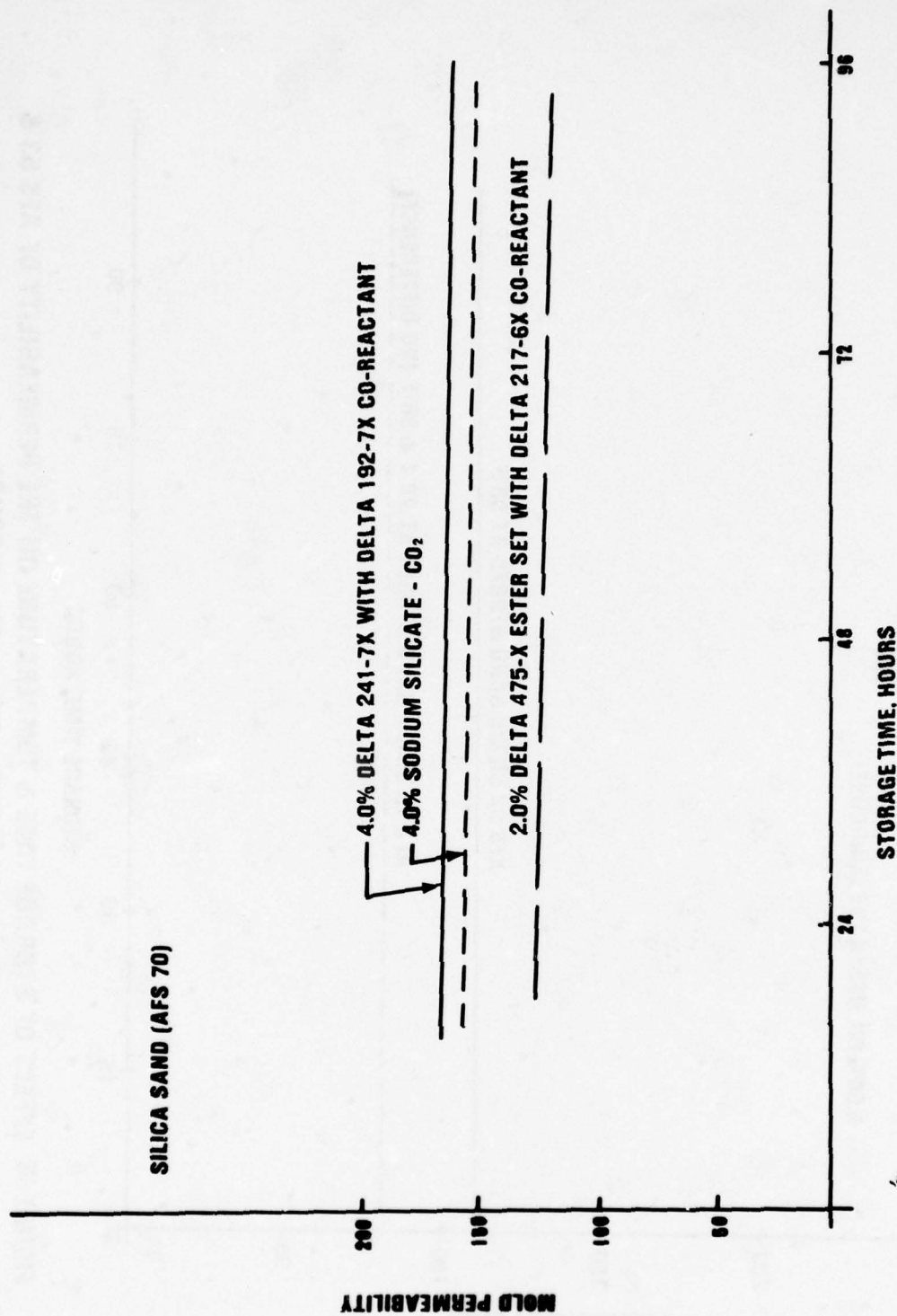


FIGURE 45 EFFECT OF STORAGE TIME ON MOLD PERMEABILITY OF AFS 70 SILICA SAND WITH VARIOUS BINDERS

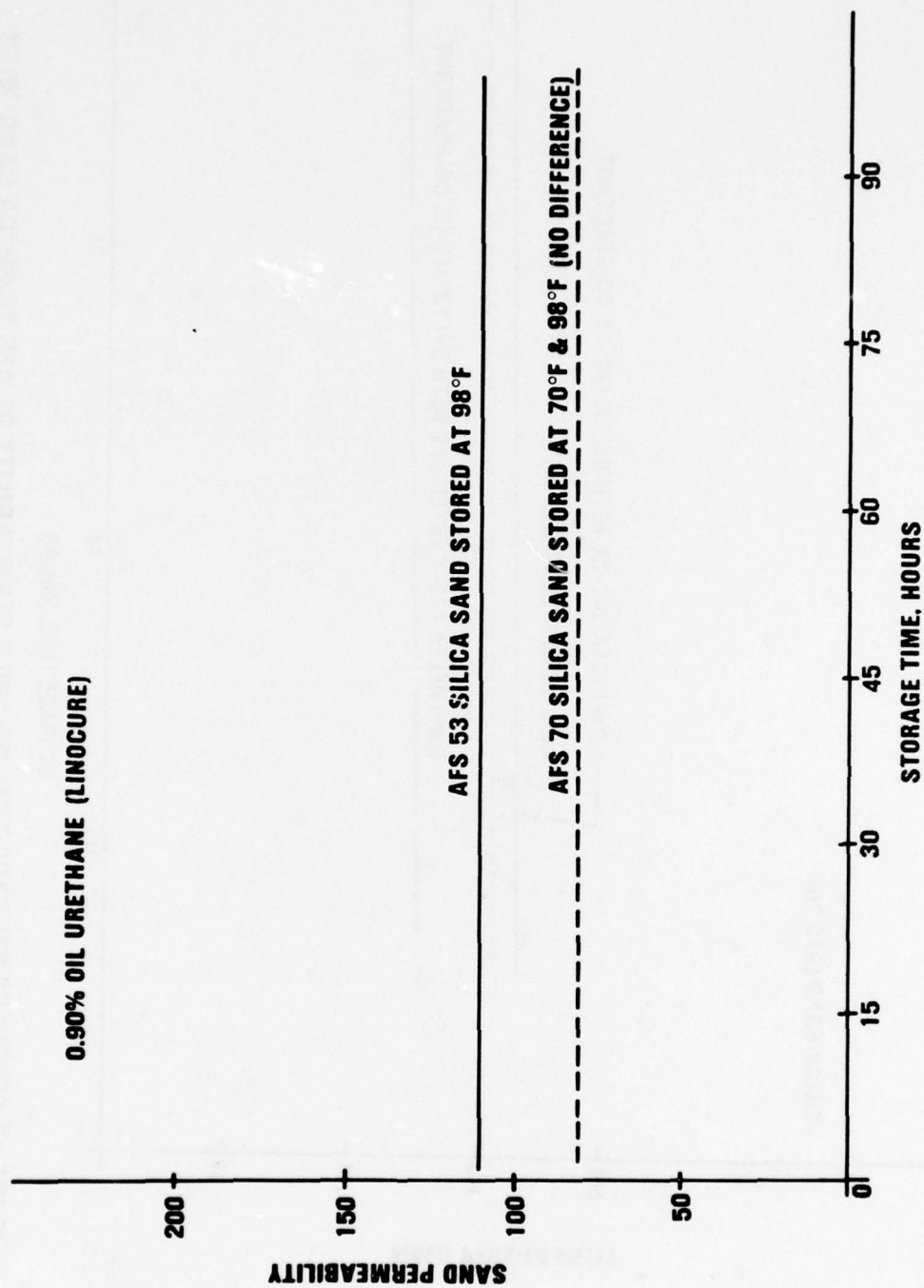


FIGURE 46 EFFECT OF STORAGE TIME & TEMPERATURE ON THE PERMEABILITY OF AFS 53 & AFS 70 SILICA SAND BONDED WITH 0.90% LINOCURE

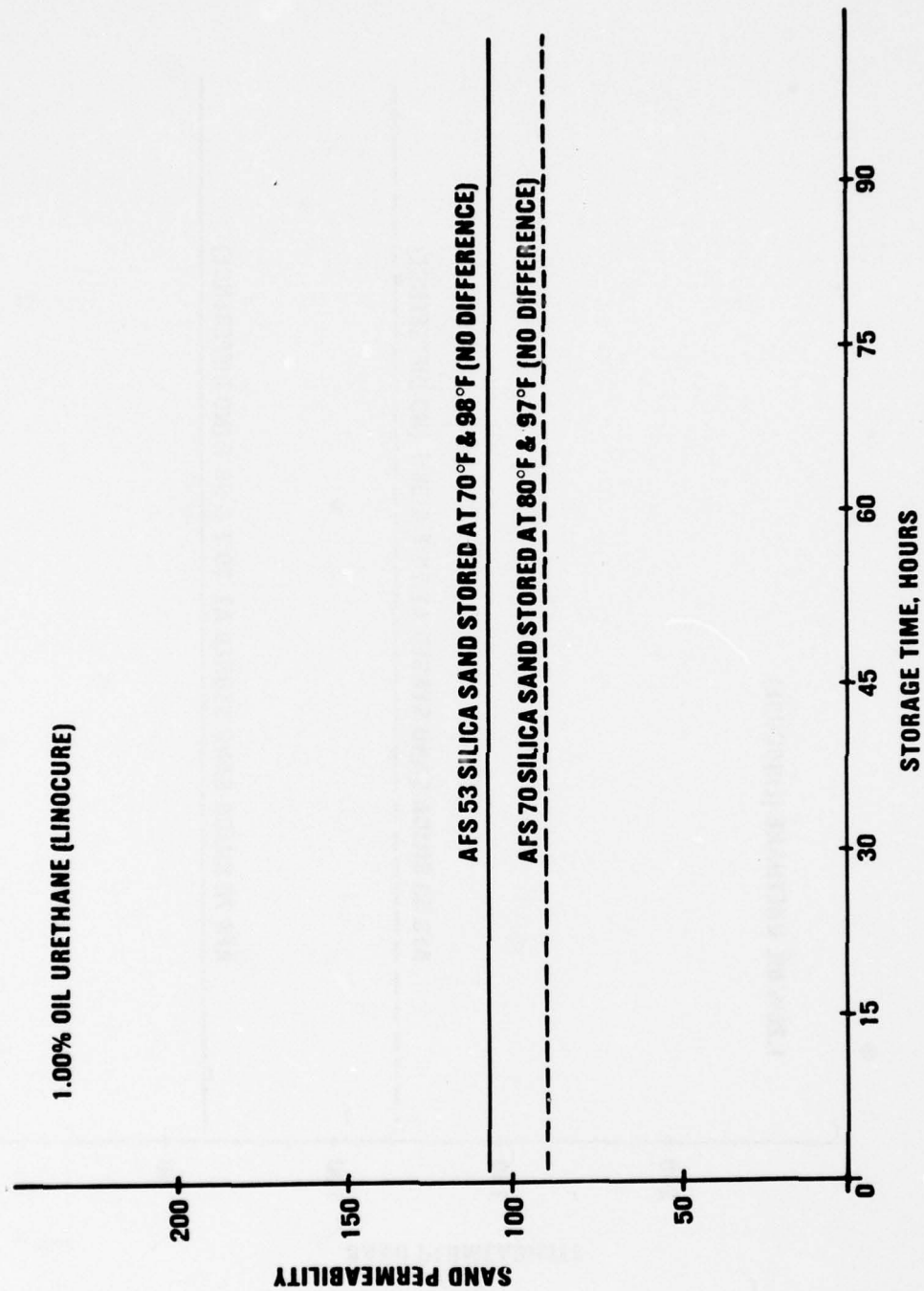


FIGURE 47 EFFECT OF STORAGE TIME & TEMPERATURE ON THE PERMEABILITY OF AFS 53 & AFS 70 SILICA SAND BONDED WITH 1.00% LINOURE

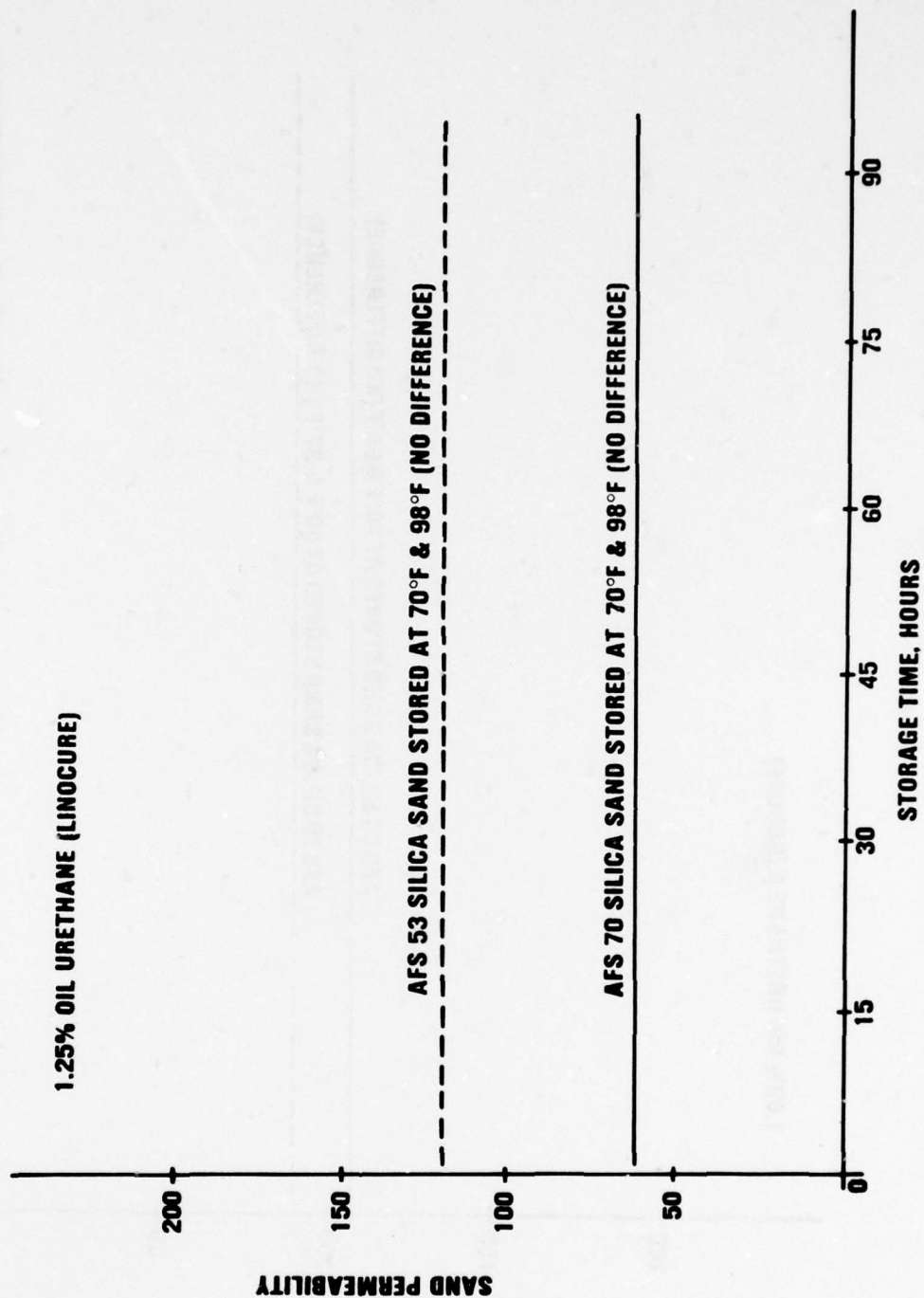


FIGURE 48 EFFECT OF STORAGE TIME & TEMPERATURE ON THE PERMEABILITY OF AFS 53 & AFS 70 SILICA SAND BONDED WITH 1.25% LINOCURE

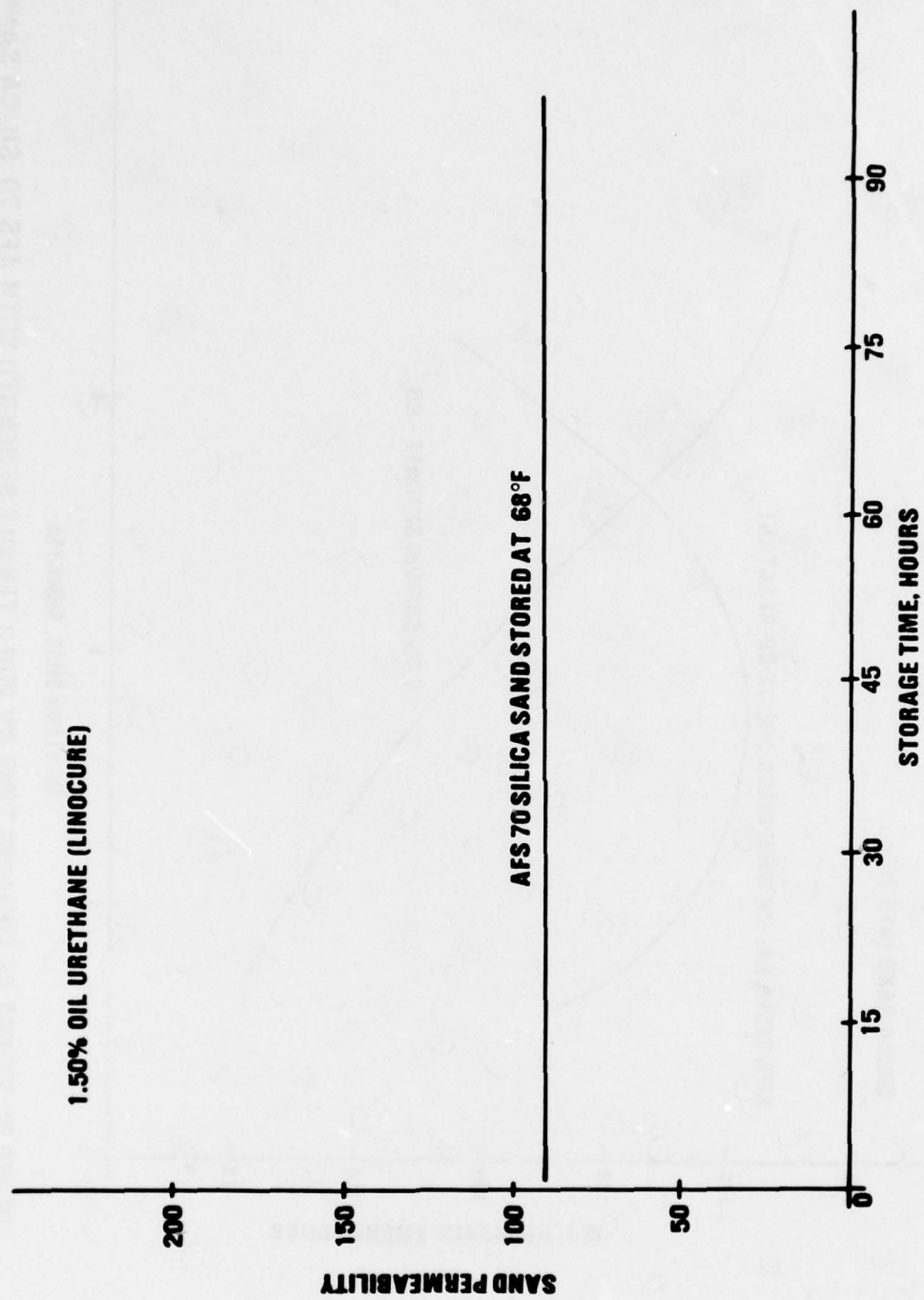


FIGURE 49 EFFECT OF STORAGE TIME & TEMPERATURE ON THE PERMEABILITY OF AFS 70 SILICA SAND BONDED WITH 1.50% LINOCURE

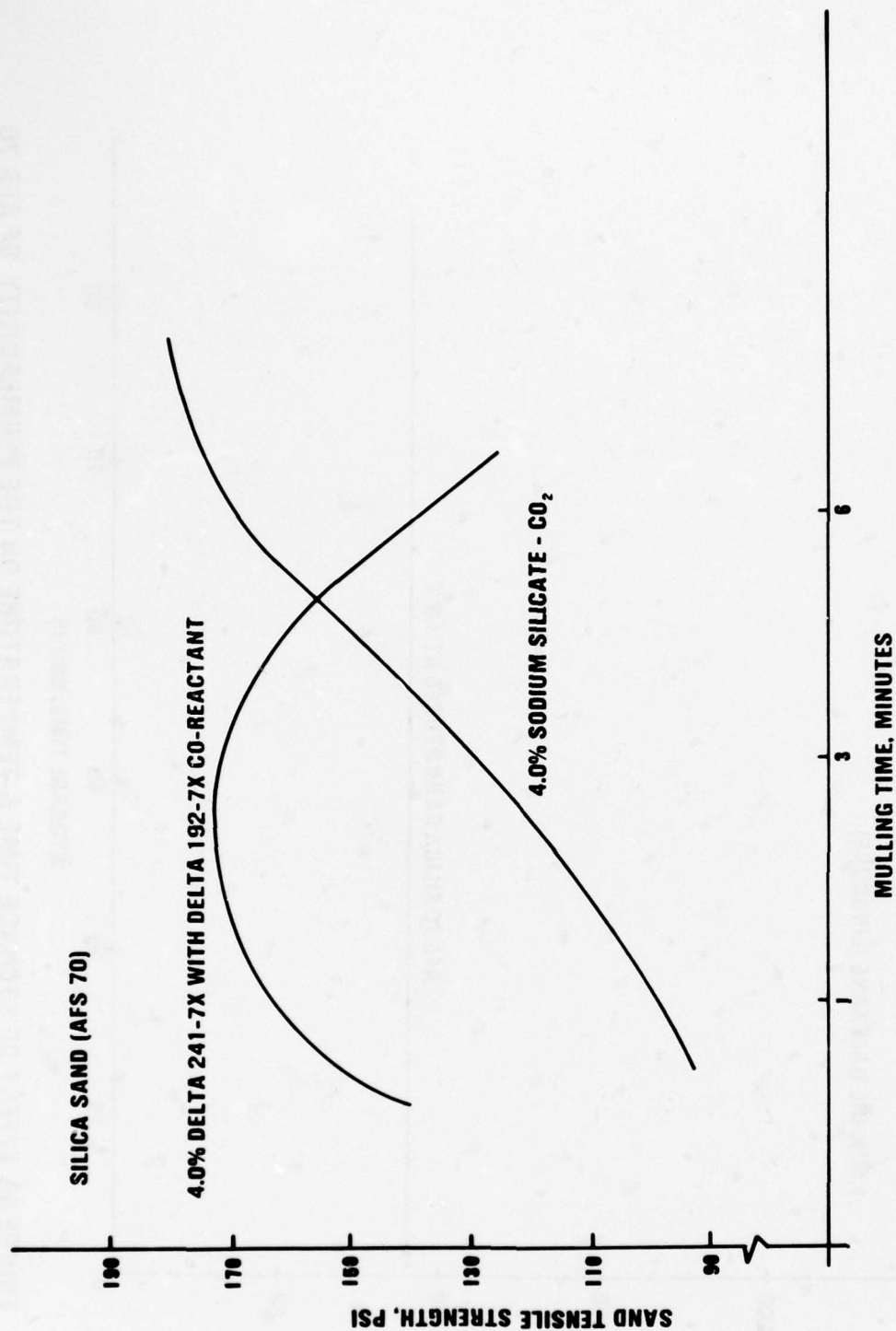


FIGURE 50 EFFECT OF MULLING TIME ON MOLD TENSILE STRENGTH WITH AFS 70 SILICA SAND & VARIOUS BINDERS

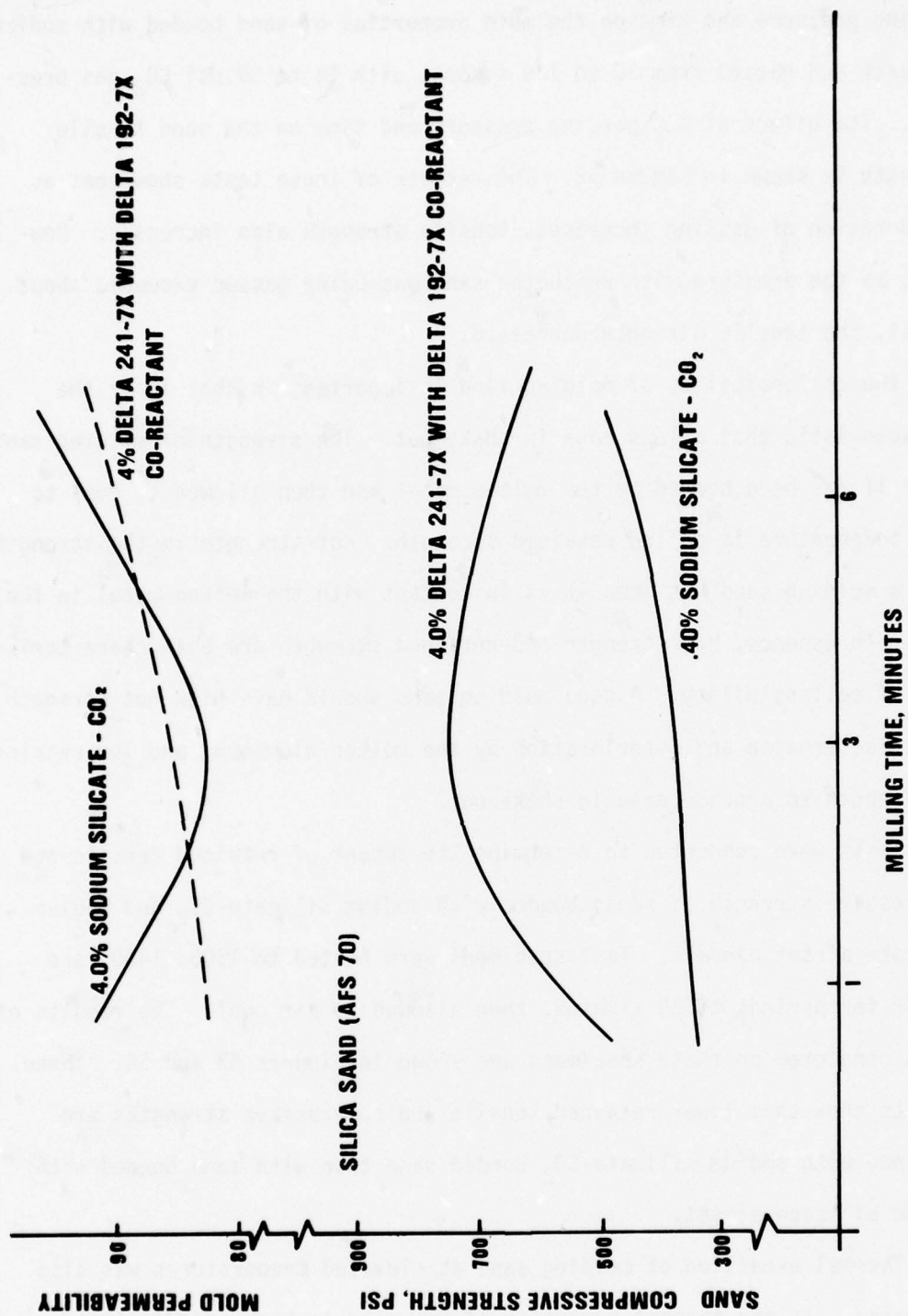


FIGURE 51 EFFECT OF MULLING TIME ON MOLD PERMEABILITY & COMPRESSIVE STRENGTH OF AFS 70 SILICA SAND WITH VARIOUS BINDERS

gassing pressure and time on the mold properties of sand bonded with sodium silicate and gassed from 30 to 120 seconds with 14 to 80 psi CO_2 gas pressure. The effect of CO_2 gassing pressure and time on the sand tensile strength is shown in Figure 52. The results of these tests show that as the duration of gassing increases, tensile strength also increases. However, as the pressure with which the sand was being gassed exceeded about 70 psi, the tensile strength decreased.

The collapsibility of molding sand is important in that it is the characteristic that allows ease in shake-out. The strength of molding sand after it has been heated by the molten metal and then allowed to cool to room temperature is called retained strength. Hot strength is the strength that a molding sand has when it is in contact with the molten metal in the mold. In essence, hot strength and retained strength are both characteristics of collapsibility. A good molding sand should have high hot strength to resist erosion and deterioration by the molten aluminum, and low retained strength to provide ease in shake-out.

Tests were conducted to determine the amount of retained tensile and compressive strength of sands bonded with sodium silicate- CO_2 and sodium silicate airset binders. Test specimens were heated to 1300, 1400, and 1500°F for periods of 20 minutes, then allowed to air cool. The results of tests conducted on these specimens are shown in Figures 53 and 54. These results show that lower retained tensile and compressive strengths are obtained with sodium silicate- CO_2 bonded sand than with sand bonded with sodium silicate airset.

Thermal expansion of molding sand at elevated temperatures was also evaluated. If the thermal expansion of the sand is high, difficulties may occur in maintaining dimensional tolerances in the casting.

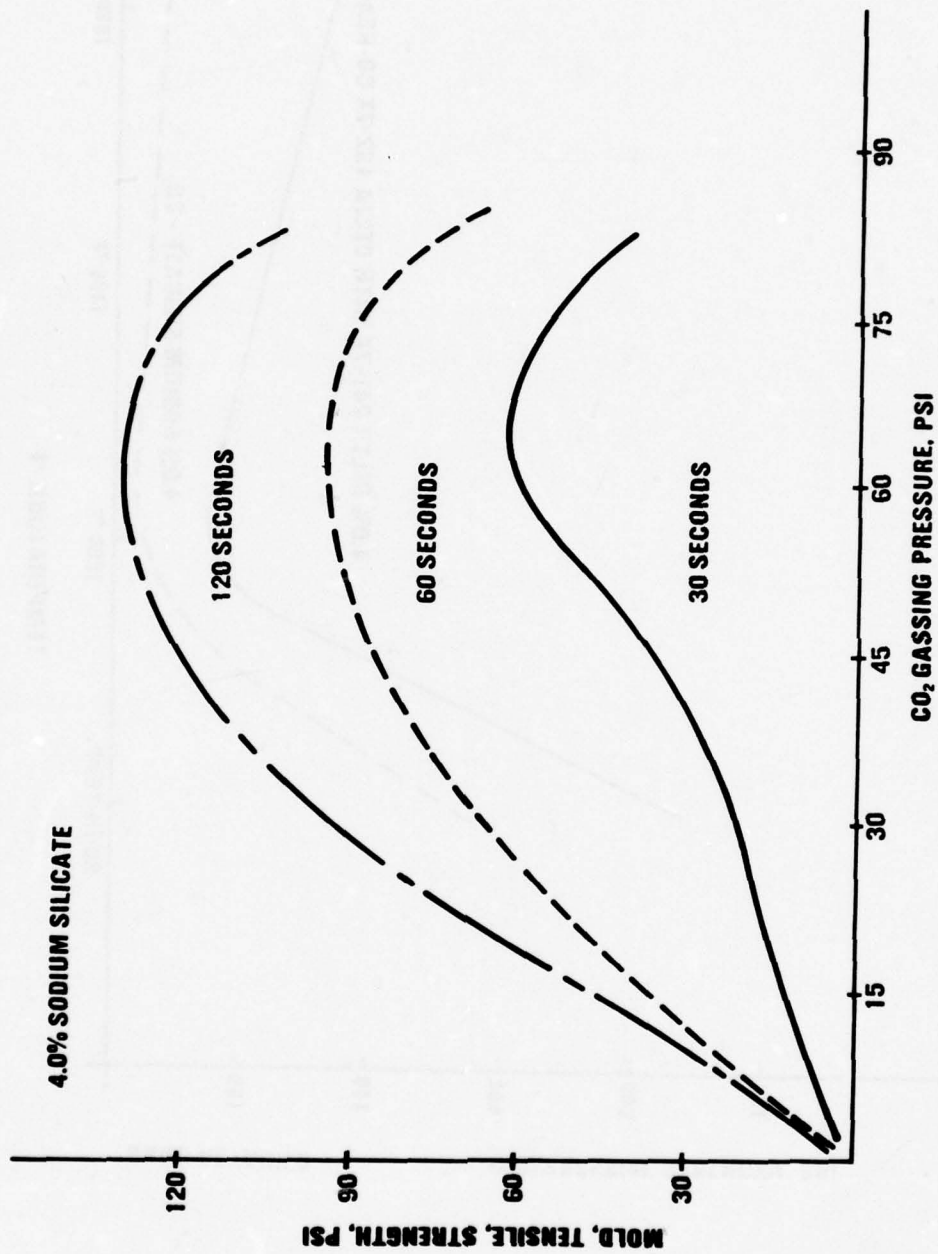


FIGURE 52 EFFECT OF CO₂ GASSING PRESSURE ON MOLD TENSILE OF AFS 70 SILICA SAND/SODIUM SILICATE AT VARIOUS GASSING TIMES

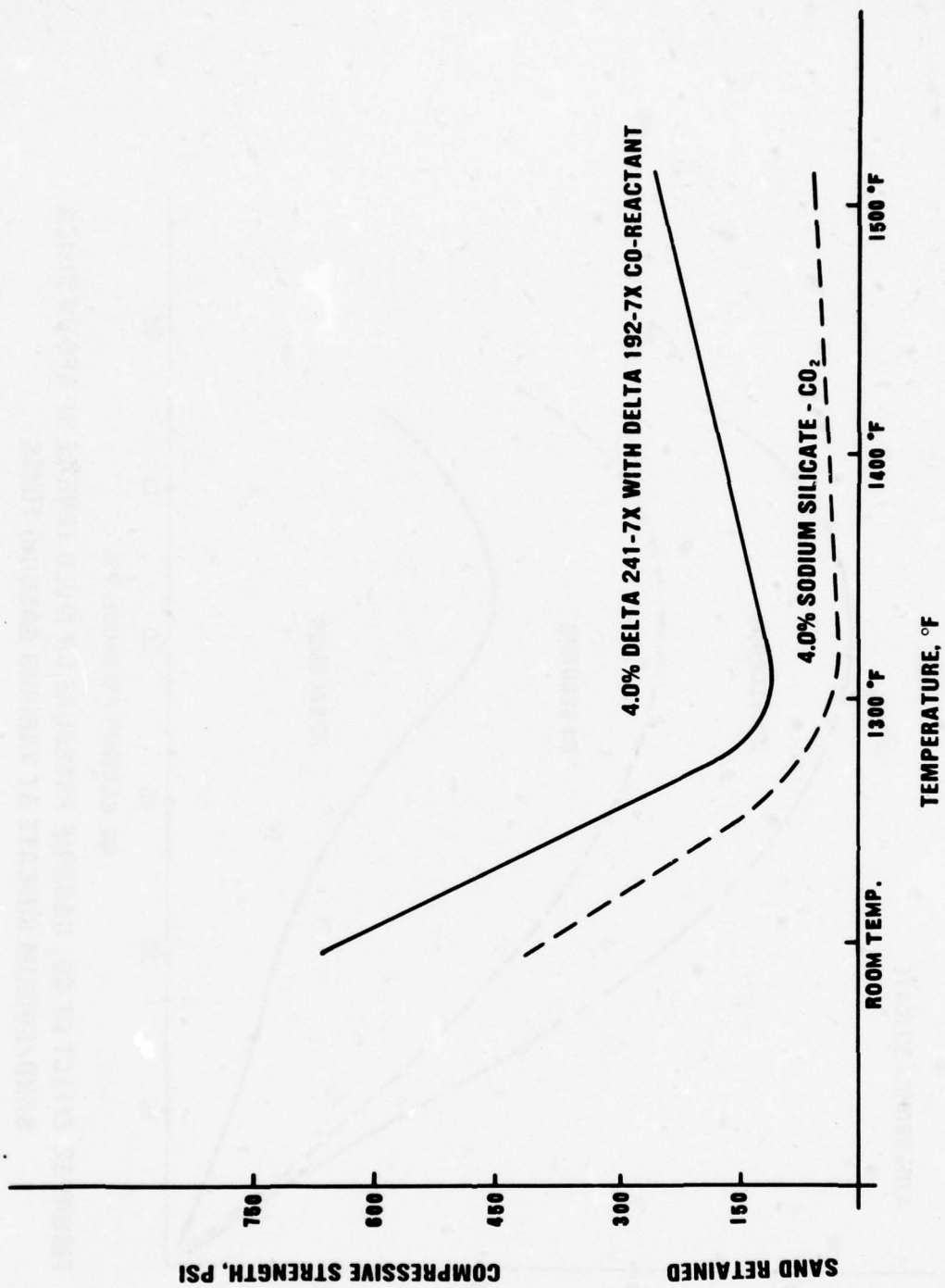


FIGURE 53 EFFECT OF ELEVATED TEMPERATURES ON RETAINED MOLD COMPRESSIVE STRENGTH OF AFS 70 SILICA SAND

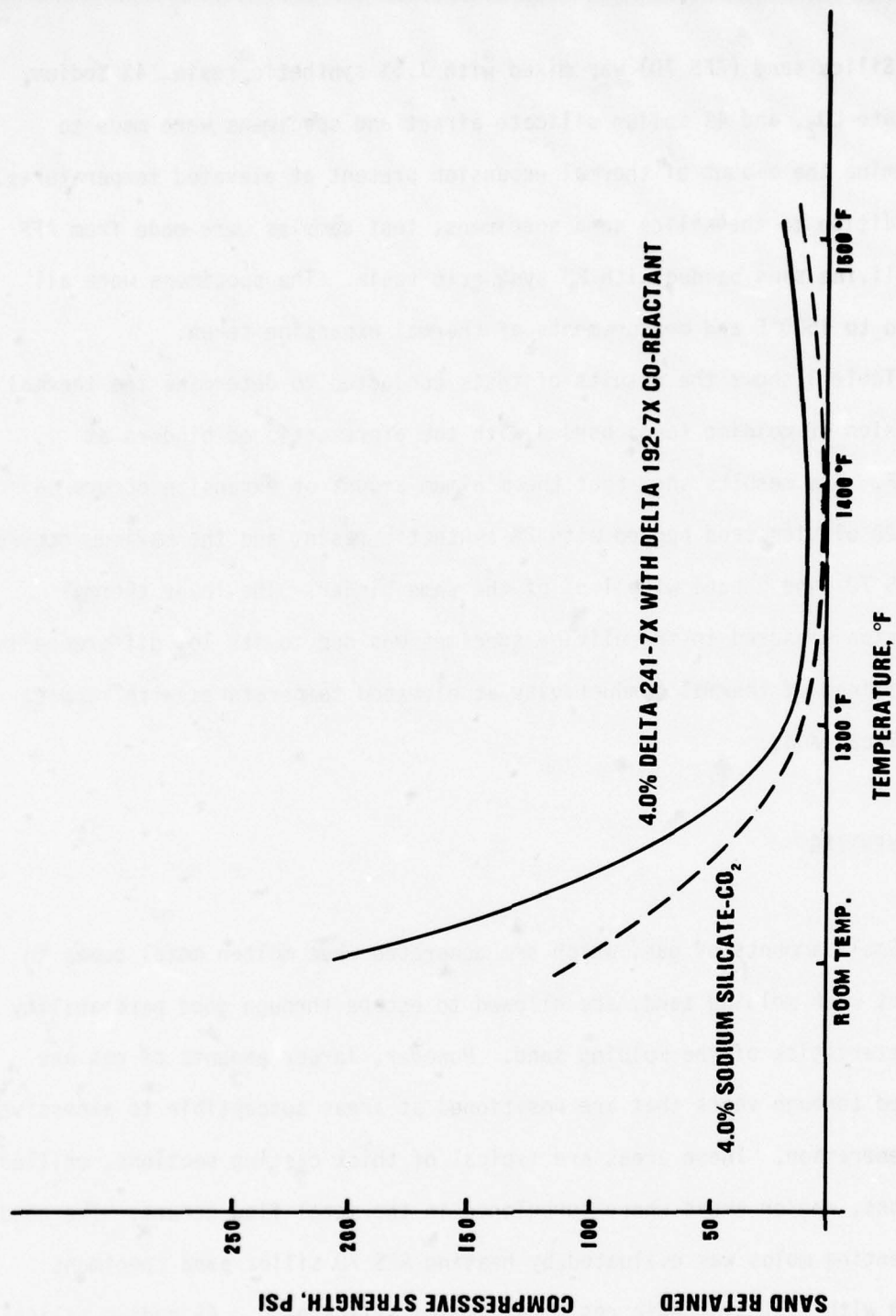


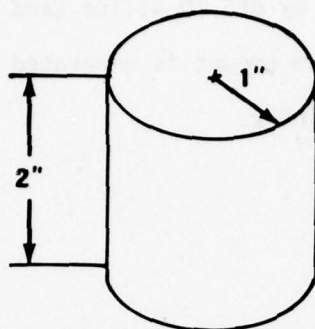
FIGURE 54 EFFECT OF ELEVATED TEMPERATURES ON RETAINED MOLD TENSILE STRENGTH OF AFS 70 SILICA SAND

Silica sand (AFS 70) was mixed with 1.5% synthetic resin, 4% sodium silicate- CO_2 , and 4% sodium silicate airset and specimens were made to determine the amount of thermal expansion present at elevated temperatures. In addition to the silica sand specimens, test samples were made from AFS 120 olivine sand bonded with 2% synthetic resin. The specimens were all heated to 1500°F and measurements of thermal expansion taken.

Table 3 shows the results of tests conducted to determine the thermal expansion of molding sands bonded with the aforementioned binders at 1500°F. The results show that the minimum amount of expansion occurs in AFS 120 olivine sand bonded with 2% synthetic resin, and the maximum occurs in AFS 70 sand bonded with 1.5% of the same binder. The lower thermal expansion measured in the olivine specimen was due to its low difference in coefficient of thermal conductivity at elevated temperatures with respect to silica sands.

3. VENTING

Small amounts of gas, which are generated when molten metal comes in contact with molding sand, are allowed to escape through good permeability characteristics of the molding sand. However, larger amounts of gas are removed through vents that are positioned at areas susceptible to excessive gas generation. These areas are typical of thick casting sections, chilled sections, and/or areas where turbulence in the metal flow occurs. The need for venting molds was evaluated by heating AFS 70 silica sand specimens bonded with 1.5% synthetic resin, 4% sodium silicate- CO_2 , 4% sodium silicate airset, and AFS 120 olivine sand bonded with 2% synthetic resin to 1500°F in a vacuum and measuring the evolved gas.

TABLE 3**THERMAL EXPANSION OF MOLD SAND AT ELEVATED TEMPERATURES****CONFIGURATION OF TEST SPECIMEN**

SAND TYPE	AFS NUMBER	BINDER TYPE	THERMAL EXPANSION
SILICA	70	1.5% DELTA 475-X ESTER SET WITH DELTA 217-6X CO-REACTANT	a. 9.2×10^{-6} IN/IN/°F b. 7.9×10^{-6} IN/IN/°F
SILICA	70	4.0% SODIUM SILICATE CO ₂	a. 4.3×10^{-6} IN/IN/°F b. 4.5×10^{-6} IN/IN/°F
SILICA	70	4.0% DELTA 241-7X WITH DELTA 192-7X CO-REACTANT	a. 1.6×10^{-6} IN/IN/°F b. 3.6×10^{-6} IN/IN/°F
OLIVINE	120	2.0% DELTA 475-X ESTER SET WITH DELTA 217-6X CO-REACTANT	a. 1.4×10^{-6} IN/IN/°F b. 2.8×10^{-6} IN/IN/°F

NOTE: ALL TESTS PERFORMED AT 1500°F

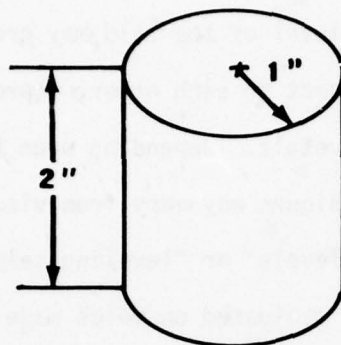
Table 4 shows the amount of gas generated by the specimens described in the preceding paragraph. The results of these tests show that the minimum amount of gas is generated by AFS 70 silica sand bonded with 4% sodium silicate airset, and the maximum amount is generated in AFS 120 olivine sand with 2% synthetic resin binder.

4. PARTING AGENTS

Other items that were given summary evaluations in this investigation include parting agents, methods of mold leveling, and methods of shaking out molds bonded with no-bake binders. Each of these items was considered, since they each represent significant variables of good molding practice.

Parting agents may be described as being fine, bondless compounds that are applied to mold joints to prevent contacting surfaces from adhering. In general, parting compounds are used to keep the molding sand from sticking to the pattern or at mold section interfaces. Various parting compounds are recommended by manufacturers of the binders evaluated in this investigation for use with the respective binder system or class (i.e., synthetic resin, oil-urethane, sodium silicate, etc.). These recommended parting agents were each used in conjunction with the respective binder system. With the Linocure binder system, and Ashland parting agents LP-15 and LP-16 "Zip-Slip" were evaluated. The LP-16 parting agent displayed superior parting characteristics, provided fine detail pickup, and lasted longer than the LP-15 agent. Although the composition of the LP-16 parting agent is unknown, it appears to be an aluminum-alcohol based solution. The parting agents evaluated in this investigation were all spray or brush applied.

TABLE 4
GAS EVOLUTION OF MOLD SAND ELEVATED TEMPERATURES



SAND TYPE	AFS NUMBER	BINDER TYPE	EVOLVED GAS
SILICA	70	1.5% DELTA 475-X ESTER SET WITH DELTA 217-6X CO-REACTANT	10.4L/kg
SILICA	70	4.0% SODIUM-SILICATE-CO ₂	10.2L/kg
SILICA	70	4.0% DELTA 241-7X WITH DELTA 192-7X CO-REACTANT	6.8 L/kg
OLIVINE	120	2.0% DELTA 475-X ESTER SET WITH DELTA 217-6X CO-REACTANT	17.6L/kg

NOTE: ALL TESTS PERFORMED AT 1500°F UNDER VACUUM.

5. MOLD LEVELING

The leveling of small molds consisting of two or three sections is typically not a problem. However, when molds using multiple flasks are made for large castings, the level of the mold may prove critical. If the flasks are not level with respect to each other, improper alignment and casting mismatch defects may result. Depending upon the sizes and number of flasks used, leveling techniques may vary from visual to using mechanical devices such as "bubble levels" or "leveling telescopes."

Leveling techniques were evaluated on molds made for parts of the configuration shown in Figure 18. The molds were leveled visually and with the aid of bubble levels, and then checked with a leveling telescope. Results of the observations proved that linear deviations as great as 0.250 inch were present when leveling was accomplished with the bubble level, but could be corrected to within 0.001 inch with optical leveling equipment.

6. SHAKE-OUT

Molds made with no-bake binders present considerable problems to shake-out operations. These molds typically retain most of their strength after pouring and resist conventional methods of shaking out. Under production situations, the sand may be separated from the casting by vibrating or mechanically breaking the sand free or by placing the entire mold in a furnace at about 850°F for 24 hours and allowing the binder to burn out. However, for large, thin-wall aluminum castings, removal of the sand by vibration severe enough to break the sand away from the casting may also

result in damage to the part. In addition, thermal break-down of the mold sand would require a furnace capable of maintaining the entire mold (less flasks) at the given temperature and time.

Although shake-out of the casting under thermal conditions is a feasible method for no-bake sand removal, it is considered a method conceivable only for high production rate castings. Consequently, since the aforementioned shake-out methods are considered unfavorable or impractical, casting shake-out is restricted to manually removing the sand from the casting. This can be accomplished by physically breaking the sand free of the casting with chisels, hammers, and/or pneumatic equipment especially designed for casting shake-out purposes. However, extreme caution must be exercised during sand removal by this method to protect the cast part from damage. This method of sand removal should be used to remove the bulk of the sand, so that the sand remaining on the part is about 1 to 2 inches thick. This thickness can be approximated by physically removing the sand until the vertical runners (discussed in a later section) are exposed. At this point, the remainder of the sand adhering to the casting may be removed by sand or grit blasting.

A means of reducing the time required for casting shake-out is by establishing a minimum sand-to-metal ratio. In aluminum casting, common sand-to-metal ratios are 10 to 1 for large, thin-wall castings and 6 to 1 for small, thick-section castings. The large, thin-wall castings require a higher sand-to-metal ratio since they represent greater total surface area than small, thick-section castings.

7. SUMMARY

Examination of the results and data discussed in this section show that molding sand to be used for producing large aluminum castings should have specific characteristics. These characteristics include good flowability, permeability, tensile strength, and compressive strength. The sand should also have high hot strength, low retained strength, and low thermal expansion and gas evolution characteristics. In general, good mold and core sand should be strong enough to withstand handling and resist deterioration by the molten metal at elevated temperatures; have good permeability to allow the passage of gas; be flowable and display good compaction and surface finish characteristics; and hold dimensional tolerances at elevated temperatures and provide ease in shake-out after cooling to room temperature.

In general, the results of this investigation show that after sand type and method of mixing have been established, the required properties of a molding sand depend upon binder type and percentage. The choice of binder type depends upon (1) obtainable mold properties, (2) applicability to required molding procedures, and (3) availability. In summarizing the results of tests conducted to determine the effect of storage time on mold properties with respect to binder type, the following conclusions were drawn:

1. Although sands bonded with sodium silicate- CO_2 and sodium silicate airset binders displayed good mold properties, the strengths obtained showed rapid deterioration after relatively short storage intervals. This decrease in strength is due to the hygroscopic nature of the binders (moisture pickup from humidity).
2. Molding sands bonded with synthetic resin binder displayed generally lower mold properties than obtained with all other binder types. In addition, the short work and strip times of molding sand using this type of binder are considered unfavorable for the production of molds for large aluminum castings.
3. Sands bonded with oil-urethane binders continued to display good mold properties after prolonged storage intervals and offered flexible work and strip times.

Due to the length of time required to construct a mold for a large aluminum casting, a binder that displays good mold properties after prolonged storage and provides flexible work and strip times is required. These characteristics were displayed by the oil-urethane binder (Linocure). The Linocure binder met each of the aforementioned criteria for binder selection and displayed favorable results in each of the tests described in this section.

In conclusion, the results of this investigation show that optimum mold properties for the examined systems were obtained from a molding sand consisting of AFS 53 or AFS 70 (depending upon application) silica sand bonded with about 1.10% Linocure when large, thin-wall aluminum parts are to be cast.

SECTION V
CHILLING AND/OR INSULATION REQUIREMENTS

1. CHILL MATERIAL, SIZE, AND LOCATION

The function of chills in a mold is to promote directional solidification and produce a microstructure with fine dendritic arm spacing (DAS). Directional solidification is the control imposed upon the liquid-to-solid transition from a solidifying section toward a molten metal reservoir (riser). The optimum distance between the chill and the riser is determined during the design of the mold gating system, and is discussed in section VI. In general, this distance is limited by the maximum area that the riser will feed to avoid shrinkage defects. The influence of the chill on cooling rate is related to the volumetric heat capacity of the chill material. Fine DAS is dependent upon rapid solidification of the cast material and is typically finest at the areas adjacent to the chill.

Chill materials that were evaluated in this investigation include copper, iron, aluminum, and graphite. Tests were conducted on parts cast in the configuration of Figure 8 ($T = 0.500$ inch) and specimens were removed to evaluate the effects of the chill materials on the mechanical properties of cast A357 aluminum alloy. In addition, the effect of chilling with respect to casting thickness was also evaluated by casting and testing parts of the same configuration as above. The effect of chill size on mechanical properties was evaluated using aluminum chills with dimensions of 6 x 2 x 2 inches and 6 x 1 x 1 inches. The effect of chill shape was evaluated by casting parts using rectangular and trapezoidal aluminum chills of equal mass.

The mechanical properties obtained from the use of different chill materials and sizes were determined by taking standard round tensile specimens from the test panels at locations 1, 4, 8, and 11 inches from the chilled end. The results of the chill material tests are shown in Figures 55 and 56, chill size in Figure 57, and chill shape in Figure 58. The results show that highest mechanical properties in terms of ultimate tensile strength, yield strength, and percent elongation occurred in test panels chilled with copper. The higher mechanical properties obtained with the copper chill were due to the higher thermal conductivity of copper relative to iron, aluminum, and graphite. In essence, the copper chill was able to transmit the heat of the molten metal away faster than with the other materials and caused a more rapid transition from liquid to solid. The result was finer dendritic arm spacing (DAS) and subsequent higher mechanical properties. The effect of DAS on the mechanical properties of cast A357 is discussed in detail in section XIII.

The results of tests to determine the effects of chill size on mechanical properties are shown in Figure 57. As chill size increases, mechanical properties increase. The reason for the higher mechanical properties displayed by the parts cast with the larger chill is that the volumetric thermal capacity is higher in the larger chill. However, it can be seen that there is a limit to the size of chill beyond which mechanical properties do not increase. In general, the mass of the chill should equal 1 to 2 times the mass of the section being chilled.

As shown in Figure 58, the difference in mechanical property development between parts cast with rectangular and trapezoidal aluminum chills of equal volume was negligible. The two shapes that were evaluated represented different surface areas in contact with the molten aluminum. The contact surface areas of the trapezoidal and rectangular chills were 6 (6 x 1) and

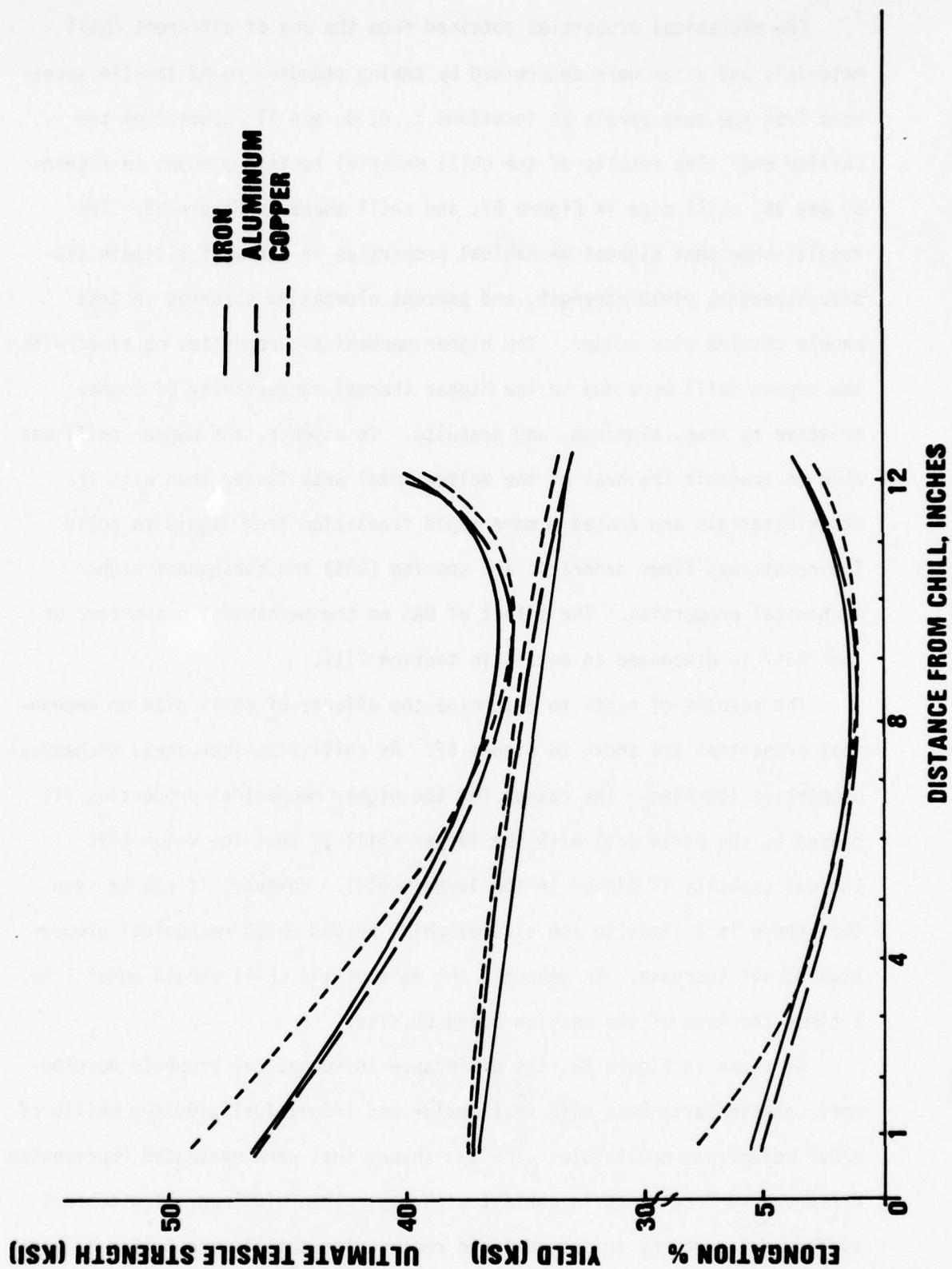


FIGURE 55 EFFECT OF CHILL MATERIAL ON MECHANICAL PROPERTIES OF A357

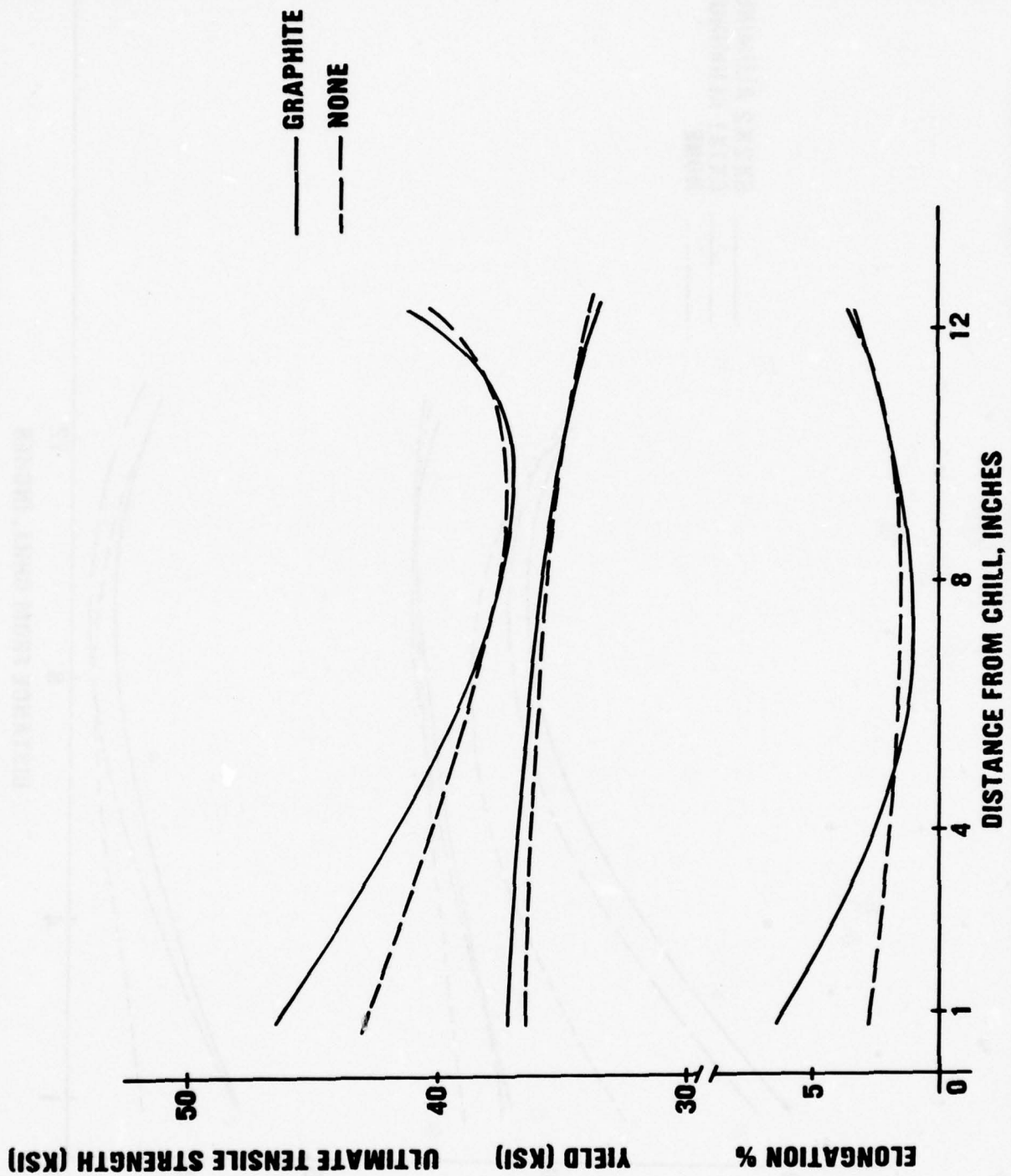


FIGURE 56 EFFECT OF CHILL MATERIAL ON MECHANICAL PROPERTIES OF A357

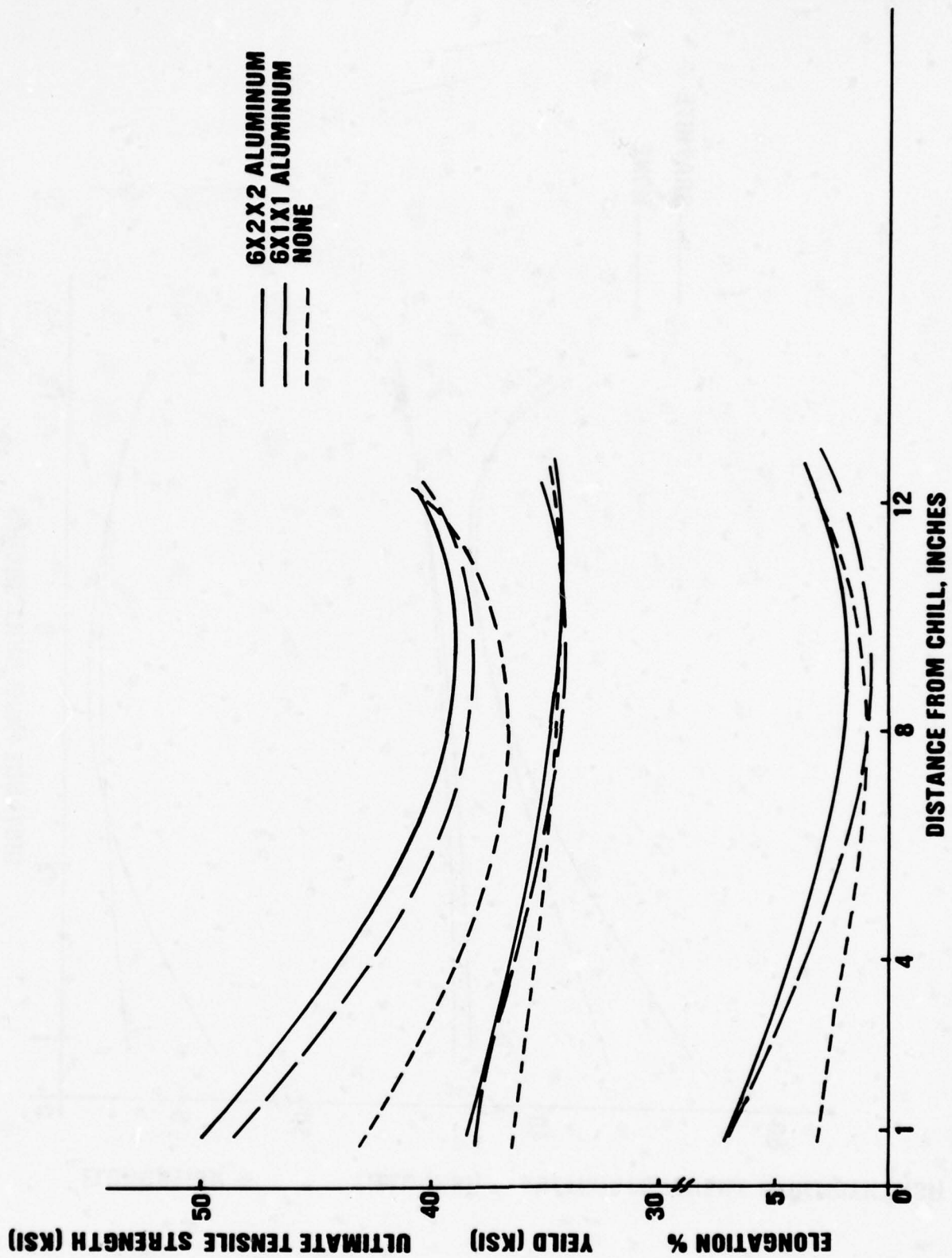


FIGURE 57 EFFECT OF CHILL MASS ON MECHANICAL PROPERTIES OF A357

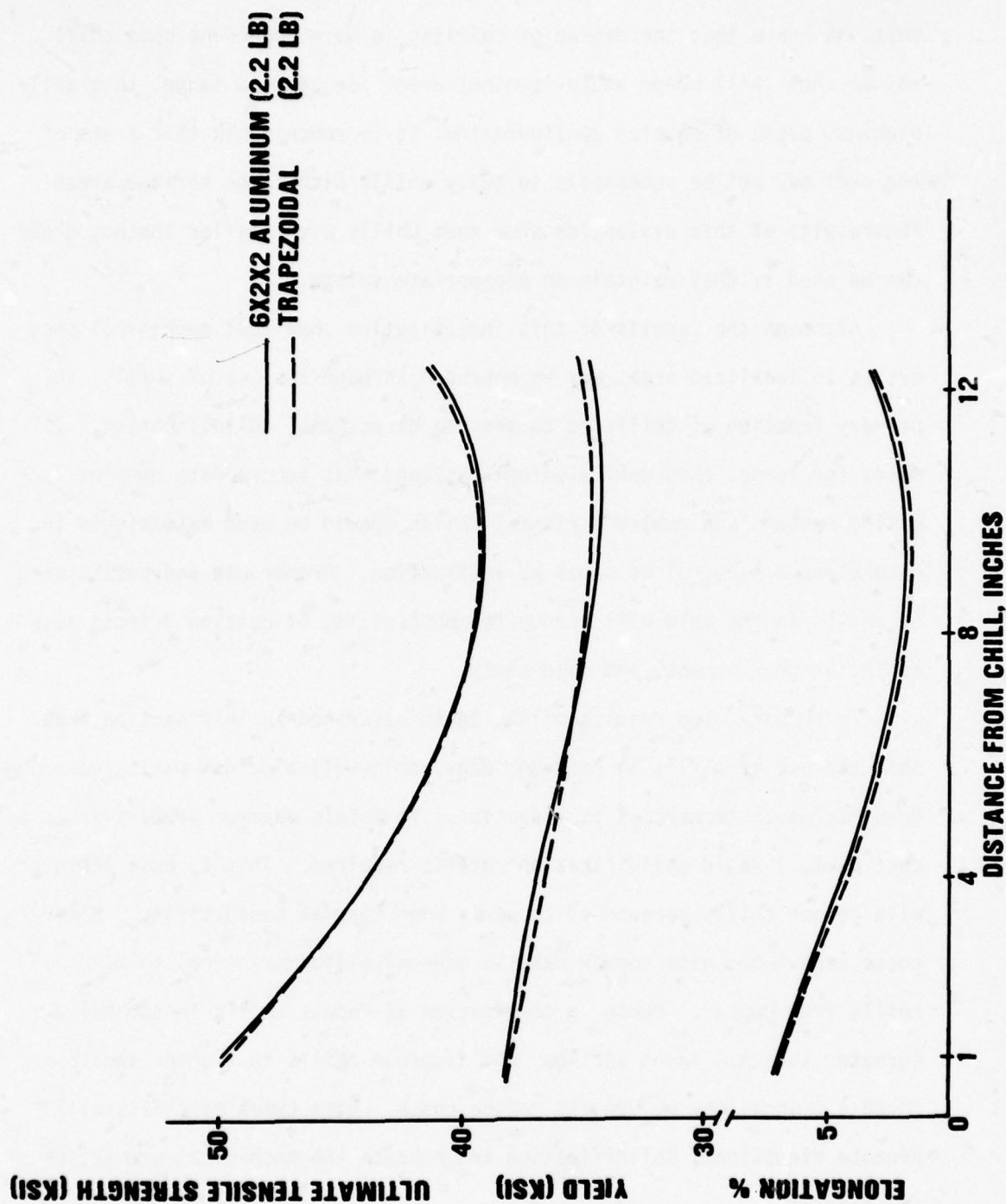


FIGURE 58 EFFECT OF CHILL CONFIGURATION WITH SAME MASS ON MECHANICAL PROPERTIES OF A 357

12 (6 x 2) square inches, respectively. These results are significant in that they show that the degree of chilling is more dependent upon chill volume than chill shape and/or contact area. In casting large, thin-wall aluminum parts of complex configuration, it is conceivable that areas of the part may not be accessible to heavy chills with large surface areas. The results of this evaluation show that chills with smaller contact areas can be used if they maintain an appropriate volume.

Although the results of this investigation show that mechanical properties in localized areas may be enhanced through the use of chills, the primary function of chills is to promote directional solidification. In molds for large, thin-wall aluminum castings that incorporate complex gating systems and numerous risers, chills should be used extensively to ensure proper control of metal solidification. Proper use and positioning of chills in the mold will reduce the possibility of casting defects such as shrinkage, misruns, and cold shuts.

In summary, the results of the tests described in this section show that the use of chills in casting large, thin-wall aluminum parts requiring good "as-cast" properties is essential. To obtain maximum properties in a cast part, a rapid solidification rate is required. This is best achieved with copper chills because of copper's high thermal conductivity. However, costs associated with copper make it economically impractical to make all chills from copper. Hence, a combination of copper chills in the heavy (greater than 1.0 inch) sections and aluminum chills in lighter sections (0.20-1.0 inch) may be used to reduce costs. Both types of chills will promote directional solidification and enhance the mechanical properties of the casting.

The configuration of the chills will be dictated by the shape of the area to be chilled. Based on our experience and that of other foundries, the total thickness of the chill should equal 1 to 2 times the thickness of the section being chilled.

2. INSULATION MATERIAL, SIZE, AND LOCATION

Insulating materials such as plaster, ceramic, and fibrous material are used by the casting industry to provide improved fluidity and/or decrease the solidification rate of molten aluminum. These materials are commonly used to insulate risers or thin sections of aluminum castings, which are susceptible to cold shut or misrun defects.

Risers, which are molten reservoirs of metal, play an important role during metal solidification. The transition from the molten metal to the solidified casting takes place in three steps: (1) the molten metal cools from the pouring temperature to the solidification temperature, (2) the metal cools through the temperature range at which it solidifies, and (3) the solidified metal cools to room temperature. As the metal cools to room temperature, contraction takes place. The contraction that occurs as the metal cools to the solidification temperature is known as liquid contraction. The contraction related to the second step in cooling is called solidification contraction, and through the third step solid-state contraction occurs. These latter forms of contraction are compensated for during pattern design by using an established shrink rule. To compensate for contraction occurring during the transition from the pouring temperature through the solidification range, risers are used. Typically, aluminum castings will display a decrease in volume during the solidification range of about 6.5%. This decrease in volume (due to liquid and solidification

contraction) may be described as metal shrinkage and is controlled by proper use and location of risers. Risers feed molten metal to the casting as it solidifies and minimize the occurrence of shrinkage porosity defects. To ensure proper feeding, the riser must remain in the molten state until the casting passes through the solidification range and becomes solid. This molten state of the metal in the risers may be controlled by insulating the riser cavity from the molding sand.

Preformed riser sleeves consisting of a fibrous material composite and cast plaster risers were evaluated in this investigation. Parts were cast in the configuration shown in Figure 59 with composite and plaster riser sleeves and the cooling rate of each monitored with thermocouples attached to a multipoint reader. The results of this evaluation are shown in Figure 60. The data from this evaluation show that there is negligible difference between the insulating characteristics of the composite sleeve and the plaster riser. However, due to the inherent hygroscopic nature of the plaster sleeve even after prolonged drying, gas defects were noted in areas of the part fed by that riser.

Since insulation of mold sections results in a reduction in the solidification rate, insulation materials may be used to induce the feeding of sections that are susceptible to misrun or cold shut defects. This theory was evaluated by casting parts in the configuration shown in Figure 61 and placing plaster or ceramic foam block pads at the middle of each test plate. The dimensions of the insulating pads used in this investigation are 6 x 2 x 0.5 inches and 6 x 2 x 1 inches. Thermocouples connected to a multipoint recorder were located above and on either side of the insulating pads and used to determine the metal cooling rate. The results of these tests are shown in Figures 62-65. These parts were poured at 1400°F and,

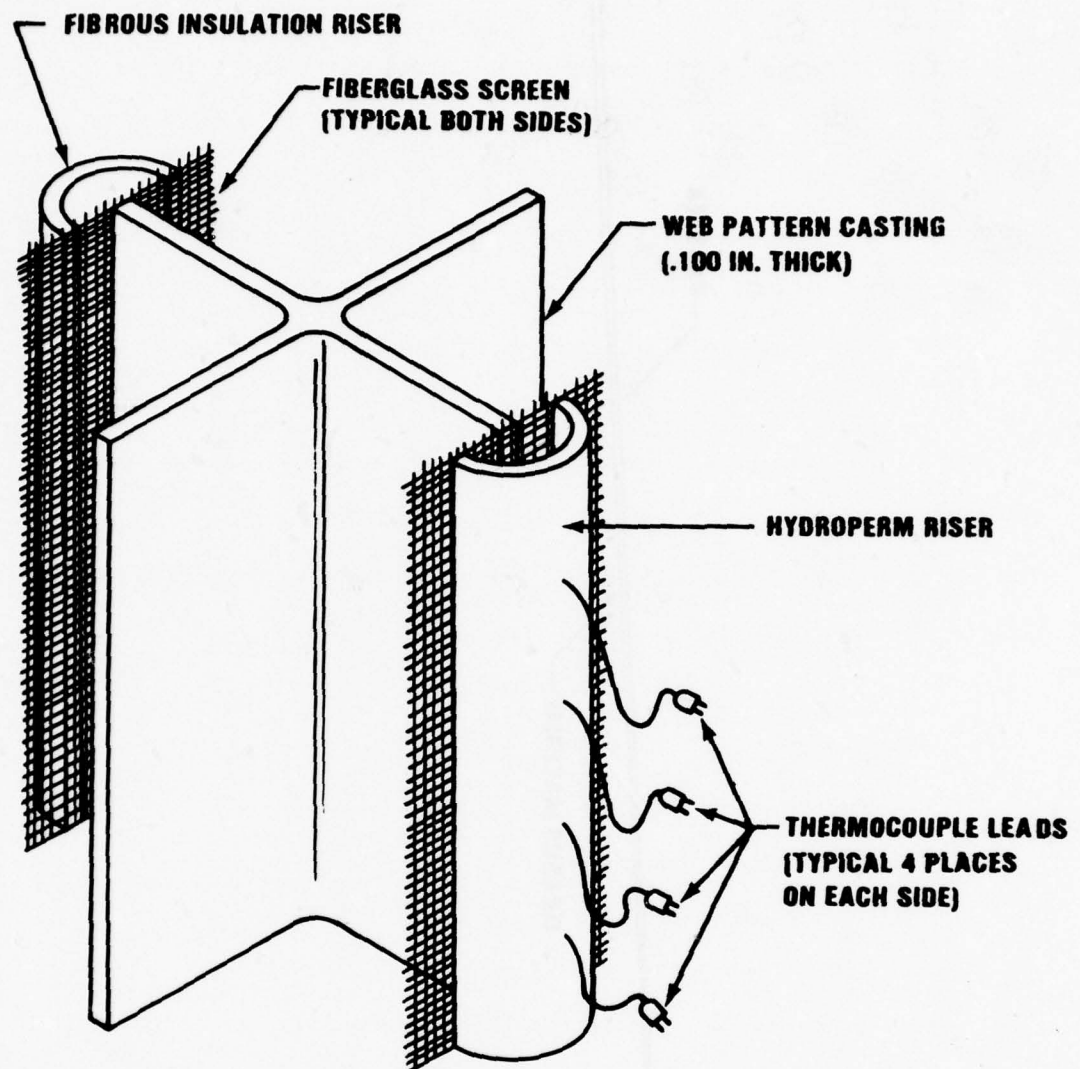


FIGURE 59 TEST CONFIGURATION FOR THE EVALUATION OF VERTICAL RUNNER INSULATION MATERIAL

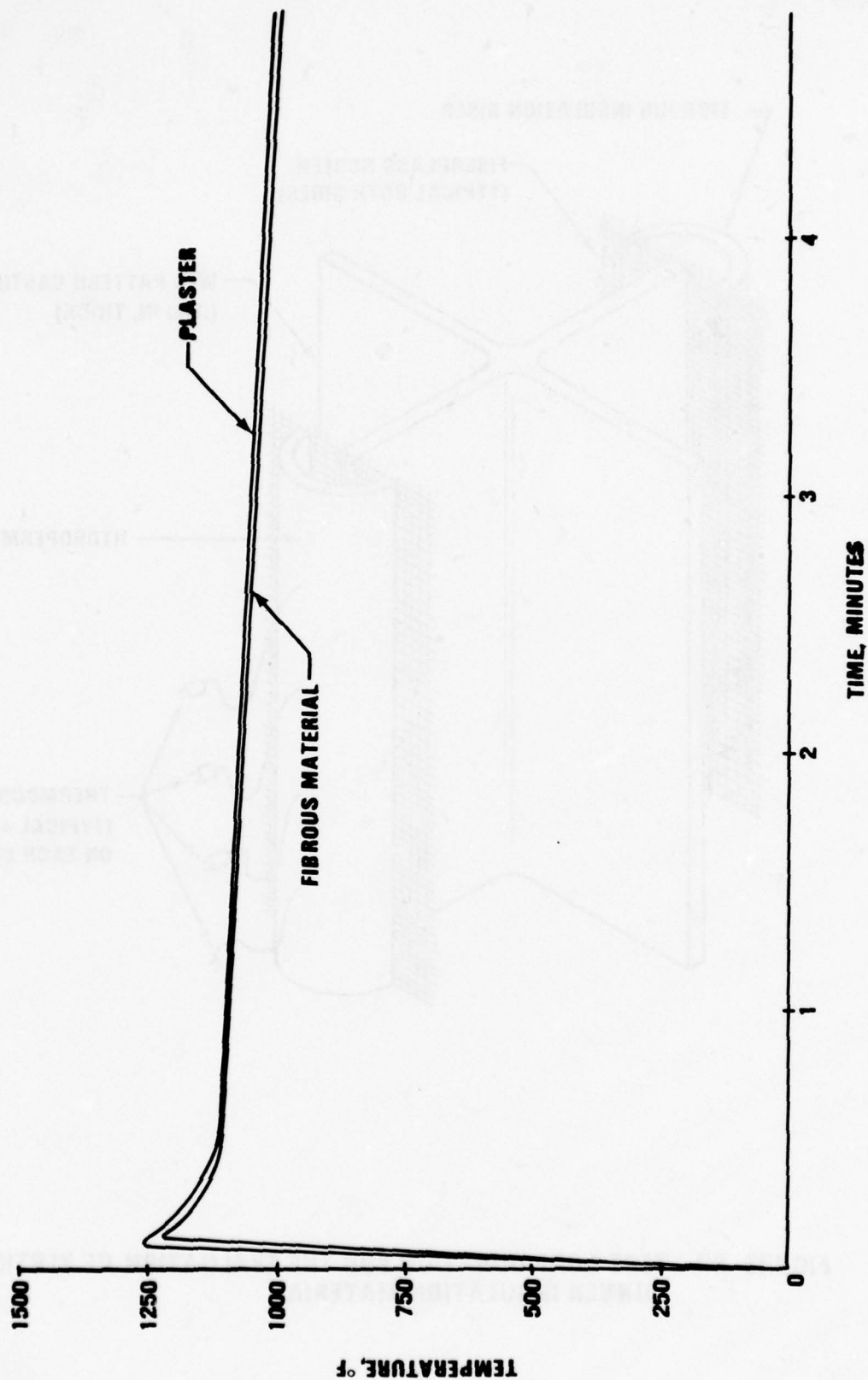


FIGURE 60 EFFECT OF INSULATING RISER MATERIAL ON THE SOLIDIFICATION RATE OF A357

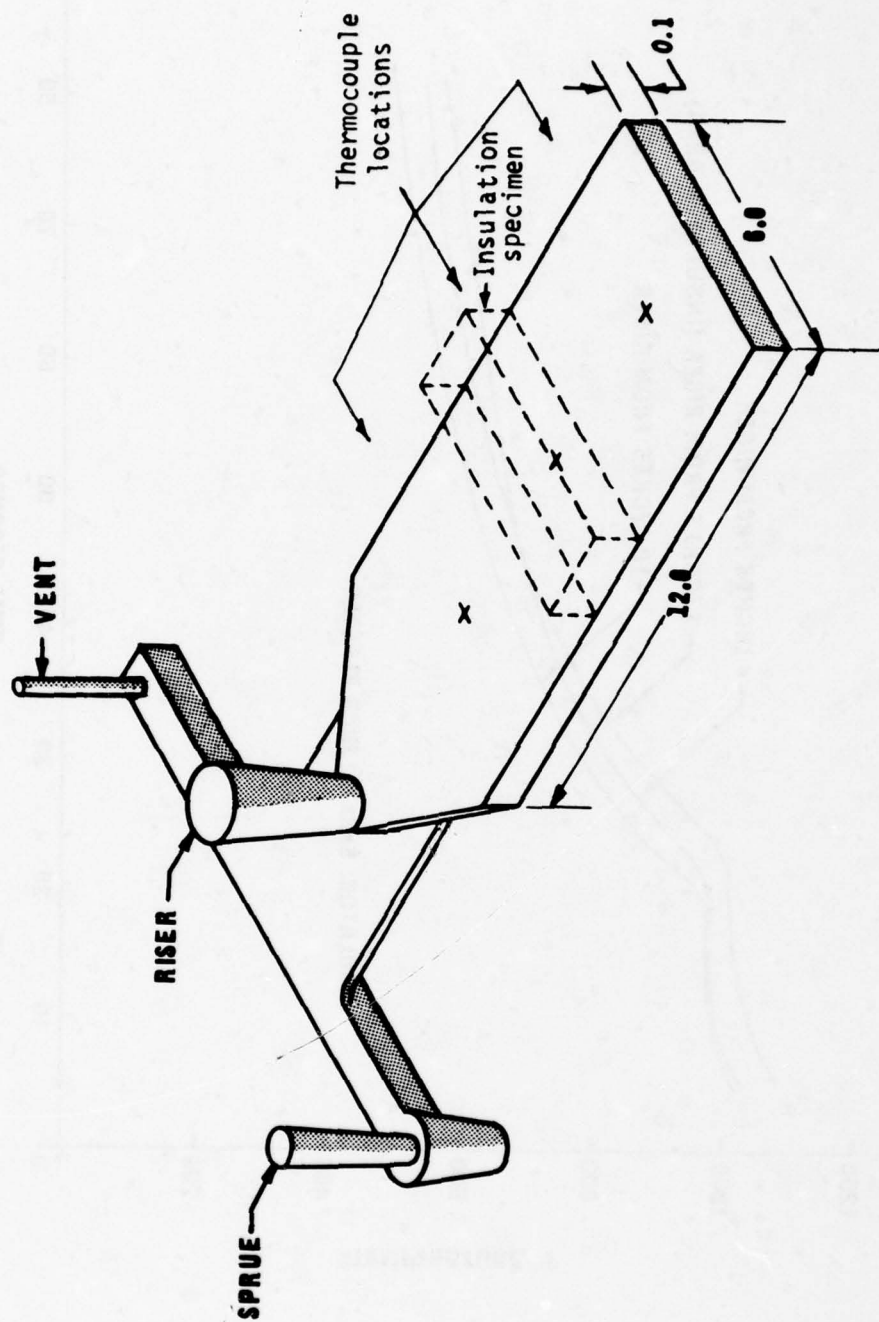


FIGURE 61 CONFIGURATION OF TEST PLATE FOR INSULATION TESTS

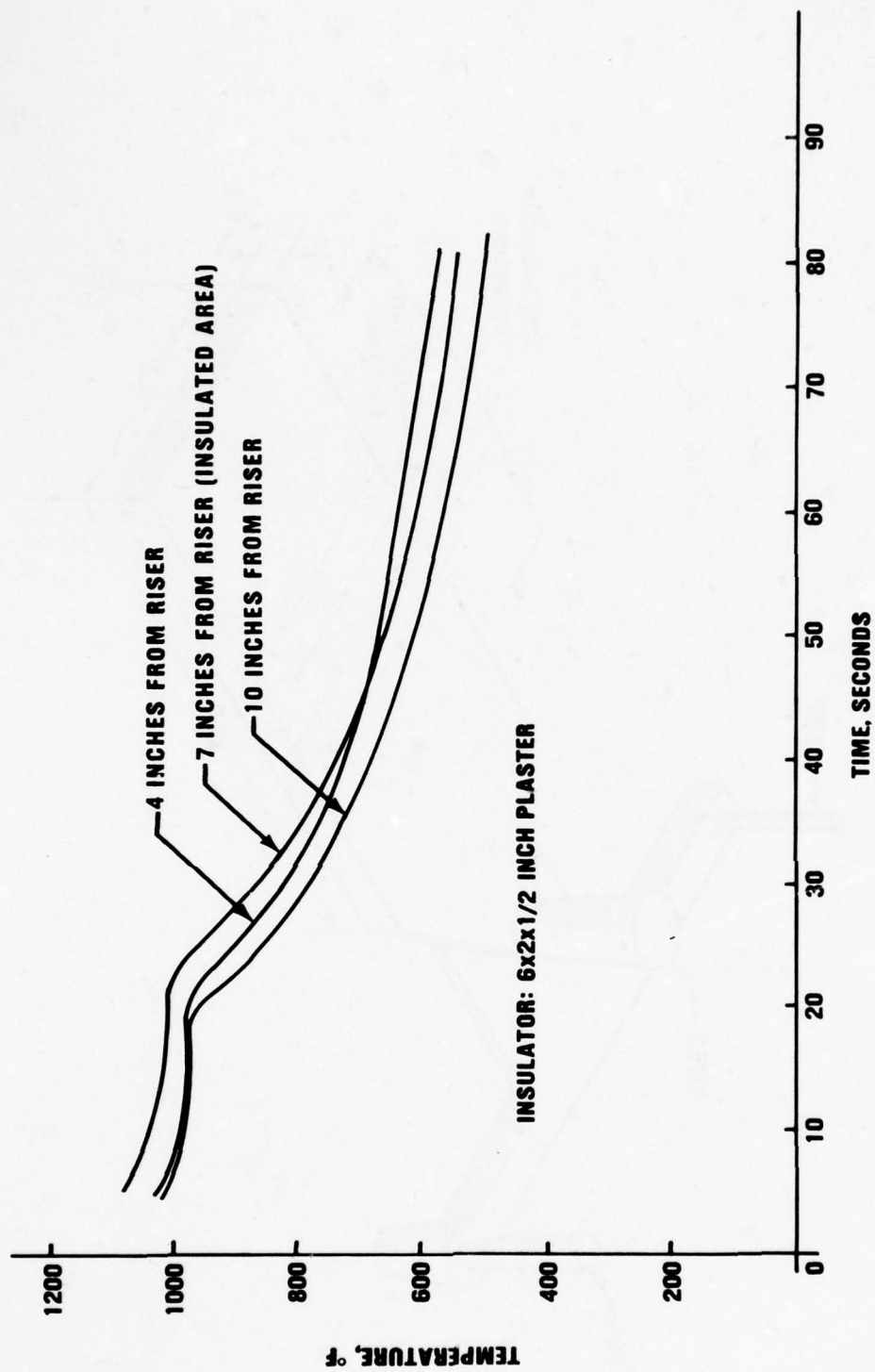


FIGURE 62 EFFECT OF .50" THICK PLASTER INSULATION ON THE SOLIDIFICATION RATE OF .10" THICK TEST PLATE

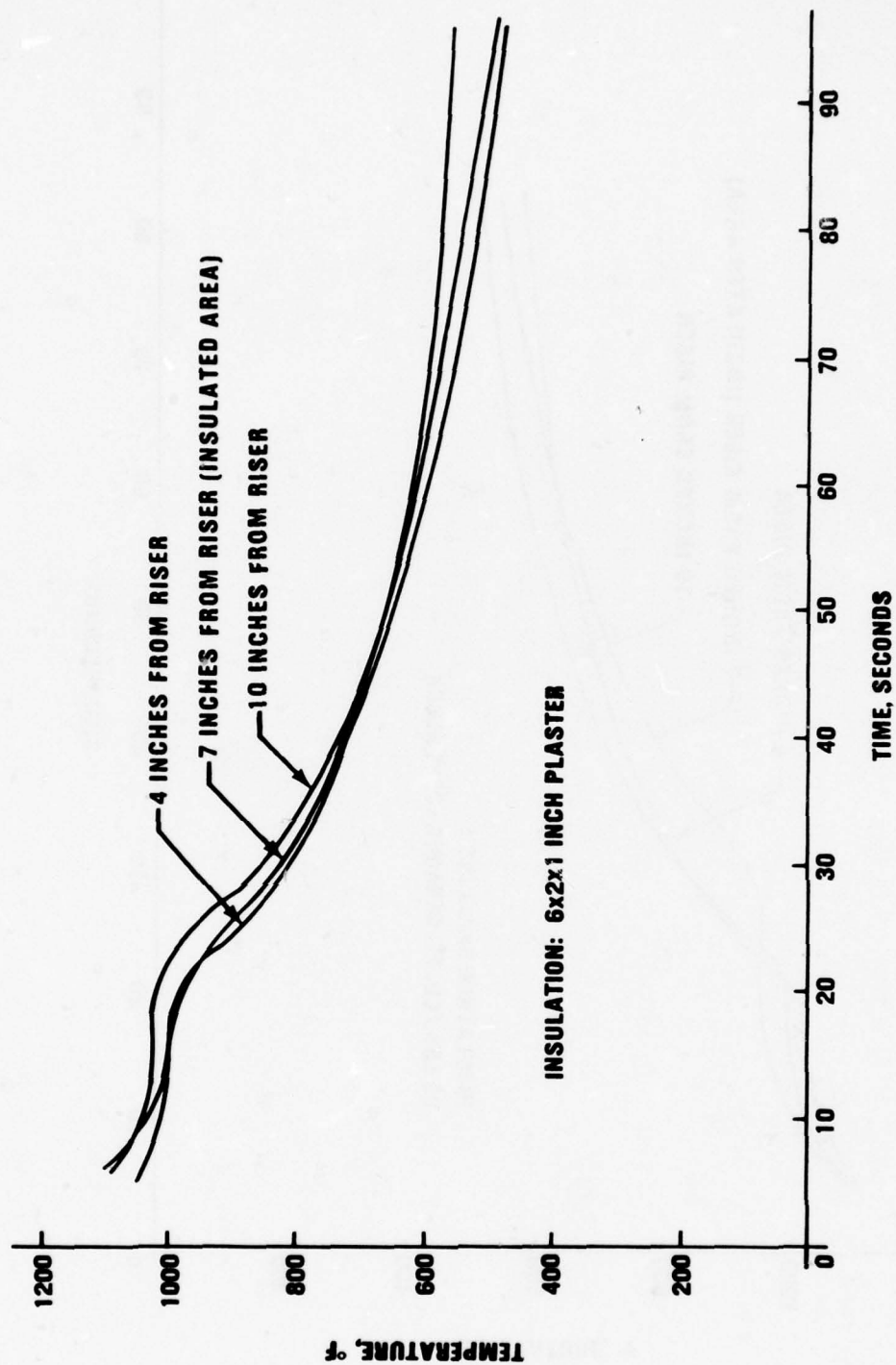


FIGURE 63 EFFECT OF 1" THICK PLASTER INSULATION ON THE SOLIDIFICATION RATE OF .10" THICK TEST PLATE

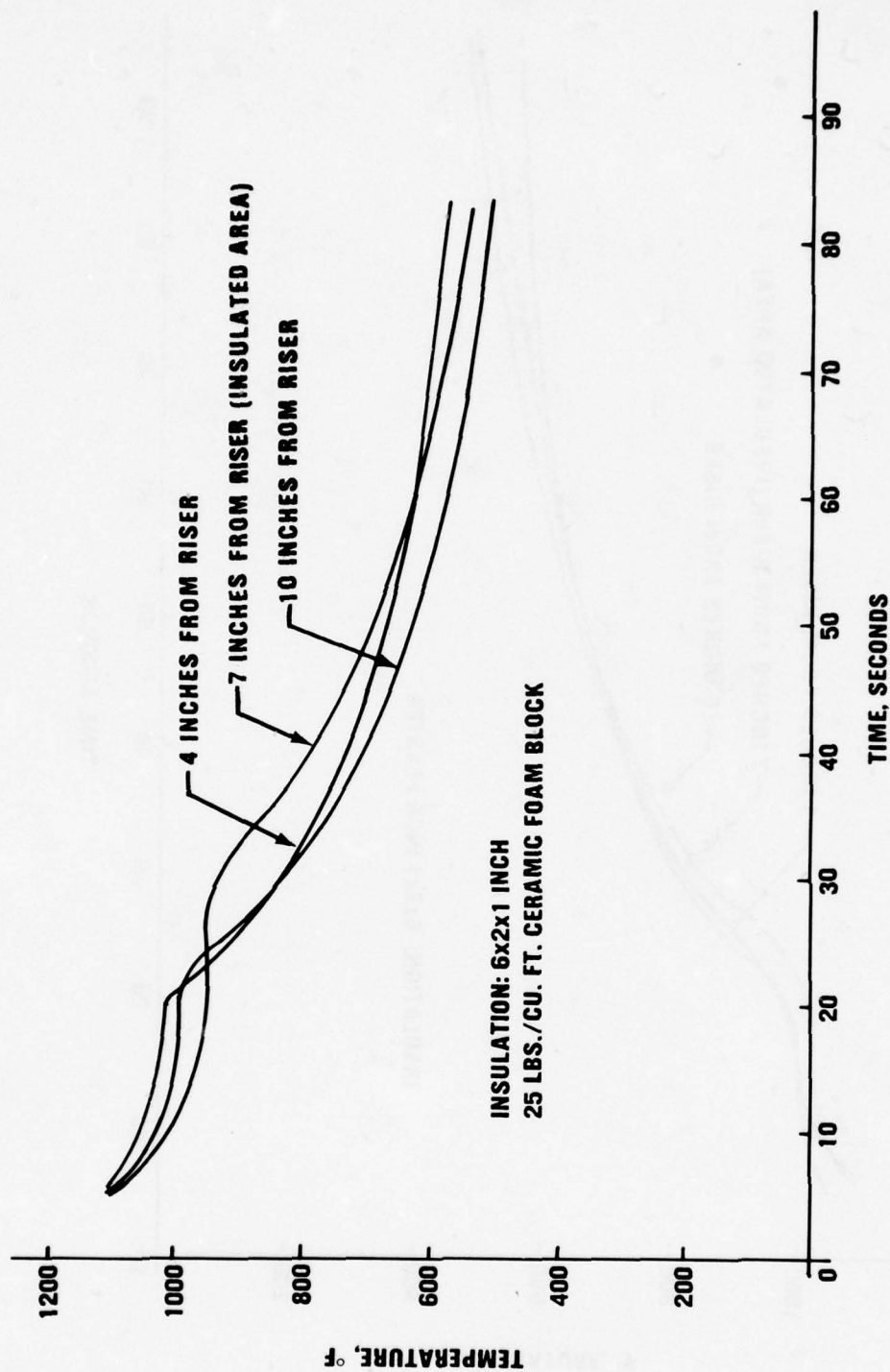


FIGURE 64 EFFECT OF 1" THICK CERAMIC FOAM BLOCK (25 LBS./CU. FT.) INSULATION ON THE SOLIDIFICATION OF .10" THICK TEST PLATE

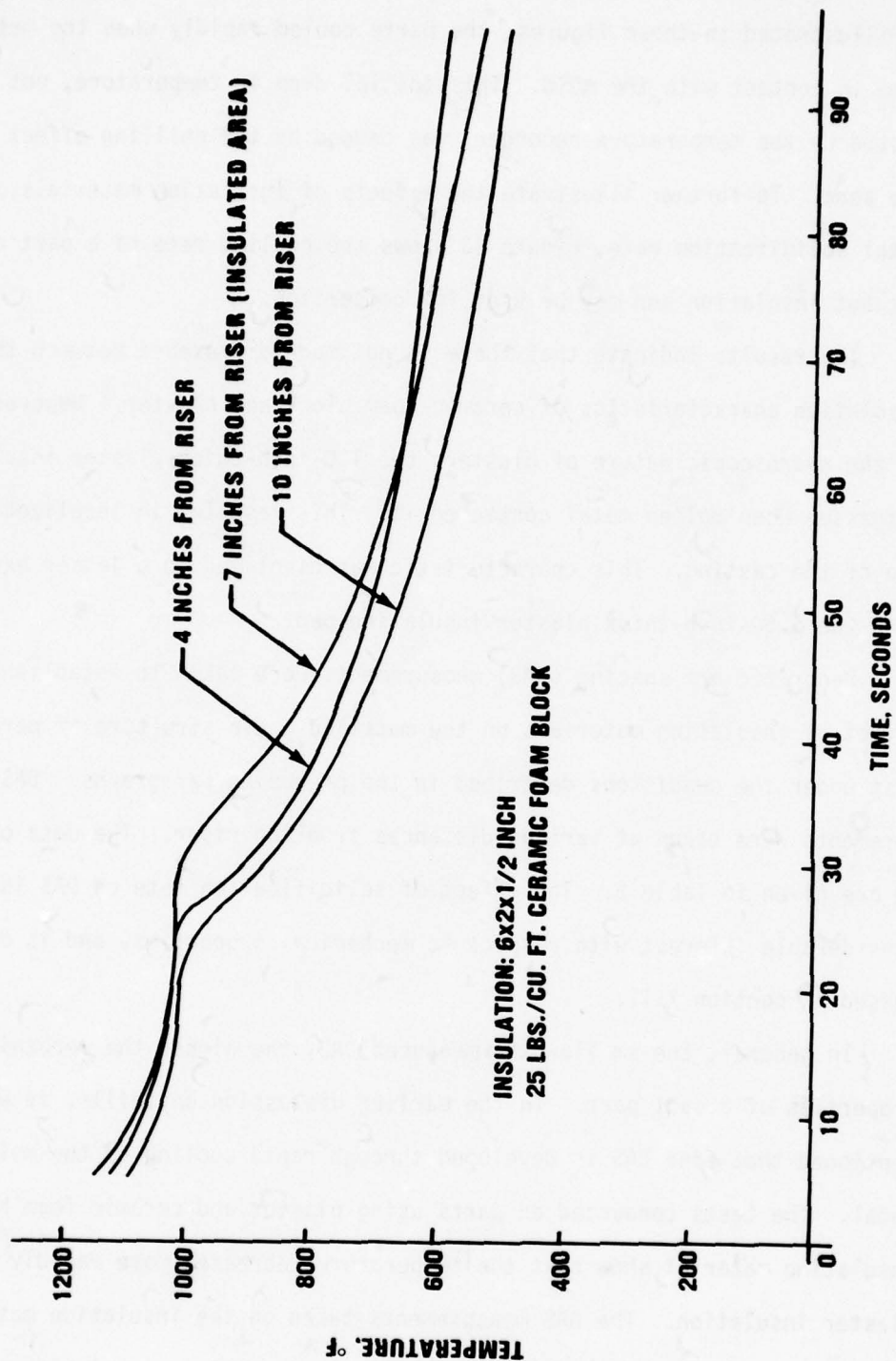


FIGURE 65 EFFECT OF 1/2" THICK CERAMIC FOAM BLOCK (25 LBS./CU. FT.) INSULATION ON THE SOLIDIFICATION RATE OF .10" THICK TEST PLATE

as illustrated in these figures, the parts cooled rapidly when the metal came in contact with the mold. This initial drop in temperature, not detected by the temperature recorder, was caused by the chilling effect of the sand. To further illustrate the effects of insulation materials on the metal solidification rate, Figure 66 shows the cooling rate of a part cast without insulation and may be used for comparison.

The results indicate that there is not much difference between the insulation characteristics of ceramic foam block and plaster. However, due to the hygroscopic nature of plaster, the 1.0-inch-thick plaster insulation outgassed when molten metal contacted it. This resulted in localized warpage of the casting. This characteristic was displayed to a lesser extent with the 0.50-inch-thick plaster insulating pad.

Dendritic arm spacing (DAS) measurements were taken to establish the effect of insulating materials on the metallic grain structure of parts cast under the conditions described in the preceding paragraphs. DAS measurements were taken at various distances from the riser. The data obtained are given in Table 5. The effect of solidification rate on DAS is of considerable interest with respect to mechanical properties, and is discussed in section XIII.

In general, the smaller the measured DAS, the higher the mechanical properties of a cast part. In the earlier discussion on chills, it was mentioned that fine DAS is developed through rapid cooling of the molten metal. The tests conducted on parts using plaster and ceramic foam block insulating material show that the temperature decreases more rapidly with plaster insulation. The DAS measurements taken on the insulation materials tested show negligible difference in DAS with respect to insulating material.

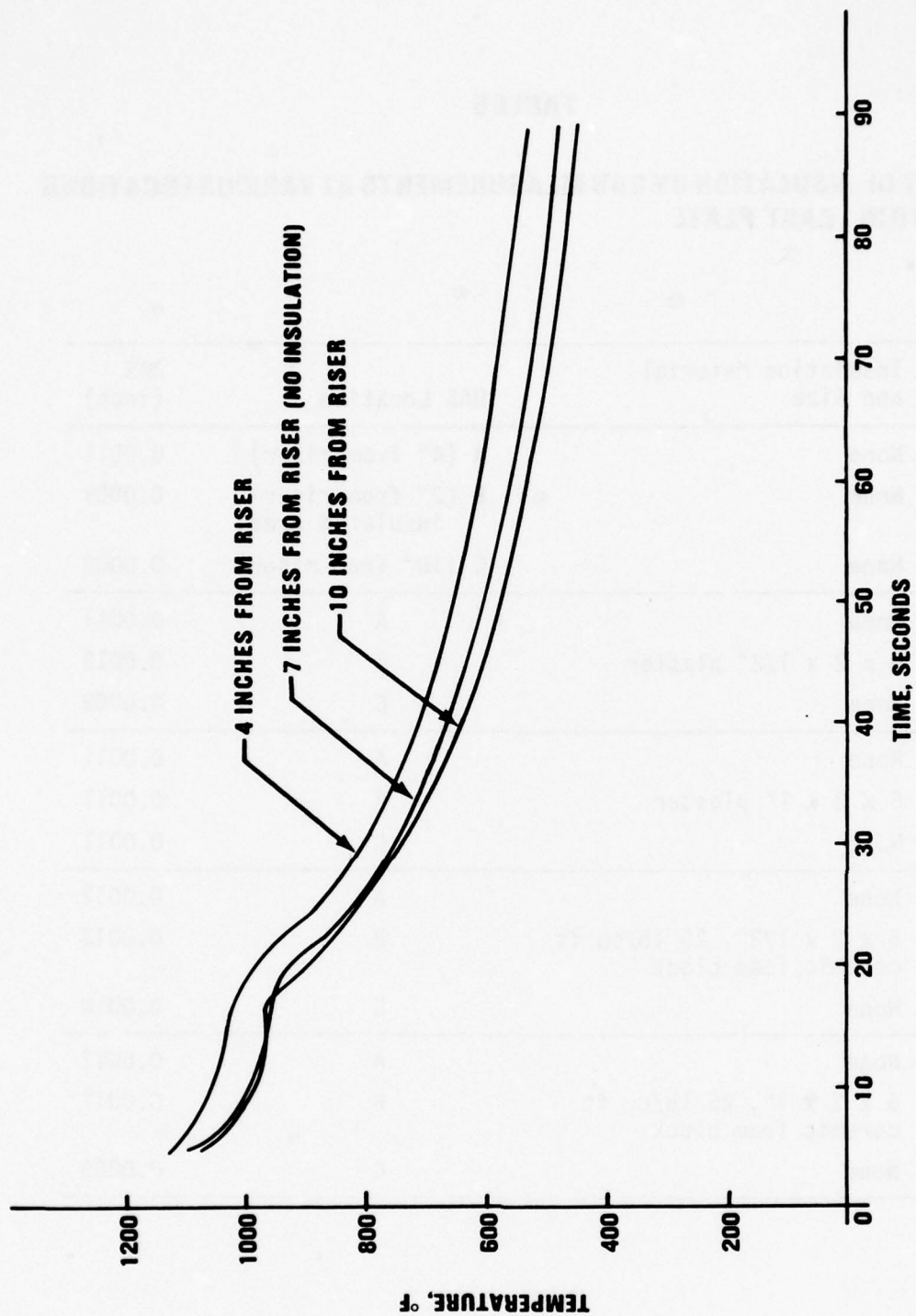


FIGURE 66 SOLIDIFICATION OF .10" THICK TEST PLATE AT VARIOUS DISTANCES FROM RISER
WITH NO INSULATION

TABLE 5**EFFECT OF INSULATION ON DAS MEASUREMENTS AT VARIOUS LOCATIONS
ON A .10 IN. CAST PLATE**

Insulation Material and Size	DAS Location	DAS (inch)
None	A (4" from riser)	0.0011
None	B (7" from riser- insulated area)	0.0009
None	C (10" from riser)	0.0009
None	A	0.0011
6 x 2 x 1/2" plaster	B	0.0012
None	C	0.0009
None	A	0.0011
6 x 2 x 1" plaster	B	0.0011
None	C	0.0011
None	A	0.0012
6 x 2 x 1/2", 25 lb/cu ft ceramic foam block	B	0.0013
None	C	0.0010
None	A	0.0012
6 x 2 x 1", 25 lb/cu ft ceramic foam block	B	0.0012
None	C	0.0009

In summary, we can conclude that plaster displayed unfavorable results when used as a riser sleeve material and as an insulating material for thin sections. When used as a riser material, it showed no significant improvement over the paper-fiberglass composite material tested and also caused gas defects in the cast test part. As an insulating material for thin-section castings, plaster displayed the same insulating properties as ceramic foam block, and outgassed when contacted with molten aluminum. Based on the results of this investigation, the optimum material for riser sleeve is paper-fiberglass composite and the best insulating material for casting thin sections is ceramic foam block. The thickness of the insulating material used should be held to the minimum required to obtain good feeding characteristics.

SECTION VI

GATING AND RISERING TECHNIQUES

1. GATING TECHNIQUES

The gating technique used to get metal into the mold cavity is one of the most important contributors to the production of sound castings. Improper gating practice can result in a wide variety of casting defects. Various gating techniques were analyzed to consistently ensure the promotion of directional solidification, adequate mold filling, proper riser feeding, and minimum turbulence. The gating parameters considered in this investigation were gating ratio, sprue height and shape, straining materials, and riser size and location. It was not the purpose of this investigation to develop data on the flow characteristics of metal in the gating system, but rather to evaluate different gating systems and assess their effectiveness to consistently produce high-quality aluminum castings.

a. Pouring Position

One of the first concerns in designing a gating system is to determine if the part should be cast vertically or horizontally. Horizontal gating is the most commonly used technique because it generally is less complicated to mold, has less hydrostatic pressure, and produces less metal turbulence. However, large, thin-wall castings are impractical to cast in a horizontal position because of nonuniform directional solidification and the potential for mold sag.

Castings horizontally cast are usually filled from the bottom of the mold through the mold cavity and then into the risers. This means that all the metal must pass through the casting before solidification can begin. This gives rise to nonuniform directional solidification which, as discussed earlier, leads to lower mechanical properties. On the other hand, when parts are cast in the vertical position, directional solidification is promoted because the metal is gated into the casting only when and where metal is required. Solidification can then be controlled by judicious placement of chills, thus allowing the metal to solidify toward each riser/ingate combination. However, the main disadvantage of vertical gating of large, thin-wall castings is a large sprue height that, if not properly designed, will cause metal turbulence.

Two test sections were selected for evaluation of gating techniques. These sections, shown in Figures 18 and 19, represent portions of the YC-14 station 170 body bulkhead. For the reasons explained above, a vertical gating system was selected for evaluation during this phase.

b. Gating Ratio

The next decision to be made in designing a gating system for large, thin-wall casting applications is to select a gating ratio. An unpressurized gating system should be used. This is one where the cross-sectional area at the base of the sprue is less than the total area of the runner and the total area of the ingates. The flow rate in this type of system is controlled at the sprue. The advantage of the unpressurized system is a slow metal flow in relatively large runners and ingates. A slow metal flow minimizes metal turbulence and prevents a rapid surge of metal entering the mold cavity.

At the start of this investigation, a 1:4:4 gating ratio was used when designing the gating system for the part shown in Figures 18 and 19. Schematic diagrams of the gating systems are shown in Figures 67 and 68. The metal flow in a vertical gating system such as shown in these figures is down the sprue into the horizontal runner, through the ingates to one of any number of vertical runners, and into the casting through a series of step gates. The gating ratio does not take into account cross-sectional areas of the vertical runner and step gates. It was determined from this investigation that as long as the cross-sectional area of the vertical runner was larger than the area of an ingate and the total areas of two step gates were larger than the area of an ingate, metal flow would not be restricted.

The size of the down sprue was determined from the standard flow rate equation (ref. 1):

$$A_B = \frac{W}{(\frac{2gh}{f})^{-1/2}}$$

where A_B = area at base of sprue (in.²)
 W = flow rate (lb/sec)
 ρ = density of aluminum (0.086 lb/in.³)
 g = gravitational acceleration (386 in./sec²)
 h = total height (in.)
 f = frictional factor (1.3 for round sprues)

- (1) Kura, John G., "Gating Calculations," American Foundryman, May 1955, pp. 123-124.

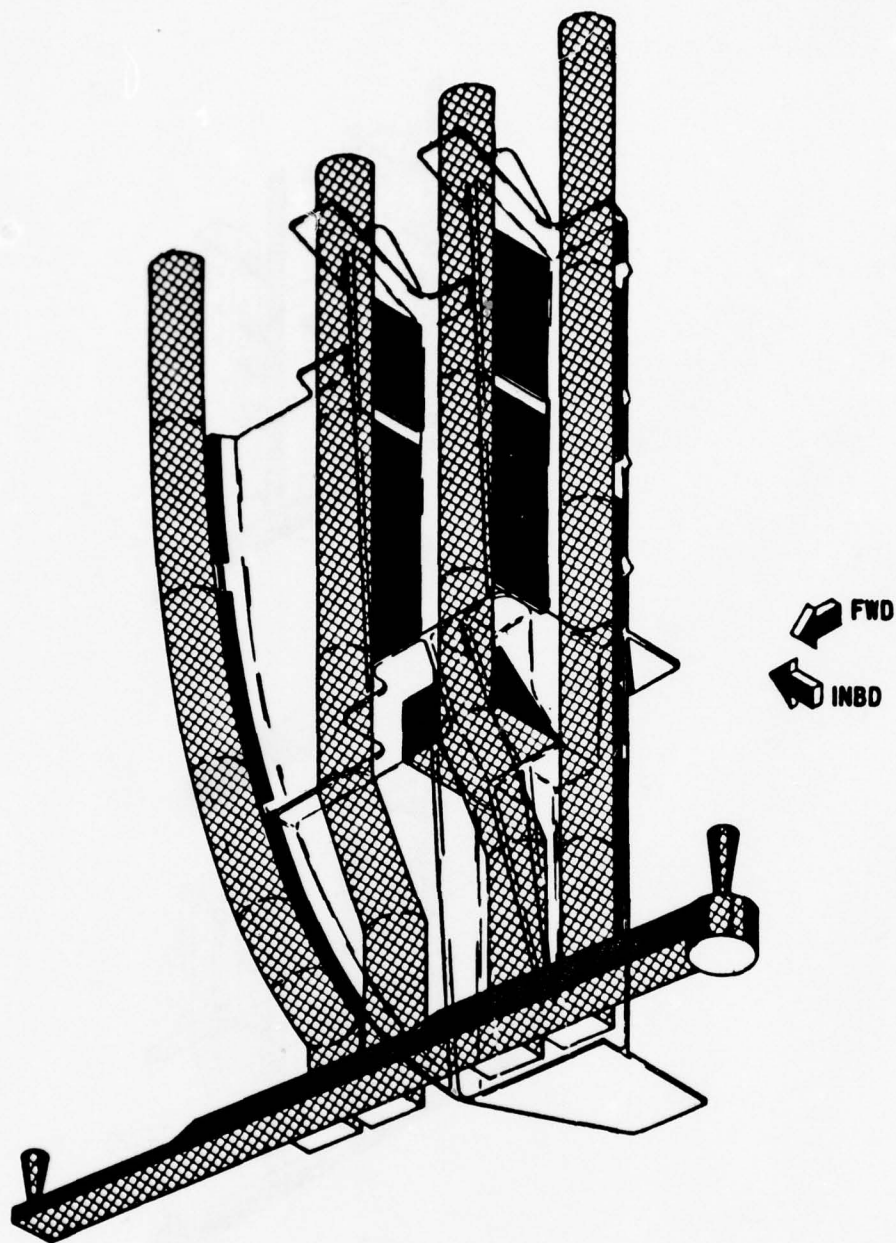


FIGURE 67 PART "A" CONFIGURATION WITH GATING SYSTEM ATTACHED

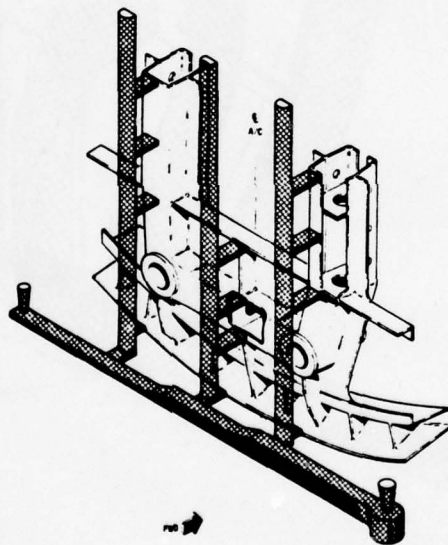
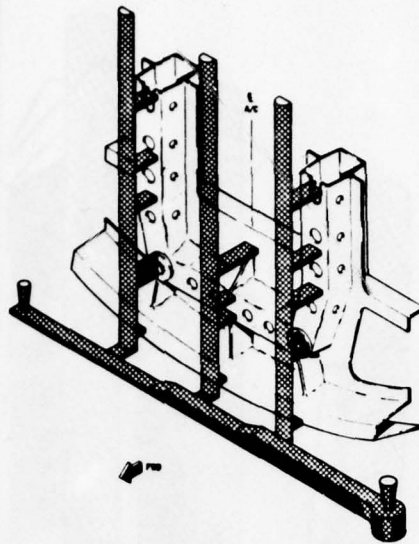


FIGURE 68 PART "B" CONFIGURATION WITH GATING SYSTEM ATTACHED

In order to arrive at the proper sprue size, a flow rate of 7 lb/sec was chosen. It was felt that this flow rate would fill the mold in the shortest amount of time while still maintaining laminar flow. From these calculations, two sprues, each 0.75 inch diameter x 52.5 inches high, were initially selected for the configuration shown in Figure 18. After pouring the part at 1450°F, radiographic inspection revealed the presence of dross and porosity throughout the part. The poor quality of this part was attributed to the 1:4:4 gating ratio. It was suspected that this gating ratio, coupled with a large sprue height, resulted in a high metal velocity at the ingates, causing turbulent flow of metal into the mold. To overcome this problem, a 1:8:8 gating ratio was evaluated.

Using the larger gating ratio with the same sprue sizes, the metal velocity from the runner to the ingates would be lower due to the larger runner and ingate area. This lower velocity should result in less turbulence and thus better radiographic quality. Another casting of the same configuration was cast under similar circumstances except with the larger gating ratio. The internal quality of this casting was indeed better than previously experienced, but unacceptable gas porosity, dross, and small misruns still persisted.

The gating ratio was then changed to 1:6:8. The advantage of having the ingate area larger than the runner area is to maintain the metal temperature by filling the runners at the same rate as with the 1:6:6 ratio while maintaining a low metal velocity in the ingates. Again, the casting, as illustrated in Figure 18, was cast under similar conditions. The overall radiographic quality of this part was better than any of those previously cast. However, some gas porosity was present in the part. The origin of the gas porosity was found not to be attributed to the gating system, but rather to the strontium modifier used in the A357. (A discussion on the

effect of strontium in A357 was given in an earlier section.) It was concluded from these castings that a 1:6:8 gating ratio provided optimum metal flow characteristics. When selecting the gating ratio for large, thin-wall structural parts, which are best cast in the vertical position, it is recommended from the results of the foregoing work that a 1:6:8 gating ratio be used.

Further evaluation of gating techniques was conducted using the same part configuration and gating ratio as above. The parts were gated in the inverted position as shown in Figure 69 to simulate a possible method of pouring the full-scale station 170 body bulkhead. Pouring the part in the inverted position will allow the thin areas to fill first since the hydrostatic head pressure is greatest and provides better feeding of the thick sections that are in the upper portion of the part.

c. Sprue Design

The key to a good gating system is to have a properly designed sprue system. The important aspects of sprue design that affect metal turbulence are sprue height and shape and the base diameter of the sprue which controls the flow rate.

The first consideration in the design of a sprue system is to determine the height of the sprue. It is generally known that large sprue heights cause metal turbulence. During this investigation, test parts of the configuration shown in Figures 18 and 19 were poured with sprue heights of 30 and 52 inches. Parts cast with sprue heights greater than 30 inches had poor radiographic quality thought to be caused by increased turbulence.

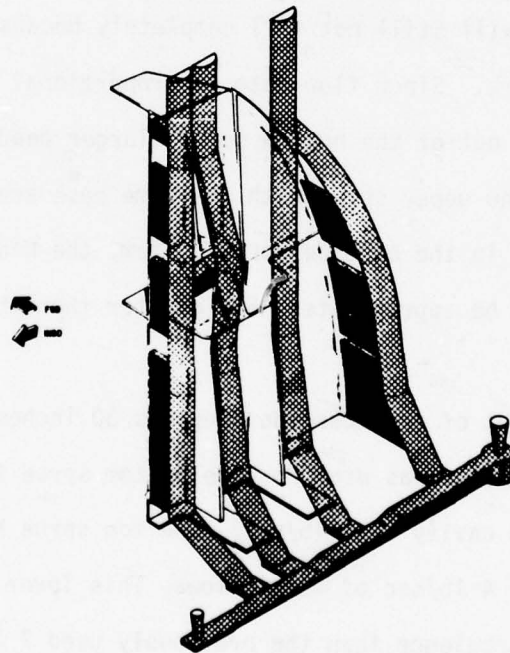
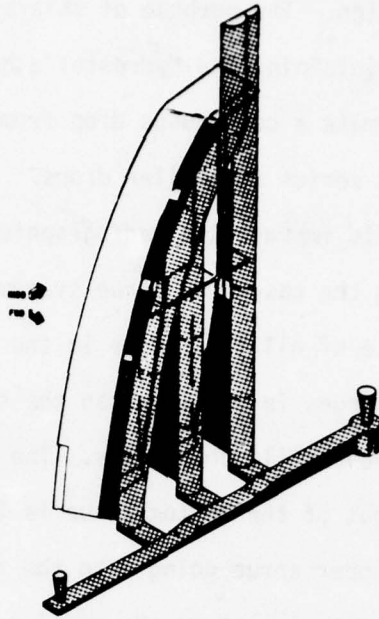


FIGURE 69 PART "A" CONFIGURATION CAST IN INVERTED POSITION WITH GATING SYSTEM ATTACHED

As shown in Figure 70, the sprue system used for these parts was a cascading sprue design. The purpose of this system is to eliminate metal turbulence while maintaining the hydrostatic head. The advantage is that the metal does not make a continuous drop from the pouring basin to the pouring well, but a series of smaller drops. This will reduce the metal turbulence and should improve the radiographic quality of the casting.

When designing the cascading sprue system, attention must be given to the area at the base of all the sprues in the cascade. If the area at the base of the upper sprues is smaller than the sprues in the bottom, the bottom sprue will never fill completely. The reason for this is simple: the flow of metal out of the bottom sprue is larger than the flow of metal coming out of the upper sprue going into the top of the lower sprues. This will result in air entrainment in the metal as it attempts to fill the bottom sprue. If the areas at the base of all sprues are the same, the bottom sprue will still not fill completely because of the effect of hydrostatic pressure. Since flow rate is proportional to the hydrostatic head, the flow rate out of the bottom sprue (larger head) will be faster than the flow out of the upper sprue with the same base areas. To ensure adequate sprue filling in the cascade sprue system, the base area of the upper sprues should be approximately 50% greater than the base area of the lower sprues.

The height of each cascade step was 30 inches. A sprue with a 0.50-inch base diameter was used for the bottom sprue to lower the flow rate into the mold cavity to 3 lb/sec. The top sprue had a base diameter of 0.70 inch, or 4 lb/sec of metal flow. This lower flow rate should cause less metal turbulence than the previously used 7 lb/sec. Several castings were poured with this gating system. The radiographic quality of the castings was better than those cast with a single sprue. However, there

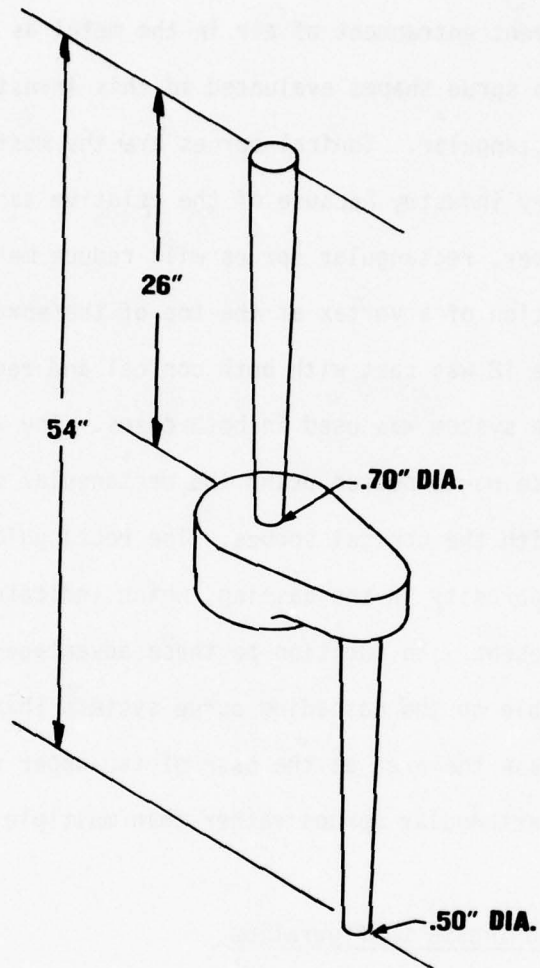


FIGURE 70 CASCADE SPRUE SYSTEM FOR CONFIGURATION "A" OF FIGURE 69

was still a small amount of gas porosity dispersed through the casting. Since the metal quality was satisfactory prior to pouring, the dispersed gas porosity was assumed to be caused by the gating system.

Consideration was then given to the sprue shape. All sprues were tapered to prevent entrapment of air in the metal as it flows down the sprue. The two sprue shapes evaluated in this investigation were conical (round) and rectangular. Conical sprues are the most commonly used in the aluminum foundry industry because of the relative ease of fabrication and molding. However, rectangular sprues will reduce metal swirling and minimize the formation of a vortex at the top of the sprue. The configuration shown in Figure 18 was cast with both conical and rectangular sprues. The cascading sprue system was used in both cases. The relative radiographic results of those parts poured using the rectangular sprues was better than those poured with the conical sprues. The rectangular sprues produced less dispersed gas porosity in the casting, which indicated that less metal turbulence was present. In addition to these advantages, rectangular sprues are more suitable to the cascading sprue systems than conical sprues. In order to increase the area at the base of the upper sprues, it is easier to use multiple rectangular sprues rather than multiple conical sprues.

d. Runner and Ingate Configuration

Another important consideration in the design of a gating system is the runner and ingate configuration. A typical configuration is shown in Figure 71. The optimum runner shape was found to be square. The reason for this is simple. Square runners provide the least amount of metal surface area exposed to the runner walls. This will result in a minimum amount of heat loss, a critical factor in the casting of thin-wall parts.

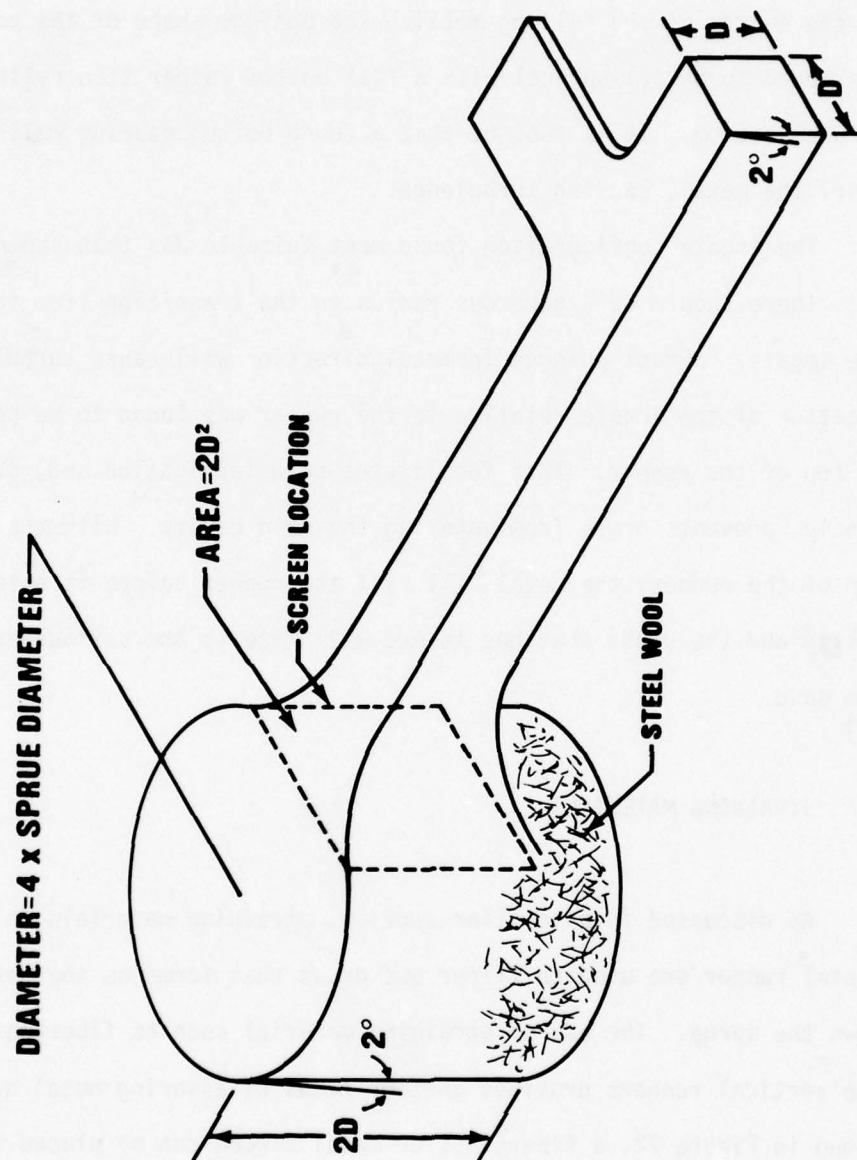


FIGURE 71 TYPICAL RUNNER, POURING WELL AND INGATE CONFIGURATION

The shape of the pouring well, which is located under the base of the sprue, is important to control metal flow entering the runner. The metal passing out of the sprue is traveling at its greatest velocity. The purpose of the pouring well is to reduce the metal velocity by absorbing some of the energy of the falling metal. The optimum shape of the pouring well was found to be cylindrical with a flat bottom rather than cylindrical with a round bottom. It is thought that a round bottom pouring well tends to swirl the metal, causing turbulence.

The ingate configuration found most suitable was that shown in Figure 71. There should be a generous radius in the transition from the runner to the ingate. Abrupt changes in metal direction will cause turbulence. The location of the ingate relative to the runner was found to be best placed on top of the runner. This facilitates mold fabrication and, most importantly, prevents dross from entering the mold cavity. With the ingates on top of the runner, the metal will fill the runner before it enters the mold cavity and the dross that has formed will rise to the surface and adhere to the sand.

2. STRAINING MATERIALS

As discussed in an earlier section, straining materials in the horizontal runner are used to filter out dross that forms as the metal comes down the sprue. The use of straining material such as fiberglass screen in the vertical runners provides another means of assuring metal quality. As shown in Figure 72, a fiberglass or metal screen can be placed between the vertical runner and the step gates. The advantage of screening the metal at this location in the mold is that the lower metal velocity in the vertical runners permits a more uniform filtering. Dross that is trapped in the

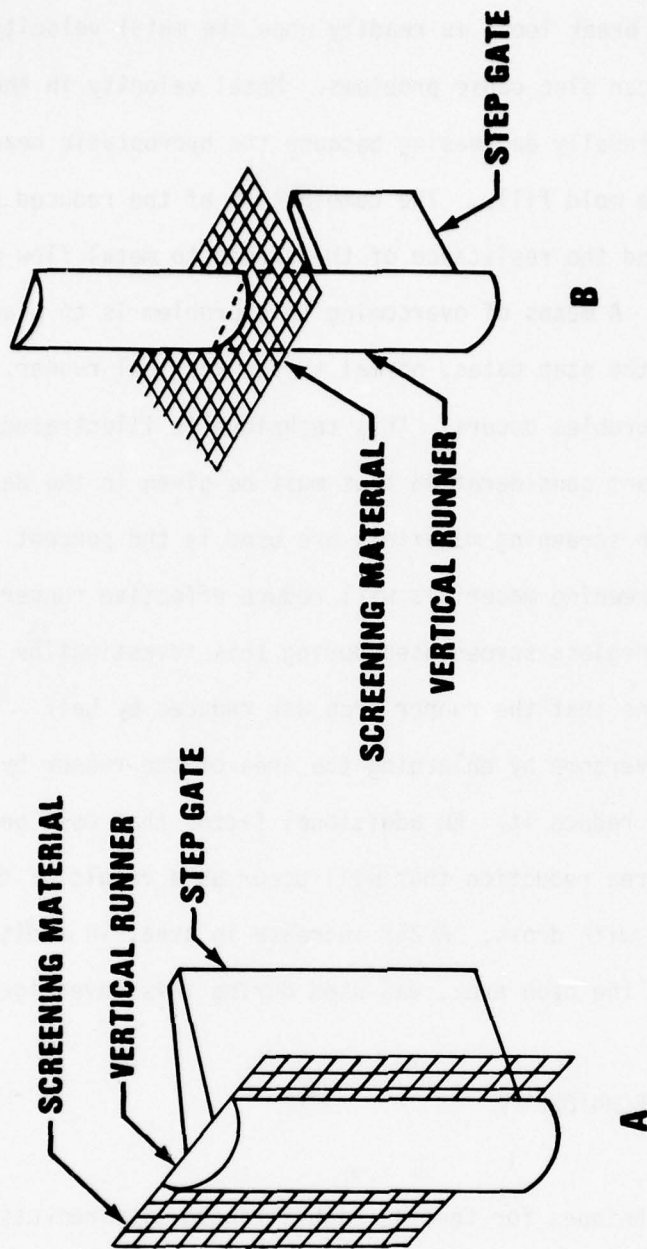


**FIGURE 72 APPLICATIONS FOR THE USE OF SCREENING MATERIAL IN
VERTICAL GATING SYSTEMS**

screen will not break loose as readily when the metal velocity is low. This advantage can also cause problems. Metal velocity in the vertical runners is continually decreasing because the hydrostatic head pressure decreases as the mold fills. The combination of the reduced hydrostatic head pressure and the resistance of the screen to metal flow may cause the part to misrun. A means of overcoming this problem is to place screening material above the step gates, normal to the vertical runner, at the location where the problem occurs. This technique is illustrated in Figure 72B.

One important consideration that must be given in the design of gating systems in which screening materials are used is the percent open area of the screen. Screening materials will reduce effective runner or ingate areas. The fiberglass screen used during this investigation had a 50% open area, which means that the runner area was reduced by half. This problem can be easily overcome by enlarging the area of the runner by the amount the screen will reduce it. An additional factor that must be considered is the amount of area reduction that will occur as a result of the screen becoming filled with dross. A 25% increase in area, in addition to the increase due to the open area, was used during this investigation.

3. RISERING TECHNIQUES

Design techniques for feeding high-strength aluminum castings must permit the solidifying metal to be continuously fed by a reservoir of molten metal. This promotion of directional solidification is the key to obtaining high-strength castings. To design such a risering system, information must be known about the effect of riser size, the distance metal will feed from a riser, and knowledge about the feeding paths that transport metal through the casting.

During this investigation, plates of the configuration shown in Figure 8 were used to determine the effect of riser size and the distance metal will feed from a riser. Since the demonstration component is a large, thin-wall casting, 0.10- and 0.50-inch-thick plates were tested. Risers with base diameters of 1, 2, and 3 inches (each 6 inches high) were evaluated on the two test plates. The riser volumes were 11.0, 29.8, and 58.1 in.³, respectively. Tests were conducted to determine the effect of chill size on the ability of these risers to feed the plates.

The effect of distance from an unchilled end and an end chilled with a 6- x 2- x 2-inch aluminum chill on the mechanical properties of a 0.10-inch-thick cast A357 plate is shown in Figures 73 and 74, respectively. The risers used in this evaluation had base diameters of 1 and 2 inches. It is readily seen that chilling a 0.10-inch-thick plate has little effect on the resultant mechanical properties. The reason for this is simple. The rate of solidification of thin sections is so rapid that the additional chilling effect from the chill is negligible. The effect of riser size on the 0.10-inch-thick plate is negligible adjacent to the riser. However, at distances away from the riser, the 2-inch-diameter feeder produces better properties. The decrease in properties between 4 and 6 inches from the riser is a result of massive shrink porosity, as verified by radiographic examination. Since the plate was gated from the riser end, the metal began to solidify as soon as it filled the mold cavity. Neither of the risers was sufficient to fill the solidification shrinkage beyond 4 inches.

The effect of distance from a 6- x 2- x 2-inch and 6- x 3- x 3-inch aluminum chill on the mechanical properties of a 0.50-inch-thick cast A357 plate are shown in Figures 75 and 76, respectively. The risers evaluated with these test plates have base diameters of 2 and 3 inches. The mechanical properties at the chilled end of the plates are not affected by the

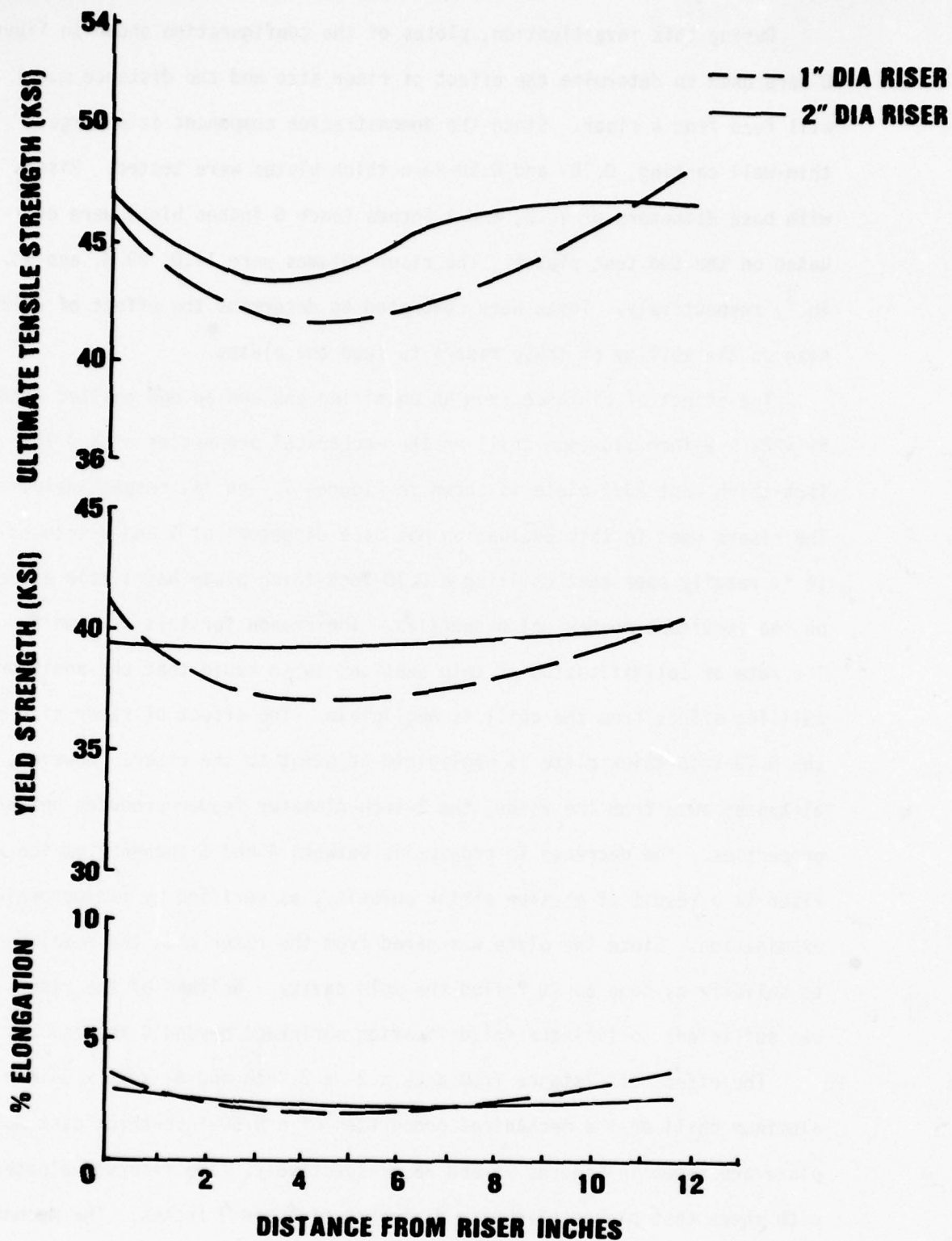


FIGURE 73 EFFECT OF RISER SIZE ON MECHANICAL PROPERTIES OF .10 IN. THICK CAST PLATE

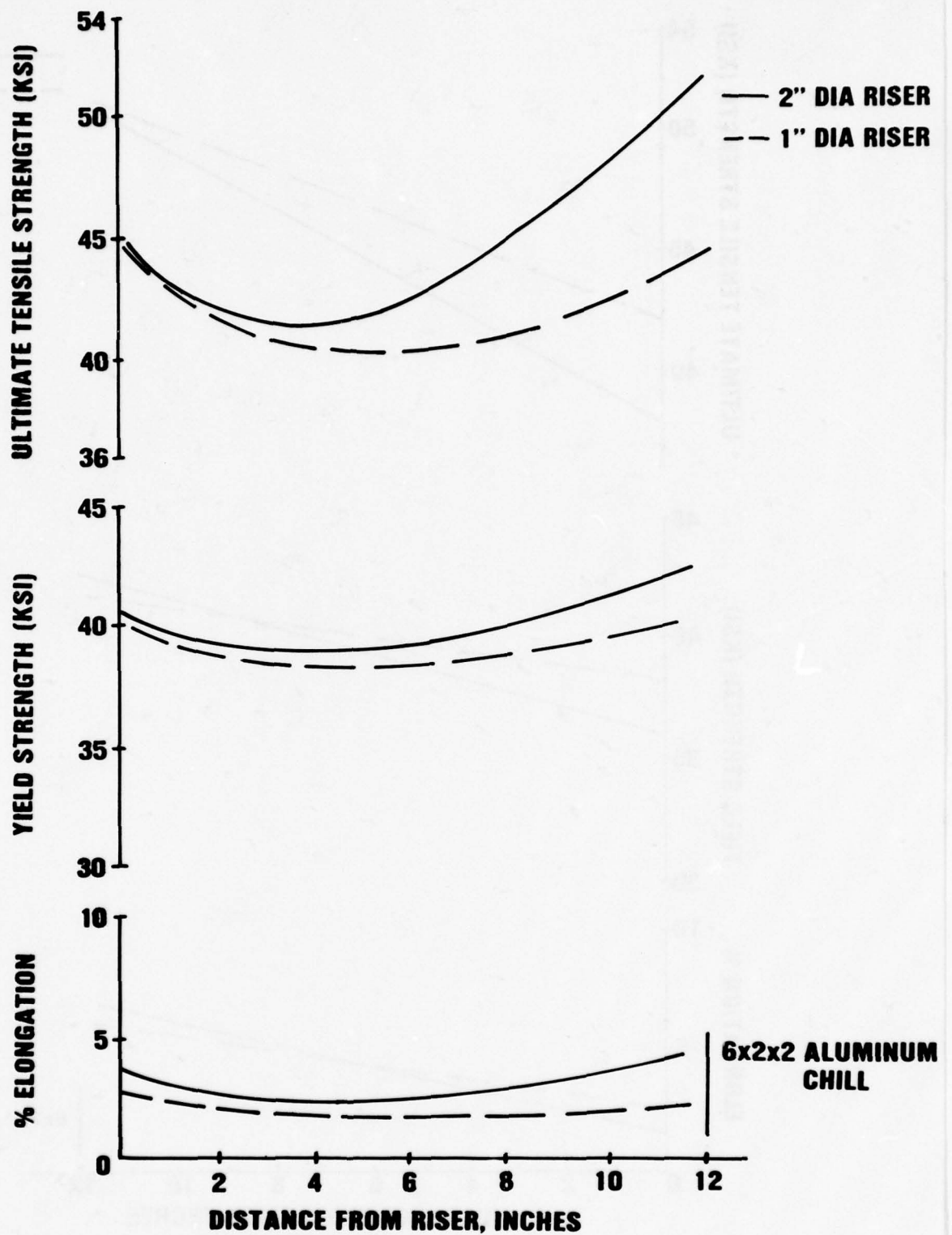


FIGURE 74 EFFECT OF RISER SIZE ON MECHANICAL PROPERTIES OF .10 IN. THICK CAST PLATE

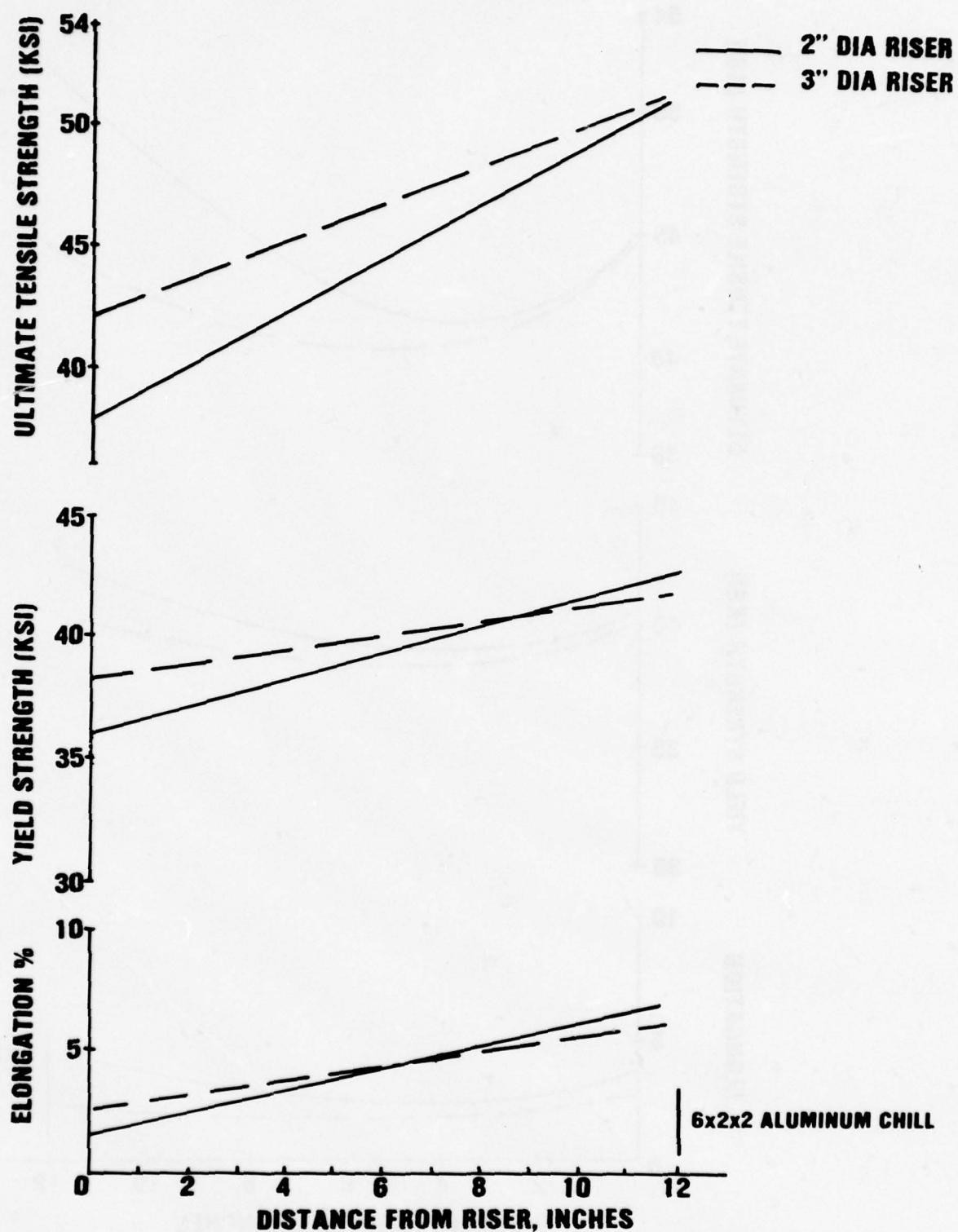


FIGURE 75 EFFECT OF RISER SIZE ON MECHANICAL PROPERTIES OF .50 IN. THICK CAST PLATE

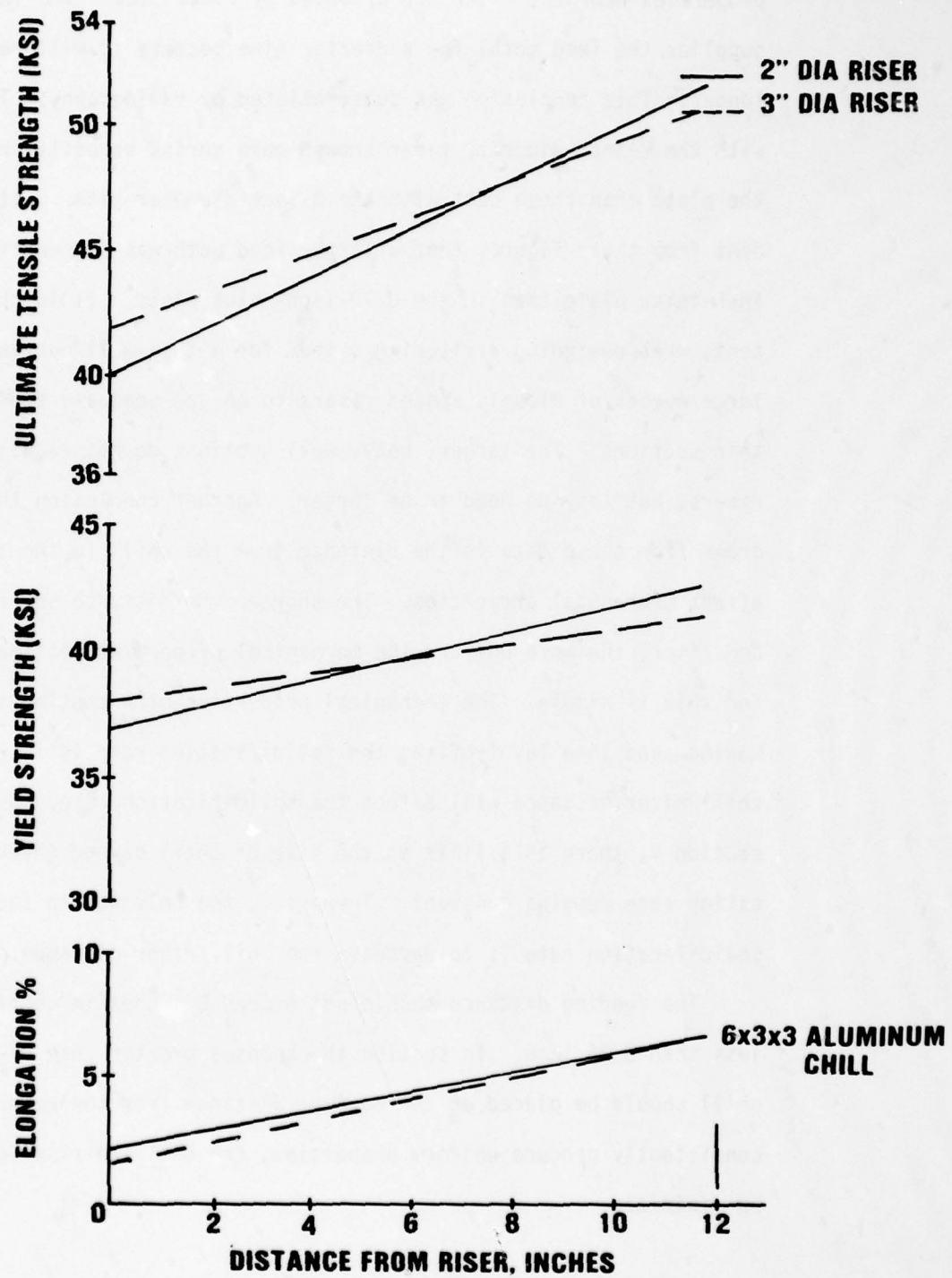


FIGURE 76 EFFECT OF RISER SIZE ON MECHANICAL PROPERTIES OF .50 IN THICK CAST PLATE

chill masses used in this evaluation. Also, the riser size does not affect the mechanical properties at the chilled end. However, the mechanical properties near the riser are affected by riser size. The larger riser supplies the feed metal for a greater time because it will retain heat longer. This conclusion was substantiated by radiography. The plates cast with the 2-inch-diameter riser showed more shrink porosity in the middle of the plate than those cast with the 3-inch-diameter riser. It is also evident from these figures that a larger feed path was present in the 0.50-inch-thick plate than in the 0.10-inch-thick plate. It is therefore important, when designing a risering system for a thin-wall casting, to use a large number of closely spaced risers to ensure adequate feeding of the thin sections. The larger, heavy wall sections do not require as many risers, but they do need to be larger. Another conclusion that can be drawn from these data is the distance from the chill to the riser that will affect mechanical properties. The shorter the distance between the chill and riser, the more uniform the mechanical properties will be. The reason for this is simple. The mechanical properties of a casting increase to a maximum and then level off as the solidification rate is increased. The chill/riser distance will affect the solidification rate. As discussed in section V, there is a limit to the size of chill beyond which the solidification rate remains constant. Therefore, the only way to increase the solidification rate is to decrease the chill/riser distance.

The feeding distance should not exceed 6 inches in section thicknesses less than 0.25 inch. In section thicknesses greater than 0.25 inch, a chill should be placed at the maximum distance from the riser. In order to consistently produce uniform properties, the chill-to-riser distance should be minimized.

Plaster and fibrous materials were evaluated for application as insulating riser sleeves. To minimize the heat loss of the metal and to ensure that the vertical runners provide adequate feeding, insulation of the vertical runners is necessary. As described earlier, the part configuration shown in Figure 59 was used to compare the insulating characteristics of these materials.

Semicircular risers, 2.5 inches in diameter, were thermocoupled at four locations and then coupled to a temperature recorder. The part was poured at 1435°F. The results shown in Figure 60 indicate that there were no appreciable differences in the insulating characteristics of these materials. However, the plaster riser sleeves are more expensive and will generate gas when placed in contact with molten aluminum. For these reasons, the fibrous insulating riser sleeves are suggested for use where insulating requirements are needed.

The information gained from these tests was applied to the design of the risering system for the parts shown in Figures 18 and 19. As discussed previously, the vertical runners and ingates act as risers to feed the solidification shrinkage. The riser size selected for the vertical runner was 2.5 inches in diameter, semicircular, and made of fibrous insulation. The size of the step gate feeding the ribs was dictated by the rib width and length. In order to eliminate as much clean-up after casting as possible, the step gate width was three times the width of the rib. The step gate covering the rib was $1/3$ to $1/2$ the height of the ribs. Tapered step gates were used to prevent the casting from feeding the vertical runners. In order to provide adequate feeding of the various section thicknesses, the large vertical runner was required. If a reverse feeding path between

the casting and the vertical runners was established, the heavy sections of the casting could act as risers to feed the vertical runners. However, when the molten metal comes in contact with the heavy sections, it will begin to solidify back to the step gate. The tapered step gates, after they have fed the shrinkage of the heavy sections, will freeze off at reduced areas (tapers), thus eliminating a reverse feeding path between the casting and vertical runner.

A simple method used during this investigation to determine if the step gates were of the proper size and providing adequate feed to the casting was radiography. In areas that were suspected of inadequate feeding, step gates were removed and radiographed. If shrink porosity was evident in step gates near the casting, vertical runners were not providing enough feed metal. The size of the vertical runner in this area was increased.

The techniques for designing a gating and risering system are not cut and dried. There are no magic formulas that, when applied, will tell the riser placement and size, gating configuration, etc. The gating and risering for each casting are unique. However, from the tests conducted in this investigation, a lot of the guesswork can be eliminated from the gating and risering design, and a more sophisticated, scientific approach can be taken.

SECTION VII
CROSS-SECTION, OVERALL DIMENSIONAL TOLERANCES,
AND STRAIGHTENING REQUIREMENTS

This purpose of this section of the investigation was to define the dimensional tolerance requirements that could be cost effectively achieved by sand casting. Based on this information, shrinkage allowances were established. Also, straightening requirements and techniques for large, thin-wall castings made from aluminum alloy A357 were developed.

1. DIMENSIONAL REQUIREMENTS

The test parts shown in Figures 8, 18, and 19 were used to define the dimensional tolerance requirements attainable in the fabrication of thin-wall aluminum castings. Parts used for previous tests were dimensionally checked and compared with the pattern to determine the amount of shrinkage. Test results are shown in Table 6.

A draft angle of $1/2$ degree per side could be readily achieved with flanges up to 11 inches in height. These small draft angles, however, must be used with a rigid pattern. It is recommended that the sections with small draft angles be made of metal. Also, it is necessary to use a good parting agent on the pattern prior to ramming the mold. Next, the method of stripping the pattern from the mold is important. The mold or pattern, whichever the case may be, must be removed normal to each other or pattern damage will result. This can be done by placing a level on the mold or pattern surface and observing alignment. The minimum section thickness in an A357 sand casting that can be consistently and economically achieved by

TABLE 6 DIMENSIONAL TOLERANCES - A357 SAND CASTING

DIMENSION	MINIMUM DIMENSION & TOLERANCE, IN.
DRAFT ANGLE	$\frac{1}{2}^{\circ}$
SECTION THICKNESS	$.100 \pm .010$
OVERALL DIMENSION, IN. (GENERAL)	
0-1.0	$\pm .010$
1.1-10.0	$\pm .030$
10.1-20.0	$\pm .050$
20.1-40.0	$\pm .10$
40.1-60.0	$\pm .15$
60.1-100.0	$\pm .25$
MACHINING ALLOWANCE UP TO 100 IN.	$+ .250$
SHRINKAGE ALLOWANCE (GENERAL)	$.125 \text{ IN./FT.}$

conventional means is 0.100 ± 0.010 inch. The area that can be cast with this section thickness is limited. Based on the ability of a riser to adequately feed a thin section and the fluidity of the metal, the maximum distance from the center of the thin section to a riser is approximately 5 inches. This limits the dimensions of any one thin area to about 10 x 10 inches.

The average dimensional requirements given in Table 6 are very general in nature. The overall dimensional requirements are controlled by the shrinkage characteristics of the metal and part geometry. The degree of success in achieving the dimensional requirements is dictated by the shrinkage allowance. In comparing the shrinkage of unrestrained plates with the pattern dimensions, a shrinkage factor of 0.125 inch per foot was selected. However, shrinkage of parts with a complex geometry does not always occur uniformly. Therefore, the shrinkage allowances must be determined differently for each part configuration.

One possible method of determining the shrinkage allowances for a part is to graphically section the part into discrete sections. Each section is then treated as either an unrestrained or partially restrained plate. Whether or not a discrete section should be treated as an unrestrained or partially restrained plate is dependent on the mold and part characteristics. If the retained strength of the mold is high, the part will experience resistance on solidification, rendering it partially restrained. Also, the larger the mass undergoing solidification, the more force that will be exerted during contraction, which approaches an unrestrained part.

After the shrinkage analysis of the entire part has been made, each discrete shrinkage allowance should be summed, giving the total shrinkage allowance of the casting.

2. STRAIGHTENING REQUIREMENTS

Experience indicates that straightening of aluminum alloy A357 is best accomplished after heat treatment, in the solution treated ("W") condition. Alloy A357, as with all heat-treatable aluminum alloys, begins to naturally age after quenching if it is not maintained at a temperature of -10°F or less. Since it is almost impossible to straighten a large, complex casting while maintaining it at -10°F , it was necessary to determine how long a part could be held at room temperature after quenching and still have enough ductility to straighten.

AFS standard cast tensile bars were made from A357. They were chilled in the drag and poured at 1325°F . These test specimens were then solution heat treated, quenched, and immediately placed on dry ice. The temperature was maintained at below -10°F for 20 hours. The specimens were removed from the dry ice and allowed to reach room temperature prior to testing. It is apparent from Figure 77 that the ductility of A357 is not affected by naturally aging up to 8 hours at room temperature. These results were substantiated by heat treating the part A section of the demonstration component and then straightening.

The tools required for straightening consisted of various sizes of rubber mallets, clamps for straightening ribs and flanges, and backing blocks. As discussed in the next section, very little distortion was observed and all distortion except for oil-canning was removed. Oil canning generally occurs in thin sections as the result of a severe quench. It is almost impossible to remove oil-canning, once it has formed. Careful design of the part is required to assure that it does not occur.

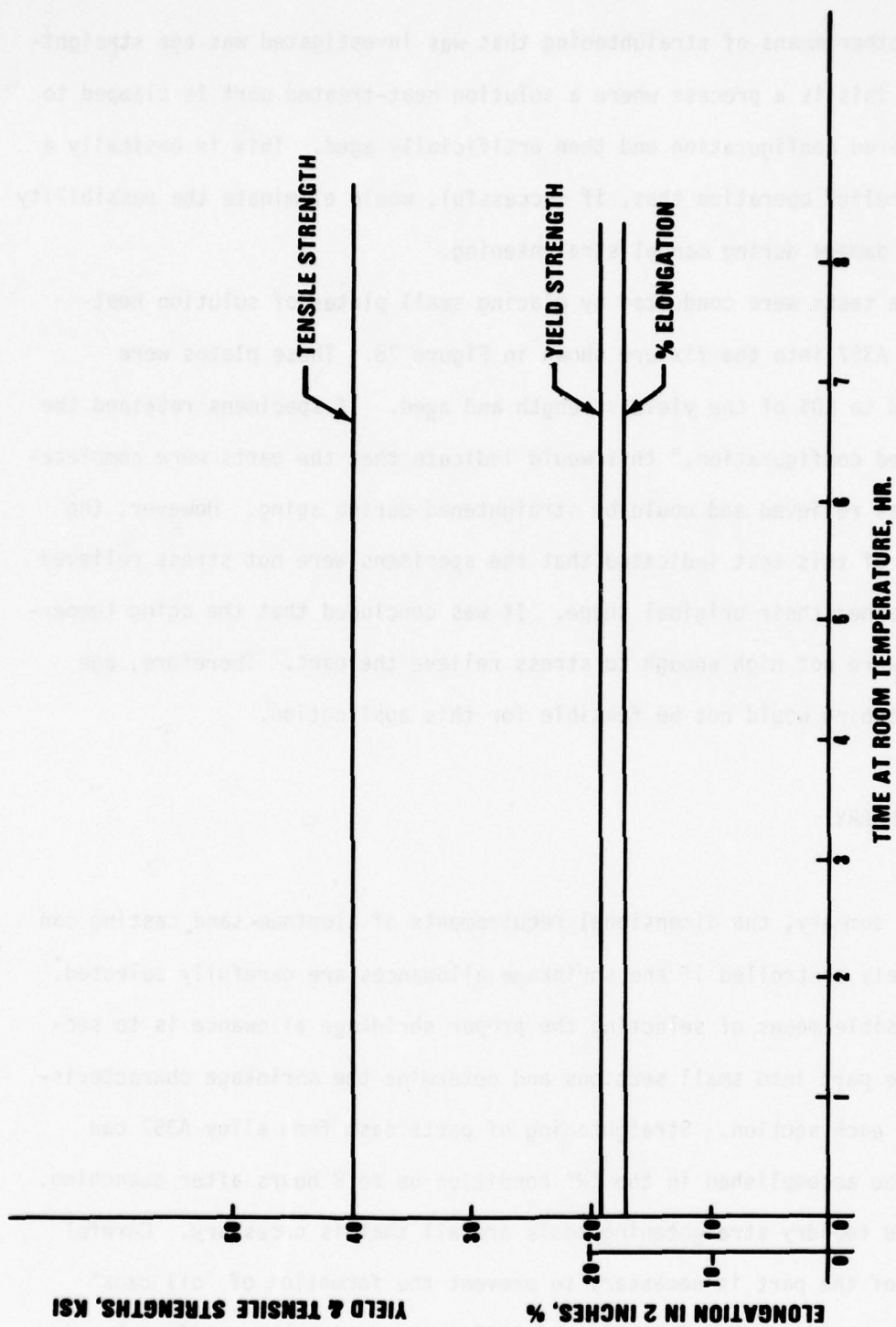


FIGURE 77 EFFECT OF NATURAL AGING ON THE MECHANICAL PROPERTIES OF A357

Another means of straightening that was investigated was age straightening. This is a process where a solution heat-treated part is clamped to the desired configuration and then artificially aged. This is basically a stress-relief operation that, if successful, would eliminate the possibility of part damage during manual straightening.

The tests were conducted by placing small plates of solution heat-treated A357 into the fixture shown in Figure 78. These plates were stressed to 80% of the yield strength and aged. If specimens retained the "stressed configuration," this would indicate that the parts were completely stress relieved and would be straightened during aging. However, the results of this test indicated that the specimens were not stress relieved and retained their original shape. It was concluded that the aging temperatures were not high enough to stress relieve the part. Therefore, age straightening would not be feasible for this application.

3. SUMMARY

In summary, the dimensional requirements of aluminum sand casting can be closely controlled if the shrinkage allowances are carefully selected. One possible means of selecting the proper shrinkage allowance is to section the part into small sections and determine the shrinkage characteristics of each section. Straightening of parts cast from alloy A357 can easily be accomplished in the "W" condition up to 8 hours after quenching. Standard foundry straightening tools are all that is necessary. Careful design of the part is necessary to prevent the formation of "oil cans" during quenching. Straightening of A357 parts during the artificial aging cycle does not appear to be feasible.

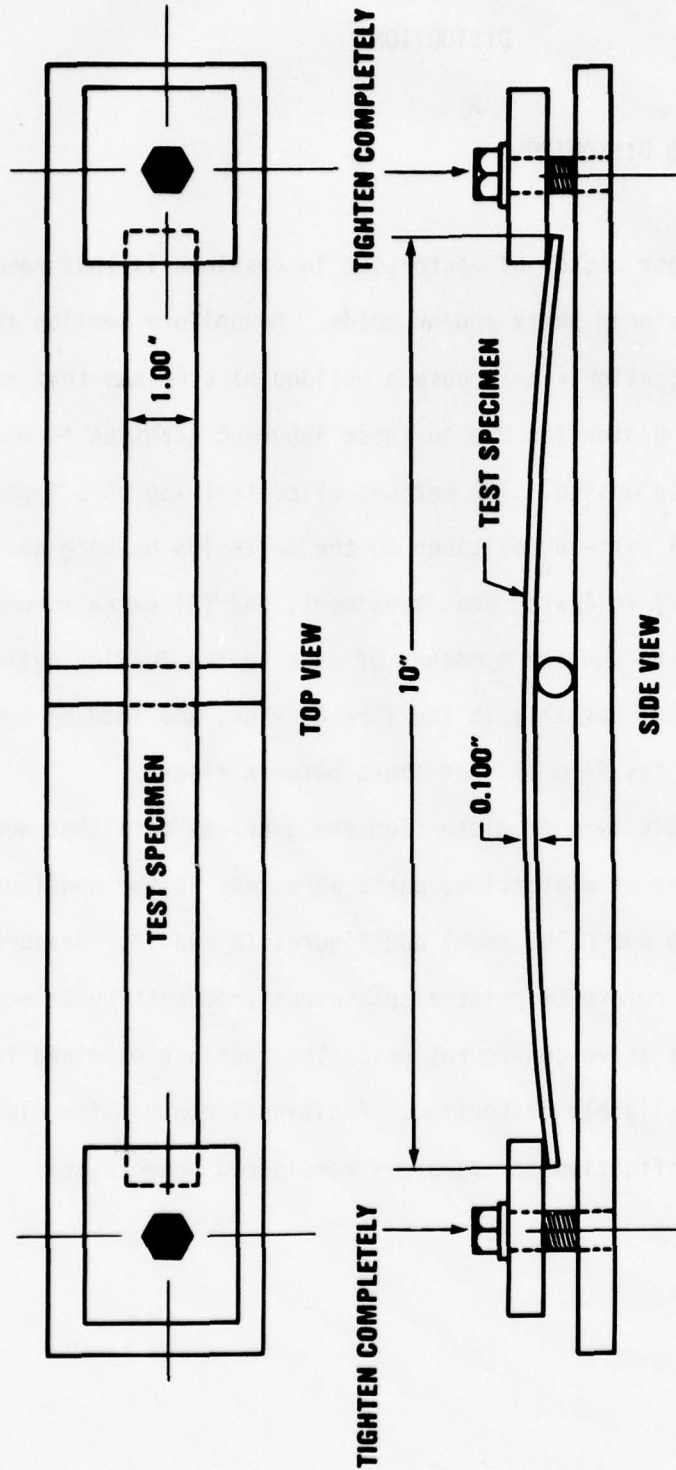


**FIGURE 78 HEAT TREAT FIXTURE FOR DETERMINING THE EFFECT OF AGING TEMPERATURES
ON THE STRAIGHTENING OF CAST PARTS**

SECTION VIII

DISTORTION

1. DESIGN-RELATED DISTORTION

One of the major causes of distortion in castings is that resulting from improperly designed parts and/or molds. Nonuniform section thicknesses and solidification rates cause a buildup of stresses that act to distort the part. Distortion due to these inherent stresses is minimized by altering the mold design. Two methods of controlling this type of distortion include (1) cast-on additions to the parts (to balance sections) that will be cut off following heat treatment, and (2) extra runners and gates placed so as to provide symmetry of mass to the feeding system. The cast-on additions are normally in the form of ribs, and feeding system alterations are in the form of cast links between risers.

To evaluate this type of distortion and generate data that would allow reliable predictions of distortion, parts were cast in the configuration of Figure 8 ($T = 0.100$ and 0.500 inch) and Figures 18 and 19. Measurements for differences in reference point displacement from pattern orientation were taken from the above configurations. The castings examined in these tests displayed negligible distortion. Additional control for distortion due to metal solidification stresses was considered unnecessary.

2. HEAT-TREAT DISTORTION

The second major cause of distortion is heat treatment. Heat-treat distortion results when the parts are rapidly quenched from the solution heat treatment temperature. Variations in the cooling rate throughout the part result in a buildup of stresses that, if large enough, will warp the part.

To determine the amount of distortion resulting from heat-treat operations, parts of the configuration shown in Figure 8 ($T = 0.100$ and 0.500 inch) were cast, solution heat treated at $1010 \pm 5^\circ\text{F}$, and quenched in either agitated (1) water at 160°F , (2) 20% glycol solution at 120°F , or (3) 28% glycol solution at 120°F . To simulate production heat-treat operations, a 10-second delay was allowed between heat treat and quenching. This 10-second quench delay was based on delay times measured during heat-treat operations of production furnaces used by Boeing. The specimens used in these tests were suspended with Ni-Cr wire in standard wire mesh heat-treat baskets during both solution heat-treat and quenching operations. This suspension allowed the entire surfaces of the parts to be uniformly heat treated in the furnace and quenched in the respective solutions. In addition to evaluating the effects of the aforementioned quenchants on distortion of cast parts, mechanical properties as a function of section thickness when quenched in the three different quench media were also evaluated. Parts of the configuration shown in Figure 8 ($T = 0.100$ inch) and Figure 79 were used to determine mechanical properties. Upon completion of heat-treat operations, test parts were dimensionally checked and inspected by penetrant and radiographic techniques to ensure casting integrity.

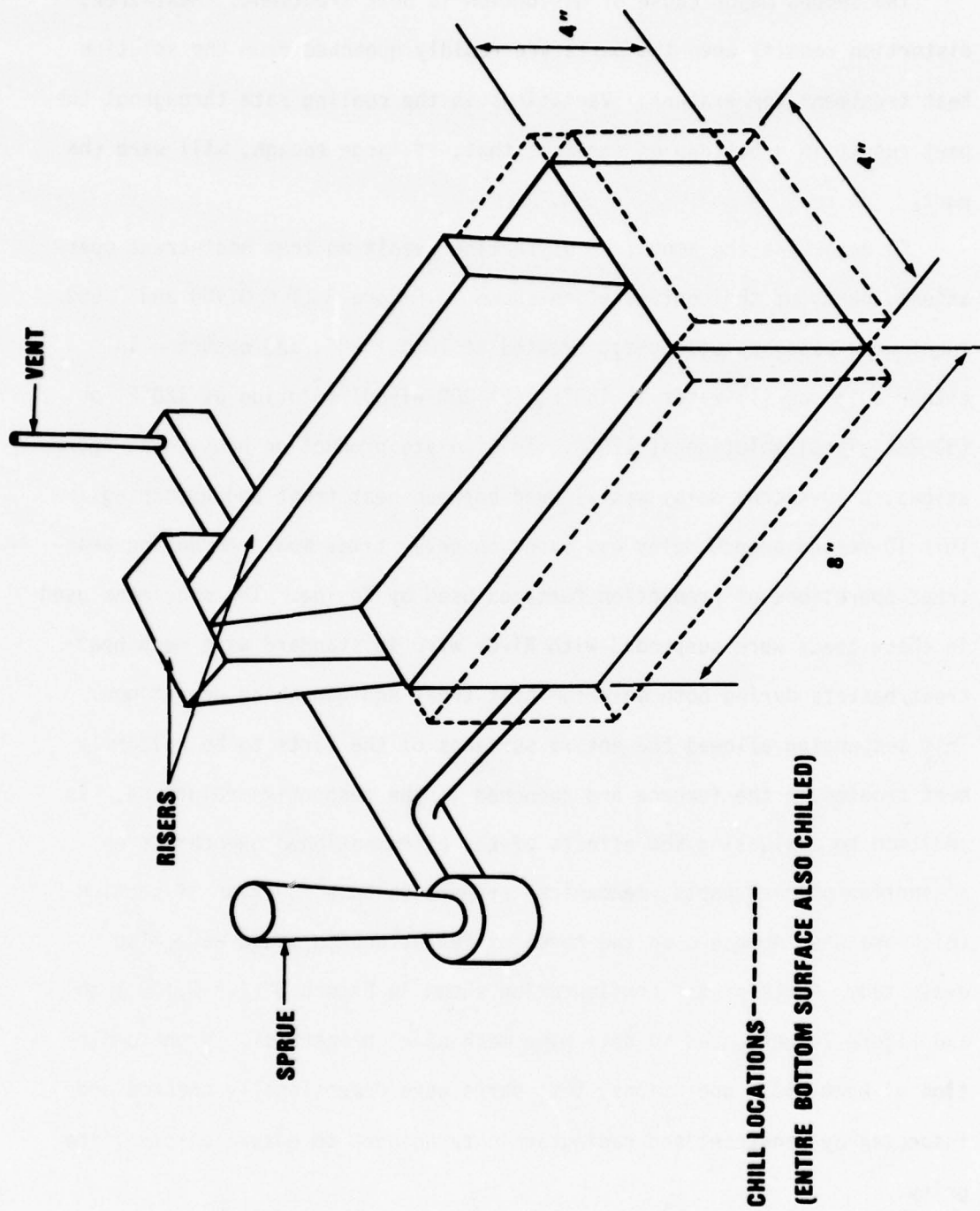


FIGURE 79 TEST BLOCK CONFIGURATION

The glycol solutions chosen for evaluation in this investigation were used because they represent quenching media less severe than water. Theoretically, the greater the severity of the quenching media, the more distortion will occur. In addition, the faster the heat-treated part is cooled, the higher the mechanical properties of the part. The 160°F quench water was used because it is a standard quenchant used in heat treatment of cast aluminum parts. The 120°F glycol solutions were used to show a comparison between water and less severe quenchants with respect to distortion and mechanical properties.

The amount of distortion that occurred in the parts quenched in the different solutions is shown in Figure 80. It was noted from the quenched parts that (1) maximum distortion occurred in the parts quenched in 160°F water (A), (2) distortion in parts quenched in 20% glycol solution at 120°F (B) was less than observed in the water-quenched parts, and (3) parts quenched in 28% glycol solution at 120°F (C) displayed the least amount of distortion with respect to all other parts tested. In essence, the parts quenched in water contained a far greater buildup of stresses than found in parts quenched in the less severe media.

The test specimens used to determine mechanical properties of cast A357 quenched under the described conditions were also subjected to production-oriented handling procedures. Typically, when precipitation-hardening alloys like A357 complete solution heat-treat and quenching operations, they are placed in cold storage at subzero temperatures to inhibit natural aging of the material. This storage can be accomplished by either placing the parts in a commercial grade freezer capable of subzero temperatures or by completely packing the parts in dry ice (CO_2), which has a melting point of -78.2°C (-109°F) at 1 atmosphere pressure. The parts are typically held

in storage until preparations for working (straightening, etc.) of the parts are complete. The parts are then removed from storage and more easily worked in the "W" condition.

The mechanical test specimens used in this investigation were packed in dry ice and held for a period of 33 hours. The parts were then taken from cold storage, straightened, and artificially aged at 325°F for 9 hours and subsequently allowed to air cool. Tensile specimens were then machined from the test parts and used to determine ultimate tensile strength, yield strength, and percent elongation in a 2-inch gage length. Results of these tests showed that optimum mechanical properties are obtained by quenching in water at 160°F. The data in Table 7 show that parts quenched in water display average strength values of round specimens to be (1) about 3.0% higher in yield strength and 7.5% higher in tensile strength than round specimens taken from parts quenched in 20% glycol solution at 120°F, and (2) slightly higher in yield strength (about 0.5%) but 5.0% higher in tensile strength than round specimens taken from parts quenched in 28% glycol solution at 120°F. Results of mechanical tests conducted on flat specimens showed that parts quenched in 160°F water were (1) about 1.0% higher in yield strength but about 3.0% lower in tensile strength than specimens quenched in 20% glycol solution at 120°F, and (2) about 4.0% higher in yield strength but about 3.5% lower in tensile strength than specimens quenched in 28% glycol solution at 120°F. The higher mechanical properties displayed by the water-quenched thick specimens are explained by the theory that intermetallics in the A357 alloy remain in solution with more rapid quench rates and tend to migrate out of solution in the form of precipitates at slower cooling rates. In the flat specimens (Fig. 8 where $T = 0.100$ inch), the lower tensile properties of the water-quenched specimens

TABLE 7 EFFECT OF VARIOUS QUENCHING MEDIUMS ON THE MECHANICAL PROPERTIES OF CAST A357

SPECIMEN NO.	QUENCHANT	SPECIMEN CONFIGURATION	YIELD (KSI)	TENSILE (KSI)	% ELONGATION*
560-1	WATER 160°F	ROUND	42.4	50.9	7.0
560-2			42.4	51.6	8.0
560-3			41.4	52.3	10.0
495-1		FLAT	39.8	46.6	4.5
495-2			40.4	43.7	2.0
495-3			39.4	47.0	5.0
562.1	20% GLYCOL 120°F	ROUND	40.1	47.0	4.0
562-2			41.8	48.3	4.0
562-3			40.7	47.9	4.5
498-1		FLAT	39.3	48.7	5.5
498-2			39.3	46.2	3.5
498-3			39.7	47.0	4.0
564-1	28% GLYCOL 120°F	ROUND	41.2	48.4	4.0
564-2			42.8	49.6	5.0
564-3			41.5	49.2	5.0
502-1		FLAT	39.8	48.1	7.0
502.2			37.3	46.0	4.0
502.3			37.9	48.3	5.0

*% ELONGATION COMPUTED IN A 2 INCH GAGE LENGTH

with respect to the glycol-quenched specimens is also attributed to section thickness and cooling rate. The section thickness of the specimens was constant (i.e., 0.100 inch) and the quenchant temperatures were 160°F for the water and 120°F for the glycol quenchants. Even though water is considered a more severe quenchant than the glycol solutions, the determining factor is the temperature of each bath and the cooling mechanism of glycol quenchants. As parts are submersed in agitated water after solution heat treatment, bubbles form on the surface of the part and tend to insulate the part and cause nonuniform cooling. However, the agitation of the bath breaks up the bubbles and allows the part to cool more uniformly. With glycol quenchants, the glycol tends to separate from solution at temperatures exceeding about 160°F (the surface of the part is above 160°F) and form a film on the part surface. This film inhibits bubble formation and allows uniform cooling of the part. In thick parts, the cooling rate is slow enough for the quench agitation to remove the bubbles and provide more uniform cooling. In thin parts, the cooling rate is so rapid that the glycol film is formed quicker than the bubbles are removed.

Significant differences in the percent elongation of the test specimens were also noted. Round test specimens quenched in 160°F water displayed average values about 50% higher than with 20% glycol solution at 120°F and about 44% higher than with 28% glycol solution. However, due to the reasons discussed in the preceding paragraph, flat specimens quenched in 160°F water displayed values about 12% lower than with 120°F-20% glycol solution and about 28% lower than with 120°F-28% glycol solution.

As shown in Figure 80, considerable distortion was obtained in thin sections from quenching in each of the three quenching media. Although the distortion observed on the specimens quenched in 28% glycol solution at 120°F was significantly less than that observed on specimens quenched in 160°F water or 120°F-20% glycol solution, the distortion present in these specimens merits concern with respect to dimensional control problems. In large aluminum castings of complex configurations (i.e., Fig. 18), distortion in thin sections between ribs or thicker sections may result in "buckling" or "oil-canning" defects. These distortion defects are very difficult and often impossible to correct when close dimensional control is required. However, this type of distortion may be avoided by minimizing the size of the thin section (with respect to distance between ribs) or adding additional ribs or supports to the thin sections.

During quenching operations, heat-treated parts tend to move about in the quench tank due to agitation of the quenching bath. This movement may result in nonuniform cooling of the part and/or damage to the part if it collides with other quenched parts, quench tank walls, etc. To avoid problems that may result from part movement while quenching large aluminum castings, a fixture should be used to restrict movement during this operation. Design of such a fixture should include provisions for holding the casting in place to minimize movement during quenching, but also allow expansion/contraction of the part during heat treatment and cooling to room temperature.



FIGURE 80 RESULTANT DISTORTION OF TEST PLATES QUENCH IN DIFFERENT MEDIA. A-WATER 160°F, B-20% GLYCOL, 120°F; C-28% GLYCOL 120°F

Although water-quenched specimens displayed elongations higher than glycol-quenched specimens, the glycol-quenched specimens displayed far less distortion. It is evident from these observations that a trade-off between distortion and elongation must be made. The decision for choice of quenching media must be based on properties required of the part with respect to maximum allowable distortion.

3. SUMMARY

To summarize the results of this investigation, we can conclude that:

1. The amount of distortion resulting from solidification stresses was found to be negligible in the parts that were cast for evaluation. However, if distortion due to these stresses should occur in large aluminum castings, it could be controlled by incorporating cast-on additions for part balance or using extra runners and gates to provide symmetry.
2. Water quenching yields high mechanical properties but poor distortion characteristics. However, if care is taken during design and heat treatment, distortion can be minimized and mechanical properties maintained.
3. A heat-treat fixture for controlling distortion during quenching of large aluminum castings is necessary.

SECTION IX

NDE PROCEDURES AND VERIFICATION OF RESULTS

Each NDE (nondestructive evaluation) method has unique capabilities and limitations, and no single method can be applied with complete assurance of detecting all conditions that may be detrimental. Inspection methods may be broadly categorized as applicable to surface or to internal quality determinations. Thorough inspection of castings requires that sufficient methods be applied to reliably detect both surface and subsurface discontinuities. However, many of the commonly applied methods or tests in one category will have some limited capability in the other. For example, cracks detectable by surface inspection methods may also be revealed by radiography during evaluation of internal soundness. Some redundancy is therefore afforded by the multiple inspections normally applied to high-integrity products.

The primary NDE methods evaluated and employed in Phase II were fluorescent penetrant for surface discontinuities and X-radiography for internal soundness. These two methods are most commonly used in the casting industry for inspection of nonferromagnetic castings. Other methods were considered that have some useful capabilities, but none were judged equal to penetrant and radiography for overall inspections. However, ultrasonic techniques demonstrated a potential capability to reveal fine porosity in heavy sections where the ability of radiography appears to be deficient. This capability will be under further investigation and development during Phase IV.

1. SURFACE INSPECTION METHODS

Initial inspection for surface irregularities, discontinuities, and finish was accomplished visually. Surface irregularities below drawing tolerances, such as underflush parting lines, core or chill impressions, pits, inclusions, and open gas holes, were sought. Discontinuities such as cracks, misruns, cold shuts, and other linear, propagating-type flaws were also noted. Surface finish was compared with NAS 823, "Cast Surface Comparison Standards," after final cleanup of the castings.

Fluorescent penetrant inspection procedures were evaluated and materials and techniques considered optimum were designated. Water-washable and PE (post-emulsifiable) penetrant systems were investigated. Significant parameters included penetrant dwell time, method of removing excess penetrant, type of developer (dry, water soluble, water suspension, nonaqueous, or none), and development time. The investigation of these various techniques was conducted in a laboratory on relatively small cast panels, and it was necessary to consider some practical aspects of inspecting the full-size casting in a production facility. For example, the emulsification step of the PE system requires close and uniform control of the dwell time. This can be difficult or impossible to achieve on large and complex-shaped parts that require crane-handling. In addition, aluminum sand castings present some rather unique surface conditions and defect characteristics, as compared to wrought material, that need consideration in arriving at the optimum penetrant inspection procedure.

Cast surface textures frequently are such that they retain sufficient penetrant for developers (particularly the more sensitive nonaqueous types) to bring out a high level of background fluorescence. This background can

reduce inspection sensitivity and reliability by reducing the visual contrast of defect indications. Also, many casting defects are relatively open and retain a large volume of penetrant. The application of most developers and the use of high-sensitivity penetrants will result in extensive "bleed-out" that can interfere with critical interpretation of discontinuities. Wide-spreading indications from groupings of small pores, as shown in Figure 81, may obscure the presence of a small crack in such locations. Laboratory tests showed that this spreading of indications is substantially curtailed by the use of dry powder developer, as is illustrated in Figure 82. However, facilities for proper application of dry developer to the full-size casting were not available.

Based on the laboratory tests, available facilities, and other practical considerations, a penetrant system using a highly self-developing, water-washable penetrant with no developer was selected for the program. This system is considered to have a sensitivity equivalent to Group V materials per MIL-I-25135, "Inspection Materials, Penetrant." Threshold indications of surface pores on cast test panels were obtained from openings less than 0.001 inch in diameter. Other studies have shown capabilities of revealing linear defects with opening widths less than 1 micron. More important to penetrant inspection reliability or effectiveness than sensitivity of the materials, however, is proper preparation of the parts prior to inspection. Sawing, grinding, and sand blasting, extensively used in cleanup of castings, are known to exert a smearing action that can completely close tight defects to the entry of the most sensitive penetrants. To alleviate this adverse effect, a requirement was imposed on the program castings that 0.0002 to 0.0004 inch be chemically removed from all surfaces. Figure 83 shows the marked improvement gained by etching a segment of casting that had been abrasively ground.

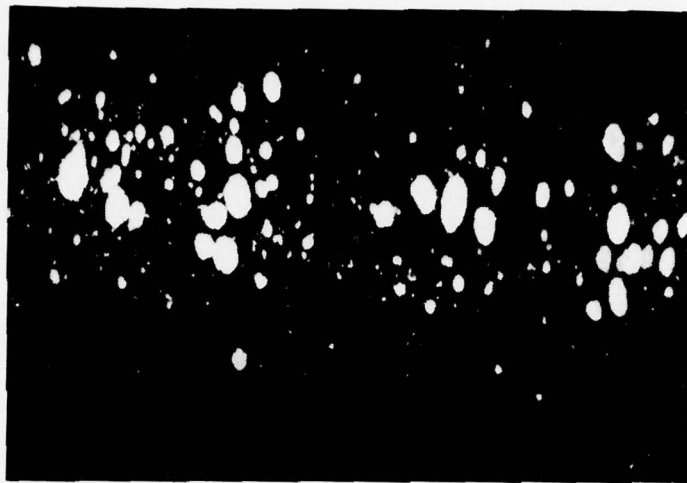


Figure 81—Penetrant Indications Obtained with Water Suspension Developer on a Cast Panel Exhibiting Excessive Surface Porosity

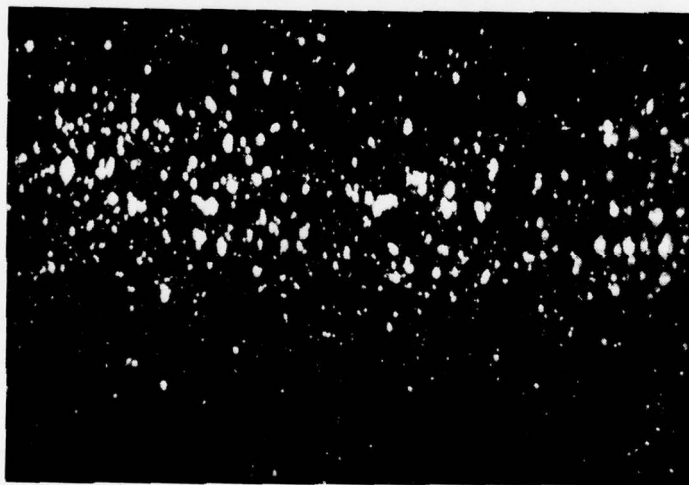


Figure 82—Penetrant Indications Obtained with Dry Powder Developer on the Panel of Figure 1

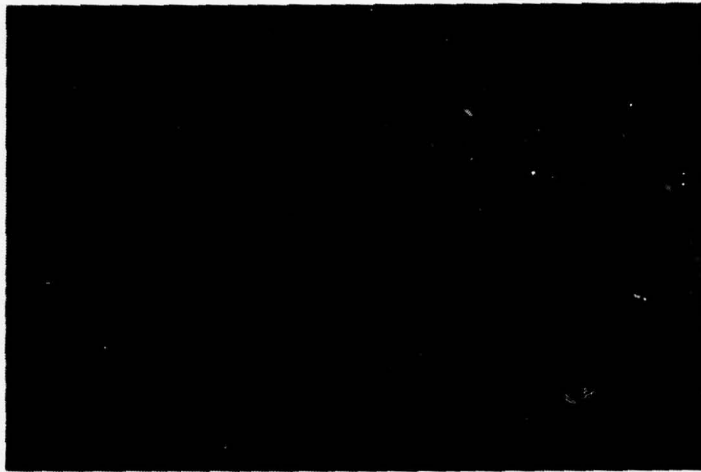


Figure 83- Penetrant Inspection Results Before and After Etching a Casting Section Which had Been Abrasively Ground

2. DETERMINATION OF DENDRITE ARM SPACING (DAS)

Dendritic arm spacing (DAS) measurements provide nondestructive means of determining mechanical properties likely to be attained in local areas of a casting. It was necessary to develop suitable methods for the microscopic measurement of DAS on designated areas of the full-size castings, as well as on the mechanical test specimens for the design allowables study, and to aid in the creation of D-XXXX, "Aluminum Alloy A357 Castings, Dendrite Arm Spacing, Process for Determination of." The local measurement area of the casting surface may be metallographically polished by either electrochemical or mechanical methods. The mechanical method was chosen for development. The resulting technique proved to be simple and rapid. A flexible shaft motor-tool was used for rough and fine grinding with three grades of rubber bonded abrasive wheels. Polishing was accomplished with cotton laps and both 6- and 1/2-micron diamond paste. After polishing, the surface was etched with 0.5% HF solution. At this point, direct examination with a portable microscope may be performed. However, it was found to be easier to prepare a plastic replica of the etched surface, which could be better examined in the laboratory. Also, the replica may be retained as a permanent record.

Eddy current conductivity measurements were made in conjunction with the DAS measurements for a period of time to determine if differences in the morphology and distribution of the interdendritic eutectic associated with different DAS values might effect the bulk conductivity. Such a correlation was not demonstrable.

3. CASTING SOUNDNESS

A uniformly sound casting is critical to the achievement of consistently high mechanical properties. Internal soundness of light alloy castings is conventionally evaluated by X-radiography, and this was the primary internal inspection method for the program. Radiographic inspection techniques were refined during foundry control development to provide consistently high-quality radiographic practices, assuring the B and C quality grades designated for the castings. However, the application of the ASTM E155-76 radiographic standards is definitely subjective and requires experienced, skilled film interpreters. This is particularly true for those conditions such as porosity and shrinkage that are acceptable in amounts or degrees up to that contained in the specified radiographic reference standards. The task of film interpretation becomes more difficult and less accurate if the thickness of the material being evaluated differs significantly from that of the reference standard. A high proportion of the program casting design consists of thicknesses of 0.100 to 0.125 inch, and the lesser proportion contains critical areas with sections several inches thick. These must be radiographically compared with standards representing 0.25- and 0.75-inch thicknesses, respectively.

Although the existing radiographic standards and the levels specified for the quality grades have been in use for many years, their adequacy for assuring a newer, higher level of integrity and strength might be questioned. Certainly there is a need for more study of the influence of internal soundness on mechanical properties of higher than customary strength castings. Two limited studies were initiated to provide additional insight into this matter.

Special radiographic reference standards were developed for seven levels of fine, dispersed porosity in 0.125-inch-thick material. All design allowable test specimens were radiographed after machining and rated according to these seven standards. The original ratings were from 0.250-inch standards and spanned only three levels (B or better, C or better, or worse than C). This expanded "Porosity Index" is being applied to all further mechanical property determinations and correlative results will be included in a later report.

Dispersions of very fine porosity become increasingly difficult to detect radiographically as section thickness increases. The maximum thickness of the program casting is 6 inches. In an attempt to improve inspection capabilities in this and other heavy sections of the casting, ultrasonic methods were examined. Ultrasonic comparison tests were made on 5- and 6-inch-thick cast material with and without porosity (equivalent to radiographic quality grades A and C). Three approaches to porosity estimation were evaluated:

- o Pulse-echo multiple back reflection loss
- o Pulse-echo direct porosity detection
- o Through-transmission

All three methods were successful with direct contact coupling and a promising ability of ultrasound to detect porosity in aluminum castings was demonstrated. The pulse-echo (contact method) direct porosity detection is the more practical approach, as the inspection can be conducted from one surface and the back surface need not be parallel. Figures 84 and 85 show comparative fluorescent penetrant indication photographs and ultrasonic porosity indication recordings obtained from the two cast blocks. Further development effort is being directed to obtaining quantitative ultrasonic porosity measurements, correlating these with radiographic quality grade, and applying the method to rating of mechanical property test material.

AD-A060 339

BOEING AEROSPACE CO SEATTLE WASH
CAST ALUMINUM STRUCTURES TECHNOLOGY (CAST) MANUFACTURING METHOD--ETC(U)
MAY 78 R G CHRISTNER, D D GOEHLER

F/G 11/6

F33615-76-C-3111

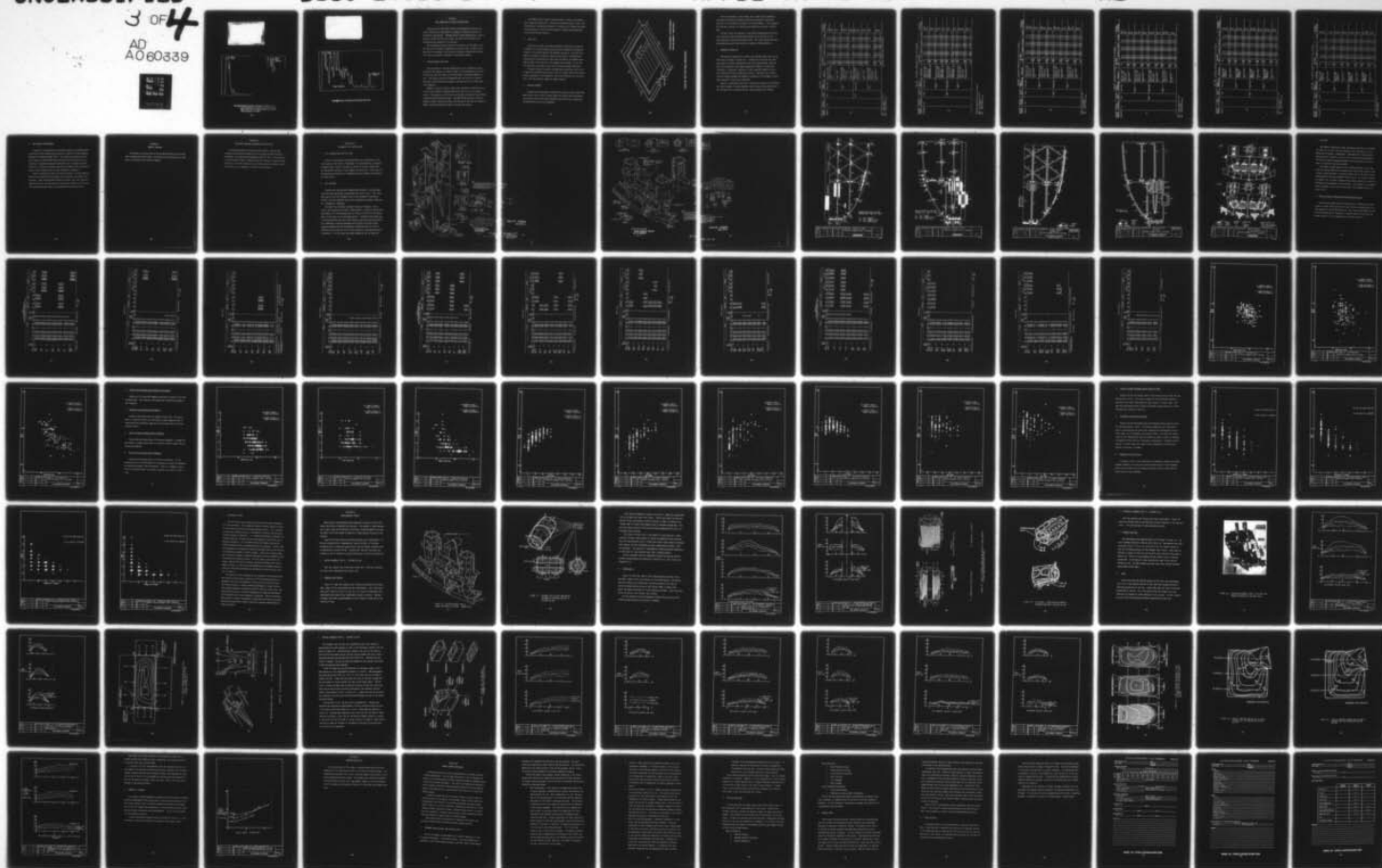
UNCLASSIFIED

D180-24610-1

AFFDL-TR-78-62

NL

3 OF 4
AD
A060339



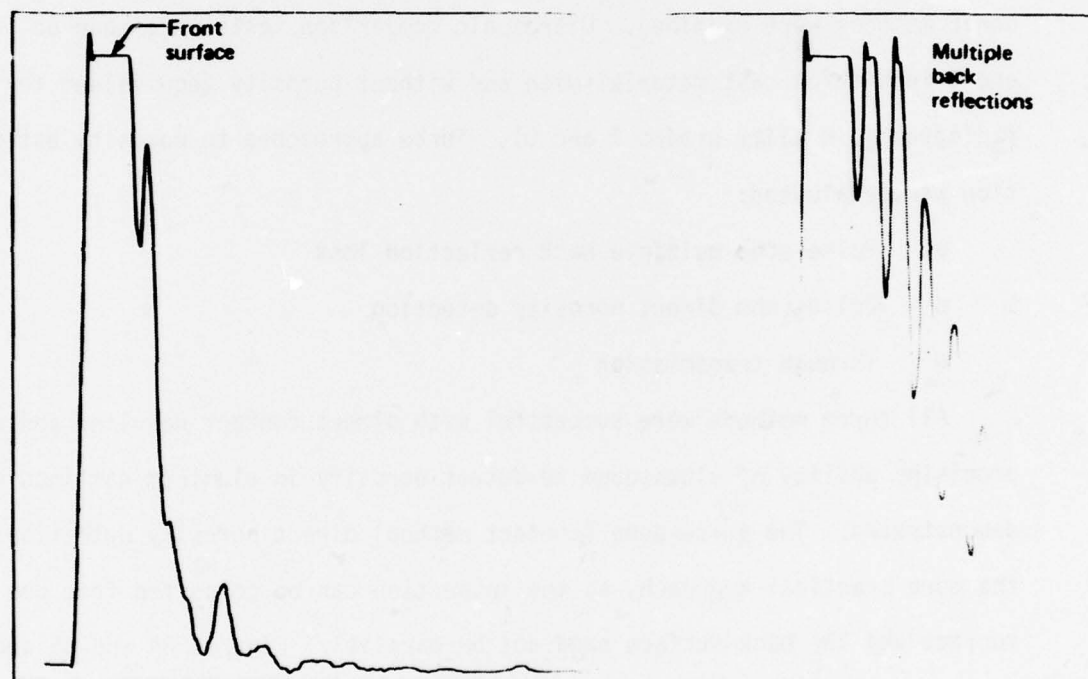
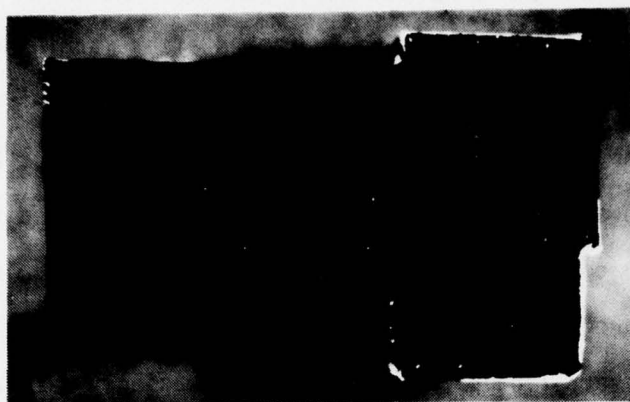


Figure 84—Florescent Penetrant Indications of Porosity (Top) with a Recording of Ultrasonic Indications (Bottom) Sound Entry from Vertical Surface at the Left with Travel Through to the Right

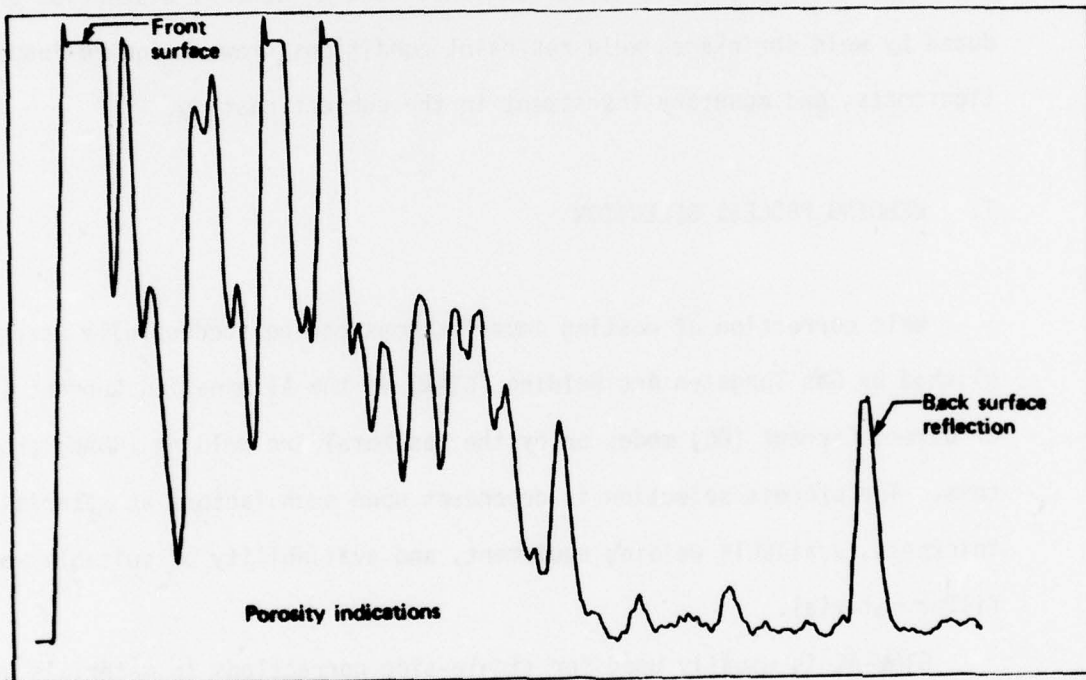


Figure 85—Same as Figure 84 but with Second Cast Block

SECTION X

WELD CORRECTION OF CASTING IMPERFECTIONS

Imperfections in A357 sand castings can frequently be corrected by fusion welding as an alternative to scrapping a casting or reducing its performance expectations. Although typical casting imperfections, such as porosity, shrink, misruns, and cracks, can usually be corrected, each casting must be evaluated on its own merit.

Due consideration must be given to such factors as the number, size, and location of individual imperfections, working access, distortion produced by weld shrinkage, weld restraint conditions, rework and re-inspection costs, and monetary investment in the subject casting.

1. WELDING PROCESS SELECTION

Weld correction of casting imperfections can be successfully accomplished by Gas Tungsten Arc Welding (GTAW) in the Alternating Current (AC) or Direct Current (DC) modes or by the Gas Metal Arc Welding (GMAW) process. The process selection is dependent upon such factors as material thickness, available welding equipment, and availability of suitable weld filler material.

GTAW-AC is usually used for single-side corrections in materials up to 1/8 inch thick without a prepared weld cavity and up to 1/4 inch with a cavity. Thicknesses up to 3/8 inch can be welded successfully using GTAW-AC by grooving and welding both sides. The GTAW-AC mode provides excellent cathodic surface cleaning and good visibility due to the high arc intensity. However, the weld penetration tends to be wide and shallow.

The GTAW-DC mode is used for heavier material sections and produces deep, narrow weld penetration. Because the DC mode produces a small, concentrated arc, the welding visibility is limited and is further restricted by the presence of soot-like surface deposits commonly encountered when using helium-rich gas mixtures.

2. WELD TESTS

During this program, tests were conducted to evaluate the relative suitability of various welding processes and to determine the mechanical properties of the weld deposits and adjacent base metal. Cast A357 test panels, configured as shown in Figure 86, were used in the evaluation. Simulated weld corrections were made using the GTAW-DC and GTAW-AC modes, A356 and A357 filler materials, and preheat and no preheat, on 1/8- and 5/8-inch-thick test panels in the as-cast and heat-treated conditions.

Although originally planned, simulated weld corrections could not be produced with the GMAW process due to lack of suitable weld filler material. During procurement of test materials, A357 filler material was only available in 36-inch straight lengths for manual welding.

3. WELDING EQUIPMENT

Although many conventional, commercially available, manual AC/DC GTAW power sources can be used to produce acceptable quality weld corrections, consistently better results were obtained using solid-state, square-wave, variable-polarity duty cycle equipment.

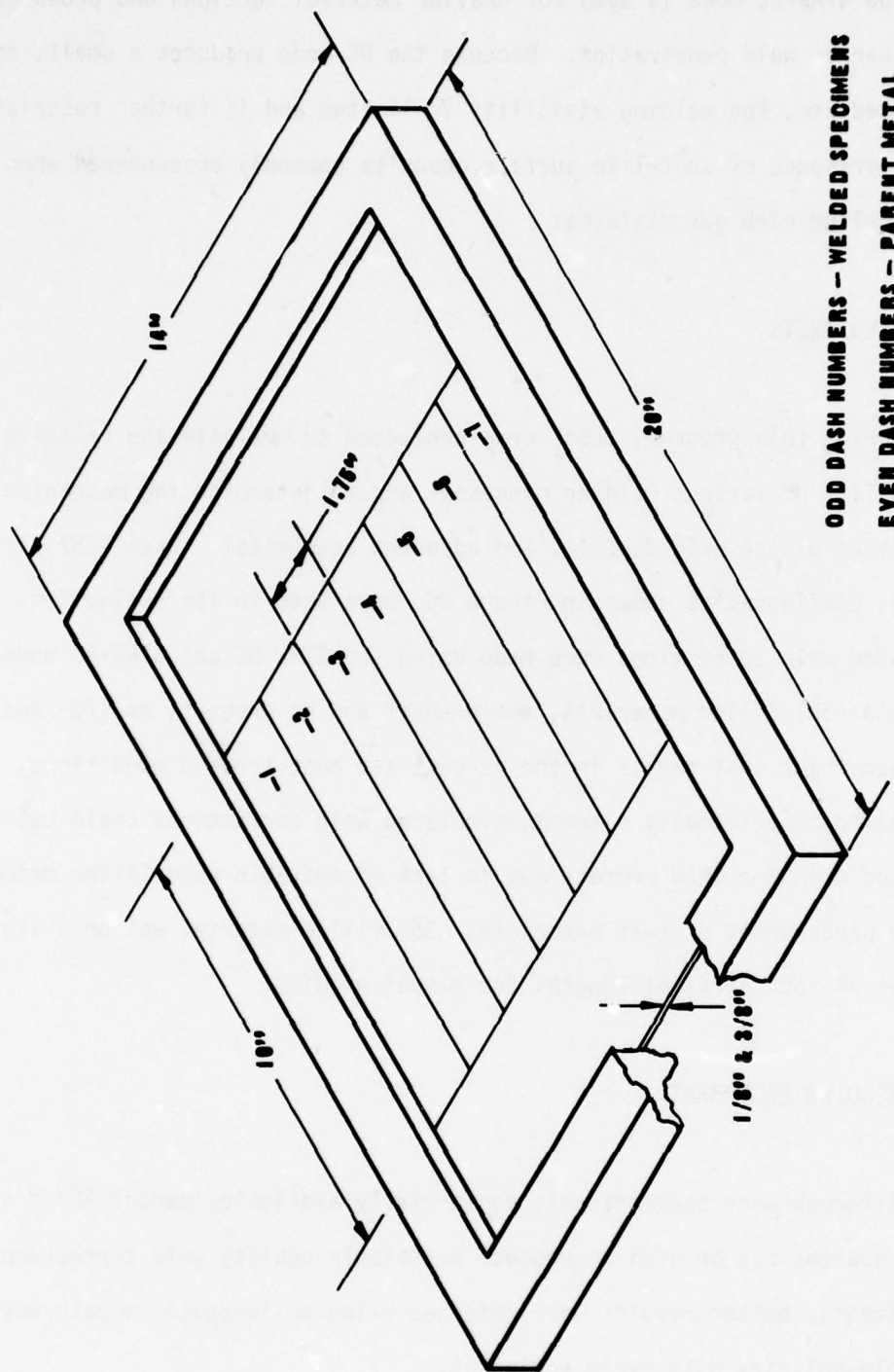


FIGURE 86 WELD TEST PANEL CONFIGURATION

During test welding in the AC mode, such a power source completely eliminated the problem of tungsten spitting and produced a substantial reduction in the incidence of porosity in the weld deposit. This equipment also provides excellent arc stability and smooth weld tailouts in the DC mode.

The power source was operated in the maximum unbalanced-polarity duty cycle condition, which provided approximately 70% of the time in the straight-polarity (electrode negative) mode. This mode produced increased weld penetration while retaining the AC cathodic cleaning benefits.

4. MECHANICAL PROPERTIES

The mechanical properties of welded test specimens taken from the cast A357 panels are shown in Tables 8-13. Examination of the test data indicates that the various combinations of AC and DC welding modes, A356 and A357 filler materials, and preweld temperature produced no significant differences in mechanical properties of test specimens welded in the as-cast condition and heat-treated after welding. There was also no significant difference between the mechanical properties of the welded and base metal specimens in the as-cast condition.

However, as predicted, there was a substantial reduction in the tensile and yield strengths of welded specimens that had been heat-treated prior to the simulated weld corrections and not re-heat-treated after welding.

TABLE 8 MECHANICAL PROPERTIES OF WELD TEST SPECIMENS

WELDING PROCESS	SECTION THICKNESS	FILLER ALLOY	PREWELD TEMPERATURE	CONDITION	SPECIMEN NO.	TUS(KSI)	TYS(KSI)	% ELONG.	LOCATION OF FAILURE
GTAW-AC	.125	A356	Room Temp.	Weld in As-Cast Condition, heat treat to -T6 after weld.	62-1	46.2	41.9	6.0	PM
					62-3	51.5	49.0	6.0	Weld Zone
					62-5	52.0	47.6	7.0	PM
					62-7	49.1	46.5	6.0	Haz
					AVE	49.7	46.3	6.3	
				Parent metal -T6	62-2	49.9	47.5	6.0	PM
					62-4	51.7	48.1	8.0	PM
					62-6	*	*	*	
					AVE	50.8	47.8	7.0	
				Weld in As-Cast condition, heat treat to -T6 after weld.	55-1	48.8	45.8	6.0	Weld Zone
					55-3	50.6	47.4	6.0	Haz
					55-5	49.5	45.4	8.0	Haz
					55-7	47.4	44.8	6.0	Haz
					AVE	49.0	45.9	6.5	
		A357	Room Temp.	Parent metal -T6	55-2	*	*	*	PM
					55-4	*	*	*	PM
					55-6	49.0	46.3	6.0	PM
					63-1	49.8	45.4	3.0	PM
					63-3	50.0	46.7	4.0	Haz
				Weld in As-Cast condition, heat treat to -T6 after weld.	63-5	50.0	41.2	6.0	PM
					63-7	48.8	44.7	5.0	Haz
					AVE	49.7	44.5	4.5	
				Parent metal -T6	63-2	49.0	46.5	5.0	PM
					63-4	49.3	45.3	5.0	PM
					63-6	48.5	43.5	6.0	PM
GTAW - Gas Tungsten Arc Weld	.125	A357	Room Temp.	Weld in As-Cast condition, heat treat to -T6 after weld.	AVE	48.9	45.1	5.3	
					51-1	50.1	45.3	4.0	Haz
					-3	50.7	47.0	5.0	Haz
				Parent metal -T6	AVE	50.4	46.2	4.5	
					51-2	48.9	46.3	5.0	PM
					-4	46.3	46.0	4.0	PM
					-6	50.5	47.3	5.0	PM
					AVE	48.6	46.5	4.7	
				Parent metal -T6	AVE	50.4	46.2	4.5	
					51-2	48.9	46.3	5.0	PM
					-4	46.3	46.0	4.0	PM
					-6	50.5	47.3	5.0	PM
					AVE	48.6	46.5	4.7	

*Specimen ruptured prior to 0.2% yield.

GTAW - Gas Tungsten Arc Weld
PM - Parent Metal
HAZ - Heat Affected Zone

TABLE 9 . MECHANICAL PROPERTIES OF WELD TEST SPECIMENS

WELDING PROCESS	SECTION THICKNESS	FILLER ALLOY	PREWELD TEMPERATURE	CONDITION	SPECIMEN NO.	TUS(KSI)	TYS(KSI)	% ELONG.	LOCATION OF FAILURE
GTAW-DCSP	.125	A356	Room Temp.	Weld in As-Cast condition, heat treat to -T6 after weld. Parent metal -T6	59-1	48.5	40.8	9.0	Weld
					-3	48.3	42.5	6.0	PM
					-5	49.0	41.2	7.0	Haz
					AVE	48.6	41.5	7.3	
					59-2	48.9	45.2	4.0	PM
					-4	46.8	45.8	4.0	PM
					-6	47.7	42.7	4.0	PM
					AVE	47.8	44.6	4.0	
					64-1	48.5	42.3	13.0	PM
					-3	49.0	44.5	6.0	PM
		A357	300°F	Weld in As-Cast condition, heat treat to -T6 after weld. Parent metal -T6	-7	49.3	43.0	12.0	Haz
					AVE	48.9	43.3	10.3	
					64-4	50.3	48.2	4.0	PM
					-6	49.3	46.9	5.0	PM
					AVE	49.8	47.6	4.5	
					60-1	50.2	44.7	9.0	PM
					-3	47.7	45.6	3.0	Haz
					AVE	48.9	45.2	6.0	
					60-2	49.3	47.1	3.0	PM
					-4	50.5	47.1	6.0	PM
			300°F	Weld in As-Cast condition, heat treat to -T6 after weld. Parent metal -T6	AVE	49.9	47.1	4.5	
					61-1	51.8	45.1	6.0	PM
					-3	48.8	44.7	5.0	PM
					-5	39.6	*	2.0	PM
					-7	50.7	46.2	7.0	PM
					AVE	47.7	45.3	5.0	
					61-2	49.5	45.3	5.0	PM
					-4	*	*	*	PM
					-6	49.4	48.6	5.0	PM
					AVE	49.5	47.0	5.0	

*Specimen ruptured prior to 0.2% yield.

GTAW - Gas Tungsten Arc Weld
 PM - Parent Metal
 HAZ - Heat Affected Zone

TABLE 10. MECHANICAL PROPERTIES OF WELD TEST SPECIMENS

WELDING PROCESS	SECTION THICKNESS	FILLER ALLOY	PREWELD TEMPERATURE	CONDITION	SPECIMEN NO.	TUS (KSI)	TYS (KSI)	% ELONG.	LOCATION OF FAILURE
GTAW-AC	.375	A356	Room Temp.	Weld in as-cast condition, heat treat to -T6 after weld.	141-1	45.8	40.0	4.0	Weld
					-3	46.9	39.1	5.0	Weld
					-5	46.8	39.3	5.0	Haz
					-7	46.3	38.3	7.0	Weld
					AVE	46.5	39.2	5.3	
					141-2	46.8	40.5	5.0	PM
			300°F	Weld in as-cast condition, heat treat to -T6 after weld.	-4	47.7	41.8	4.0	PM
					-6	48.6	41.5	6.0	PM
					AVE	47.7	41.3	5.0	
					136-1	48.7	39.5	5.0	PM
					-3	45.7	40.2	4.0	Weld
					-5	48.0	39.7	5.0	PM
	A357	Room Temp.	Weld in as-cast condition, heat treat to -T6 after weld.	-7	48.6	41.6	6.0	PM	
				AVE	47.8	40.3	5.0		
				136-2	49.7	42.6	6.0	PM	
				-4	42.2	34.4	6.0	PM	
				-6	41.6	35.8	4.0	PM	
				AVE	44.5	37.6	5.3		
	300°F	Weld in as-cast condition, heat treat to -T6 after weld.	Parent metal -T6	196-1	49.2	40.0	8.0	Weld	
				-3	49.2	41.3	6.0	PM	
				-5	48.4	40.9	5.0	Haz	
				-7	49.6	41.6	5.0	PM	
				AVE	49.1	40.9	6.0		
				196-2	49.4	41.3	7.0	PM	
Weld in as-cast condition, heat treat to -T6 after weld.		Parent metal -T6	-4	47.4	40.7	4.0	PM		
			-6	45.5	39.6	4.0	PM		
			AVE	47.3	40.5	5.0			
			138-1	46.7	41.1	4.0	Weld		
			-3	47.6	40.7	5.0	PM		
			-5	47.1	40.7	5.0	Haz		
A357	Room Temp.	Weld in as-cast condition, heat treat to -T6 after weld.	-7	48.8	41.1	5.0	Weld		
			AVE	47.6	40.9	4.8			
			138-2	47.6	41.2	5.0	PM		
			-4	46.7	39.7	4.0	PM		
			-6	48.0	40.5	5.0	PM		
			AVE	47.4	40.5	4.7			

180

GTAW - Gas Tungsten Arc Weld
PM - Parent Metal
HAZ - Heat Affected Zone

TABLE 11 MECHANICAL PROPERTIES OF WELD TEST SPECIMENS

WELDING PROCESS	SECTION THICKNESS	FILLER ALLOY	PREWELD TEMPERATURE	CONDITION	SPECIMEN NO.	TUS (KSI)	TYS (KSI)	% ELONG.	LOCATION OF FAILURE
GTAW-DCSP	.375	A356	Room Temp.	Weld in as-cast condition, heat treat to -T6 after weld.	193-1	45.6	40.6	5.0	Weld
					-3	46.2	40.1	5.0	Haz
					-5	47.4	39.3	5.0	Haz
					-7	48.8	40.3	7.0	PM
					AVE	47.0	40.1	5.5	
			300°F	Parent metal -T6	193-2	49.0	41.8	7.0	PM
					-4	43.3	40.5	3.0	PM
					-6	47.8	41.7	4.0	PM
					AVE	46.7	41.3	4.7	
				Weld in as-cast condition, heat treat to -T6 after weld.	139-1	46.4	41.3	5.0	PM
					-3	43.5	39.2	3.0	PM
					-5	45.8	40.3	3.0	Haz
					-7	44.9	40.9	5.0	Haz
					AVE	45.2	40.4	4.0	
				Parent metal -T6	139-2	46.6	40.5	4.0	PM
					-4	46.4	40.8	5.0	PM
					-6	47.3	41.2	5.0	PM
					AVE	46.8	40.8	4.7	
			Room Temp.	Weld in as-cast condition, heat treat to -T6 after weld.	140-1	46.6	39.9	6.0	PM
					-3	45.4	40.0	5.0	PM
					-5	44.6	39.6	4.0	PM
					-7	48.2	41.2	6.0	Haz
					AVE	46.2	40.2	5.3	
		A357	Room Temp.	Parent metal -T6	140-2	45.7	40.4	4.0	PM
					-4	46.3	40.3	5.0	PM
					-6	45.7	39.8	5.0	PM
					AVE	45.9	40.2	4.7	
			300°F	Weld in as-cast condition, heat treat to -T6	137-1	46.7	41.9	5.0	Haz
					-3	46.2	40.0	4.0	Haz
					-5	46.4	42.1	4.0	Haz
					-7	46.7	40.8	4.0	Haz
					AVE	46.5	41.2	4.3	
				Parent metal to -T6	137-2	46.6	40.4	4.0	PM
					-4	46.5	41.1	4.0	PM
					-6	46.1	39.7	4.0	PM
					AVE	46.4	40.4	4.0	

GTAW - Gas Tungsten Arc Weld
PM - Parent Metal
HAZ - Heat Affected Zone

TABLE 12 MECHANICAL PROPERTIES OF WELD TEST SPECIMENS

WELDING PROCESS	SECTION THICKNESS	FILLER ALLOY	PREWELD TEMPERATURE	CONDITION	SPECIMEN NO.	TUS(KSI)	TYS(KSI)	% ELONG.	LOCATION OF FAILURE
GTAW-AC	.375	A356	Room Temp.	WELD IN HEAT TREATED -T6 CONDITION	298-1	24.9	18.1	9.0	PM
					-3	24.9	18.5	7.0	PM
					-5	23.7	16.7	10.0	PM
					-7	24.7	17.6	10.0	PM
					AVE	24.6	17.7	9.0	
				Parent metal -T6	298-2	45.2	40.9	3.0	PM
					-4	47.2	42.2	4.0	PM
					-6	48.2	42.8	5.0	PM
					AVE	46.9	41.9	4.0	
			300°F	WELD IN HEAT TREATED -T6 CONDITION	307-1	23.2	17.7	8.0	PM
					-3	23.3	15.6	8.0	PM
					-5	22.5	15.2	7.0	PM
					-7	23.3	15.5	9.0	PM
					AVE	23.1	16.0	8.0	
				Parent metal -T6	307-2	38.8	34.8	6.0	PM
					-4	36.8	32.1	4.0	PM
					-6	38.2	34.1	4.0	PM
					AVE	37.9	33.7	4.7	
	A357	Room Temp	WELD IN HEAT TREATED -T6 CONDITION	306-1	26.0	17.5	7.0	Haz	
				-3	24.4	17.0	8.0	Haz	
				-5	24.4	17.1	8.0	Haz	
				-7	25.6	16.6	10.0	Haz	
				AVE	25.1	17.1	8.3		
			Parent metal -T6	306-2	46.7	41.7	5.0	PM	
-4	45.8	40.7		4.0	PM				
-6	45.9	40.6		3.0	PM				
AVE	46.1	41.0		4.0					
300°F	WELD IN HEAT TREATED -T6 CONDITION	212-1		23.7	15.4	11.5	PM		
		-3	23.5	14.6	11.5	PM			
		-5	24.0	14.6	11.0	PM			
		-7	23.5	15.4	11.0	PM			
		AVE	23.7	15.0	11.3				
	Parent metal -T6	212-2	41.3	34.4	6.5	PM			
-4		36.7	30.3	8.0	PM				
-6		38.6	31.8	7.0	PM				
AVE		38.9	32.2	7.2					

182

GTAW - Gas Tungsten Arc Weld
PM - Parent Metal
HAZ - Heat Affected Zone

TABLE 13 MECHANICAL PROPERTIES OF WELD TEST SPECIMENS

WELDING PROCESS	SECTION THICKNESS	FILLER ALLOY	PREWELD TEMPERATURE	CONDITION	SPECIMEN NO.	TUS (KSI)	TYS (KSI)	% ELONG.	LOCATION OF FAILURE
GTAW-DCSP	.375	A356	Room Temp.	WELD IN HEAT TREATED -T6 CONDITION	296-1	27.1	19.5	7.0	PM
					-3	28.6	19.7	7.5	PM
					-5	28.9	21.3	6.0	PM
					-7	27.1	18.9	7.5	PM
					AVE	27.9	19.9	7.0	
				Parent metal -T6	296-2	46.0	43.3	2.5	PM
					-4	48.1	44.5	2.5	PM
					-6	48.1	43.8	3.5	PM
		A357	300°F	WELD IN HEAT TREATED -T6 CONDITION	AVE	47.4	43.9	2.8	
					297-1	25.2	17.8	8.0	PM
					-3	24.3	18.4	7.0	PM
					-5	25.4	17.2	9.0	PM
					-7	25.0	16.8	11.0	PM
					AVE	24.9	17.6	8.8	
				Parent metal -T6	297-2	43.0	40.6	3.0	PM
					-4	45.3	40.5	5.0	PM
					-6	41.8	37.7	4.0	PM
		A357	Room Temp.	WELD IN HEAT TREATED -T6 CONDITION	AVE	43.4	39.6	4.0	
					211-1	25.8	21.4	8.0	PM
					-3	46.4	40.9	5.0	PM
					-5	25.5	19.0	9.0	PM
					-7	26.3	20.0	8.0	PM
					AVE	31.0	25.3	7.4	
				Parent metal -T6	211-2	45.6	40.2	3.0	PM
					-4	25.4	19.7	7.0	PM
					-6	47.3	41.6	5.0	PM
GTAW - Gas Tungsten Arc Weld PM - Parent Metal	.375	A356	300°F	WELD IN HEAT TREATED -T6 CONDITION	AVE	39.4	33.8	5.0	
					308-1	24.4	15.5	9.0	PM
					-3	26.1	17.5	7.0	PM
					-5	22.1	14.8	9.0	Weld
					-7	23.3	14.6	10.0	Weld
					AVE	24.0	15.6	8.8	
		A357	Room Temp.	WELD IN HEAT TREATED -T6 CONDITION	308-2	40.9	37.6	4.0	PM
					-4	39.4	35.2	4.0	PM
					-6	39.7	34.8	6.0	PM
					AVE	40.0	35.9	4.7	

5. WELD CORRECTION PROCEDURES

In general, the procedures and techniques required to accomplish weld correction of A357 aluminum sand castings are identical to those commonly employed for weldable wrought alloys. The experience gained during this test program has demonstrated that high-quality weld corrections can be consistently produced by employing reasonable care and standard industry practices. The detail procedures required to accomplish weld correction of typical casting imperfections has been documented in Appendix A.

Specific standards and limits for weld correction of casting imperfections will be controlled by the detail casting material and process specifications. These specifications establish the type, size, and location of imperfections that are permitted to be corrected by welding, and also establish what requirements apply to the completed weld correction zone.

SECTION XI
SURFACE FINISHING

The effects of surface finish on the fatigue properties of cast A357 were evaluated during this phase. The results will be reported at a later date, in the Phase V Full Scale Test Report.

SECTION XII

PRELIMINARY MATERIAL AND PROCESS SPECIFICATION

A preliminary material and process specification, covering A357 aluminum alloy castings produced for use as primary aircraft structural components, was prepared and transmitted to the Air Force. This preliminary specification, M-XXXX, "Aluminum Alloy A357 Castings, Primary Aircraft Structure," will form the basis for the final material and process specification that will be completed in Phase VI of the program.

SECTION XIII

ALLOWABLES TEST CASTINGS DATA

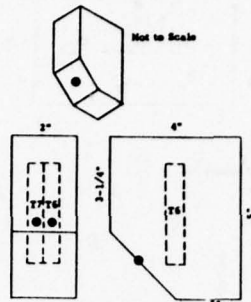
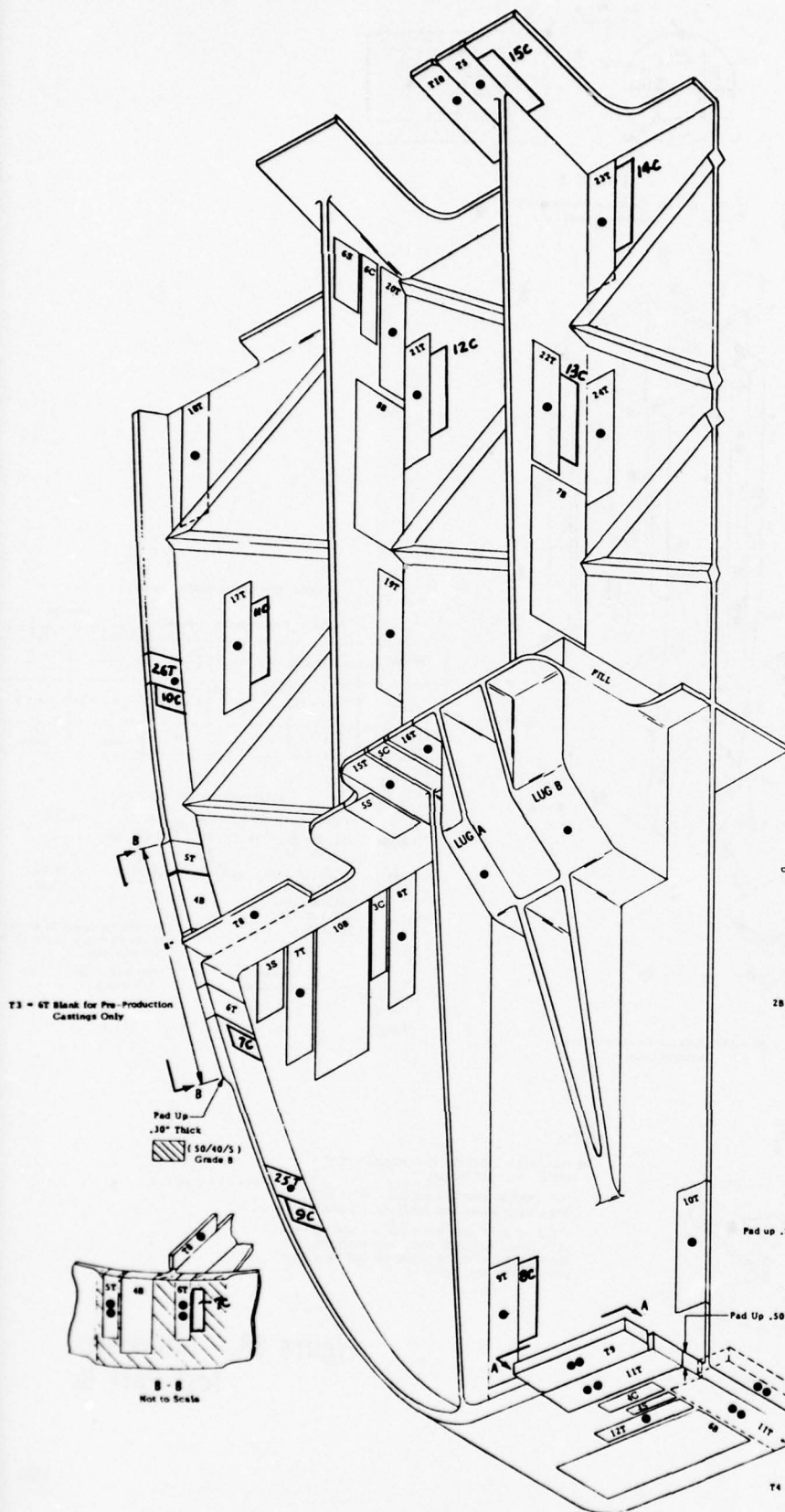
1. TEST CONFIGURATIONS AND TEST PLAN

Two test configurations were established, each representing a full-scale region of the station 170 bulkhead. The configurations, designated allowables parts A and B, are shown in Figures 87 and 88, respectively. The approximate locations of test coupons are also shown. A test plan for the generation and analysis of allowables data was prepared and submitted to the Air Force.

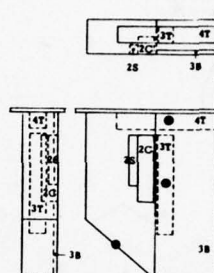
2. TEST CASTINGS

Fourteen test castings were produced during Phase II, and specimens were fabricated and tested in accordance with the test plan. Four allowables parts A and five allowables parts B were produced by the Boeing foundry, and five allowables parts A were produced by Hitchcock Industries, Inc., Minneapolis, Minnesota.

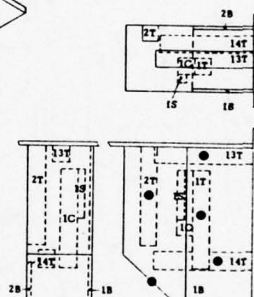
The details of the molds including locations of ingates, risers, chills, and insulation are shown in Figures 89-93. Figures 89 and 90 show these details for the Hitchcock parts A, Figures 91 and 92 for the Boeing parts A, and Figure 93 for the Boeing parts B. The Boeing parts were cast in the vertical position, while the Hitchcock parts were cast horizontally. This difference in casting techniques was utilized to provide a basic comparison between the two orientations, recognizing that the vertical position would be used for the full-scale casting as discussed previously in Section VI. All test parts were heat treated to the -T6 condition.



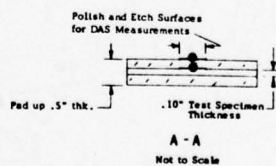
INTEGRAL CAST LUG
(50/40/5)
Grade B
To be located during pre-production



LUG A
(50/40/5)
Grade B
T2 = 3T Blank for Pre-Production Castings Only



LUG B
(50/40/5)
Grade B
T1 = 1T Blank for Pre-Production Castings Only



A - A
Not to Scale

NOTES:

1. INDICATES REQUIRED DAS MEASUREMENT LOCATION. SEE DETAIL A - A FOR DOUBLE DAS MEASUREMENT REQUIREMENTS.
2. DESIGNATED STRESS AREAS INDICATED BY (50/40/5) GRADE B. ALL OTHER AREAS (40/30/3), GRADE C.
3. ALL FLAT TEST SPECIMEN BLANKS WHICH EXCEED .15\"/>

ALLOWABLES TEST COUPONS

BOEING CASTINGS

	Tension	Shear	Bearing
Rounds	1T, 2T, 3T, 4T, 12T, 13T, 14T		
Flats	5T, 6T, 7T, 8T, 9T, 10T, 11T, 15T, 16T, 17T, 18T, 19T, 20T, 21T, 22T, 23T, 24T, 25T, 26T		
Rounds	1C, 2C, 4C	1S, 2S, 4S	
Flats	3C, 5C, 6C	3S, 5S, 6S	18, 28, 38, 48, 68, 78, 88, 108

HITCHCOCK CASTINGS

	Tension	Compression	Shear	Bearing
Rounds	Same as from Boeing castings	1C, 2C	1S, 2S	
Flats		6C	6S	18, 28, 38, 48, 108, 68

	Integral Cast Coupons	Pre-Production Coupons
Rounds	T6, T7	T1, T2
Flats	T8, T9, T10	T3, T4, T5

No 58 or 98 Bearing Specimens

COUPON BLANK SIZES (inches)

	Tension	Compression	Shear	Bearing
Rounds	.5 x .5 x 3	.5 x .5 x 2	.25 x .25 x 1.5	e/D = 1.5 e/D = 2.0
Flats	1 x 4 x t	.625 x 2.645 x t	1 x 2 x t	2 x 5 x t
Specimen Code	T	C	S	B odd B even

ALLOWABLES STATIC TEST COUPONS

**BOEING PATTERN 6R672039
STA 170 BULKHEAD**

SCALE: 1/2\"/>

REV. 1 9/77
BOEING

DRAWN BY: D. L. McLELLAN 4/77

13
14

REQUIREMENTS.
V60/51 GRADE B.

15" THICK
SIDES TO

-- REV. 1

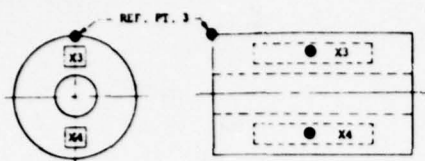
-- REV. 1

FD-2.0
1.5 x 1
0
OVER

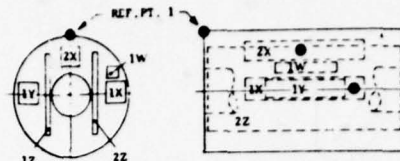
Figure 87. Allowables
Test Part A.

9/77 REPLACE PT. A 5TH
BOEING CASTING WITH
7C, 8C, 9C, 10C, 11C, 12C,
13C, 14C, 15C, 25T, 26T
ADDITIONS TO ACAT.
INBS. DINGL-

2

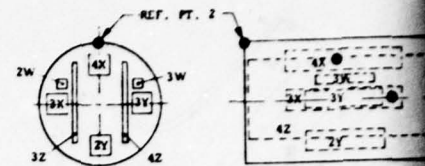


DETAIL 2
INTEGRAL CAST FITTING



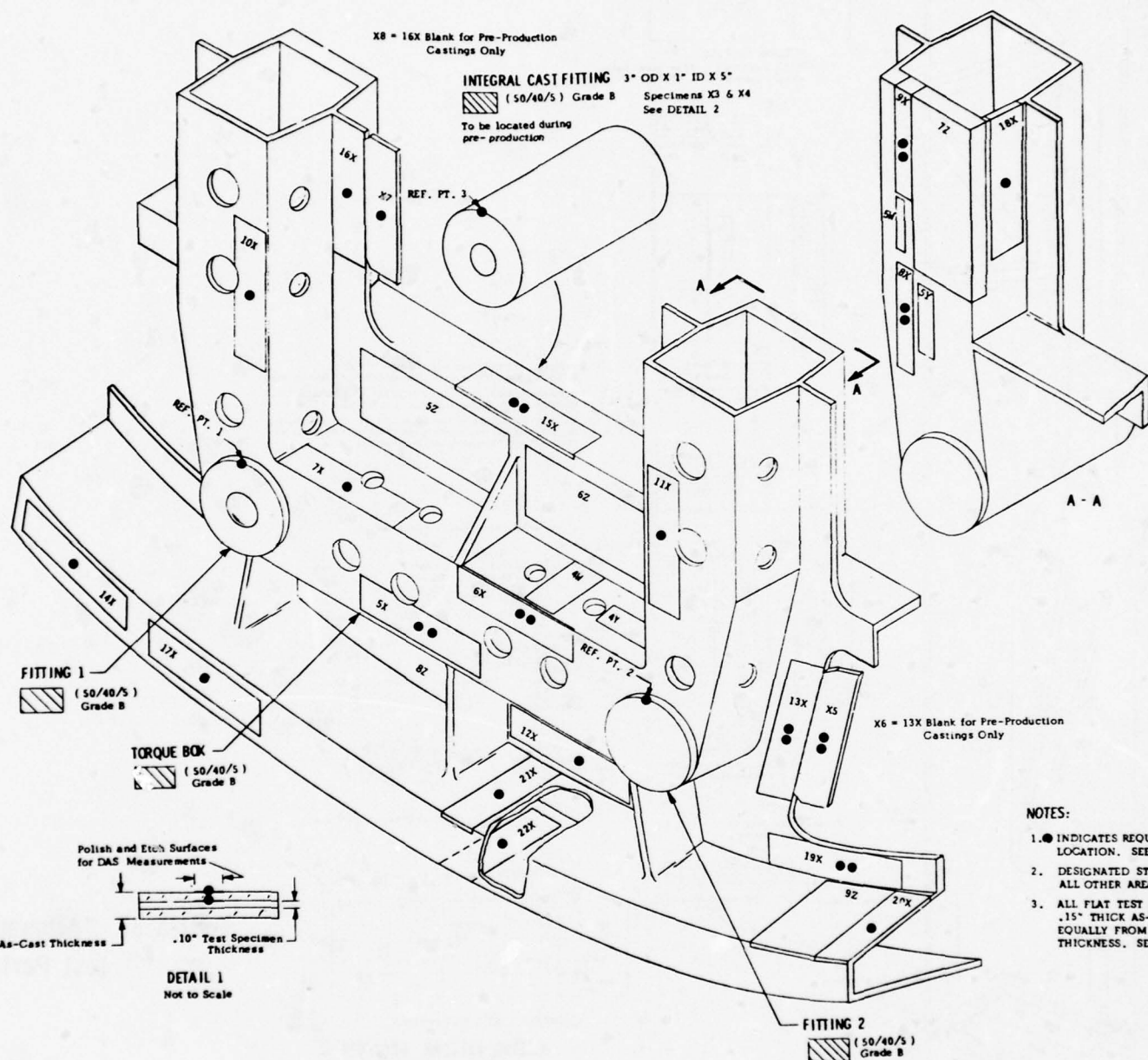
FITTING 1

X1 = 2X Blank for Pre-Production Castings Only



FITTING 2

X2 = 4X Blank for Pre-Production Castings Only



NOTES:

1. ● INDICATES REQUIRED DAS MEASUREMENT LOCATION. SEE DETAIL 1.
2. DESIGNATED STRESS AREA INDICATED. ALL OTHER AREAS ARE (40/30/5).
3. ALL FLAT TEST SPECIMEN BLANKS .15" THICK AS-CAST SHALL BE EQUALLY FROM BOTH SIDES TO THICKNESS. SEE DETAIL 1.

ALLOWABLES STATIC TEST COUPONS

BOEING PATTERN NO. 7R672039
STA 170 BULKHEAD

SCALE: 1/2" = 1"

DRAWN BY: R.E.
REVISED: D.M.


COUPON BLANK SIZES (inches)

	Tension	Compression	Shear	Bearing	
				$e/D = 1.5$	$e/D = 2.0$
Rounds	.5 x .5 x 3	.5 x .5 x 2	.25 x .25 x 1.5	----	----
Flats	1 x 4 x t	.625 x 2.645 x t	1 x 2 x t	2 x 5 x t	2 x 5 x t
Specimen Code	X	Y	W	2 odd	2 even

ALLOWABLES TEST COUPONS

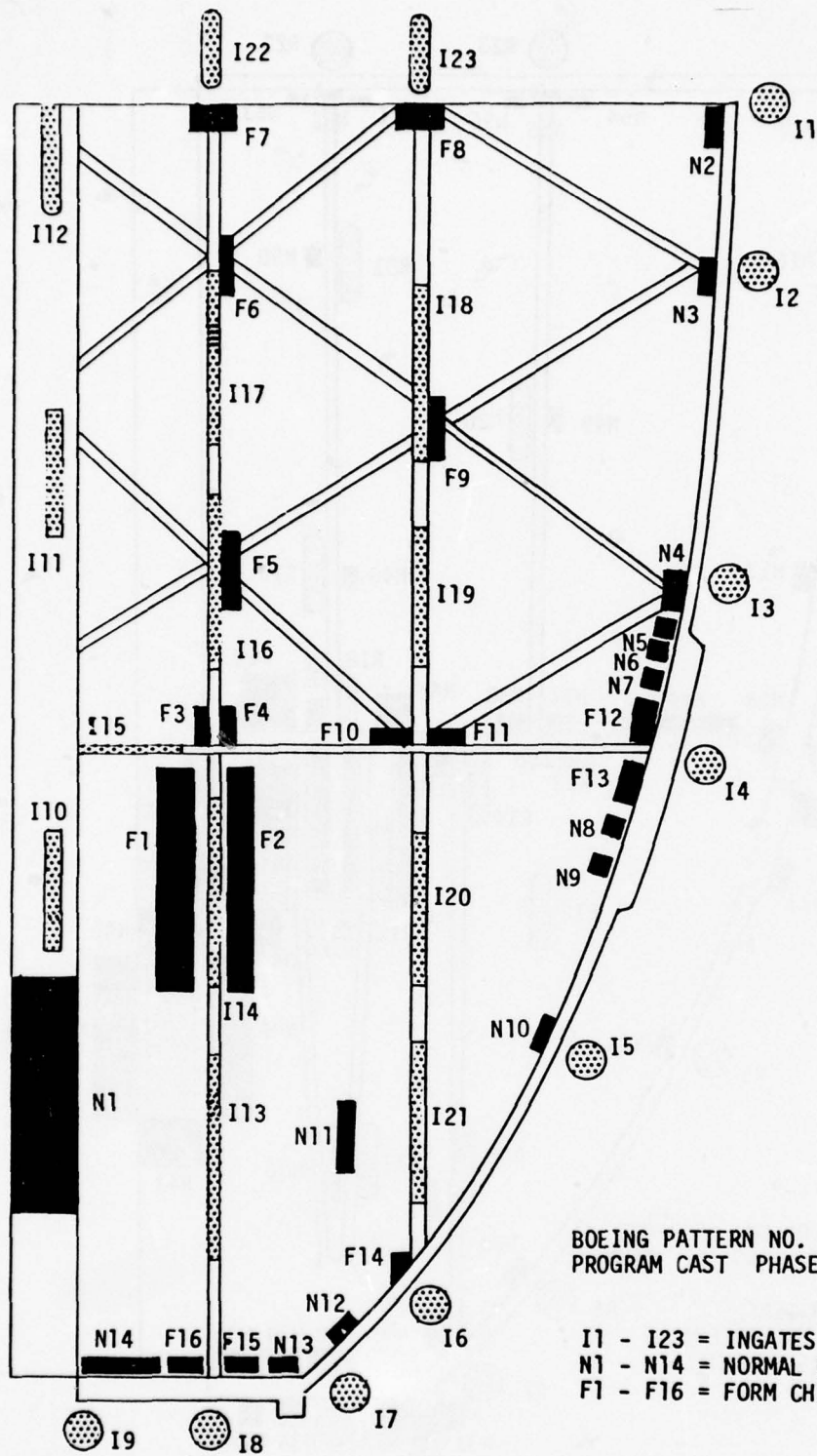
	Tension	Compression	Shear	Bearing
Rounds	1X, 2X, 3X, 4X, 8X, 9X	1Y, 2Y, 3Y	1W, 2W, 3W	----
Flats	5X, 6X, 7X, 10X, 11X, 12X, 13X, 14X, 15X, 16X, 17X, 18X, 19X, 20X, 21X, 22X	4Y, 5Y	4W, 5W	1Z, 2Z, 3Z, 4Z, 5Z, 6Z, 7Z, 8Z, 9Z
				Bearing Specimen 9Z to be tested from four selected castings only.
	Integral Cast Coupons		Pre-Production Coupons	
Rounds	X3, X4		X1, X2	
Flats	X5, X7		X6, X8	

REQUIRED DAS MEASUREMENT
SEE DETAIL 1.

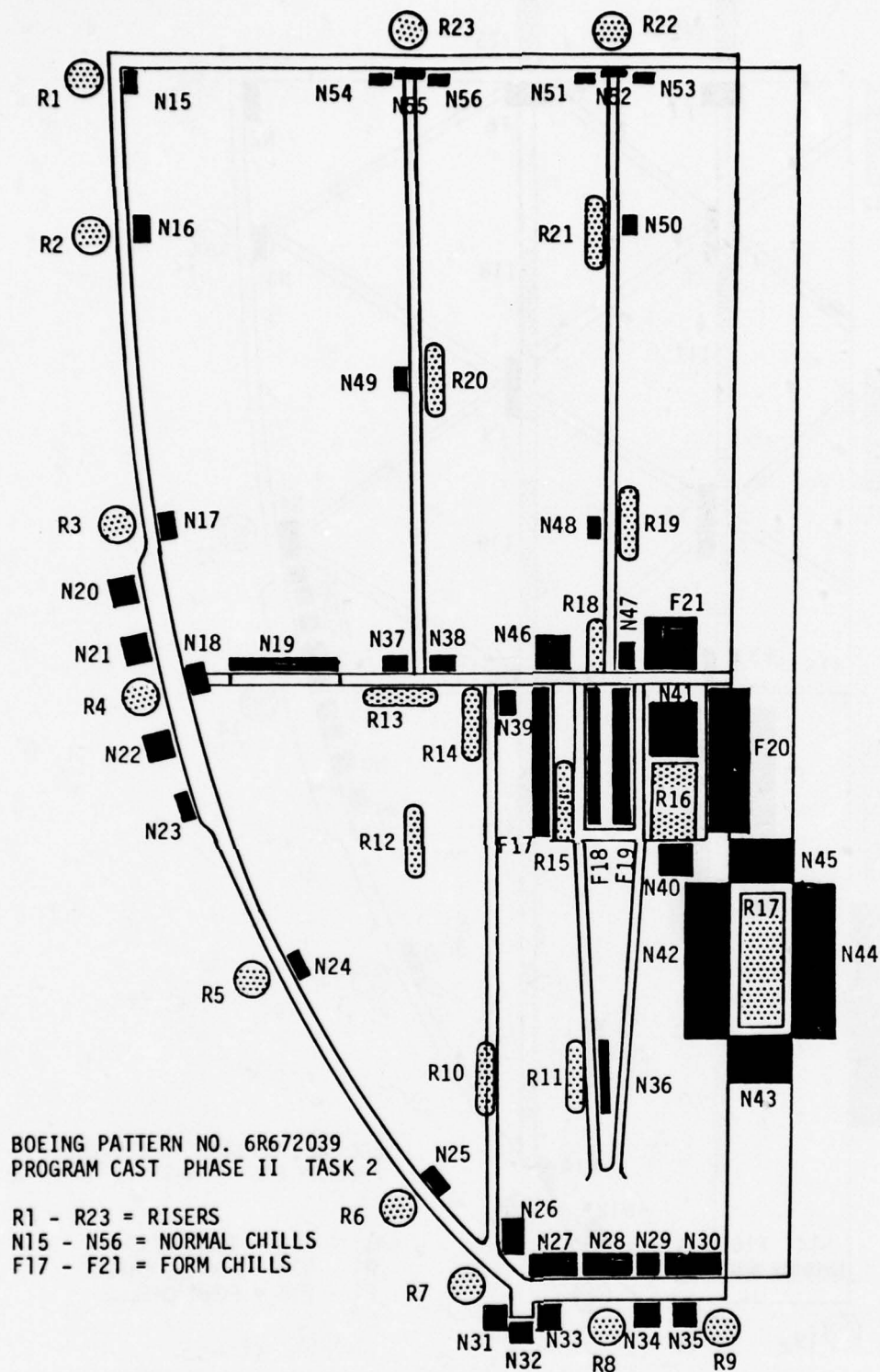
STRESS AREA INDICATED BY:  (50/40/5) GRADE B
INSEAS ARE (40/30/3), GRADE C.

DO NOT SPECIMEN BLANKS WHICH EXCEED
AS-CAST SHALL BE MACHINED
ON BOTH SIDES TO OBTAIN A .10"
SEE DETAIL 1.

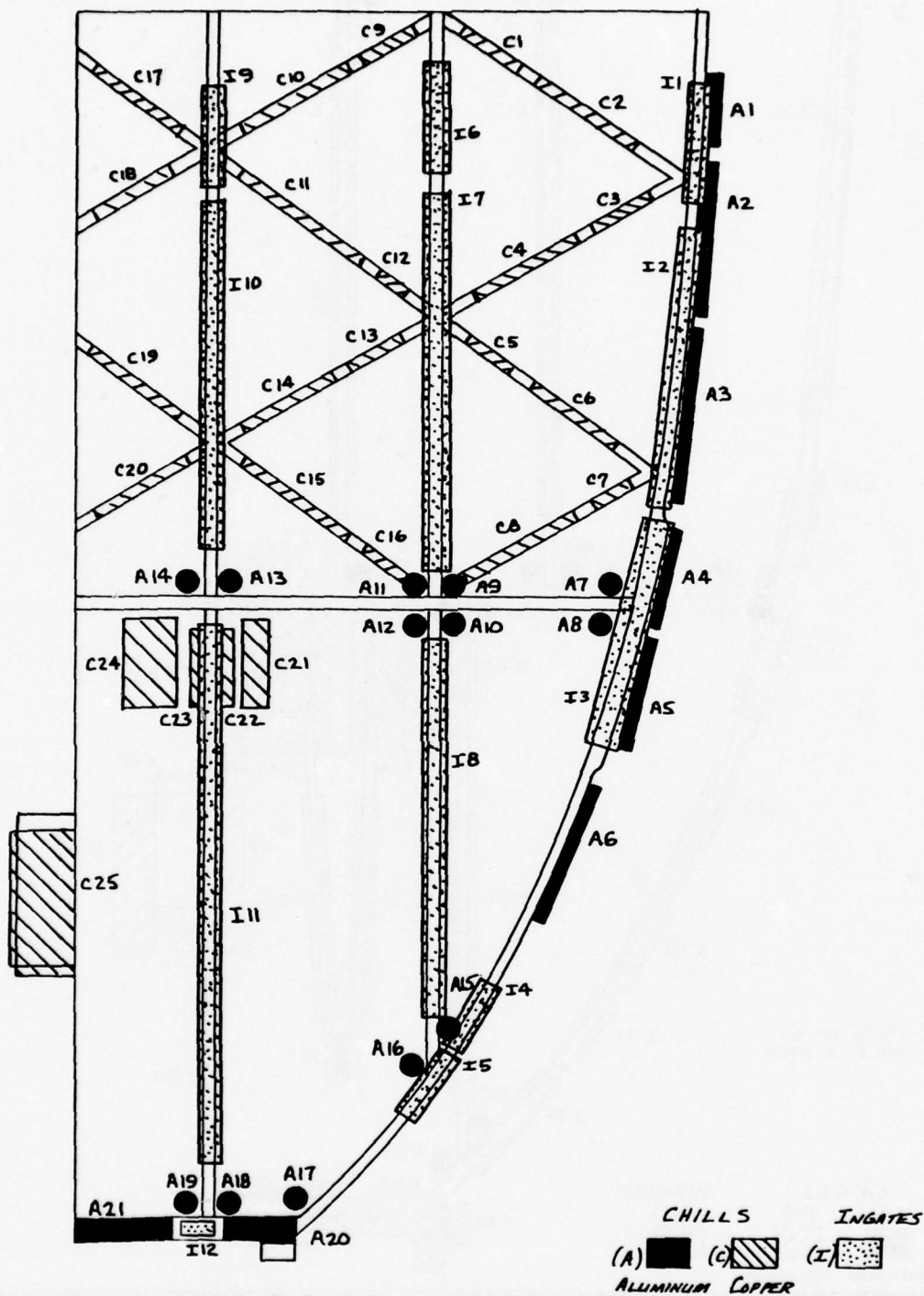
Figure 88. Allowables
Test Part B.



ENGR.	D. M. Lellan	7/77	REVISED	DATE	FIGURE 89. DETAILS OF DRAG-- HITCHCOCK ALLOWABLES PART A CASTINGS.	
CHECK						
APR						
APR						
					BOEING	191

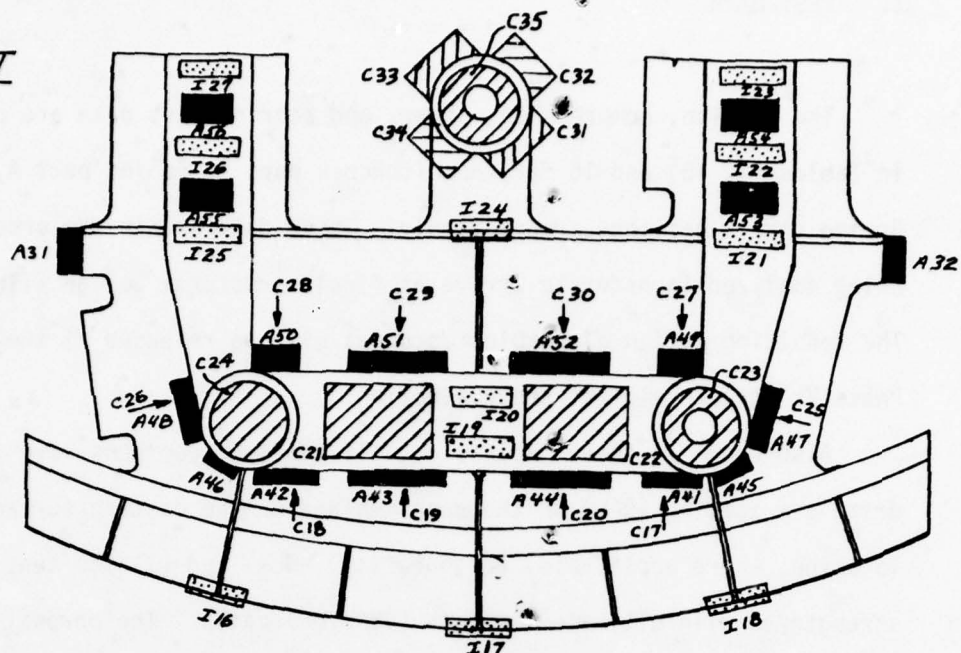


ENGR.	D. McCallan	7/77	REVISED	DATE	FIGURE 90. DETAILS OF COPE--	
CHECK					HITCHCOCK ALLOWABLES PART A CASTINGS.	
APR						
APR						
					BOEING	192

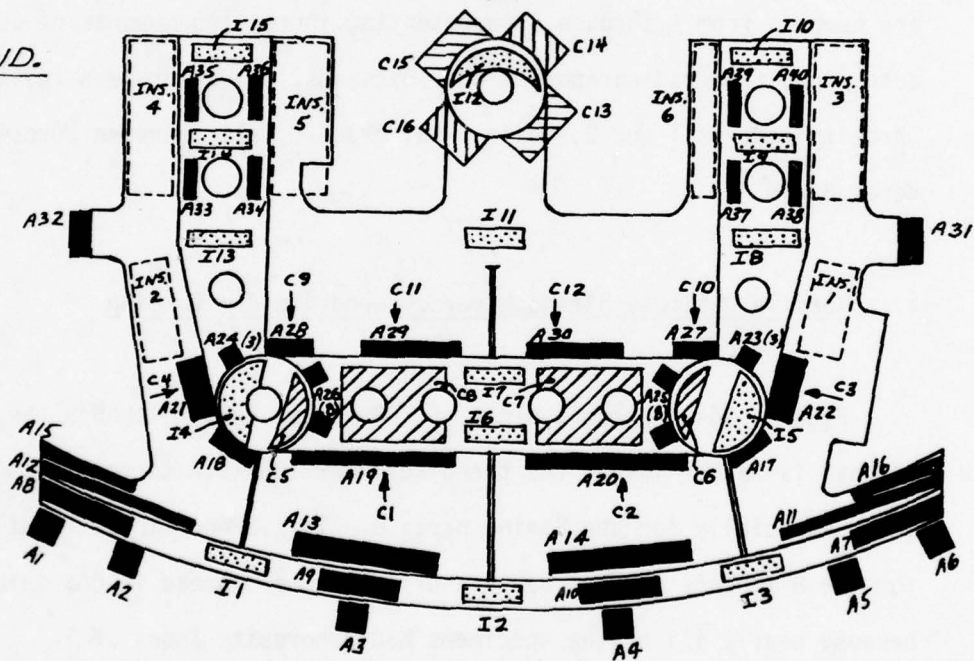


ENGR.	P. McEllan	8/97	REVISED	DATE	FIGURE 91. DETAILS OF MOLD, FORWARD SIDE-- BOEING ALLOWABLES PART A CASTINGS.	BOEING PATTERN 6R672039
CHECK						
APR						
APR						
THE BOEING COMPANY RENTON, WASHINGTON						193

AFT



FWD.



CHILLS
ALUMINUM (A) COPPER (C)

INGATE
(I)

INSULATOR
PLASTER (INS)

NOTE: SYMBOL C ↓
INDICATES COPPER
CHILL LOCATED BEHIND
ALUMINUM CHILL

ENGR.	D.M. Lellan	T/Y	REVISED	DATE	FIGURE 93. DETAILS OF MOLD, AFT AND FORWARD SIDES OF BOEING ALLOWABLES PART B CASTINGS.	
CHECK						
APR						
APR						
BOEING						195

3. TEST DATA

The tension, compression, shear, and bearing test data are presented in Tables 14, 15, and 16 for the Hitchcock part A, Boeing part A, and Boeing part B castings, respectively. These data are in the process of being analyzed in order to arrive at final structural design allowables. The resulting design allowables document will be released at the end of Phase V, Structural Test and Evaluation.

Also shown in these tables, for all tension specimens, are (1) dendrite arm spacing (DAS) on the specimen and on the casting surface at that location, where applicable, (2) porosity index, and (3) the tensile yield strength/tensile ultimate strength (TYS/TUS) ratio. The porosity indexes are numbers from 1 through 7 representing increasing amounts of porosity as determined from radiographs of the specimens. X-ray grade B falls between porosity indexes 1 and 2, while X-ray grade C falls between porosity indexes 3 and 4.

a. Tensile Ultimate Strength versus Dendrite Arm Spacing

Figures 94-96 present plots of TUS versus DAS. Although the scatter in data is rather large, the trend to lower TUS with increasing DAS can be seen, especially for the Boeing parts B. This trend cannot readily be seen for the Hitchcock parts A because of a narrower spread in DAS values and because nearly all of the specimens had a porosity index of 1.

TABLE 14
STATIC MECHANICAL PROPERTIES DATA
HITCHCOCK ALLOWABLES PART A CASTINGS -- A357-T6

Part Location	Non- inal Thick- ness (in.)	Tension					Compression			Shear		Bearing																									
		Part No.	TUS (ksi)	Elong. (%)	TYS (ksi)	DAS (0.0001 in.)	Por- osity Index	Part No.	CYS (ksi)	Part No.	SUS (ksi)	e/D = 1.5		e/D = 2.0																							
												Part No.	BYS (ksi)	Part No.	BUS (ksi)	Part No.	BYS (ksi)																				
Lug B Center	2.0	1T5H	48.4	40.4	5	0.835	18	26	1	1C5H	42.2	155H	34.6	185H	81.0	63.0	285H	103.6	79.8																		
		1T6H	48.7	40.0	5	0.821	20	28	1	1C6H	42.2	156H	34.8							186H	77.8	67.0	286H	102.7	80.5												
		1T7H	47.2	42.0	3	0.890	20	29	1	1C7H	42.0	157H	34.6													187H	84.3	65.0	287H	100.1	81.0						
		1T8H	47.2	40.4	3	0.856	21	26	1	1C8H	41.7	158H	33.9																			188H	78.8	65.8	288H	103.0	80.9
		1T9H	48.7	40.7	4	0.836	21	30	1	1C9H	42.9	159H	34.6																								
Lug B Edge	2.0	2T5H	49.4	39.5	6	0.800	16	26	1					185H	81.0	63.0	285H	103.6	79.8																		
		2T6H	48.6	38.8	5	0.798	17	28	1											186H	77.8	67.0	286H	102.7	80.5												
		2T7H	48.5	39.2	5	0.808	15	29	1																	187H	84.3	65.0	287H	100.1	81.0						
		2T8H	48.2	38.8	5	0.805	18	26	1																							188H	78.8	65.8	288H	103.0	80.9
		2T9H	48.6	40.0	4	0.823	18	30	1																												
Lug B Top	2.0	13T5H	50.4	40.7	6	0.808	15	26	1					185H	81.0	63.0	285H	103.6	79.8																		
		13T6H	50.1	40.1	6	0.800	15	28	1											186H	77.8	67.0	286H	102.7	80.5												
		13T7H	49.3	40.3	6	0.817	18	29	1																	187H	84.3	65.0	287H	100.1	81.0						
		13T8H	49.2	40.7	5	0.827	20	26	1																							188H	78.8	65.8	288H	103.0	80.9
		13T9H	49.8	40.9	5	0.821	19	30	1																												
Lug B Bottom	2.0	14T5H	47.9	40.3	4	0.841	23	26	1					185H	81.0	63.0	285H	103.6	79.8																		
		14T6H	48.2	40.0	4	0.830	21	28	1											186H	77.8	67.0	286H	102.7	80.5												
		14T7H	46.8	39.6	4	0.846	23	29	1																	187H	84.3	65.0	287H	100.1	81.0						
		14T8H	47.3	39.9	3	0.844	20	26	1																							188H	78.8	65.8	288H	103.0	80.9
		14T9H	47.9	41.4	3	0.864	21	30	1																												
Lug A Center	1.0	3T5H	48.3	40.6	4	0.841	14	23	1	2C5H	42.1	255H	34.8	385H	80.3	66.4	485H	101.9	81.6																		
		3T6H	49.0	40.1	4	0.818	16	27	1	2C6H	42.3	256H	35.0							386H	75.2	64.5	486H	92.4	78.1												
		3T7H	48.7	40.4	5	0.830	17	23	1	2C7H	41.8	257H	35.4													387H	80.0	66.9	487H	100.6	81.8						
		3T8H	49.8	41.0	5	0.823	16	22	1	2C8H	41.9	258H	35.2																			388H	75.4	68.6	488H	94.8	83.0
		3T9H	--	(1)	--	--	16	26	2	2C9H	42.8	259H	35.6																								
Lug A Top	1.0	4T5H	50.0	39.0	8	0.780	16	27	1					385H	80.3	66.4	485H	101.9	81.6																		
		4T6H	49.7	39.3	7	0.791	16	23	1											386H	75.2	64.5	486H	92.4	78.1												
		4T7H	49.7	39.7	7	0.799	18	23	1																	387H	80.0	66.9	487H	100.6	81.8						
		4T8H	49.3	39.4	6	0.799	15	22	1																							388H	75.4	68.6	488H	94.8	83.0
		4T9H	50.0	40.3	7	0.806	20	26	1																												
Pad Up Attchmt. Flange	0.30	5T5H	49.8	39.7	6	0.797	16	15	1					385H	80.3	66.4	485H	101.9	81.6																		
		5T6H	47.4	40.0	3	0.844	15													386H	75.2	64.5	486H	92.4	78.1												
		5T7H	50.0	41.0	5	0.820	18																			387H	80.0	66.9	487H	100.6	81.8						
		5T8H	49.4	41.6	4	0.842	19																									388H	75.4	68.6	488H	94.8	83.0
		5T9H	49.5	40.4	6	0.816	15																														

(1) Premature failure Specimen Casting surface 1 - Least 7 - Most

TABLE 14 (Cont.)

Part Location	Nominal Thickness (in.)	Tension				Compression				Shear				Bearing						
		Part No.	TUS (ksi)	Elong. (%)	TYS (ksi)	DAS (0.0001 in.)	Porosity Index	Part No.	CYS (ksi)	Part No.	SUS (ksi)	Part No.	BUS (ksi)	BYS (ksi)	Part No.	BUS (ksi)	BYS (ksi)			
e/D = 1.5																		e/D = 2.0		
Pad Up Attchmt. Flange	.30	6T5H	50.0	41.3	6	0.826	16	1												
		6T6H	47.6	41.1	4	0.863	18	1												
		6T7H	48.8	41.5	4	0.850	20	1												
		6T8H	48.7	41.5	4	0.852	19	1												
Lwr. Web Left	.10	6T9H	49.5	41.9	4	0.846	18	1												
		7T5H	48.4	40.3	2	0.833	18	1												
		7T6H	48.1	39.8	3	0.827	17	1												
		7T7H	45.0	41.3	1	0.918	17	3												
Lwr. Web Left	.10	7T8H	46.6	41.9	3	0.899	21	1												
		7T9H	46.8	41.3	2	0.882	13	1												
		8T5H	47.3	39.3	4	0.831	17	1												
		8T6H	47.6	41.6	5	0.874	16	1												
Web Bottom	.10	8T7H	44.1	39.3	0	0.891	22	1												
		8T8H	46.2	40.3	3	0.872	19	1												
		8T9H	45.0	40.0	1	0.889	13	1												
		9T5H	49.0	41.3	5	0.843	15	1												
Web Bottom	.10	9T6H	48.7	40.2	4	0.825	15	1												
		9T7H	45.4	40.1	4	0.883	21	1												
		9T8H	46.9	40.3	4	0.859	21	1												
		9T9H	49.3	40.5	5	0.822	13	1												
Web Bottom	.10	10T5H	--	(1)	--	--	14	1												
		10T6H	47.9	39.7	4	0.829	19	1												
		10T7H	46.7	39.1	5	0.837	19	1												
		10T8H	47.2	40.2	4	0.852	19	1												
Pad Up Base Flange	.50	10T9H	45.4	39.3	3	0.866	16	3												
		11T5H	48.1	39.8	5	0.827	17	16	1											
		11T6H	46.7	38.1	5	0.816	19	16	1											
		11T7H	47.0	39.5	4	0.840	19	20	1											
Pad Up Base Flange	.50	11T8H	47.1	40.3	4	0.856	20	18	1											
		11T9H	48.0	39.8	5	0.829	18	12	1											
		12T5H	48.7	39.5	6	0.811	17	16	1											
		12T6H	47.9	37.9	8	0.791	17	16	1											
Pad Up Base Flange	.50	12T7H	47.3	38.7	6	0.818	18	20	1											
		12T8H	47.8	38.9	6	0.814	17	18	1											
		12T9H	48.9	39.5	6	0.808	13	12	1											
																		685H	96.5	75.2
																		686H	97.1	82.0
																		687H	92.6	80.0
																		1088H	94.2	82.3
																		1089H	90.0	76.1
																		685H	96.5	75.2
																		686H	97.4	73.8
																		687H	93.0	76.9
																		688H	92.5	75.0
																		689H	96.3	75.1

(1) Failed through weld-correctable pore

Specimen

Casting surface

1 - Least
7 - Most

TABLE 14 (Cont.)

Part Location	Nominal Thickness (in.)	Tension					DAS (0.0001 in.)	Porosity Index	Compression			Shear			Bearing		
		Part No.	TUS (ksi)	TYS (ksi)	Elong. (%)	TYS/TUS			Part No.	CYS (ksi)	Part No.	SUS (ksi)	Part No.	BUS (ksi)	Part No.	BYS (ksi)	
																	e/D = 1.5
WL 130 Deck	.25	15TSH	44.8	39.7	2	0.886	19	1									
		15TGH	44.0	39.3	2	0.893	22	2									
		15T7H	44.9	38.9	2	0.866	22	1									
		15T8H	45.5	39.1	2	0.859	21	2									
		15T9H	44.1	39.4	2	0.893	23	2									
WL 130 Deck	.25	16TSH	49.2	39.4	8	0.801	14	1									
		16TGH	--	(1)	--	--	15	1									
		16T7H	48.2	39.4	6	0.817	18	1									
		16T8H	47.1	38.8	5	0.823	13	1									
		16T9H	48.5	39.3	5	0.810	17	1									
Web Up. Left	.10	17TSH	--	(2)	--	--	20	7									
		17TGH	45.6	40.7	2	0.892	20	1									
		17T7H	44.8	40.0	2	0.893	20	3									
		17T8H	44.5	40.6	2	0.912	21	1									
		17T9H	45.6	40.3	2	0.884	22	1									
Web Up. Left	.10	18TSH	48.8	42.4	3	0.869	22	1									
		18TGH	47.7	41.2	3	0.864	21	1									
		18T7H	--	(3)	--	--	23	1									
		18T8H	47.5	42.9	2	0.903	23	1									
		18T9H	46.8	41.8	2	0.893	20	1									
Flange Up. Left	.20	19TSH	48.6	41.6	2	0.856	18	1									
		19TGH	48.9	42.1	3	0.861	21	1									
		19T7H	47.8	42.0	3	0.878	21	1									
		19T8H	47.8	40.1	3	0.840	18	1									
		19T9H	47.8	41.4	3	0.866	18	1									
Flange Up. Left	.20	20TSH	47.8	42.0	3	0.878	22	1									
		20TGH	47.0	41.8	3	0.889	16	1									
		20T7H	47.1	41.6	3	0.883	20	1									
		20T8H	47.2	42.7	3	0.904	22	1									
		20T9H	48.3	41.0	4	0.849	18	1									
Web Up. Center	.10	21TSH	--	(5)	--	--	15	1									
		21TGH	45.7	39.7	2	0.869	17	1									
		21T7H	--	(6)	--	--	17	1									
		21T8H	46.6	40.2	2	0.863	18	1									
		21T9H	--	(7)	--	--	16	1									

(1) Failed through sand inclusion (2) Failed through 2 large weld-correctable pores (3) Failed through surface discontinuity
 (4) Specimen buckled (5) Multiple cracks in specimen (6) Premature failure through thfn area
 (7) Failed through weld-correctable pore at center line (8) Casting surface 1 - Least 7 - Most

TABLE 14 (Concluded)

Part Location	Nominal Thickness (in.)	Tension					DAS (0.0001 in.)	Porosity Index	Compression		Shear		Bearing					
		Part No.	TUS (ksi)	TYS (ksi)	Elong. (%)	TYS TUS			Part No.	CYS (ksi)	Part No.	SUS (ksi)	Part No.	BYS (ksi)	Part No.	BUS (ksi)	BYS (ksi)	BUS (ksi)
Flange Upr. Right	.20	22T5H	47.9	40.0	4	0.835	14	1										
		22T6H	47.3	39.8	4	0.841	18	1										
		22T7H	46.8	39.8	4	0.850	19	1										
		22T8H	47.6	40.2	4	0.844	14	1										
		22T9H	47.6	40.3	4	0.846	16	1										
Web Upr. Right	.10	23T5H	49.2	42.3	3	0.860	17	1										
		23T6H	47.4	41.0	3	0.865	19	1										
		23T7H	46.6	39.7	3	0.852	24	1										
		23T8H	45.1	41.2	2	0.913	23	1										
		23T9H	46.9	41.3	2	0.880	25	1										
Web Upr. Right	.10	24T5H	47.9	40.6	3	0.847	21	1										
		24T6H	46.4	39.6	3	0.853	16	1										
		24T7H	46.4	40.2	2	0.866	17	2										
		24T8H	46.7	40.3	3	0.863	22	1										
		24T9H	46.5	40.4	2	0.869	16	1										
Integral Lug Center	2.0	T6/5H	46.7	39.4	2	0.843	21	17										
		T6/6H	46.7	38.6	2	0.826	26	15										
		T6/7H	45.1	38.2	2	0.847	20	18										
		T6/8H	45.5	39.2	1	0.861	18	18										
		T6/9H	46.8	38.7	3	0.827	20	14										
Integral Lug Center	2.0	T7/5H	46.0	38.2	2	0.830	22	17										
		T7/6H	46.5	38.5	2	0.828	22	15										
		T7/7H	45.1	38.1	2	0.845	20	18										
		T7/8H	--	(1)	--	--	18	18										
		T7/9H	46.9	39.9	2	0.851	18	14										
Integral WL 130	.25	T8/5H	48.2	40.9	4	0.848	22	17										
		T8/6H	48.6	40.1	7	0.825	18	21										
		T8/7H	--	(2)	--	--	23	16										
		T8/8H	45.9	41.3	3	0.900	23	18										
		T8/9H	48.7	40.2	5	0.825	14	16										
Pad Up Base Flange	.50	T9/5H	49.4	39.2	7	0.793	21	16										
		T9/6H	48.1	37.6	8	0.782	13	16										
		T9/7H	48.4	39.2	5	0.810	19	20										
		T9/8H	48.9	39.0	6	0.797	20	18										
		T9/9H	49.0	38.7	7	0.790	13	12										
Integral WL 150	.15	T10/5H	48.3	39.7	3	0.822	25	15										
		T10/6H	49.7	42.6	4	0.857	25	20										
		T10/7H	48.7	40.6	3	0.834	21	16										
		T10/8H	48.0	39.3	3	0.819	20	16										
		T10/9H	48.1	40.2	3	0.836	20	14										

(1) Premature failure

(2) Failed through punch mark

Specimen

Casting surface

1 - Least
7 - Most

(1) Premature failure (2) Failed through punch mark




 Specimen
  Casting surface
  1 - Least
 7 - Most

TABLE 15
STATIC MECHANICAL PROPERTIES DATA
BOEING ALLOWABLES PART A CASTINGS -- A357-T6

Part Location	Nominal Thickness (in.)	Tension					Compression		Shear		Bearing							
		Part No.	TUS (ksi)	TYS (ksi)	Elong. (%)	TYS/TUS	DAS (0.0001 in.)	Porosity Index	Part No.	CYS (ksi)	Part No.	SUS (ksi)	e/D = 1.5		e/D = 2.0			
													Part No.	BYS (ksi)	Part No.	BYS (ksi)		
Lug B Center	2.0	1T3	47.7	40.9	5	0.857	15	21	1C3	42.9	1S3	34.0						
		1T4	48.7	40.8	5	0.838	17	25	1C4	43.9	1S4	34.1						
		1T5	47.7	40.8	6	0.855	17	17	1C5	41.2	1S5	33.9						
		1T6	48.7	42.6	5	0.875	16	19	1C6	44.5	1S6	34.0						
Lug B Edge	2.0	2T3	49.5	39.5	8	0.798	10	21					183	81.9	63.1	283	97.5	76.2
		2T4	48.8	40.0	7	0.820	17	25					184	82.2	65.5	284	103.1	78.0
		2T5	48.2	40.1	7	0.832	16	17					185	77.4	63.4	285	98.1	79.9
		2T6	49.0	41.9	5	0.855	17	19					186	80.2	67.1	286	100.0	82.3
Lug B Top	2.0	13T3	49.6	40.0	8	0.806	14	21										
		13T4	50.5	40.5	10	0.802	11	25										
		13T5	49.5	39.5	10	0.798	15	17										
		13T6	49.3	40.4	7	0.819	14	19										
Lug B Bottom	2.0	14T3	46.1	38.8	4	0.842	21	21										
		14T4	48.4	40.2	5	0.831	17	25										
		14T5	47.2	38.0	8	0.805	17	17										
		14T6	46.6	39.5	5	0.848	21	19										
Lug A Center	1.0	3T3	49.1	40.6	5	0.827	10	17	2C3	42.0	2S3	34.0	383	80.8	64.2			
		3T4	--	(1)	--	--	14	21	2C4	42.9	2S4	34.8	384	82.2	68.2			
		3T5	48.2	40.8	4	0.846	14	14	2C5	42.6	2S5	35.5	385	75.0	63.8			
		3T6	48.2	42.3	5	0.878	15	19	2C6	43.7	2S6	34.6	386	80.0	64.8			
Lug A Top	1.0	4T3	50.0	40.5	10	0.810	13	17										
		4T4	50.2	40.1	8	0.799	14	21										
		4T5	48.1	41.2	3	0.857	15	14										
		4T6	47.9	40.8	5	0.852	17	19										
Pad Up Attachmt. Flange	.30	5T3	50.0	41.2	7	0.824	14									483	103.9	86.7
		5T4	52.3	41.7	8	0.797	14									484	90.8	79.3
		5T5	47.7	40.5	6	0.849	15									485	87.1	75.6
		5T6	47.7	43.2	4	0.906	17									486	88.0	79.3
Pad Up Attachmt. Flange	.30	6T3	49.4	41.2	6	0.834	10		7C3	43.4								
		6T4	49.0	42.5	3	0.867	10		7C4	44.9								
		6T5	44.8	39.3	3	0.877	22		7C5	43.5								
		6T6	45.2	40.2	4	0.889	18		7C6	44.2								

(1) Failed outside gage area

Specimen

Castling surface

1 - Least
7 - Most

1 - Least
7 - Most

Specimen
Casting surface

(1) Failed outside gage area

TABLE 15 (Cont.)

Part Location	Nominal Thickness (in.)	Tension					Compression			Shear			Bearing		
		Part No.	TUS (ksi)	TYS (ksi)	Elong. (%)	TYS/TUS	DAS (0.0001 in.)	Porosity Index	Part No.	CYS (ksi)	Part No.	SUS (ksi)	Part No.	BUS (ksi)	BYS (ksi)
Lwr. Web Left	.10	773	44.1	39.0	3	0.884	15	4				353	34.0	1083	91.9
		774	46.8	41.5	3	0.887	15	3				354	33.8	1084	91.5
		775	42.8	37.8	3	0.883	12	4				355	30.0	1085	94.0
		776	44.4	41.3	4	0.930	13	3				356	30.0	1086	91.7
		873	46.9	40.3	4	0.859	13	1	3C3	42.6					
Lwr. Web Left	.10	874	45.8	40.8	4	0.891	15	2	3C4	45.1					
		875	47.9	39.8	7	0.831	17	2	3C5	44.1					
		876	45.6	40.1	4	0.879	17	3	3C6	42.1					
		973	47.0	40.5	5	0.862	13	3	8C3	43.8					
Web Bottom	.10	974	46.4	41.9	5	0.903	14	2	8C4	43.4					
		975	45.2	39.3	4	0.869	13	2	8C5	43.8					
		976	45.8	40.7	4	0.889	14	3	8C6	43.9					
		1073	45.1	38.8	5	0.860	13	3							
Web Bottom	.10	1074	--	(1)	--	--	12	2							
		1075	45.5	40.2	3	0.884	14	2							
		1076	47.9	43.1	3	0.900	13	2							
		1173	47.0	40.6	5	0.864	20	3	4C3	43.6	453	32.9			
Pad Up Base Flange	.50	1174	(2)	--	--	--	13	2	4C4	42.5	454	32.4			
		1175	50.0	40.7	4	0.814	14	1	4C5	40.6	455	32.8			
		1176	46.7	40.4	5	0.865	16	3	4C6	41.8	456	33.4			
		1273	48.4	42.2	4	0.872	21	3							
Pad Up Base Flange	.50	1274	46.2	41.5	3	0.898	17	2							
		1275	44.7	40.7	3	0.911	16	1							
		1276	48.7	41.7	5	0.856	21	3							
		1573	47.2	40.7	3	0.862	24	3							
WL 130 Deck	.25	1574	45.6	42.4	4	0.930	18	4							
		1575	44.3	40.3	4	0.910	15	4							
		1576	51.3	42.8	7	0.834	14	1							
		1673	--	(3)	--	--	15	1	5C3	43.9	553	32.2			
WL 130 Deck	.25	1674	51.3	38.0	10	0.741	15	1	5C4	45.0	554	33.8			
		1675	50.1	41.3	7	0.824	15	1	5C5	41.9	555	35.2			
		1676	49.8	43.3	5	0.869	16	4	5C6	39.6	556	33.4			

(1) Failed prior to yield

(2) Failed in grip

(3) Inaccurate TVS recording

Specimen

Casting surface

1 - Least
7 - Most

TABLE 15 (Cont.)

Part Location	Nominal Thickness (in.)	Tension					Compression		Shear		Bearing					
		Part No.	TUS (ksi)	Elong. (%)	TYS (ksi)	DAS (0.0001 in.)	Porosity Index	Part No.	CYS (ksi)	Part No.	SUS (ksi)	e/D = 1.5		e/D = 2.0		
												Part No.	BYS (ksi)	Part No.	BYS (ksi)	
Web Up. Left	.10	1773	47.4	0	41.6	13	2	1103	42.2							
		1774	47.4	4	43.1	13	2	1104	42.3							
		1775	45.2	4	40.8	11	3	1105	40.1							
		1776	46.4	4	43.3	15	4	1106	43.9							
Web Up. Left	.10	1873	39.6	3	33.5	14	3									
		1874	(1)	--	--	13	2									
		1875	45.5	4	40.3	14	3									
		1876	41.9	7	35.2	16	1									
Flange Up. Left	.20	1973	45.2	3	40.2	19	6									
		1974	44.3	3	41.0	21	5									
		1975	44.8	40.6	3	3	906	19								
		1976	47.7	43.2	3	3	906	15								
Flange Up. Left	.20	2073	44.8	39.9	3	0.891	21	4	603	(2)	653	35.0			883	96.5
		2074	47.5	42.6	3	0.897	28	3	604	43.0	654	34.5			884	86.7
		2075	47.6	41.4	3	0.870	23	3	605	44.6	655	35.1			885	92.8
		2076	46.3	42.9	3	0.927	19	5	606	44.0	656	34.7			886	95.4
Web Up. Center	.10	2173	47.6	42.1	3	0.884	16	3	1203	43.0						
		2174	43.3	41.0	3	0.947	25	4	1204	44.6						
		2175	48.7	41.2	7	0.846	15	2	1205	42.6						
		2176	45.6	41.5	3	0.910	15	4	1206	44.0						
Flange Up. Rt.	.20	2273	46.0	40.1	3	0.872	20	5	1303	42.6			783	--	(3)	
		2274	45.9	41.8	3	0.911	18	3	1304	46.5			784	76.2	70.1	
		2275	46.2	41.2	4	0.892	17	4	1305	43.3			785	65.4	65.4	
		2276	48.7	42.9	5	0.881	18	3	1306	45.7			786	76.8	73.0	
Web Up. Rt.	.10	2373	47.8	42.9	5	0.897	19	3	1403	43.3						
		2374	48.9	42.3	5	0.865	17	1	1404	44.0						
		2375	46.4	39.4	5	0.849	14	3	1405	42.5						
		2376	49.4	42.8	5	0.866	17	4	1406	48.1						
Web Up. Rt.	.10	2473	45.6	40.8	4	0.895	15	4								
		2474	47.0	41.8	3	0.889	14	2								
		2475	46.0	39.7	3	0.863	14	4								
		2476	47.5	43.0	3	0.905	14	3								
(1) Failed in grip		(2) Specimen buckled	(3) Failed prematurely					Specimen	Casting surface							
								1 - Least								
								7 - Most								

TABLE 15 (Concluded)

Part Location	Non- inal Thick- ness (in.)	Tension					Compression		Shear		Bearing					
		Part No.	TUS (ksi)	TYS (ksi)	Elong. (%)	TYS TUS	DAS (0.0001 in.)	Por- osity Index	Part No.	CYS (ksi)	Part No.	SUS (ksi)	e/D = 1.5		e/D = 2.0	
													Part No.	BYS (ksi)	Part No.	BYS (ksi)
Side Flange Lower	.20	25T3	48.3	40.3	5	0.834	13	3	9C3	42.8						
		25T4	50.3	43.1	7	0.857	17	1	9C4	43.5						
		25T5	46.1	39.6	5	0.859	17	2	9C5	43.0						
		25T6	49.7	43.4	5	0.873	20	3	9C6	44.3						
Side Flange Upper	.20	26T3	53.7	44.4	6	0.827	11	2	10C3	43.2						
		26T4	44.5	37.5	4	0.843	12	1	10C4 (1)							
		26T5	47.7	39.8	4	0.834	11	1	10C5	41.2						
		26T6	43.4	38.0	4	0.876	17	5	10C6	41.5						
Integral Lug Center	2.0	T6/3	44.4	38.0	5	0.856	17	3								
		T6/4	48.4	39.0	7	0.806	21	30	1							
		T6/5	44.3	36.8	4	0.831	16	26	4							
		T6/6	46.5	39.5	4	0.849	18	22	3							
Integral Lug Center	2.0	T7/3	45.4	38.0	3	0.837	18	17	1							
		T7/4	48.2	39.2	6	0.813	21	30	1							
		T7/5	45.0	37.2	5	0.827	21	26	3							
		T7/6	46.3	39.5	4	0.853	21	22	3							
Integral WL 130	.25	T8/3	44.2	37.6	4	0.851	18	4								
		T8/4	42.7	39.5	2	0.925	21	2								
		T8/5	45.2	39.1	5	0.865	17	2								
		T8/6	41.5	38.5	3	0.928	24	4								
Integral Pad Up Base Flange	.50	T9/3	49.5	39.4	10	0.796	15	7	1							
		T9/4	49.4	39.6	8	0.802	15	9	1							
		T9/5	49.5	40.1	9	0.810	19	9	1							
		T9/6	49.4	39.7	8	0.804	13	9	1							
Integral WL 150	.15	T10/3	(2)	40.1	5	--	13	3	15C3	40.9						
		T10/4	44.8	40.3	4	0.900	11	2	15C4 (3)							
		T10/5	42.7	37.7	3	0.883	12	2	15C5	41.7						
		T10/6	48.3	40.8	6	0.845	14	1	15C6	40.3						

(1) Specimen buckled

(2) TUS not recorded

(3) Specimen damaged prior to test

Specimen

Casting surface

1 - Least

7 - Most

(1) Specimen buckled

(2) TUS not recorded

(3) Specimen damaged prior to test

Casting surface

Specimen

1 - Least
7 - Most

TABLE 16
STATIC MECHANICAL PROPERTIES DATA
BOEING ALUMINUM PART 8 CASTINGS -- A357-T6

Part Location	Nominal Thickness (in.)	Tension				Compression			Shear		Bearing			
		TUS (ksi)	Elong. (%)	TYS (ksi)	DAS (0.0001 in.)	Porosity Index	Part No.	CYS (ksi)	Part No.	SUS (ksi)	e/D = 1.5		e/D = 2.0	
											Part No.	BUS (ksi)	Part No.	BUS (ksi)
Fitting 1	1.0	1X7 45.2	39.4	2	0.872	22	1V7 42.1	1V7 33.8	1V7 33.8	127 80.2	66.3	227 98.6	227 98.6	77.4
		1X8 45.5	39.2	2	0.861	23	1V8 40.8	1V8 32.9	1V8 32.9	128 61.2	(1)	228 98.2	228 98.2	78.1
		1X9 46.3	40.5	2	0.875	19	1V9 42.4	1V9 33.8	1V9 33.8	129 79.9	69.4	229 98.6	229 98.6	81.1
		1X10 45.7	40.8	2	0.893	22	1V10 42.2	1V10 33.6	1V10 33.6	1210 58.8	(1)	2210 94.9	2210 94.9	79.5
		1X11 44.8	41.3	2	0.922	23	1V11 42.8	1V11 33.0	1V11 33.0	1211 60.9	(1)	2211 97.0	2211 97.0	81.0
Fitting 1	1.0	2X7 45.0	40.0	2	0.889	23	24	3						
		2X8 44.6	39.7	2	0.890	30	27	5						
		2X9 45.6	40.3	2	0.884	21	23	2						
		2X10 45.6	40.5	2	0.888	22	24	2						
		2X11 44.1	40.8	1	0.925	28	19	5						
Fitting 2	3.0	3X7 44.4	39.2	2	0.883	22	20	6	2V7 40.1	2V7 34.0	79.2	427 88.1	427 88.1	78.8
		3X8 44.7	39.4	2	0.881	23	23	4	2V8 (2)	2V8 33.6	77.7	428 91.0	428 91.0	78.7
		3X9 47.7	41.5	3	0.870	18	24	3	2V9 42.0	2V9 34.6	65.8	429 95.6	429 95.6	80.6
		3X10 46.0	40.2	3	0.874	25	20	2	2V10 42.0	2V10 33.0	70.8	4210 103.5	4210 103.5	80.6
		3X11 45.3	39.2	2	0.865	22	25	5	2V11 43.5	2V11 34.3	70.7	4211 96.3	4211 96.3	84.2
Fitting 2	3.0	4X7 42.7	39.7	2	0.930	22	20	5	3V7 43.4	3V7 35.3				
		4X8 44.7	41.9	2	0.937	22	23	5	3V8 42.9	3V8 33.7				
		4X9 42.4	38.4	2	0.906	22	24	3	3V9 43.6	3V9 33.5				
		4X10 45.6	40.1	2	0.879	22	20	2	3V10 43.4	3V10 33.6				
		4X11 45.8	41.5	2	0.906	26	25	6	3V11 44.4	3V11 33.7				
Horiz. Torque Box	.30	5X7 45.2	37.0	4	0.818	16		3						
		5X8 46.6	37.9	4	0.813	17		3						
		5X9 45.8	38.8	4	0.847	13		2						
		5X10 47.5	41.2	5	0.867	20		2						
		5X11 50.6	41.7	3	0.824	18		3						
Horiz. Torque Box	.30	6X7 47.7	39.5	6	0.828	17		2						
		6X8 46.1	38.2	3	0.829	17		3						
		6X9 44.8	38.5	3	0.859	18		2						
		6X10 47.4	40.1	4	0.846	17		2						
		6X11 46.9	42.3	3	0.902	17		3						
Horiz. Torque Box	.20	7X7 51.1	40.4	9	0.790	10		1	4V7 45.5	4V7 36.0				
		7X8 51.3	41.4	9	0.807	13		1	4V8 44.6	4V8 35.5				
		7X9 51.9	41.6	9	0.801	9		1	4V9 45.1	4V9 36.2				
		7X10 51.7	41.9	8	0.810	8		1	4V10 44.3	4V10 35.2				
		7X11 51.9	43.7	6	0.842	11		1	4V11 46.0	4V11 36.1				

1 - Least
7 - Most

Specimen
Casting surface

(1) Failed prior to yield
(2) Specimen buckled

TABLE 16 (Cont.)

Part Location	Nominal Thickness (in.)	Tension				Compression				Shear				Bearing			
		Part No.	TUS (ksi)	Elong. (%)	TYS (ksi)	DAS (0.0001 in.)	Porosity Index	Part No.	CYS (ksi)	Part No.	SUS (ksi)	Part No.	BUS (ksi)	BYS (ksi)	Part No.	BUS (ksi)	BYS (ksi)
Vertical Box Rt. Rear	.50	8X7	44.9	40.8	2	0.908	24	5Y7	43.1	5W7	33.7	7Z7	69.6	68.5			
		8X8	45.6	41.7	2	0.914	23	5Y8	42.3	5W8	35.1	7Z8	64.7	(1)			
		8X9	46.1	41.5	2	0.900	26	5Y9	42.1	5W9	35.1	7Z9	66.3	(1)			
		8X10	46.1	41.7	2	0.904	23	5Y10	43.4	5W10	34.5	7Z10	71.5	70.7			
		8X11	45.3	42.7	2	0.942	25	5Y11	40.9	5W11	34.6	7Z11	64.7	(1)			
Vertical Box Rt. Rear	.50	9X7	46.3	41.0	2	0.885	23										
		9X8	47.5	42.3	2	0.890	23										
		9X9	47.1	42.3	3	0.898	22										
		9X10	47.7	42.4	2	0.889	22										
		9X11	47.4	43.2	2	0.911	25										
Vertical Box Left Front	.30	10X7	45.4	43.4	2	0.956	14										
		10X8	--	(2)	--	--	15										
		10X9	49.0	44.1	3	0.900	12										
		10X10	46.7	42.2	3	0.903	12										
		10X11	49.0	44.9	2	0.916	16										
Vertical Box Right Front	.30	11X7	51.4	43.7	6	0.850	10										
		11X8	50.2	43.0	4	0.856	15										
		11X9	50.1	44.4	3	0.886	15										
		11X10	49.3	43.7	3	0.886	13										
		11X11	53.9	46.8	8	0.868	14										
Web Lwr. Left	.10	12X7	49.3	40.5	7	0.821	12										
		12X8	47.0	38.6	6	0.821	14										
		12X9	45.2	37.3	5	0.825	12										
		12X10	45.4	39.7	4	0.874	13										
		12X11	48.6	42.2	3	0.868	11										
Flange Right Outside	.10	13X7	52.5	43.8	3	0.834	15										
		13X8	50.0	40.0	4	0.800	14										
		13X9	49.8	43.0	5	0.863	11										
		13X10	--	(2)	--	--	13										
		13X11	51.0	42.3	5	0.829	12										
Attachment Flange Left Vertical	.30	14X7	48.1	42.6	3	0.886	17										
		14X8	49.9	39.3	12	0.788	13										
		14X9	48.9	41.2	7	0.842	12										
		14X10	50.8	40.6	10	0.799	13										
		14X11	49.6	41.8	3	0.843	16										

(1) Failed prior to yield

(2) Failed through machining marks

Specimen

Casting surface

1 - Least
7 - Most

TABLE 16 (Cont.)

Part Location	Non- inal Thick- ness (in.)	Tension					Compression			Shear			Bearing			
		Part No.	TUS (ksi)	TYS (ksi)	Elong. (%)	TYS TUS	DAS (0.0001 in.)		Por- osity Index	Part No.	CYS (ksi)	Part No.	e/D = 1.5		e/D = 2.0	
							△	▽					BUS (ksi)	BYS (ksi)	BUS (ksi)	BYS (ksi)
Horiz. Flange	.30	15X7	48.1	41.3	4	0.859	21	2	2	527	73.5	68.4	627	96.7	79.6	
		15X8	46.9	42.1	2	0.897	17	2	2	528	73.0	65.6	628	91.5	79.9	
		15X9	48.0	41.4	3	0.862	16	2	2	529	72.9	69.7	629	100.5	85.4	
		15X10	47.2	42.3	2	0.896	20	2	2	5210	74.5	69.1	6210	104.9	81.4	
		15X11	48.0	43.4	1	0.904	18	4	4	5211	70.1	68.7	6211	96.8	83.8	
Flange Left Inside	.10	16X7	48.4	41.2	2	0.851	17	2	2							
		16X8	49.8	42.5	4	0.853	15	2	2							
		16X9	--	(1)	--	--	15	7	7							
		16X10	--	(2)	--	--	16	4	4							
		16X11	50.0	44.0	3	0.880	16	3	3							
Attachmt. Flange Left Vertical	.30	17X7	46.9	41.3	4	0.881	19	2	2							
		17X8	46.2	40.9	3	0.885	26	2	2							
		17X9	47.2	40.8	2	0.864	19	2	2							
		17X10	44.2	37.4	3	0.842	26	3	3							
		17X11	44.6	40.2	2	0.901	26	4	4							
Vertical Box Right Inside	.10	18X7	42.6	35.4	4	0.831	15	2	2							
		18X8	42.5	38.1	3	0.896	15	5	5							
		18X9	--	(3)	--	--	17	2	2							
		18X10	--	(3)	--	--	14	3	3							
		18X11	48.5	43.3	3	0.893	15	2	2							
Flange Lwr. Rt.	.25	19X7	51.5	42.7	7	0.829	12	1	1							
		19X8	49.8	42.3	5	0.849	16	1	1							
		19X9	49.8	43.8	3	0.879	10	3	3							
		19X10	51.0	43.8	5	0.859	12	1	1							
		19X11	52.0	43.8	3	0.842	14	1	1							
Attachmt. Flange Lwr. Rt.	.10	20X7	48.6	40.7	5	0.837	16	1	1							
		20X8	51.0	42.4	7	0.831	12	1	1							
		20X9	48.1	39.7	5	0.825	14	1	1							
		20X10	48.1	39.7	8	0.825	13	1	1							
		20X11	50.0	43.2	4	0.864	14	1	1							
Attachmt. Flange Lwr. Center	.10	21X7	--	(2)	--	--	13	2	2							
		21X8	47.0	38.8	7	0.826	14	1	1							
		21X9	46.8	40.8	3	0.872	13	2	2							
		21X10	48.7	40.7	5	0.836	14	1	1							
		21X11	50.0	43.8	3	0.876	15	1	1							

(1) Failed prior to yield in defect outside of gage area (2) Failed through weld-correctable pore (3) Failed through vibratool mark

△ Specimen ▽ Casting surface ▽ 1 - Least
7 - Most

TABLE 16 (Concluded)

Part Location	Nominal Thickness (in.)	Tension					Compression			Shear			Bearing			
		Part No.	TUS (ksi)	TYS (ksi)	Elong. (%)	TYS TUS	DAS (0.0001 in.)	Porosity Index	Part No.	CYS (ksi)	Part No.	SUS (ksi)	Part No.	BUS (ksi)	Part No.	BUS (ksi)
Attachmt. Flange Lwr. Center	.10	22X7	48.1	41.0	5	0.852	17	3								
		22X8	47.9	40.6	3	0.848	20	2								
		22X9	46.3	40.2	3	0.868	18	1								
		22X10	45.8	40.8	2	0.891	22	2								
		22X11	47.4	43.3	3	0.914	16	2								
Integral Fitting	3.0	X3/7	44.8	39.2	2	0.875	19	24								
		X3/8	44.5	38.9	2	0.874	25	5								
		X3/9	44.6	39.0	2	0.874	19	20								
		X3/10	46.6	39.0	3	0.874	18	23								
		X3/11	45.1	39.9	2	0.885	25	26								
Integral Fitting	3.0	X4/7	45.2	39.4	2	0.872	19	24								
		X4/8	44.9	39.5	2	0.880	21	25								
		X4/9	44.8	39.2	2	0.875	21	20								
		X4/10	47.2	39.5	3	0.837	16	23								
		X4/11	43.1	39.6	2	0.919	26	26								
Integral Flange Lwr. Rt.	.10	X5/7	47.6	41.6	3	0.874	15	15								
		X5/8	50.5	42.7	5	0.846	17	17								
		X5/9	49.8	41.9	5	0.841	12	12								
		X5/10	48.9	40.0	4	0.818	12	12								
		X5/11	--	(1)	--	--	17	19								
Integral Flange Upr. Left	10	X7/7	49.8	44.1	6	0.886	16	16								
		X7/8	49.8	44.6	3	0.896	16	16								
		X7/9	48.4	43.3	3	0.895	15	15								
		X7/10	49.2	44.7	2	0.909	12	12								
		X7/11	--	(2)	--	--	15	15								

1

Specimen

3

1 - Least
7 - Most

2

Casting surface

(1) Bad stress-strain curve

(2) Failed through weld-correctable surface flaw

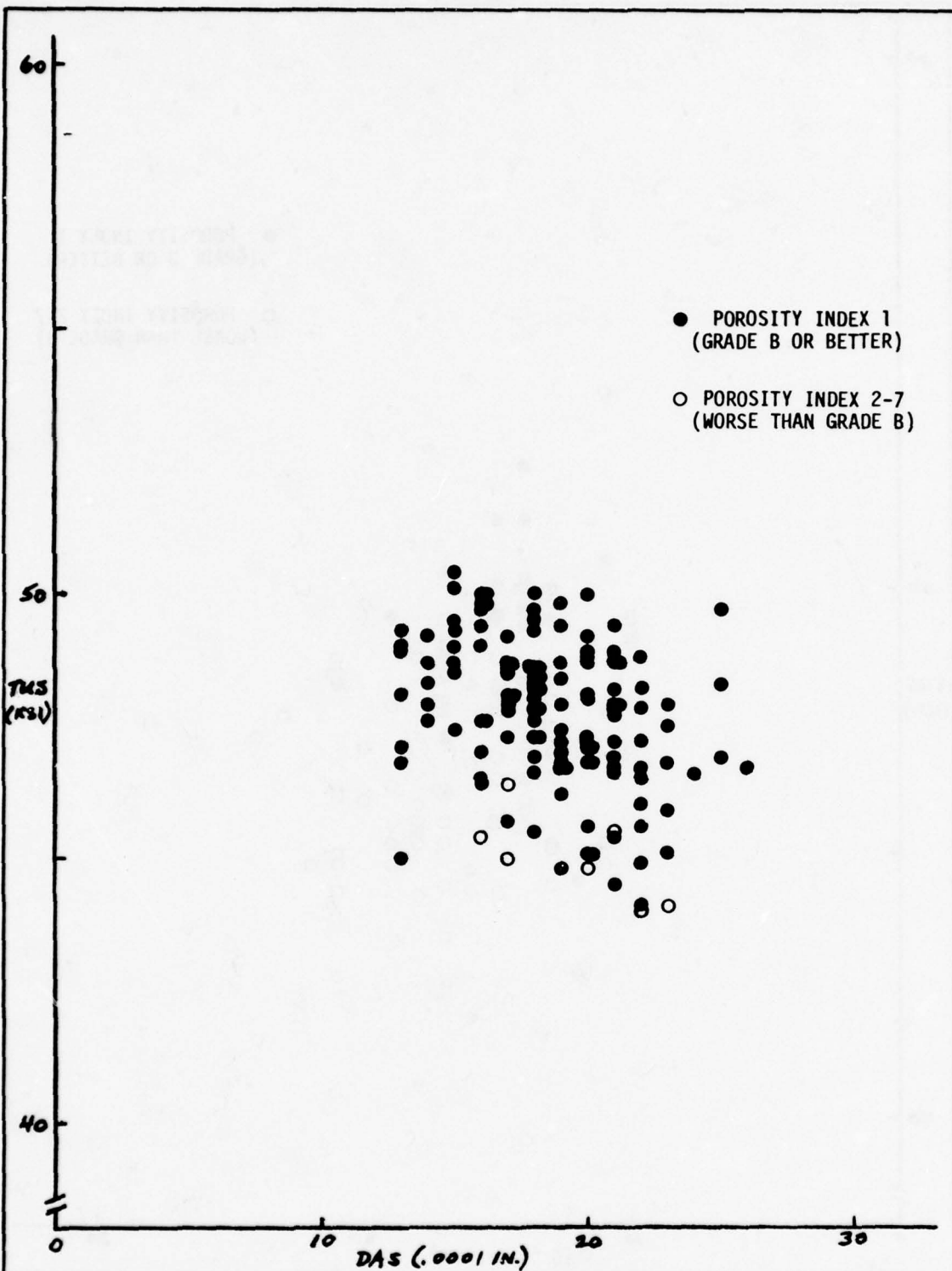
(1) Bad stress-strain curve (2) Failed through weld-correctable surface flaw

Specimen

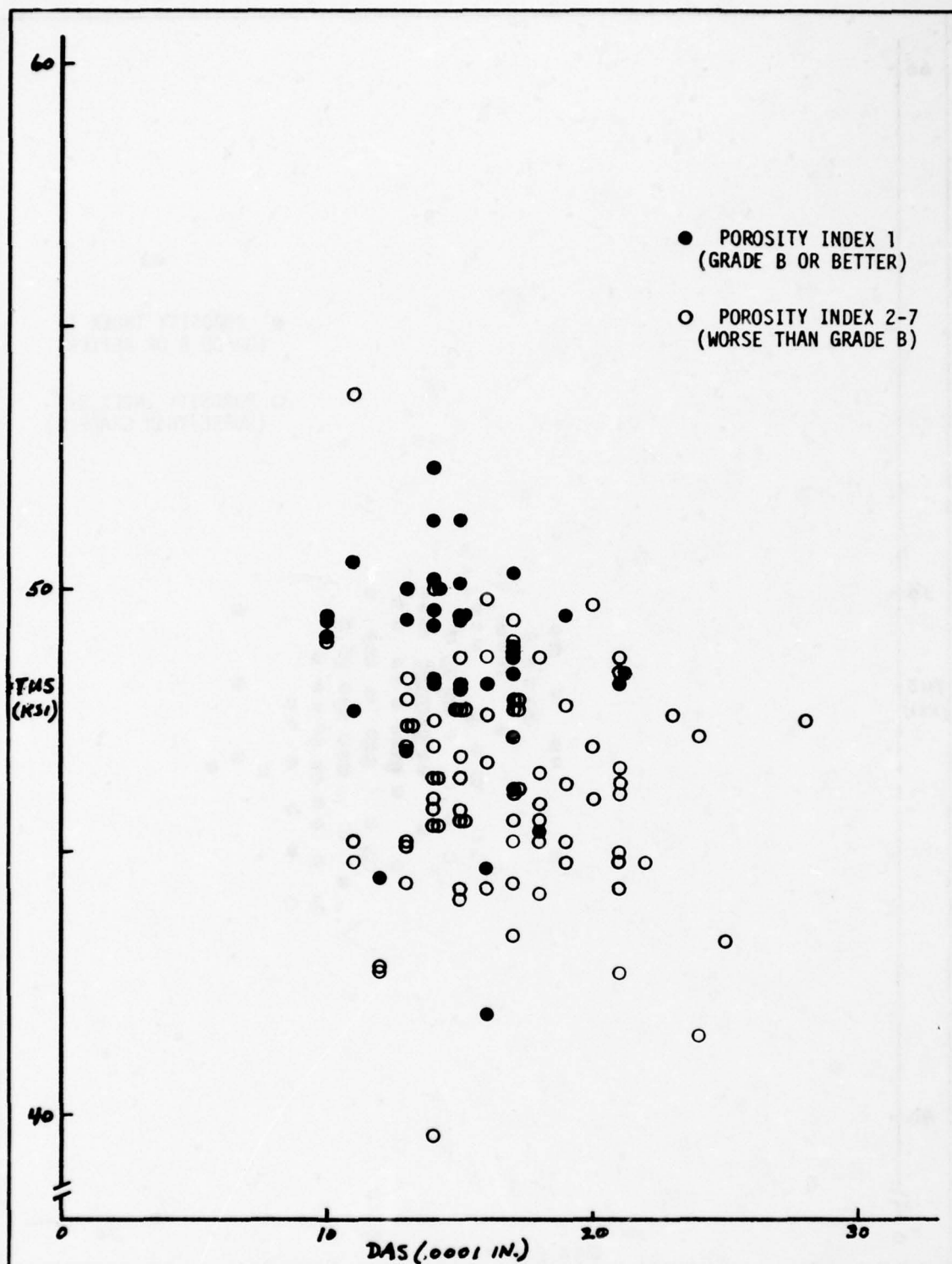
1 - Least

7 - Most

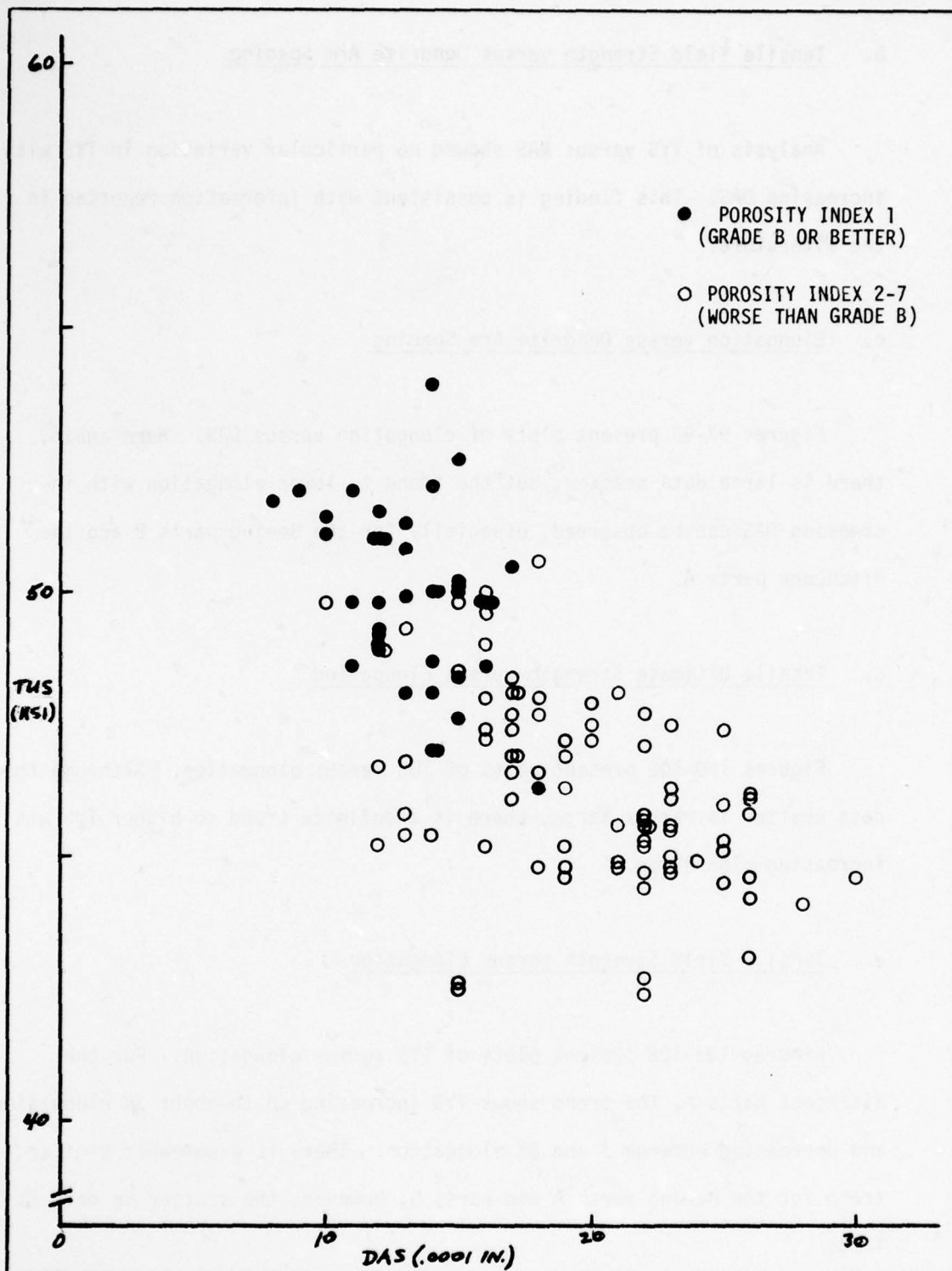
Casting surface



CALC			REVISED	DATE	FIGURE 94. TUS VERSUS DAS-- HITCHCOCK ALLOWABLES PART A CASTINGS.	
CHECK						
APR						
APR						
					THE BOEING COMPANY	PAGE 209



CALC			REVISED	DATE	FIGURE 95. TUS VERSUS DAS-- BOEING ALLOWABLES PART A CASTINGS.	
CHECK						
APR						
APR						
					THE BOEING COMPANY	PAGE 210



CALC			REVISED	DATE	FIGURE 96. TUS VERSUS DAS-- BOEING ALLOWABLES PART B CASTINGS.	
CHECK						
APR						
APR						
					THE BOEING COMPANY	PAGE 211

b. Tensile Yield Strength versus Dendrite Arm Spacing

Analysis of TYS versus DAS showed no particular variation in TYS with increasing DAS. This finding is consistent with information reported in the literature.

c. Elongation versus Dendrite Arm Spacing

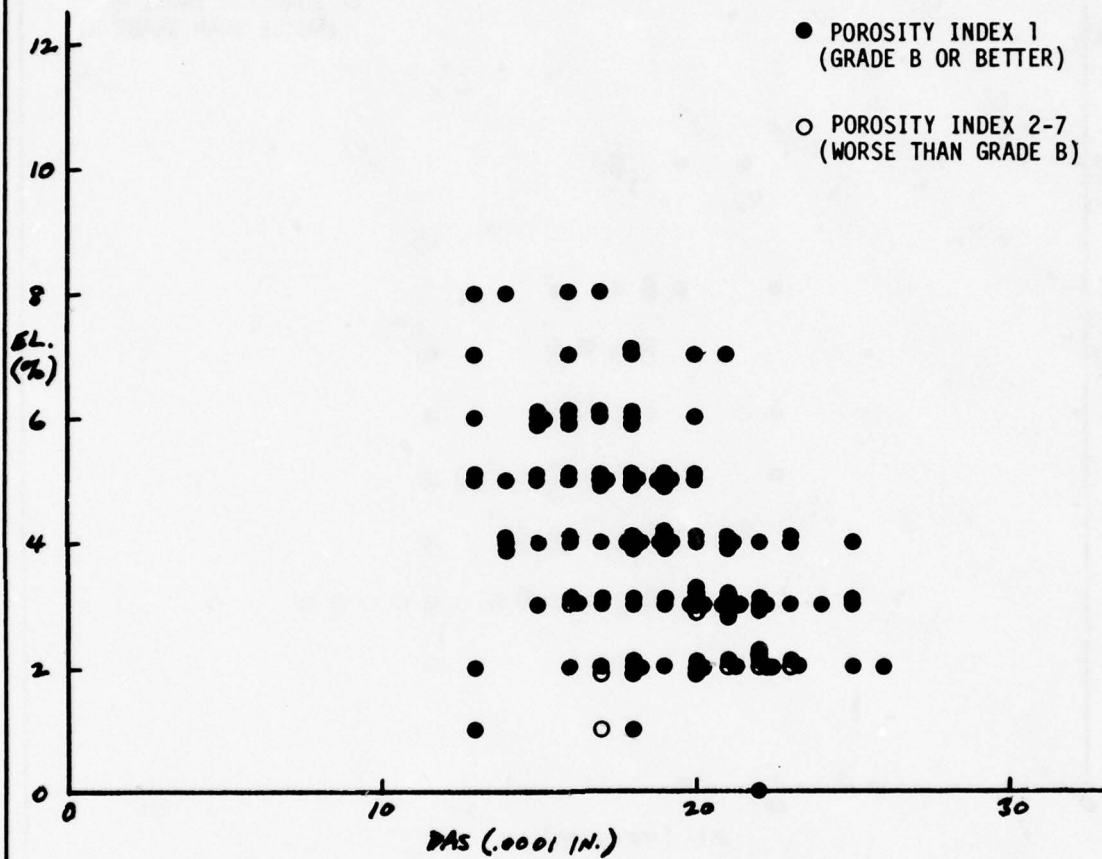
Figures 97-99 present plots of elongation versus DAS. Here again, there is large data scatter, but the trend to lower elongation with increasing DAS can be observed, especially for the Boeing parts B and the Hitchcock parts A.

d. Tensile Ultimate Strength versus Elongation

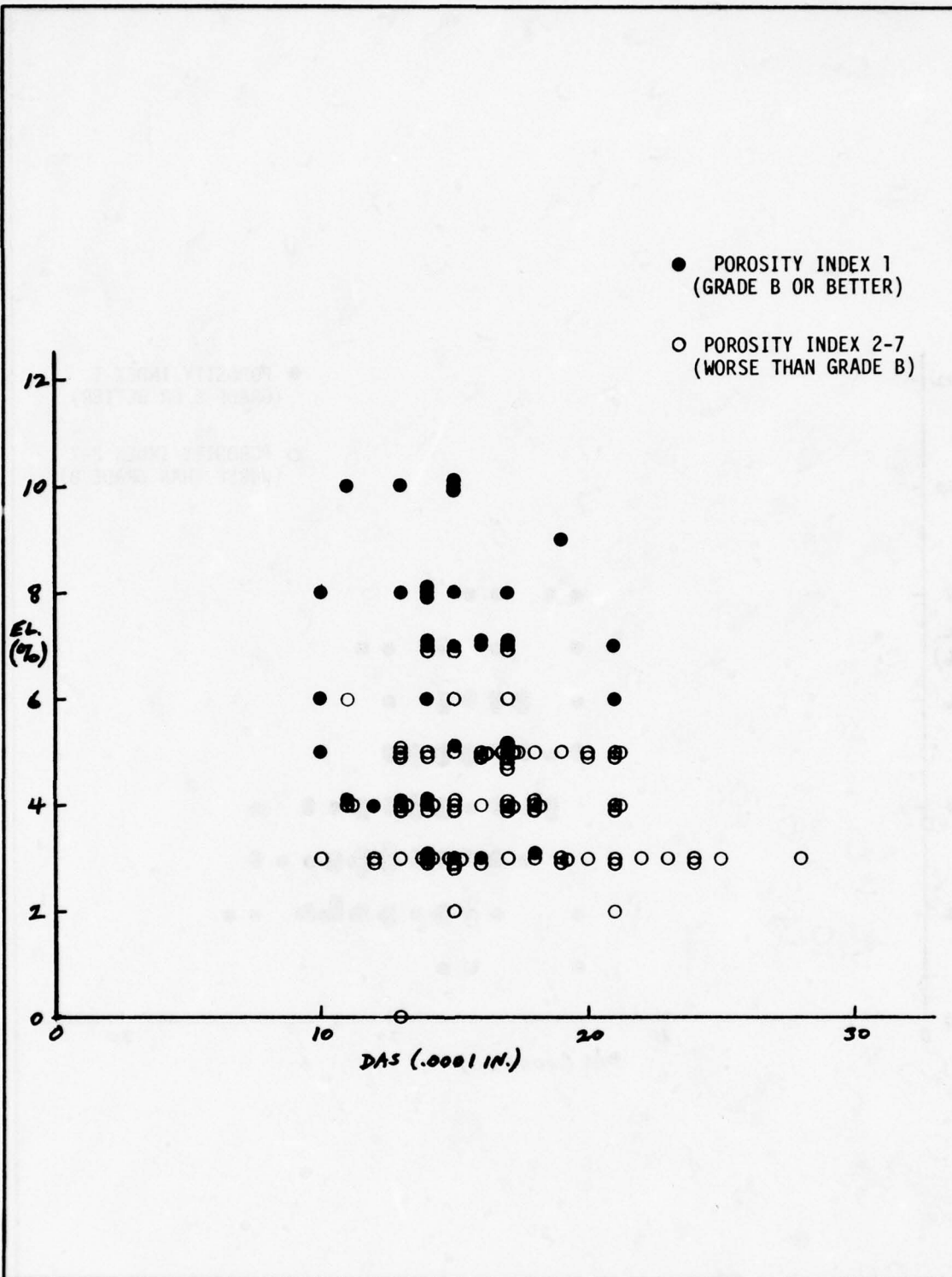
Figures 100-102 present plots of TUS versus elongation. Although the data scatter is rather large, there is a definite trend to higher TUS with increasing elongation.

e. Tensile Yield Strength versus Elongation

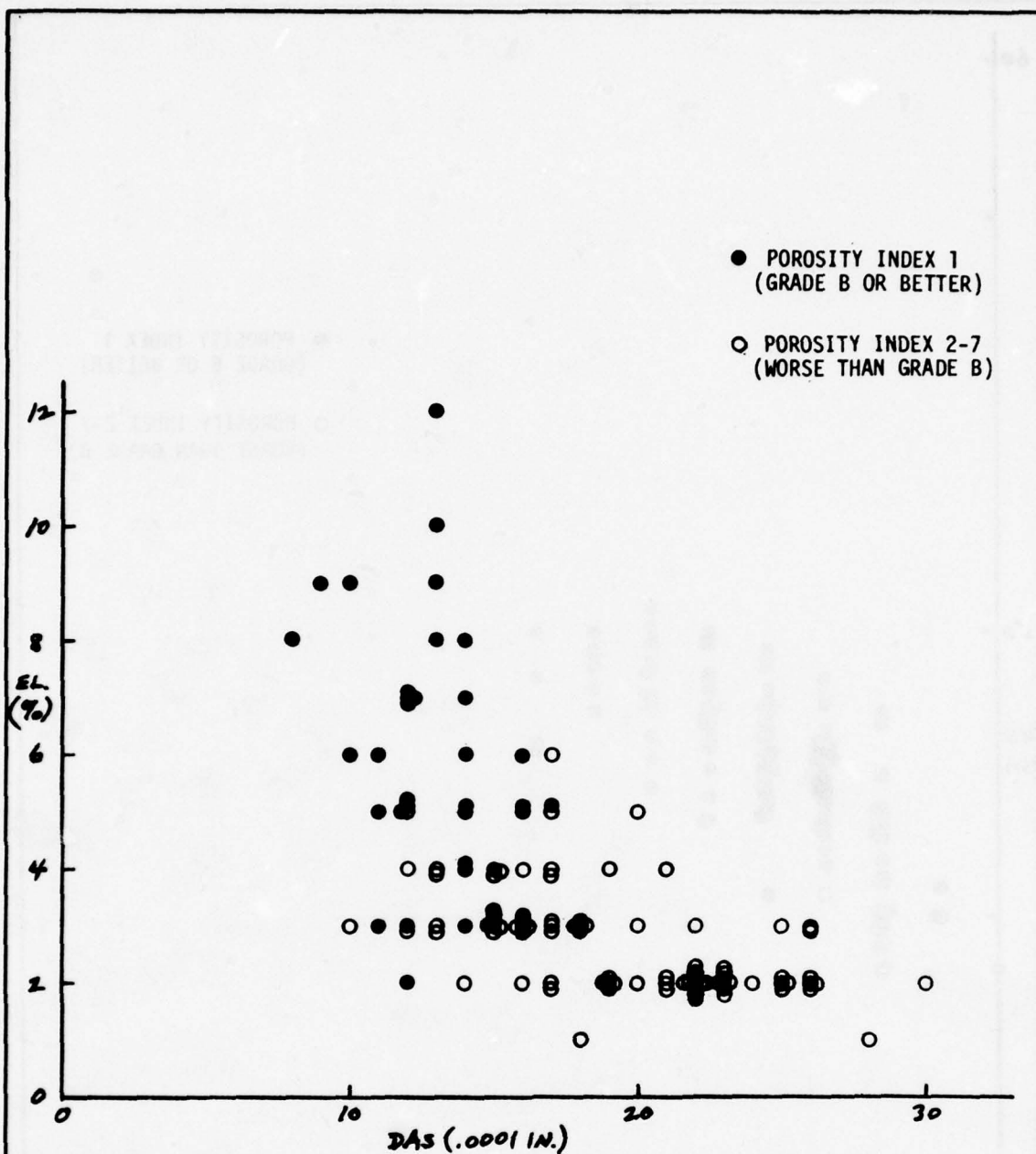
Figures 103-105 present plots of TYS versus elongation. For the Hitchcock parts A, the trend shows TYS increasing up to about 3% elongation and decreasing between 3 and 8% elongation. There is a somewhat similar trend for the Boeing parts A and parts B; however, the scatter in data is large.



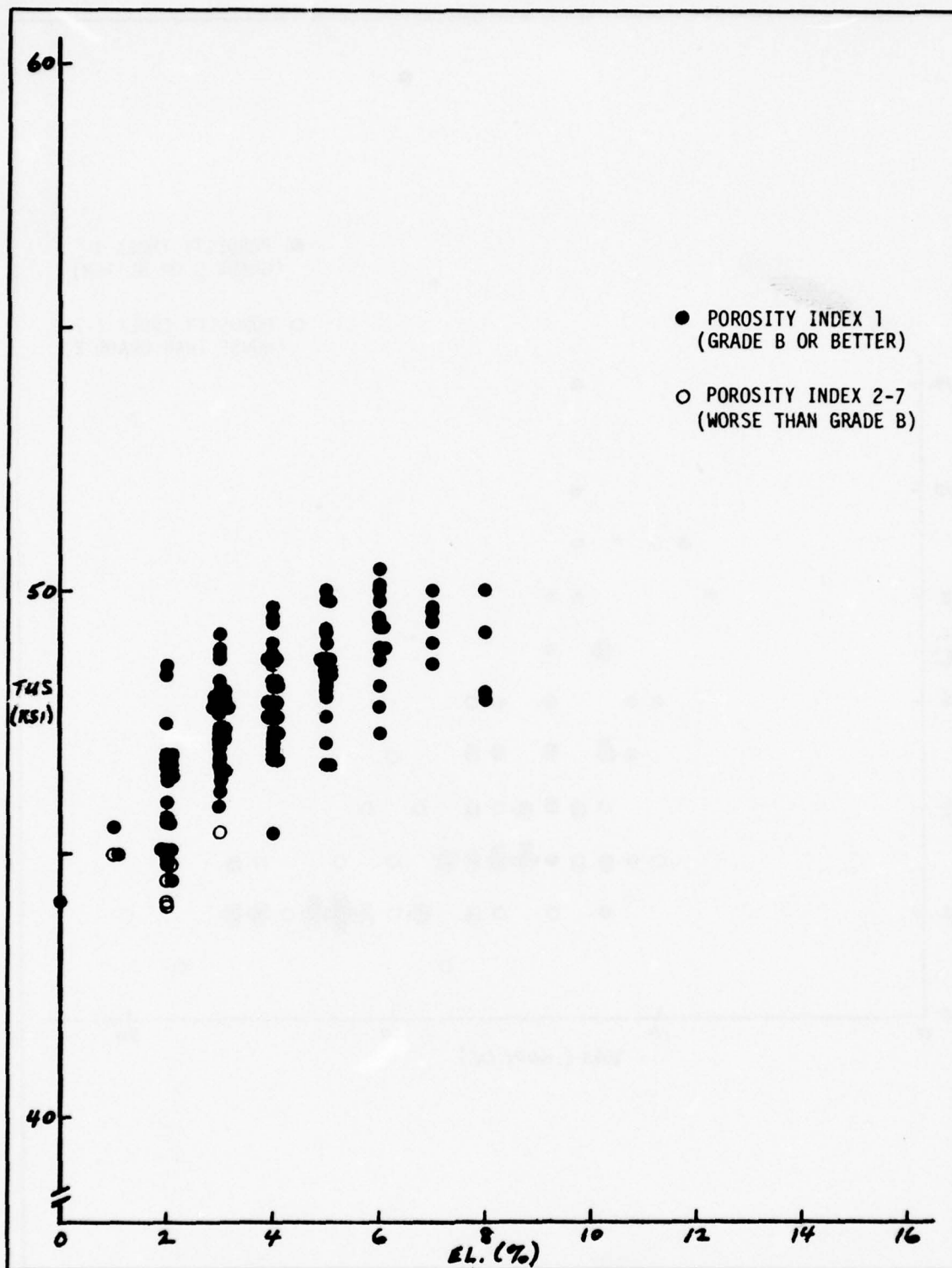
CALC			REVISED	DATE	FIGURE 97. ELONGATION VERSUS DAS-- HITCHCOCK ALLOWABLES PART A CASTINGS.	
CHECK						
APR						
APR						
					THE BOEING COMPANY	PAGE 213



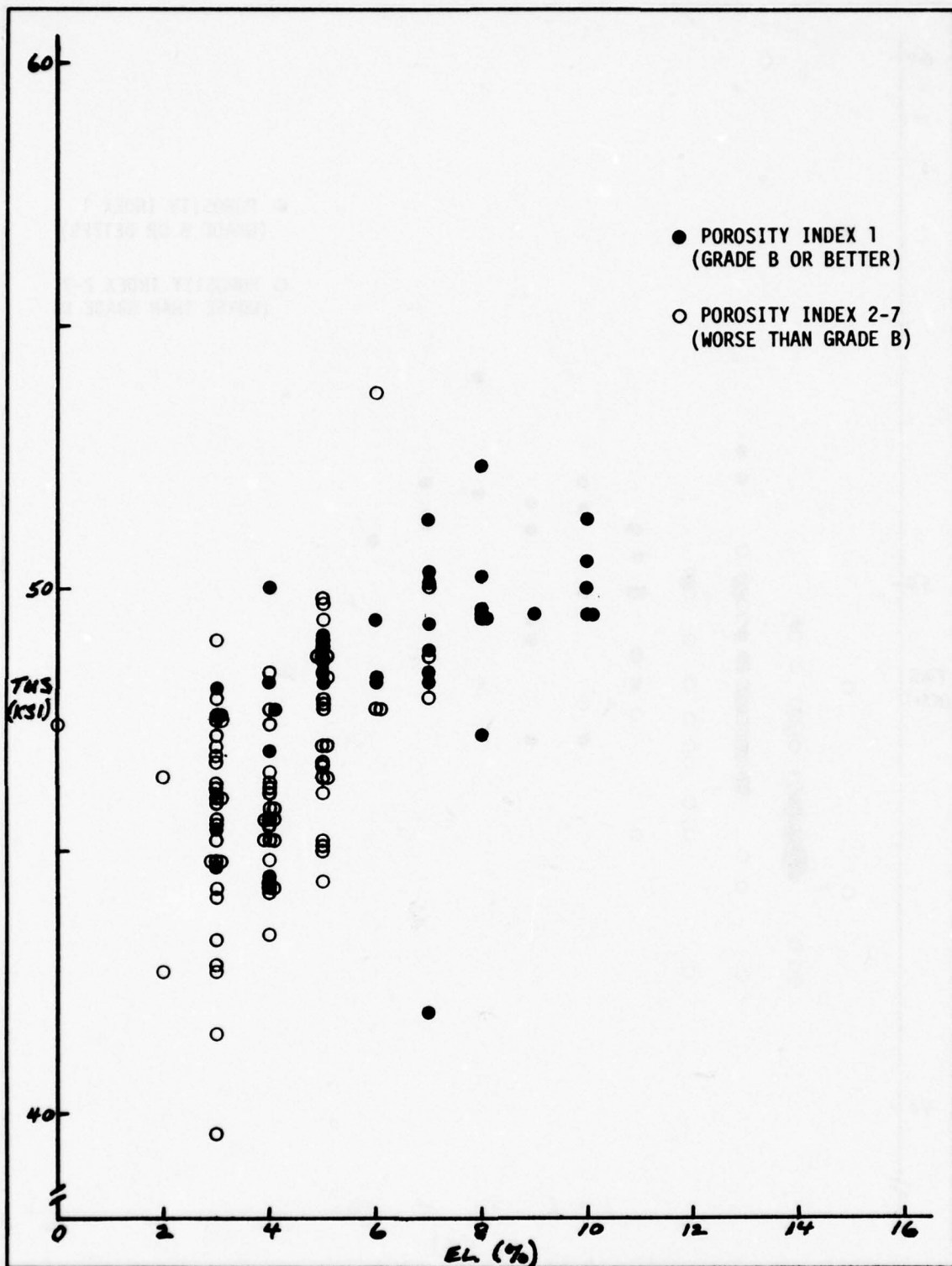
CALC			REVISED	DATE	FIGURE 98. ELONGATION VERSUS DAS-- BOEING ALLOWABLES PART A CASTINGS.	
CHECK						
APR						
APR						
THE BOEING COMPANY						PAGE 214



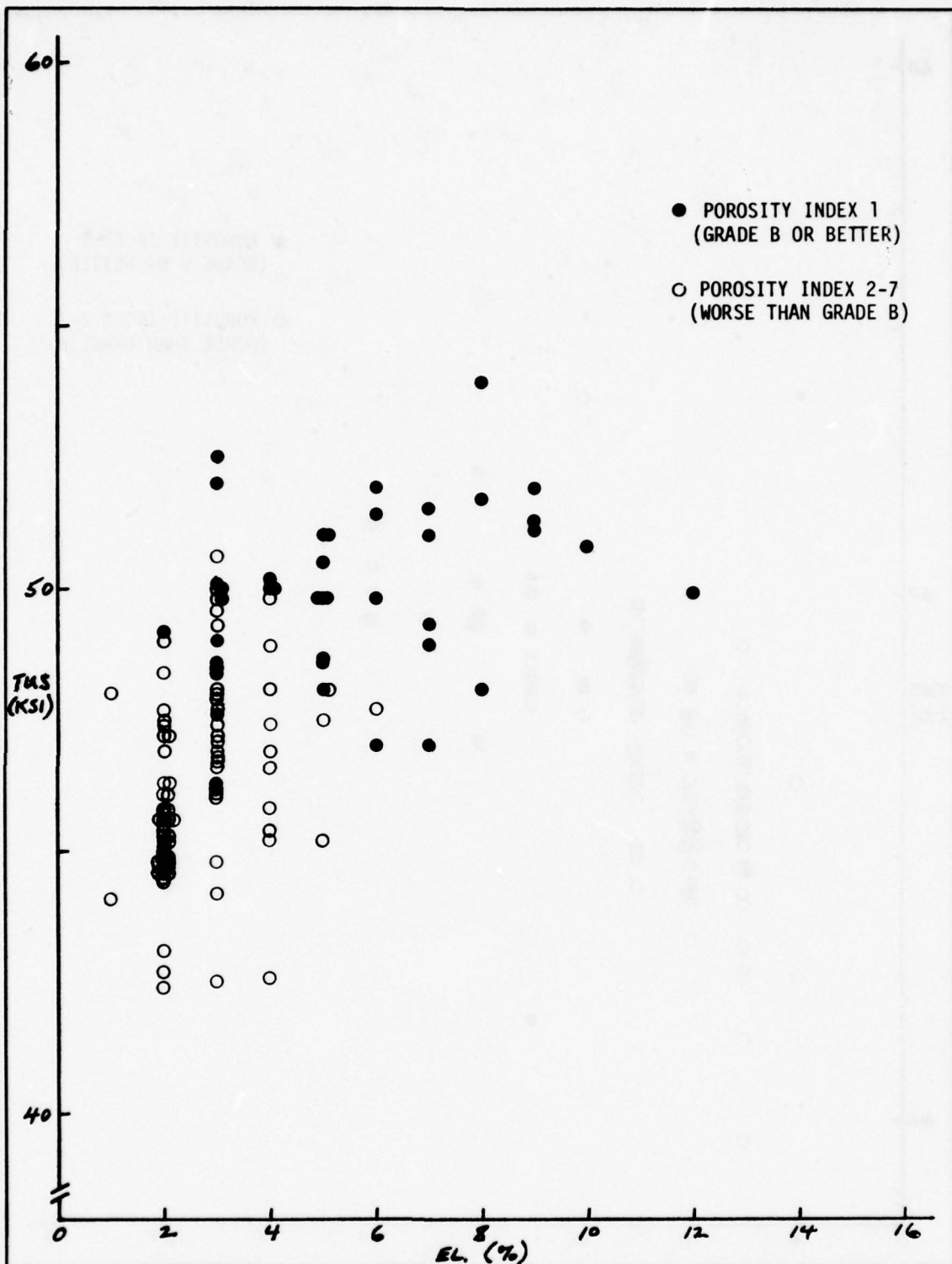
CALC			REVISED	DATE	FIGURE 99. ELONGATION VERSUS DAS-- BOEING ALLOWABLES PART B CASTINGS.	
CHECK						
APR						
APR						
					THE BOEING COMPANY	PAGE 215



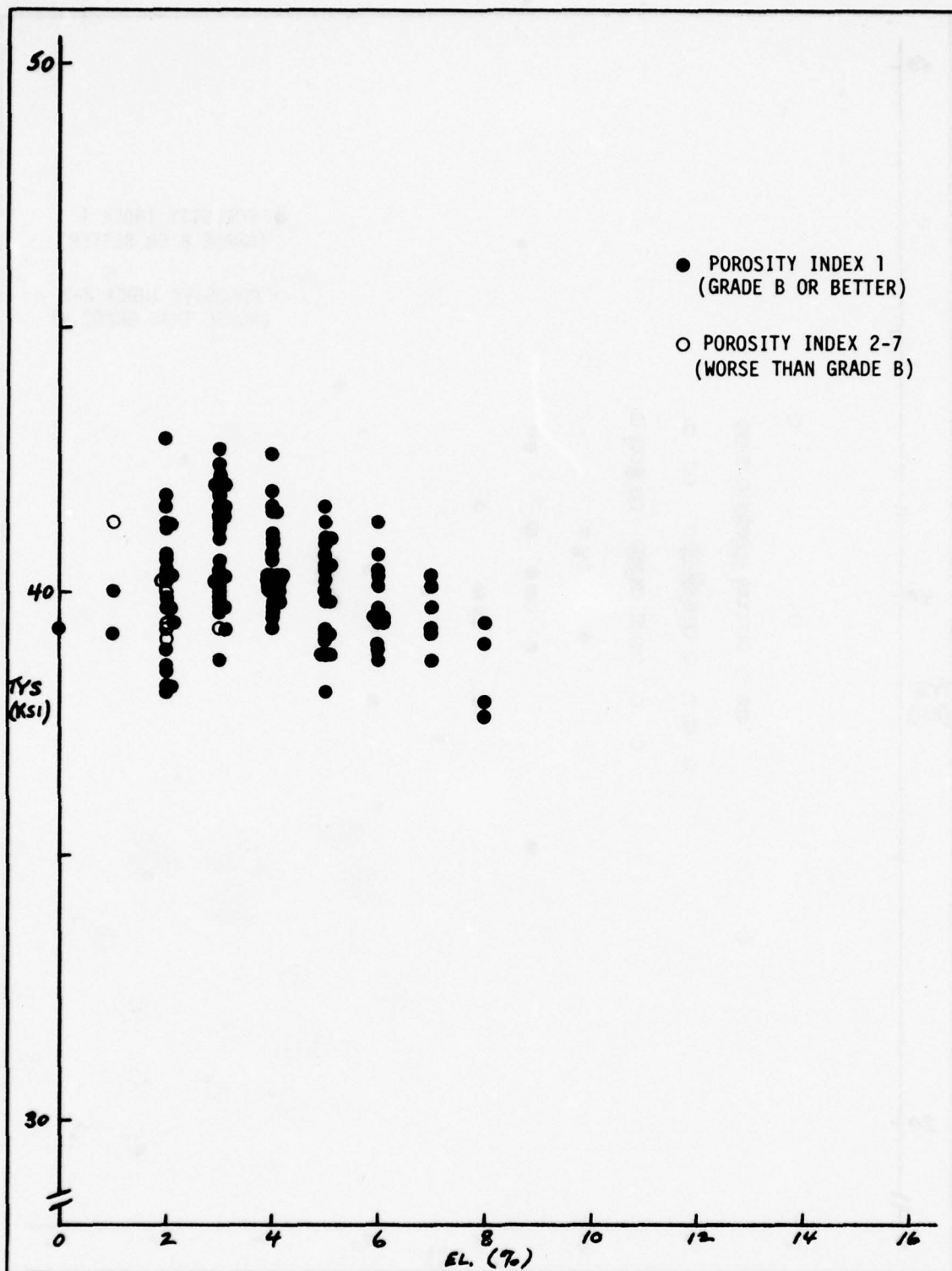
CALC			REVISED	DATE	FIGURE 100. TUS VERSUS ELONGATION-- HITCHCOCK ALLOWABLES PART A CASTINGS.	
CHECK						
APR						
APR						
					THE BOEING COMPANY	PAGE 215



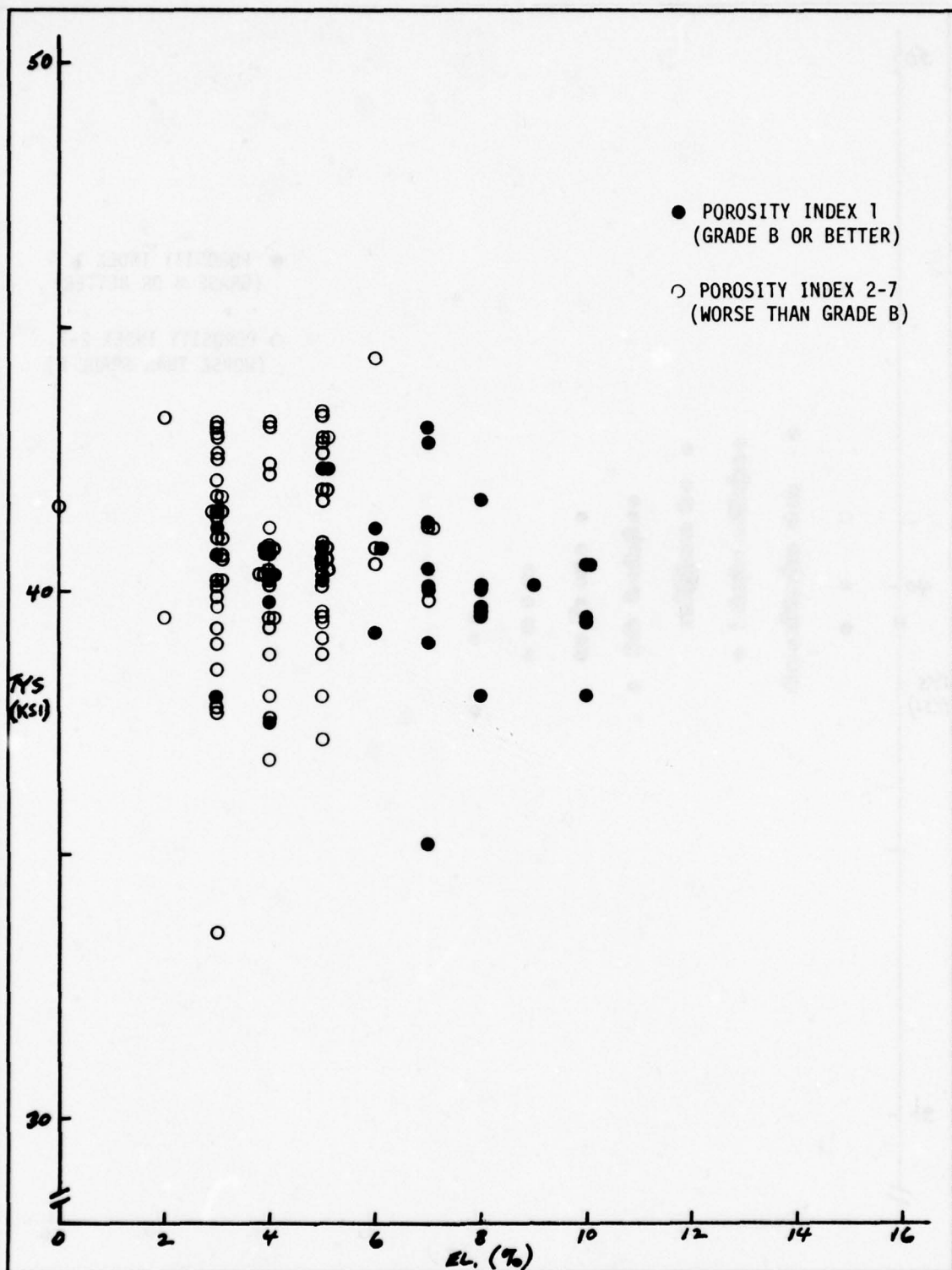
CALC			REVISED	DATE	FIGURE 101. TUS VERSUS ELONGATION-- BOEING ALLOWABLES PART A CASTINGS.	
CHECK						
APR						
APR						
					THE BOEING COMPANY	PAGE 217



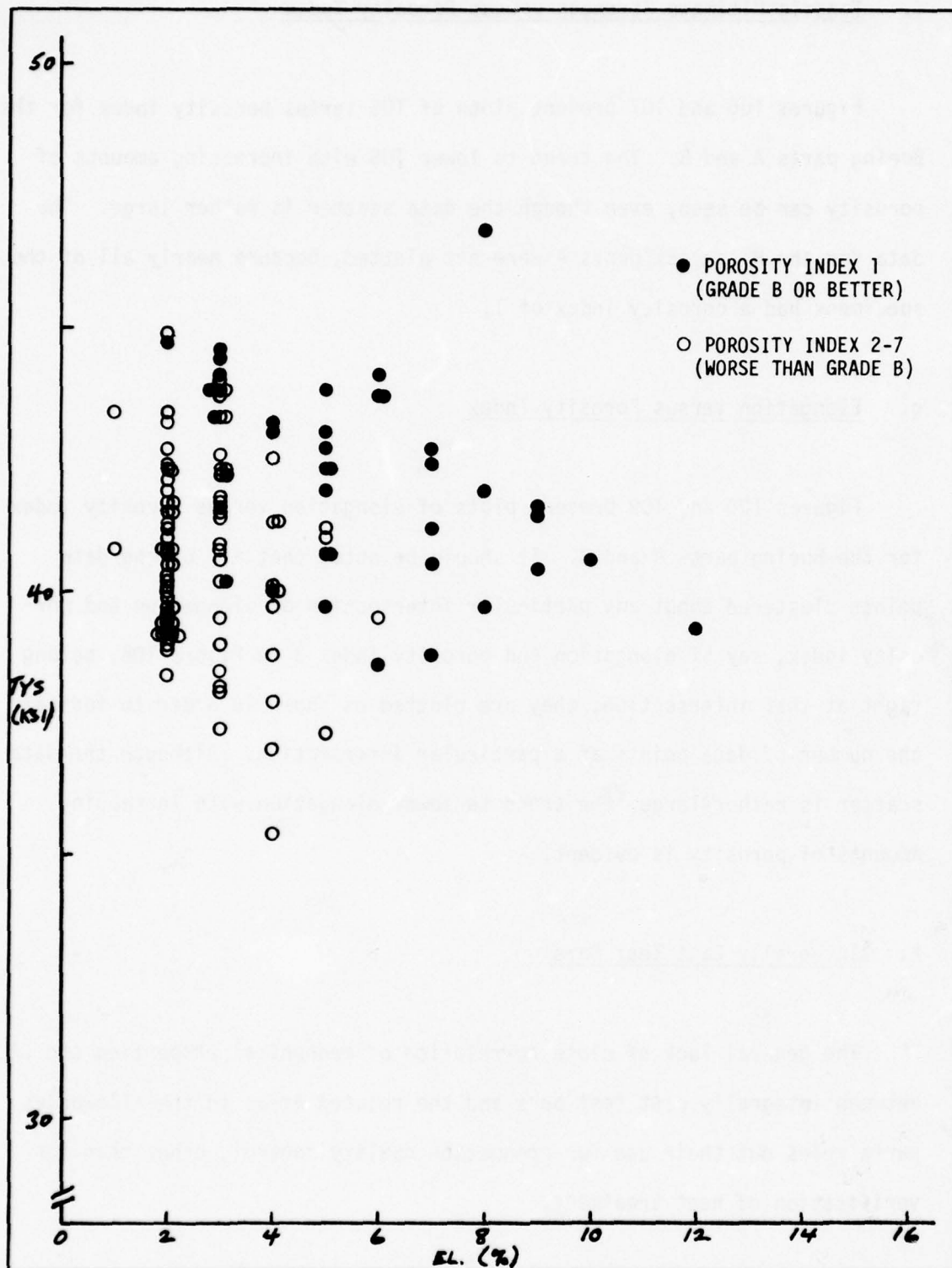
CALC			REVISED	DATE	FIGURE 102. TUS VERSUS ELONGATION-- BOEING ALLOWABLES PART B CASTINGS.	
CHECK						
APR						
APR						
					THE BOEING COMPANY	PAGE 218



CALC			REVISED	DATE	FIGURE 103. TYS VERSUS ELONGATION-- HITCHCOCK ALLOWABLES PART A CASTINGS.	
CHECK						
APR						
APR						
THE BOEING COMPANY					PAGE	219



CALC			REVISED	DATE	FIGURE 104. TYS VERSUS ELONGATION-- BOEING ALLOWABLES PART A CASTINGS.	
CHECK						
APR						
APR						
THE BOEING COMPANY					PAGE	220



CALC			REVISED	DATE	FIGURE 105. TYS VERSUS ELONGATION-- BOEING ALLOWABLES PART B CASTINGS.	
CHECK						
APR						
APR						
THE BOEING COMPANY					PAGE	221

f. Tensile Ultimate Strength versus Porosity Index

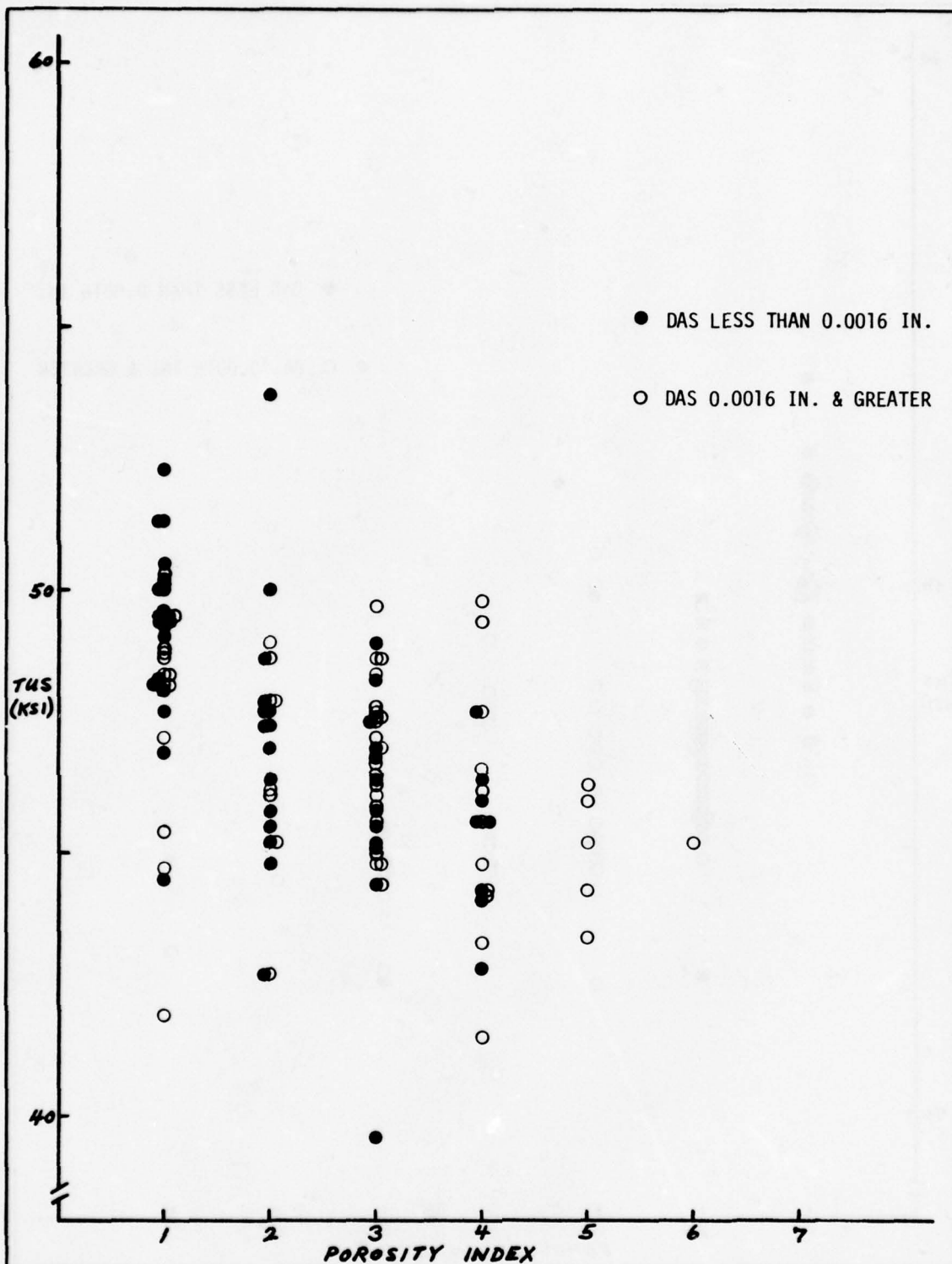
Figures 106 and 107 present plots of TUS versus porosity index for the Boeing parts A and B. The trend to lower TUS with increasing amounts of porosity can be seen, even though the data scatter is rather large. The data for the Hitchcock parts A were not plotted, because nearly all of the specimens had a porosity index of 1.

g. Elongation versus Porosity Index

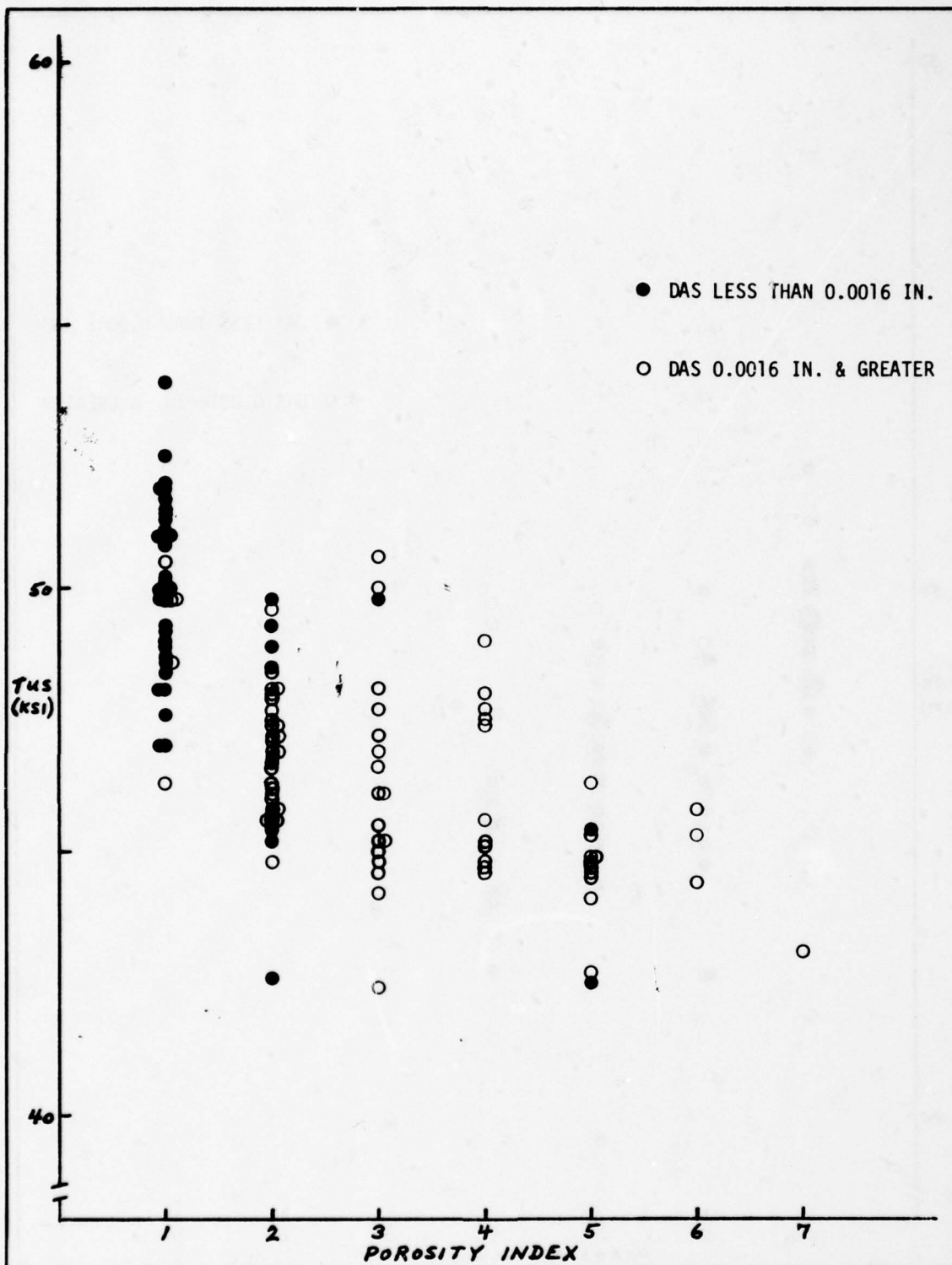
Figures 108 and 109 present plots of elongation versus porosity index for the Boeing parts A and B. It should be noted that all of the data points clustered about any particular intersection of elongation and porosity index, say 5% elongation and porosity index 3 in Figure 108, belong right at that intersection; they are plotted as shown in order to indicate the number of data points at a particular intersection. Although the data scatter is rather large, the trend to lower elongation with increasing amounts of porosity is evident.

h. Integrally Cast Test Bars

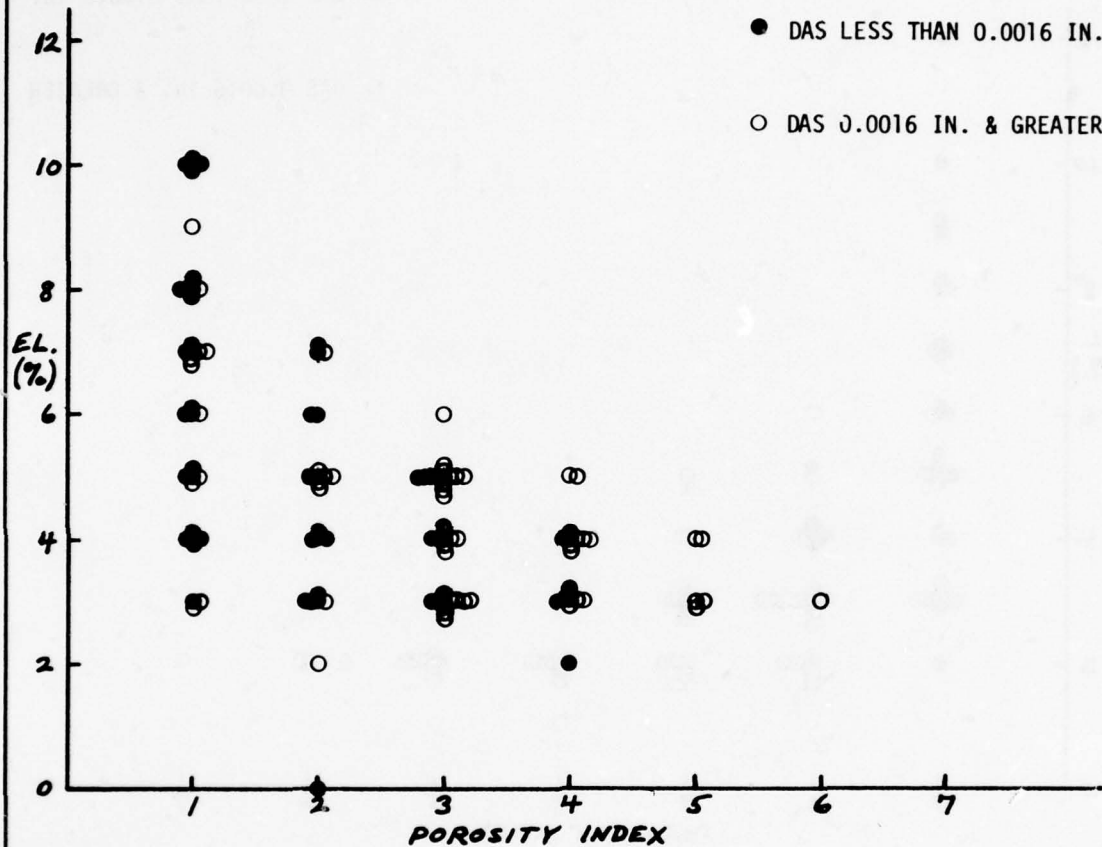
The general lack of close correlation of mechanical properties and DAS between integrally cast test bars and the related areas in the allowables parts rules out their use for production quality control, other than for verification of heat treatment.



CALC			REVISED	DATE	FIGURE 106. TUS VERSUS POROSITY INDEX-- BOEING ALLOWABLES PART A CASTINGS.	
CHECK						
APR						
APR						
THE BOEING COMPANY					PAGE	223



CALC			REVISED	DATE	FIGURE 107. TUS VERSUS POROSITY INDEX-- BOEING ALLOWABLES PART B CASTINGS.	
CHECK						
APR						
APR						
					THE BOEING COMPANY	PAGE 224



CALC			REVISED	DATE	FIGURE 108. ELONGATION VERSUS POROSITY INDEX--BOEING ALLOWABLES PART A CASTINGS.	
CHECK						
APR						
APR						
THE BOEING COMPANY					PAGE	225

4. DISCUSSION OF DATA

The tension test data provide the base from which design allowables will be established. Such allowables should be directly related to material and process specification minimum acceptance levels. It is desirable to base these acceptance levels on the physical variables that cause the resulting mechanical behaviors. It is therefore important to identify the prominent physical variables and to provide methods by which they can be measured accurately. It is believed that both allowables and specific tensile minimums should be categorized by DAS and soundness. Current ASTM E155 standards for radiographic inspection have been found to lack accuracy in establishing soundness in thick sections. Efforts are currently under way to develop ultrasonic inspection techniques from which soundness can be established with improved accuracy. For this reason, the material and process specification will be revised, and design allowables will be completed in Phase V, at which time the methodology for soundness determinations will have been established and verified with future full-size castings in Phase IV.

The trends for both increasing TUS and elongation with decreasing DAS and porosity and the general constancy of TYS with decreasing DAS are in agreement with other investigations of A357 and similar casting alloys. The relative scatter in results prevents development of unique relationships between mechanical properties and DAS or porosity at this time. DAS alone cannot be used as a reliable nondestructive inspection measurement for the prediction of either strength or elongation. There are obviously other physical variables represented in these data that must be accurately measured and quantified in order to provide an adequate understanding of material behavior.

SECTION XIV

METALLURGICAL STUDIES

Metallurgical investigations were conducted on several lugs and fittings from various allowables test castings. The purpose of these analyses was to obtain data on the effects of chilling, including dendrite arm spacing (DAS), and on the extent of porosity in these heavier portions of the castings.

Lugs and fittings from the following castings were investigated: (1) Boeing allowables part B preproduction casting S/N 369, (2) Hitchcock allowables part A production casting S/N 9, and (3) Boeing allowables part A preproduction casting S/N 578. Casting S/N's 369 and 9 had been heat treated to the -T6 condition; casting S/N 578 was in the as-cast condition.

1. BOEING ALLOWABLES PART B -- CASTING S/N 369

Both the integral cast fitting and fitting no. 2 from this preproduction part were investigated (see Figure 110).

a. Integral Cast Fitting

Figure 111 shows the integral cast fitting and locations of the step-gate, copper chills, and section cut for investigation. This figure also shows grid lines (A-A, B-B, C-C, D-D, X-X, Y-Y, and Z-Z) along which DAS measurements were made on the longitudinal section on piece B. DAS measurements were made at approximately 1/8-inch intervals along each of the seven grid lines.

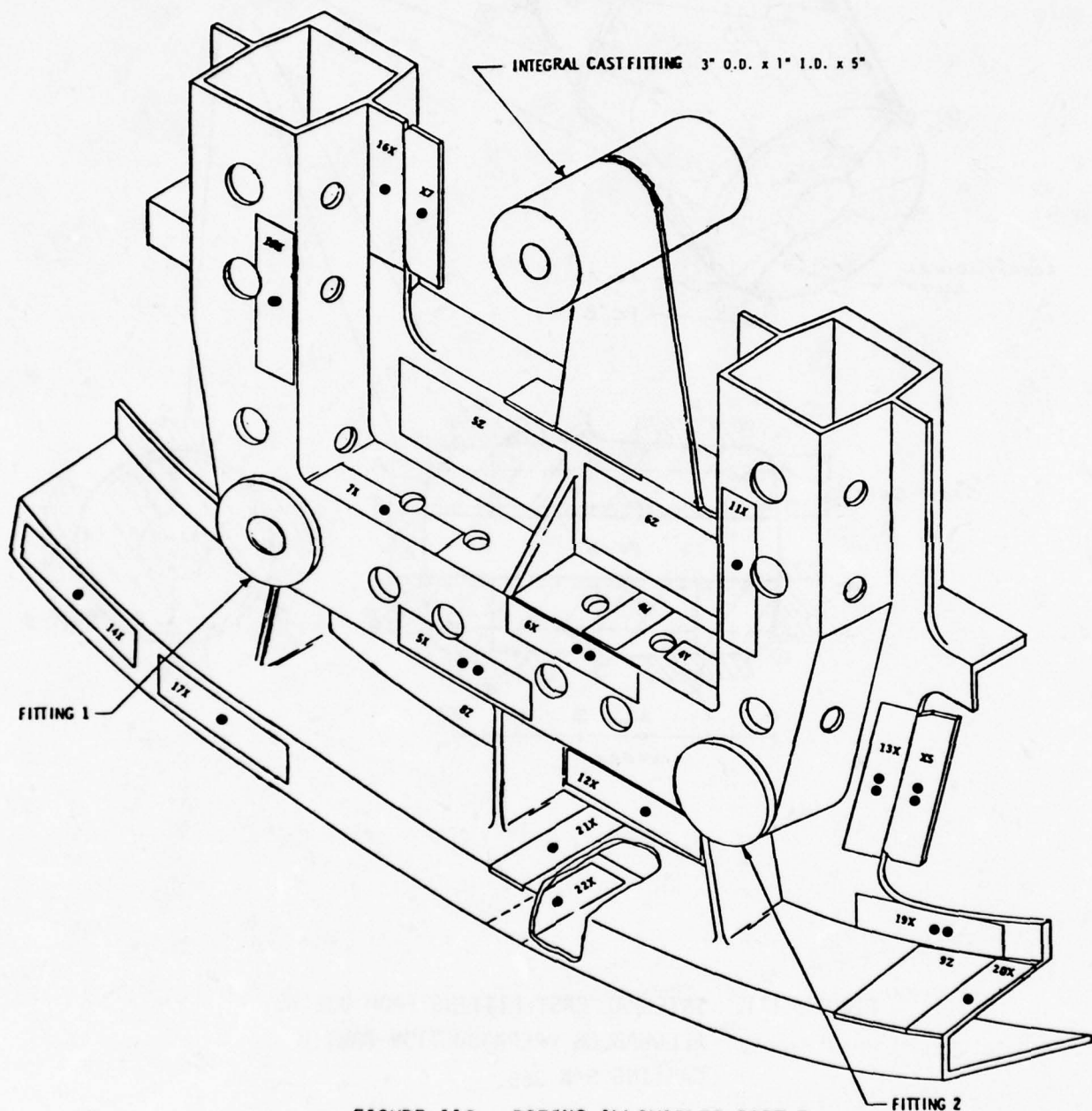


FIGURE 110. BOEING ALLOWABLES PART B,
SHOWING LOCATIONS OF FITTINGS. FORWARD SIDE.

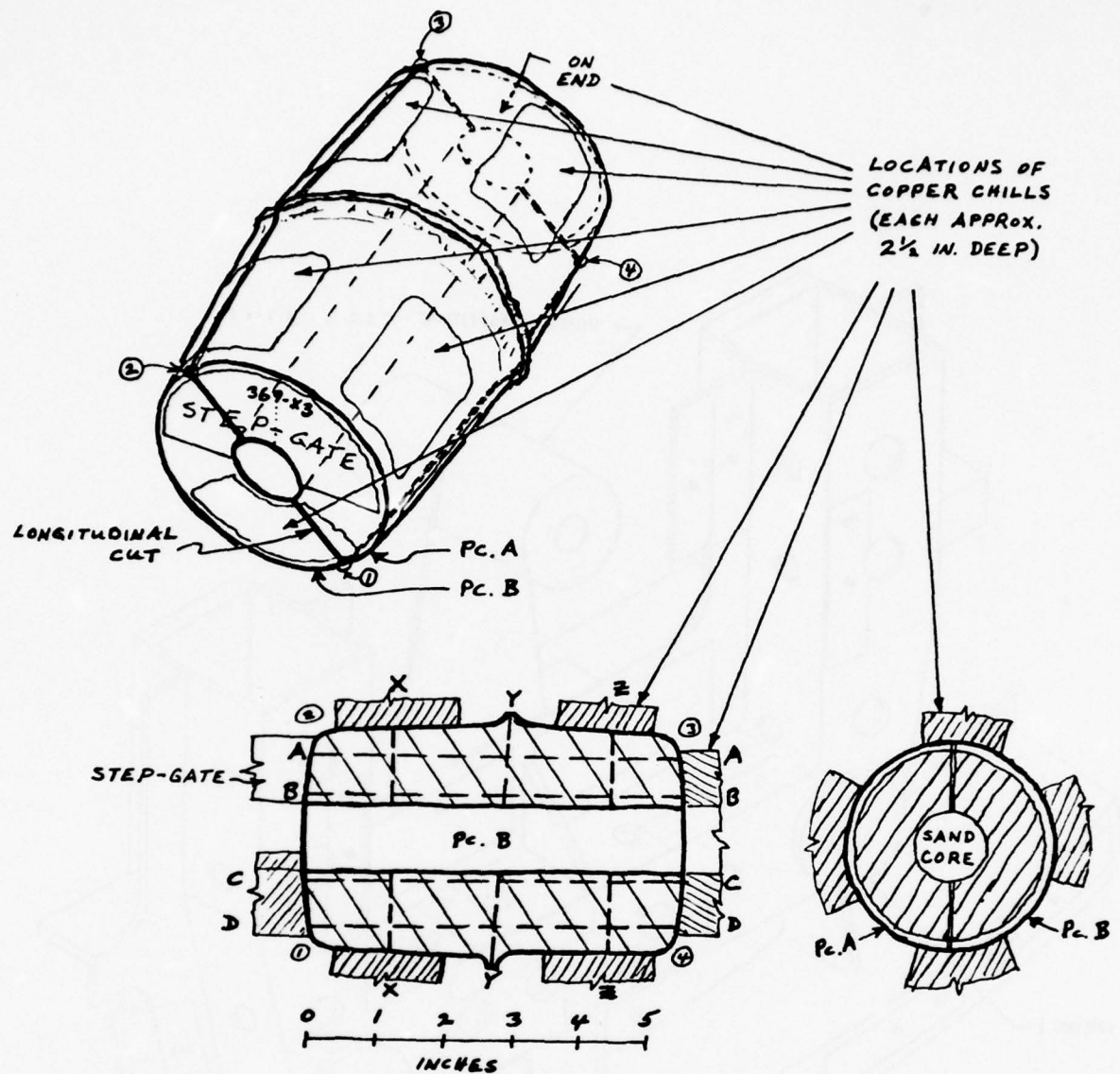


FIGURE 111. INTEGRAL CAST FITTING FROM BOEING ALLOWABLES PREPRODUCTION PART B CASTING S/N 369.

These data are plotted in Figures 112 and 113. Shown are average DAS curves and upper and lower limit curves. Points were taken from the average DAS curves and plotted on the cut section in order to construct the "contour map" of Figure 114A showing lines of constant average DAS. This map thus gives a picture of how solidification progressed from chills to step-gate during cooling.

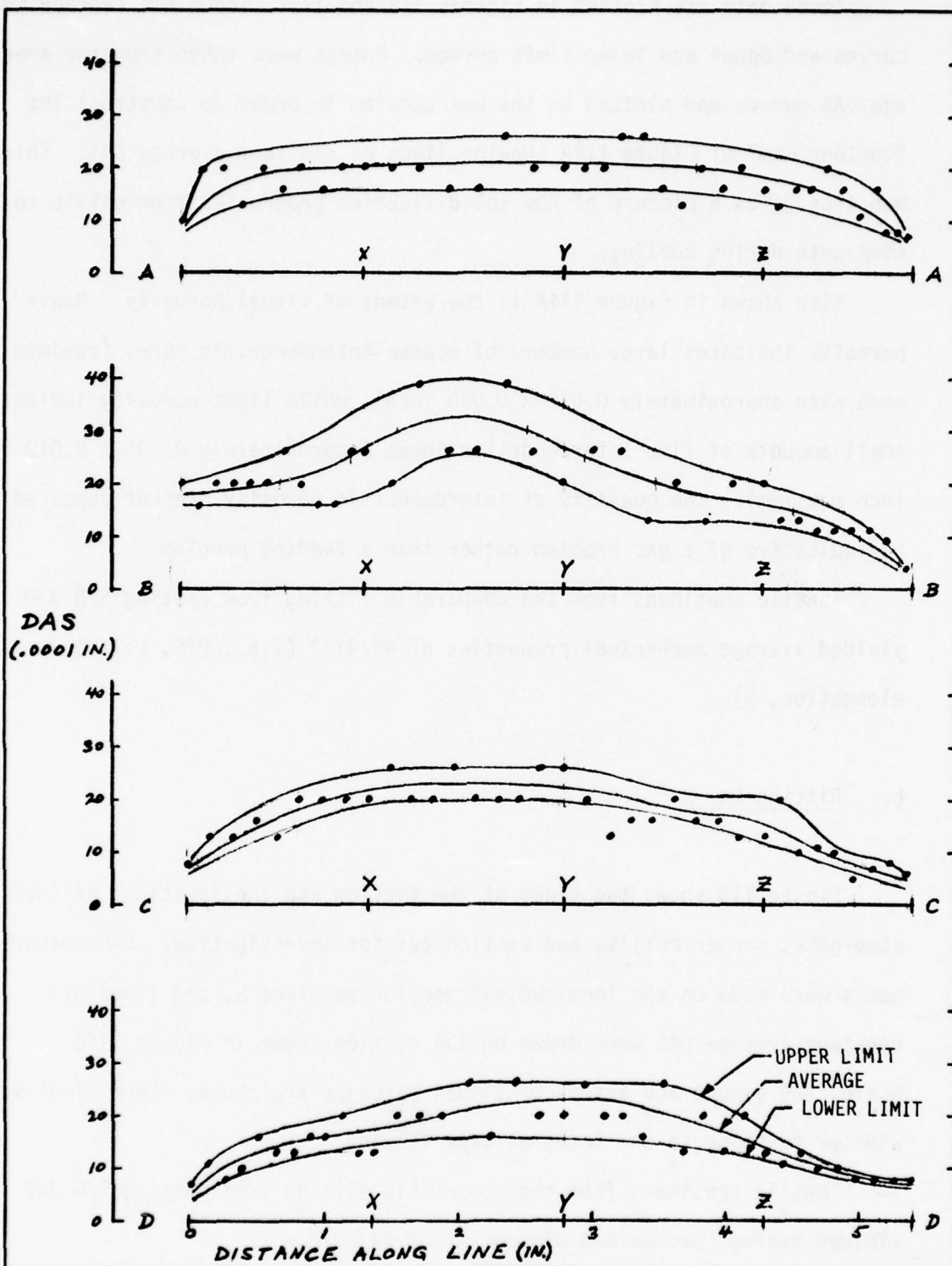
Also shown in Figure 114A is the extent of visual porosity. Heavy porosity indicates large numbers of coarse interdendritic pores (maximum pore size approximately 0.015 x 0.050 inch), while light porosity indicates small amounts of fine interdendritic pores (approximately 0.005 x 0.010 inch maximum). The quantity of interdendritic porosity present appeared to be indicative of a gas problem rather than a feeding problem.

Tensile specimens from the comparable fitting from casting S/N 330 yielded average mechanical properties of 45/41/2 (i.e., UTS, ksi/YS, ksi/elongation, %).

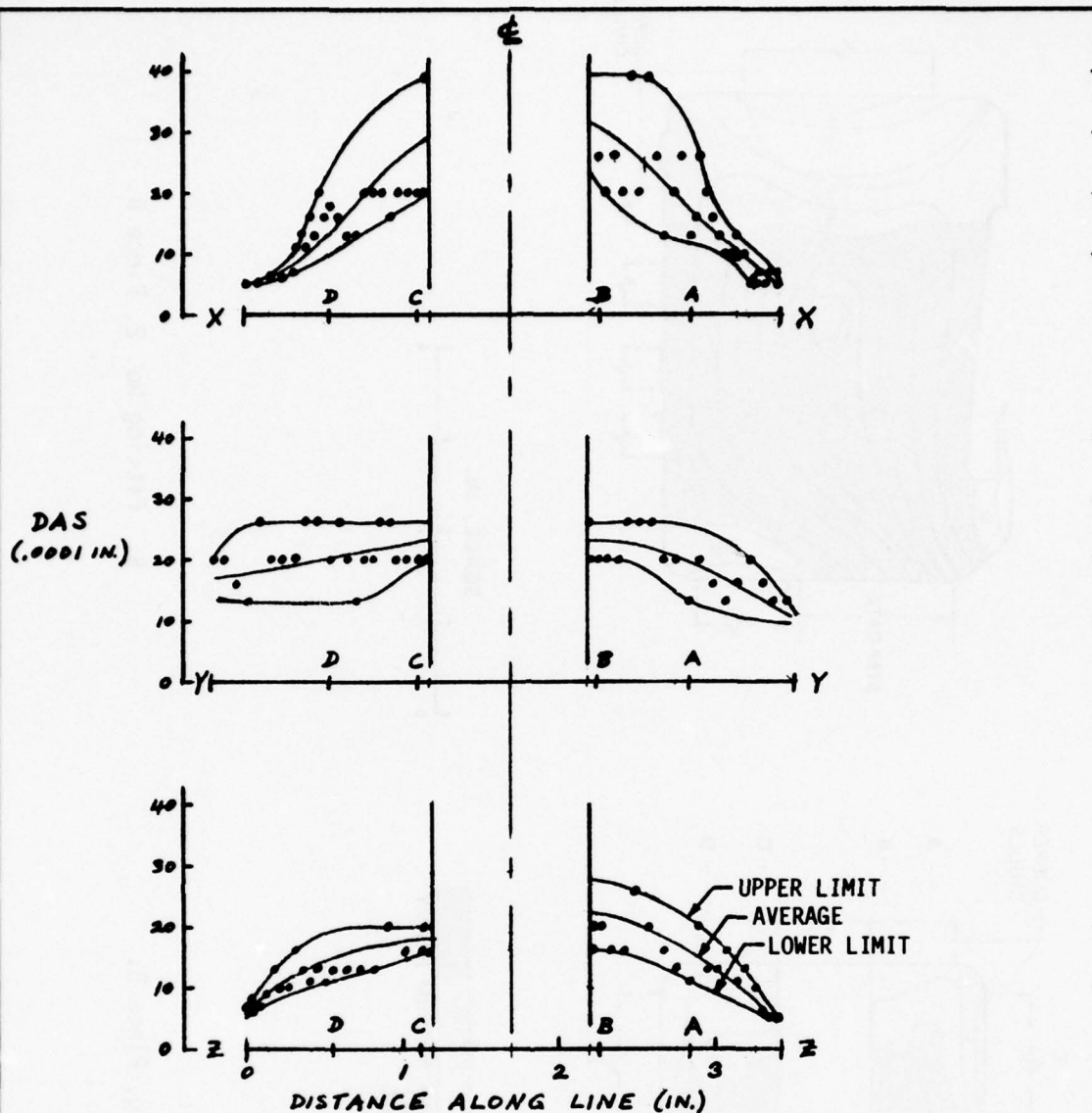
b. Fitting No. 2

Figure 115 shows two views of the fitting and the locations of the step-gate, copper chills, and section cut for investigation. DAS measurements were made on the longitudinal section on piece B, and lines of constant average DAS were drawn on the section shown in Figure 114B. Again, the amount and extent of visual porosity are shown. Pore sizes were similar to those in the integral cast fitting.

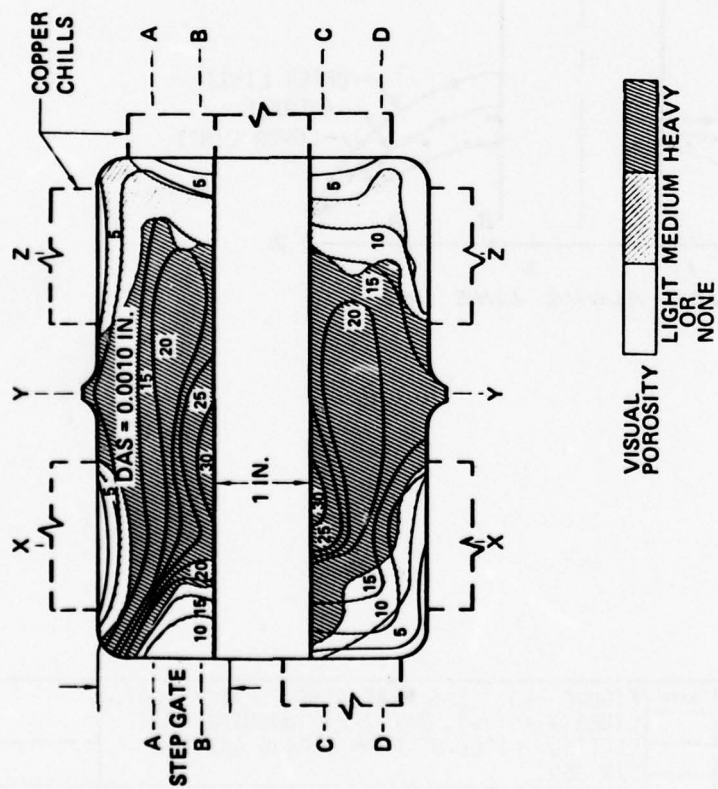
Tensile specimens from the comparable fitting from casting S/N 330 yielded average mechanical properties of 44/40/2.



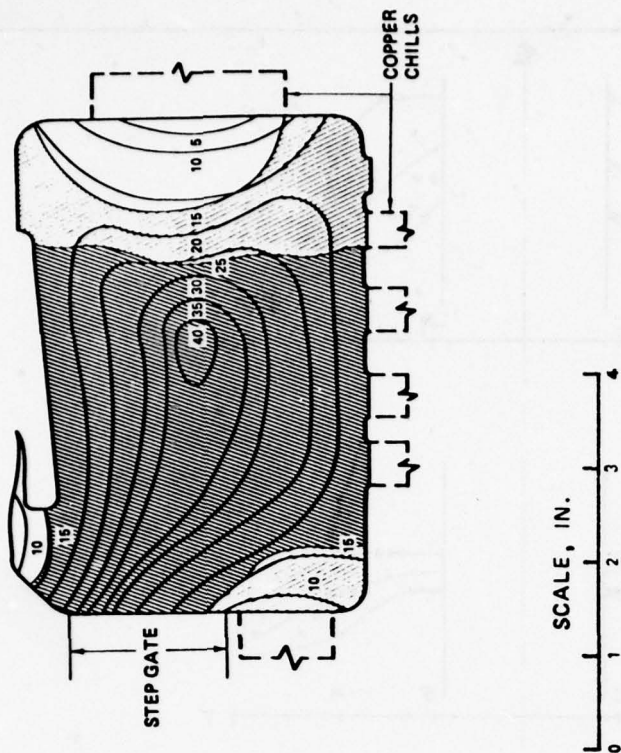
CALC			REVISED	DATE	FIGURE 112. DAS MEASUREMENTS ALONG GRID LINES A-A, B-B, C-C, AND D-D; INTEGRAL CAST FITTING, PIECE B, FROM BOEING CASTING S/N 369.	
CHECK						
APR						
APR						
THE BOEING COMPANY					PAGE	232



CALC			REVISED	DATE	FIGURE 113. DAS MEASUREMENTS ALONG GRID LINES X-X, Y-Y, AND Z-Z; INTEGRAL CAST FITTING, PIECE B, FROM BOEING CASTING S/N 369.	
CHECK						
APR						
APR						
					THE BOEING COMPANY	PAGE 233



A. Integral Cast Fitting, Piece B.



B. Fitting No. 2, Piece B.

FIGURE 114. LINES OF CONSTANT AVERAGE DAS AND EXTENT OF VISUAL POROSITY. FITTINGS FROM BOEING CASTING S/N 369.

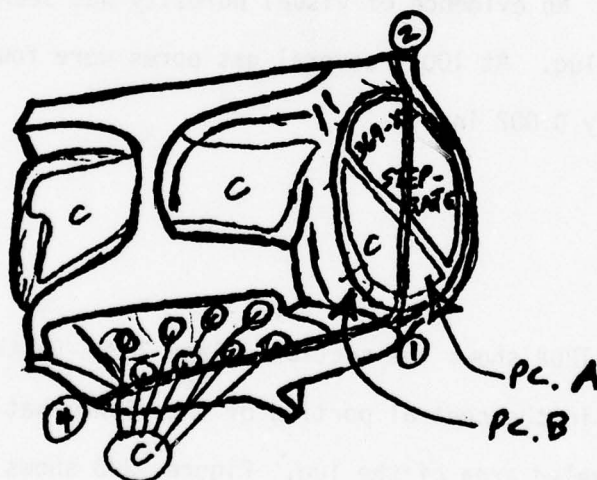
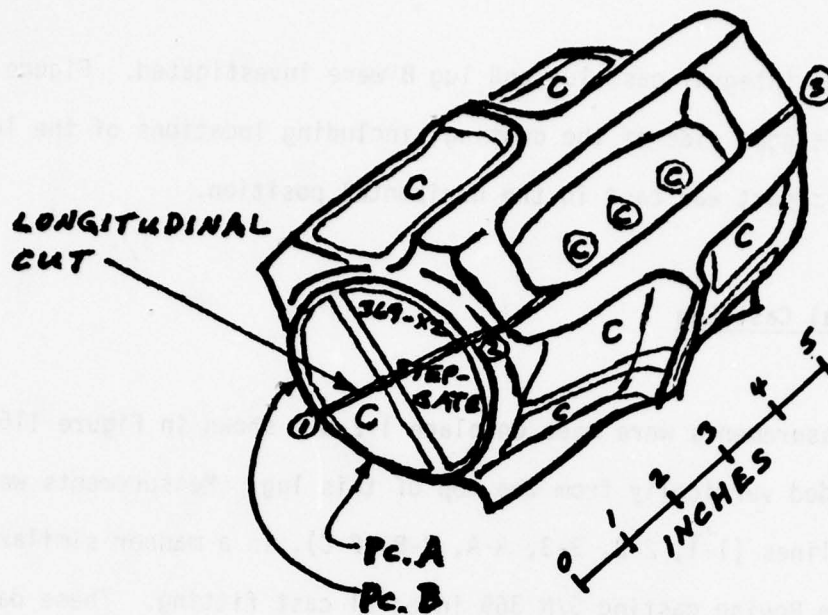


FIGURE 115. FITTING NO. 2 FROM BOEING ALLOWABLES
PREPRODUCTION PART B CASTING S/N 369.

2. HITCHCOCK ALLOWABLES PART A -- CASTING S/N 9

Both the integral cast lug and lug B were investigated. Figure 116 shows the aft/cope side of the casting, including locations of the lugs and chills. This part was cast in the horizontal position.

a. Integral Cast Lug

DAS measurements were made on plane 1-2-3-4 shown in Figure 116. The riser extended vertically from the top of this lug. Measurements were made along grid lines (1-1, 2-2, 3-3, A-A, B-B, C-C), in a manner similar to that for the Boeing casting S/N 369 integral cast fitting. These data are plotted in Figures 117 and 118, and the grid lines used are illustrated in Figure 119. Figure 119 also presents the map showing lines of constant average DAS. No evidence of visual porosity was seen in this section through the lug. At 100X, several gas pores were found (maximum diameter approximately 0.002 inch).

b. Lug B

Figure 120A shows the section (plane 2-3-4-5) that was investigated. Line 3-4 is in the central portion of the riser that extended vertically from the beveled area of the lug. Figure 120B shows the lines of constant average DAS in the lug. As in the section from the integral cast lug, there was no evidence of visual porosity in this section. At 100X, several gas pores were found (maximum diameter approximately 0.004 inch).

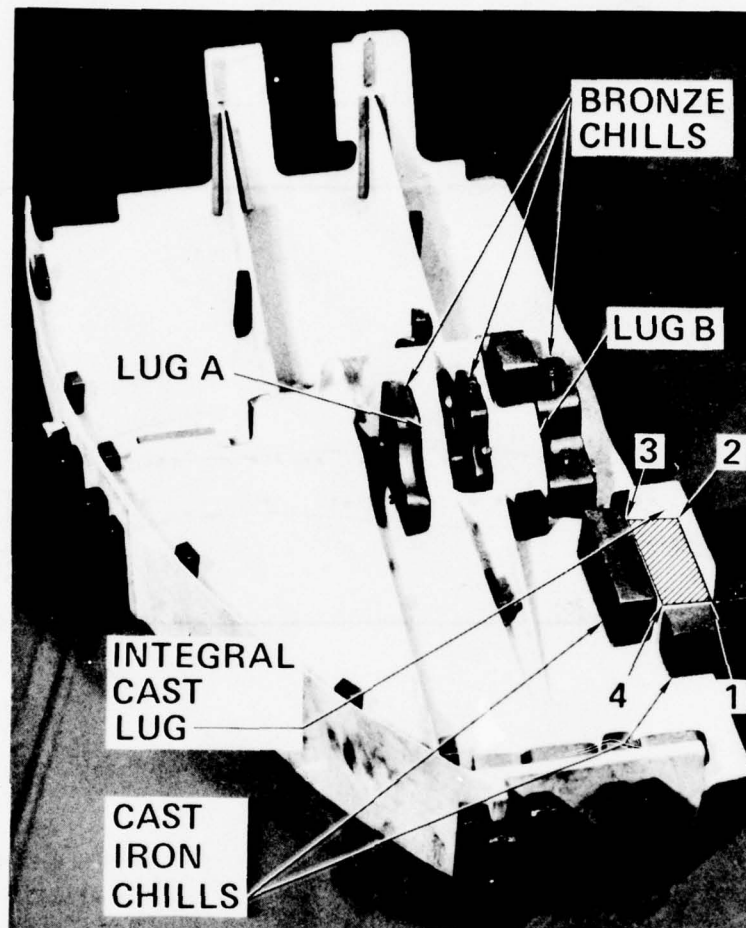
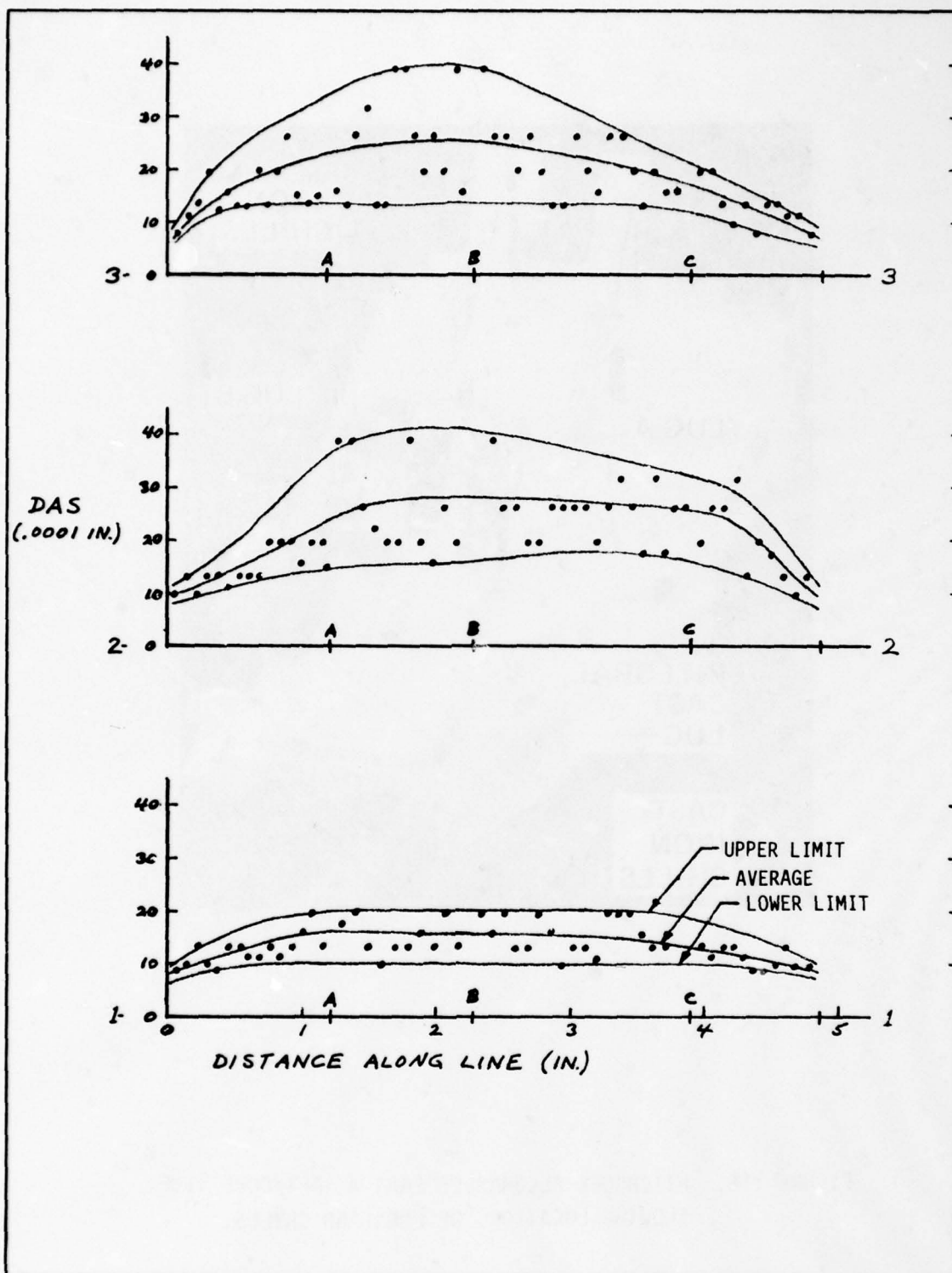
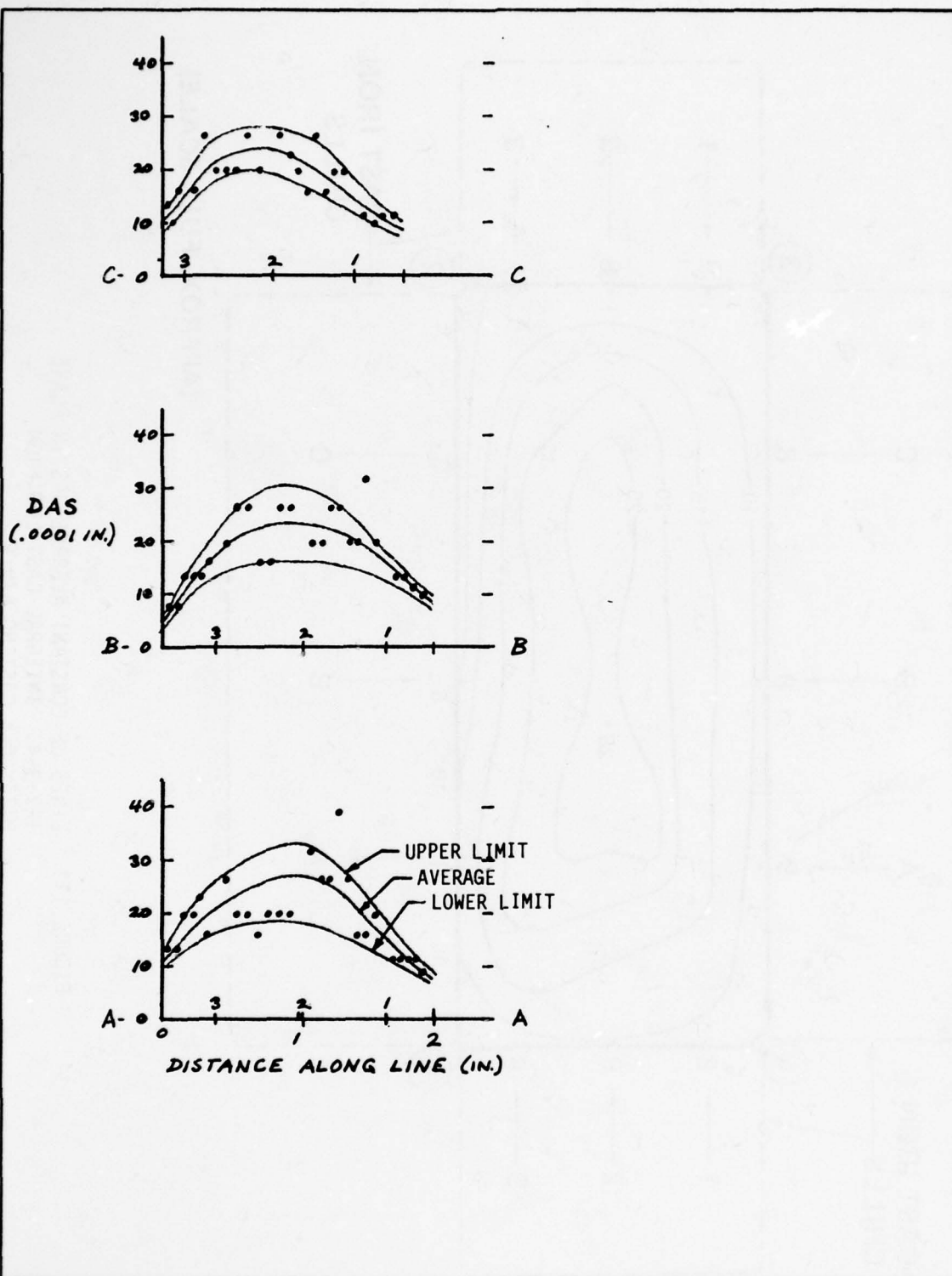


FIGURE 116. HITCHCOCK ALLOWABLES PART A, AFT/COPE SIDE,
SHOWING LOCATIONS OF LUGS AND CHILLS.



CALC			REVISED	DATE	FIGURE 117. DAS MEASUREMENTS ALONG GRID LINES 1-1, 2-2, AND 3-3; INTEGRAL CAST LUG, PLANE 1-2-3-4, FROM HITCHCOCK CASTING S/N 9.	
CHECK						
APR						
APR						
					THE BOEING COMPANY	PAGE 238



CALC			REVISED	DATE	FIGURE 118. DAS MEASUREMENTS ALONG GRID LINES A-A, B-B, AND C-C; INTEGRAL CAST LUG, PLANE 1-2-3-4, FROM HITCHCOCK CASTING S/N 9.	
CHECK						
APR						
APR						
					THE BOEING COMPANY	PAGE 239

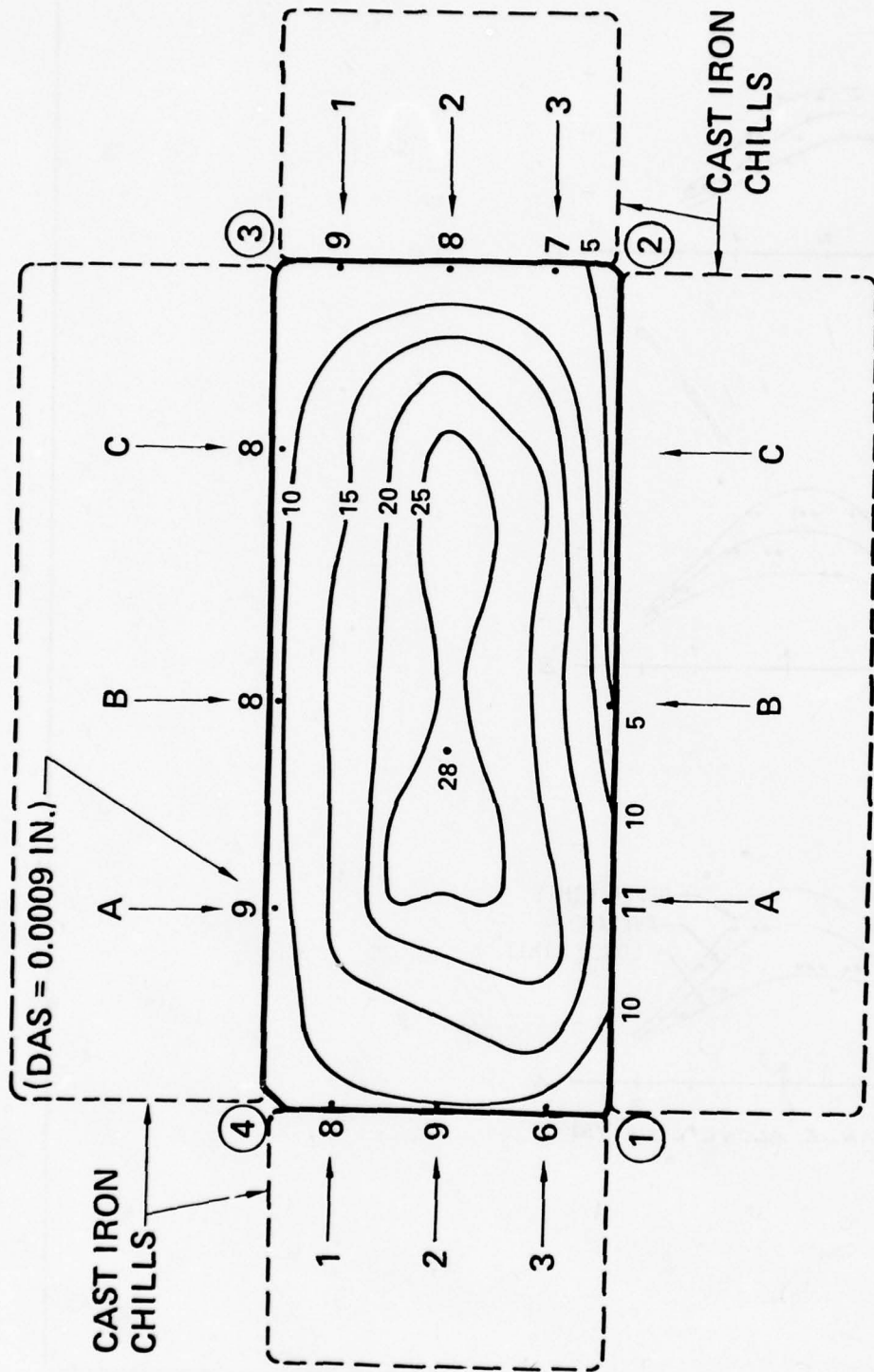
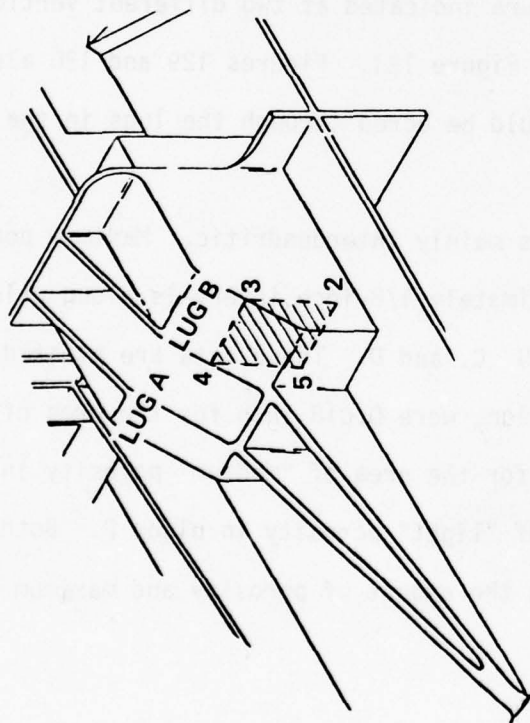
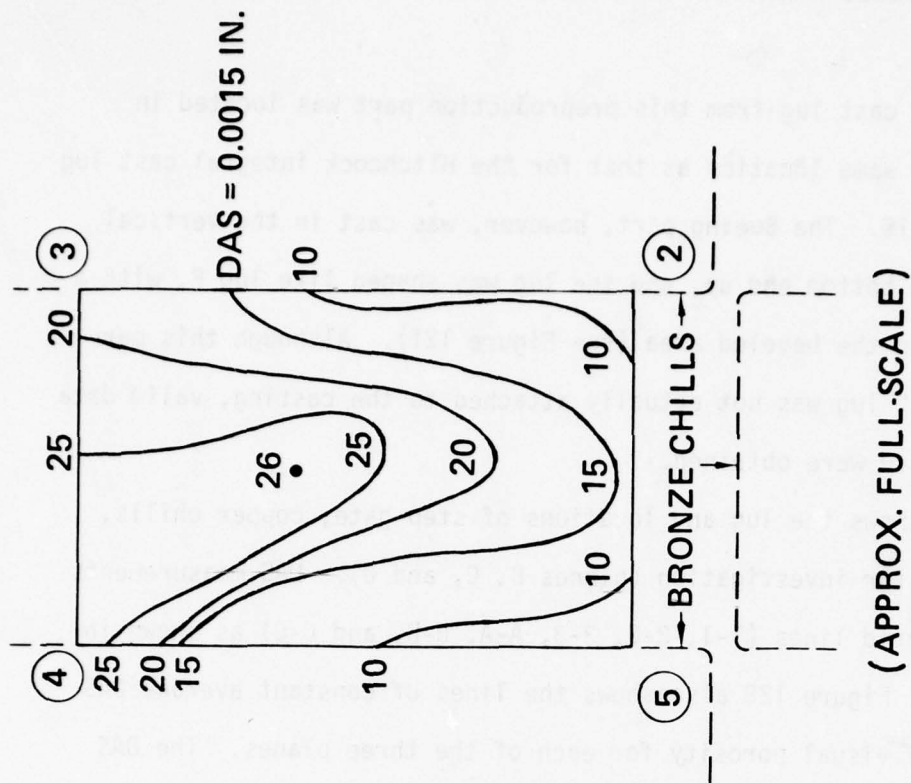


FIGURE 119. LINES OF CONSTANT AVERAGE DAS IN PLANE 1-2-3-4. INTEGRAL CAST LUG FROM HITCHCOCK CASTING S/N 9.



241



A. SECTION INVESTIGATED-- PLANE 2-3-4-5.

B. LINES OF CONSTANT AVERAGE DAS IN PLANE 2-3-4-5.

FIGURE 120. LUG B FROM HITCHCOCK CASTING S/N 9.

3. BOEING ALLOWABLES PART A -- CASTING S/N 578

The integral cast lug from this preproduction part was located in approximately the same location as that for the Hitchcock integral cast lug shown in Figure 116. The Boeing part, however, was cast in the vertical position with the bottom end up, and the lug was shaped like lug B, with a step-gate entering the beveled area (see Figure 121). Although this particular "integral" lug was not actually attached to the casting, valid data on DAS and porosity were obtained.

Figure 121 shows the lug and locations of step-gate, copper chills, and sections cut for investigation (planes B, C, and D). DAS measurements were made along grid lines (1-1, 2-2, 3-3, A-A, B-B, and C-C) as shown in Figures 122-128. Figure 128 also shows the lines of constant average DAS and the extent of visual porosity for each of the three planes. The DAS plots in Figure 128 were used to construct Figures 129 and 130, which give some idea of the internal structure indicated at two different vertical planes illustrated by E and F in Figure 121. Figures 129 and 130 also show the location of the hole that would be bored through the lugs in the actual bulkhead casting.

The porosity in this lug was mainly interdendritic. Maximum pore dimension was measured at approximately 1/8-inch intervals along grid line 2-2 on each of the three planes B, C, and D. These data are plotted in Figure 131. Maximum pore dimensions were 0.018 inch for the area of "heavy" porosity in plane B, 0.015 inch for the area of "medium" porosity in plane C, and 0.011 inch for the area of "light" porosity in plane D. Both Figures 128 and 131 show the increase in the amount of porosity and maximum pore size from chill to step-gate.

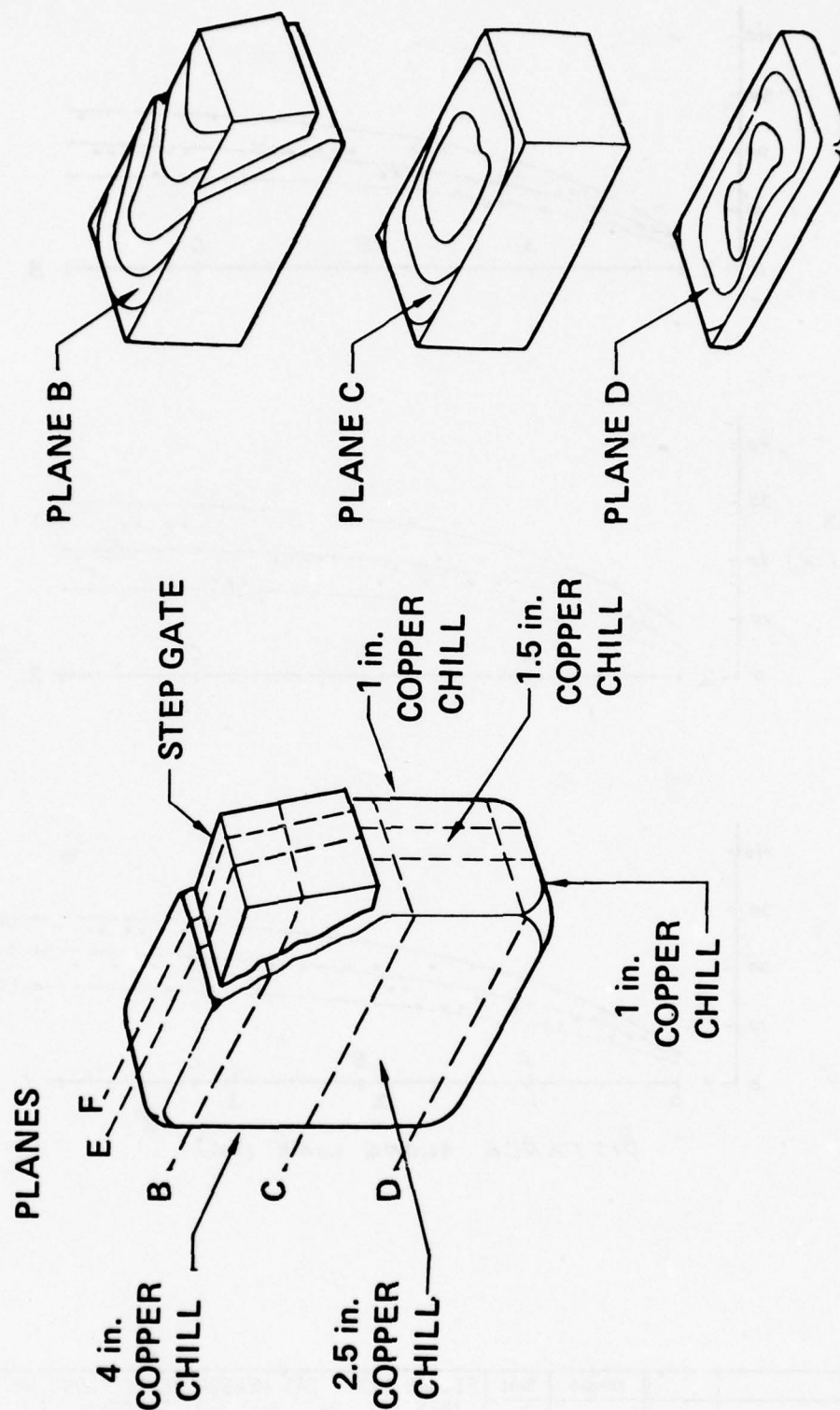
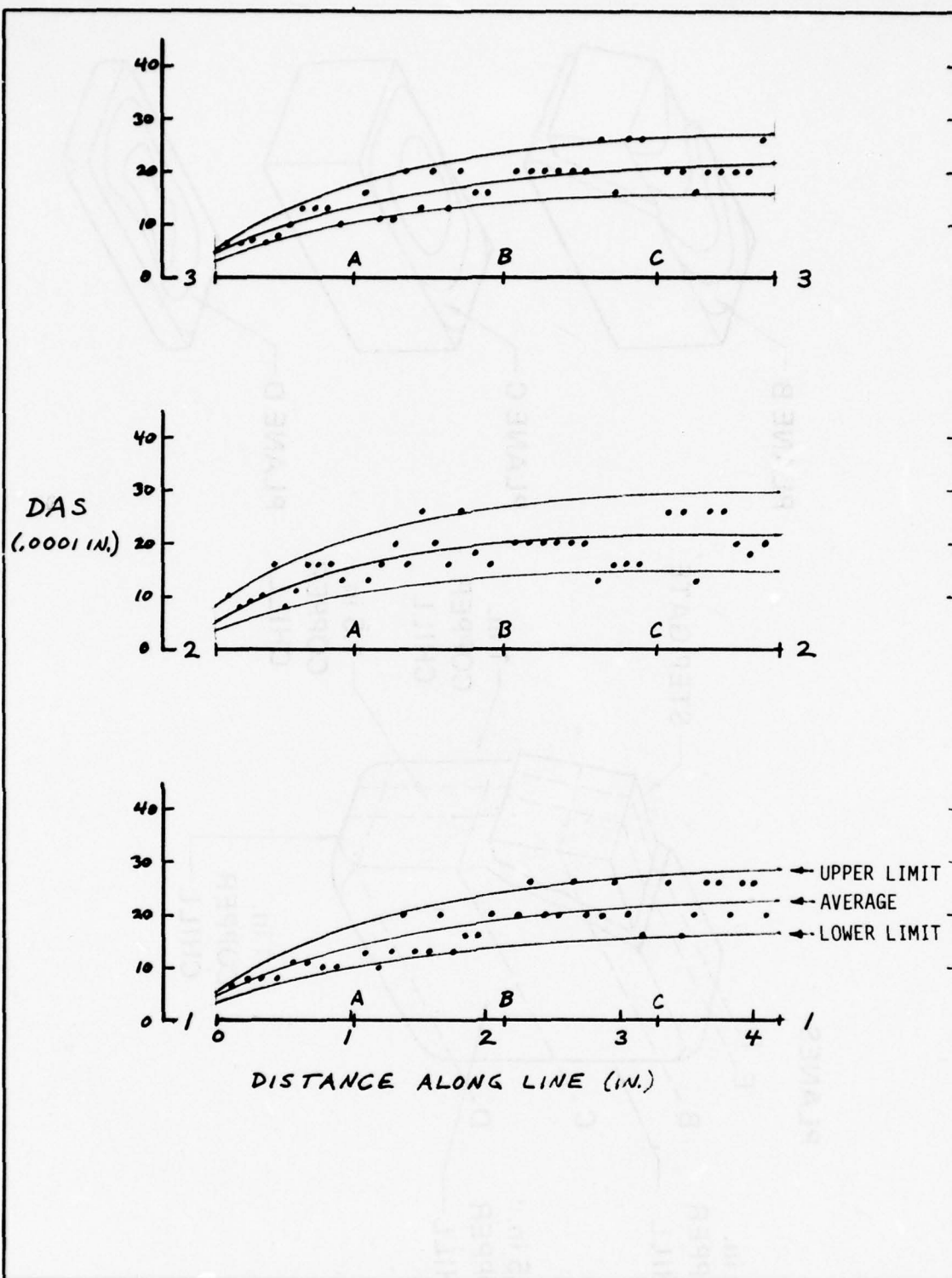
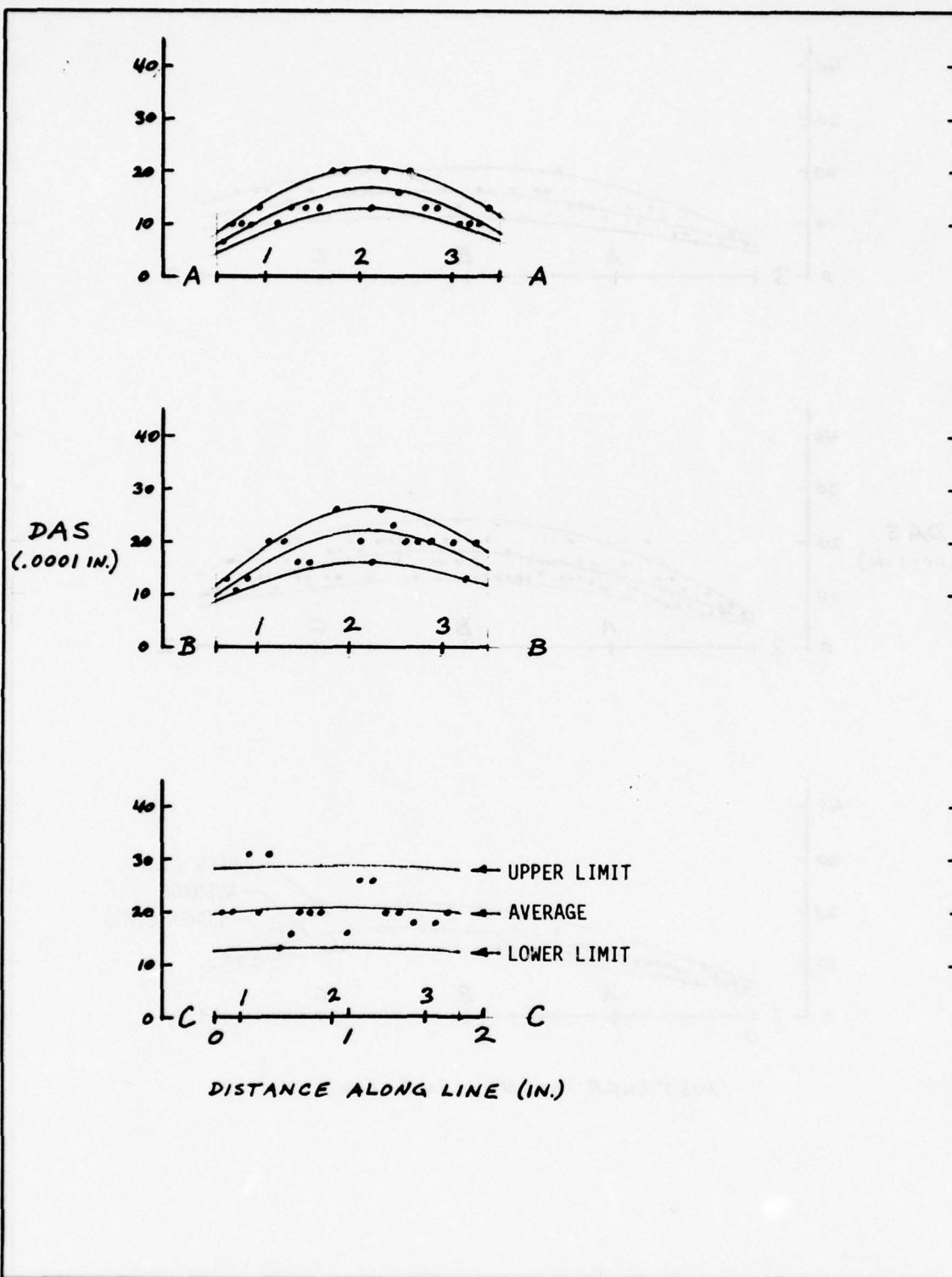


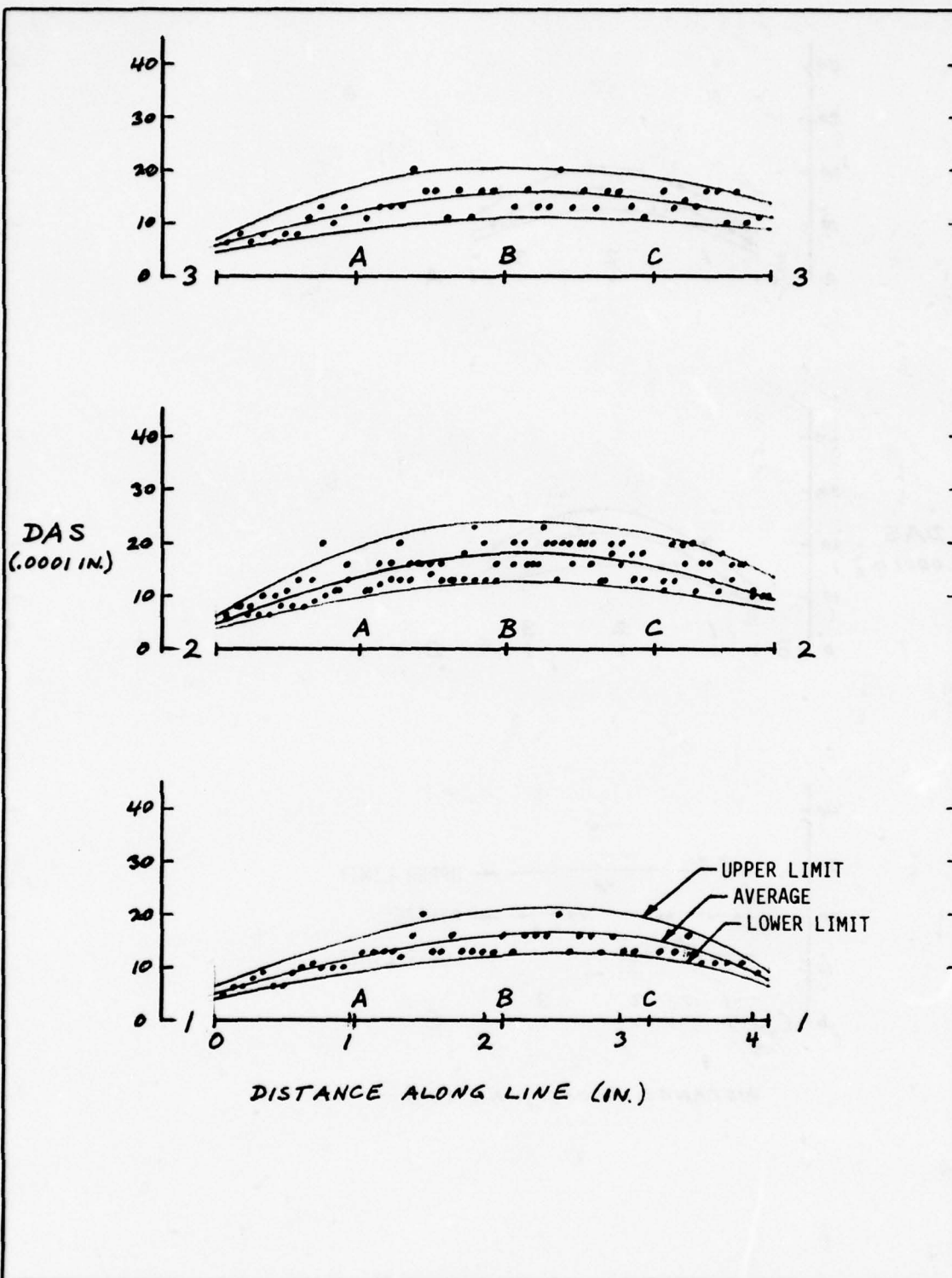
FIGURE 121. INTEGRAL CAST LUG FROM BOEING ALLOWABLES PART A CASTING S/N 578.



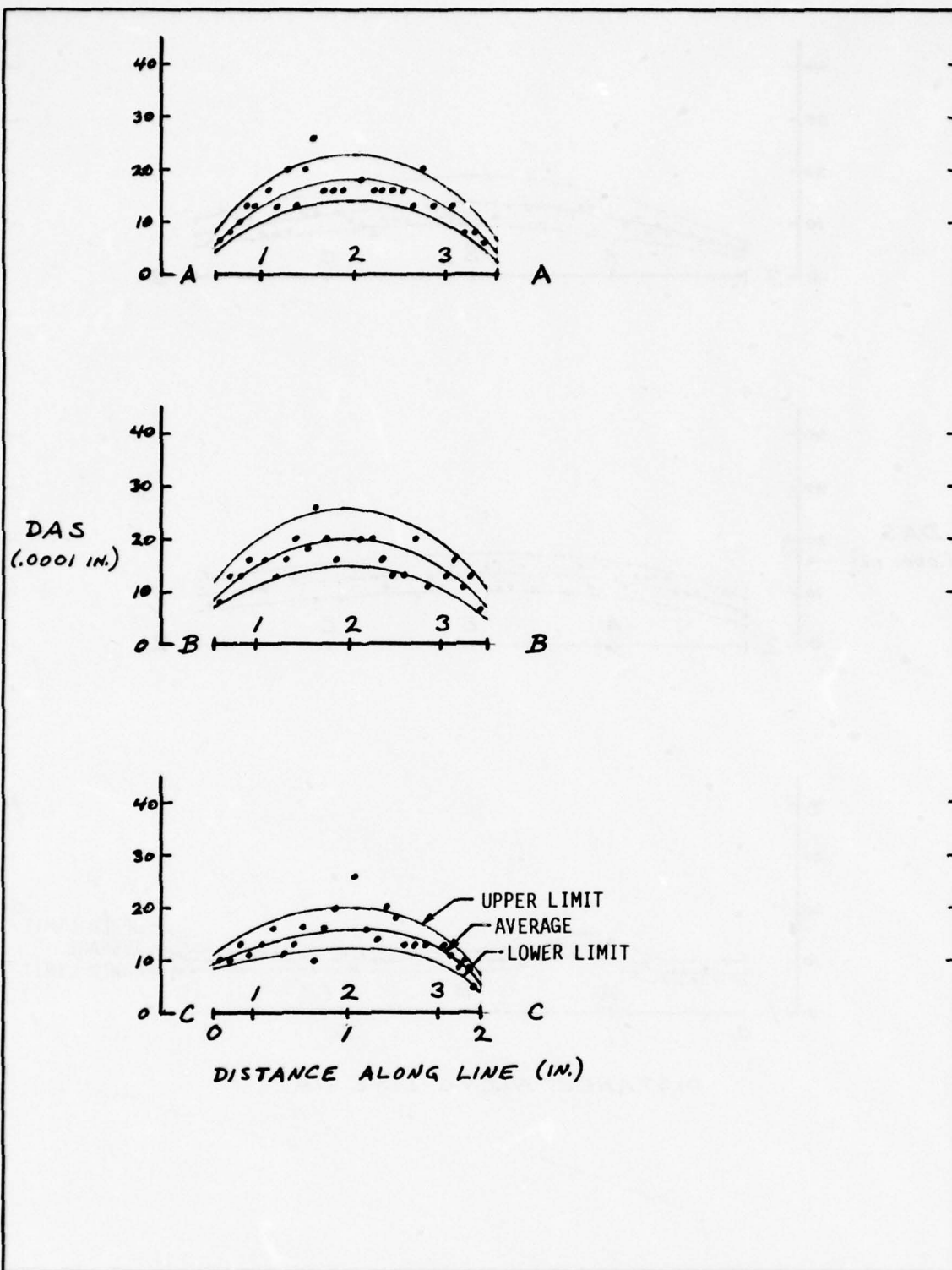
CALC			REVISED	DATE	FIGURE 122. DAS MEASUREMENTS ALONG GRID LINES 1-1, 2-2, AND 3-3; INTEGRAL CAST LUG, PLANE B, FROM BOEING CASTING S/N 578.	
CHECK						
APR						
APR						
					THE BOEING COMPANY	PAGE 244



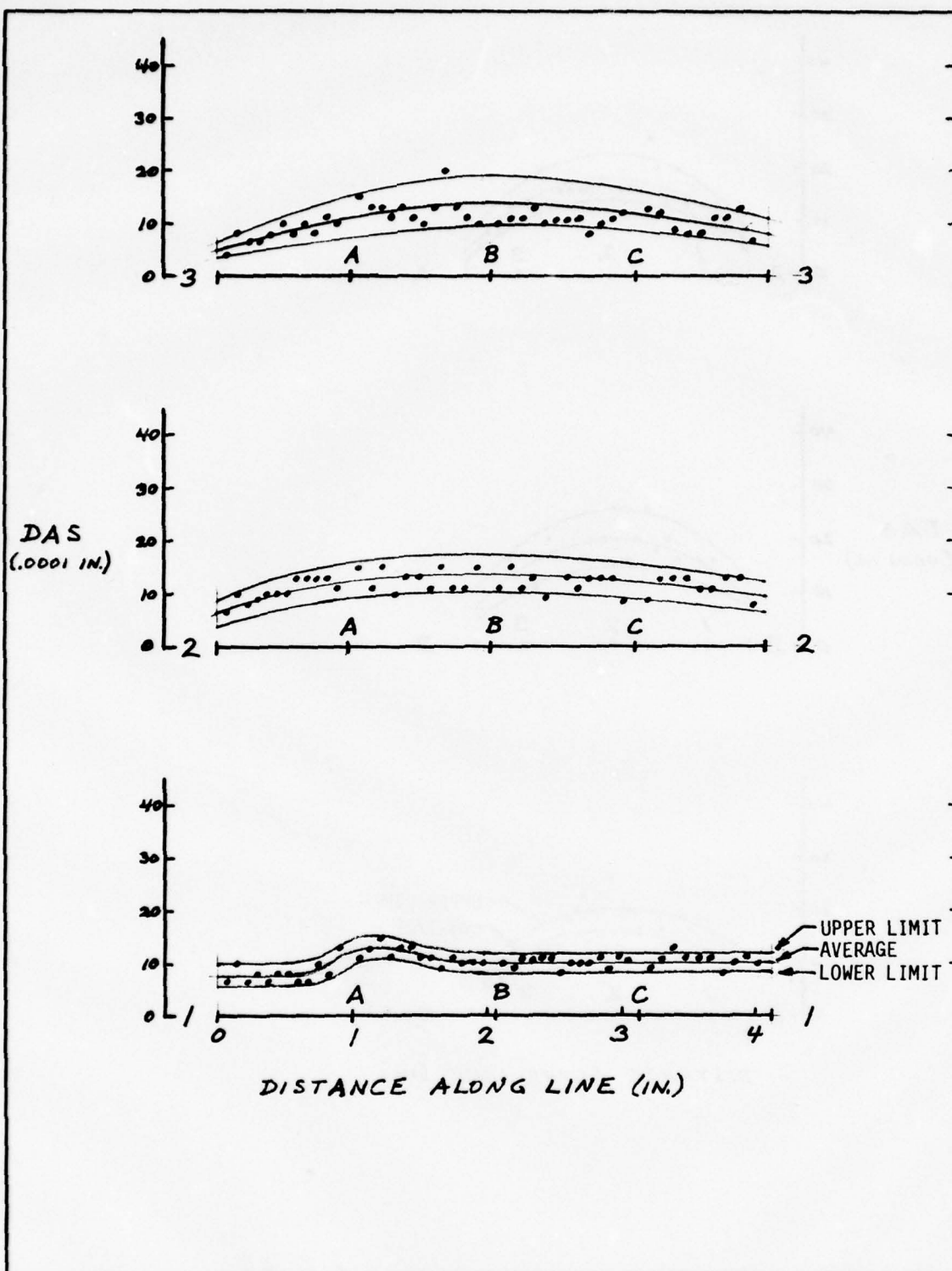
CALC			REVISED	DATE	FIGURE 123. DAS MEASUREMENTS ALONG GRID LINES A-A, B-B, AND C-C; INTEGRAL CAST LUG, PLANE B, FROM BOEING CASTING S/N 578.	
CHECK						
APR						
APR						
THE BOEING COMPANY					PAGE	245



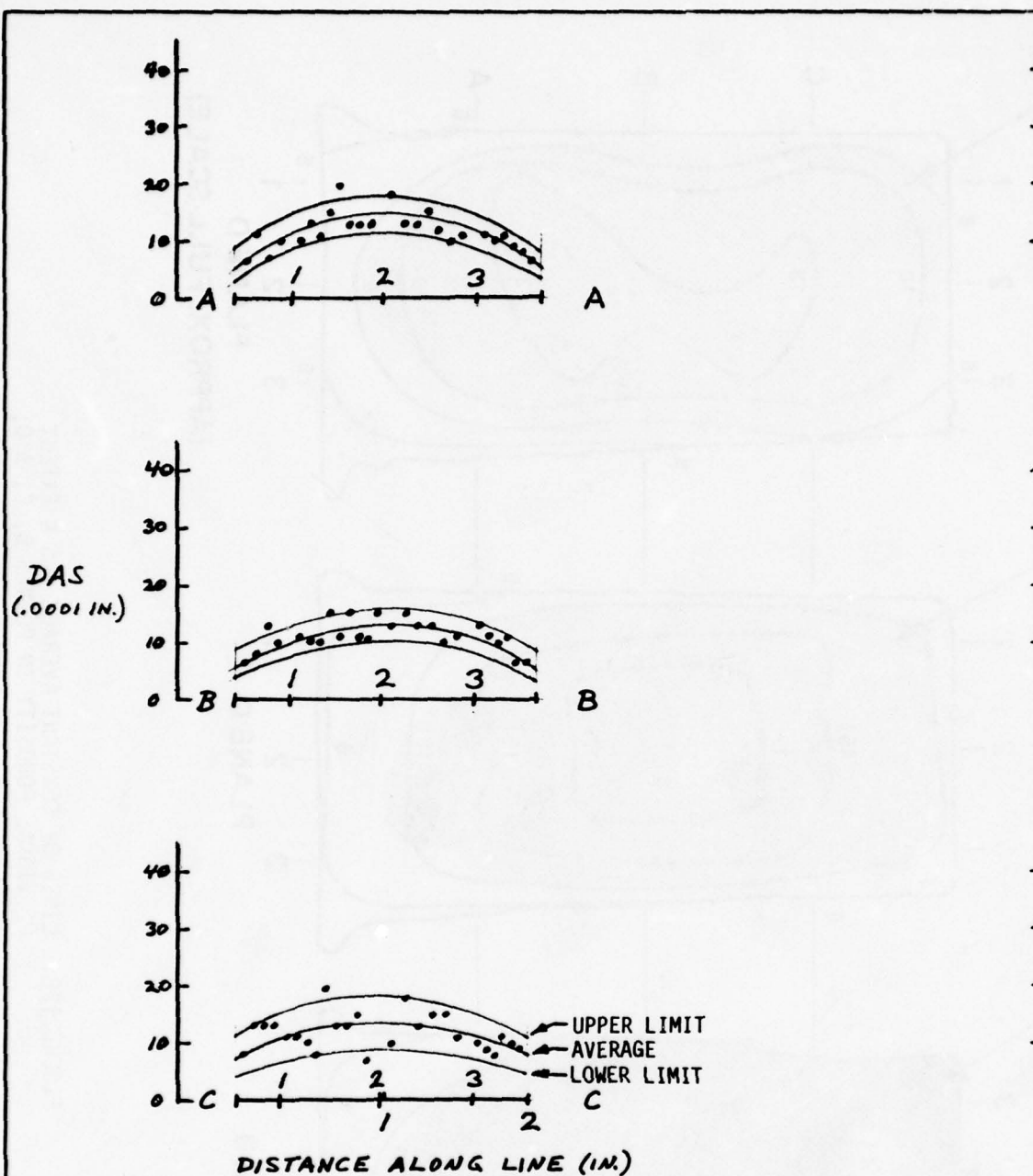
CALC			REVISED	DATE	FIGURE 124. DAS MEASUREMENTS ALONG GRID LINES 1-1, 2-2, AND 3-3; INTEGRAL CAST LUG, PLANE C, FROM BOEING CASTING S/N 578.	
CHECK						
APR						
APR						
THE BOEING COMPANY					PAGE	246



CALC			REVISED	DATE	FIGURE 125. DAS MEASUREMENTS ALONG GRID LINES A-A, B-B, AND C-C; INTEGRAL CAST LUG, PLANE C, FROM BOEING CASTING S/N 578.	
CHECK						
APR						
APR						
					THE BOEING COMPANY	PAGE 247



CALC			REVISED	DATE	FIGURE 126. DAS MEASUREMENTS ALONG GRID LINES 1-1, 2-2, & 3-3; INTEGRAL CAST LUG, PLANE D, FROM BOEING CASTING S/N 578	
CHECK						
APR						
APR						
					THE BOEING COMPANY	PAGE 248



CALC			REVISED	DATE	FIGURE 127. DAS MEASUREMENTS ALONG GRID LINES A-A, B-B, & C-C; INTEGRAL CAST LUG, PLANE D, FROM BOEING CASTING S/N 578.	
CHECK						
APR						
APR						
					THE BOEING COMPANY	PAGE 249

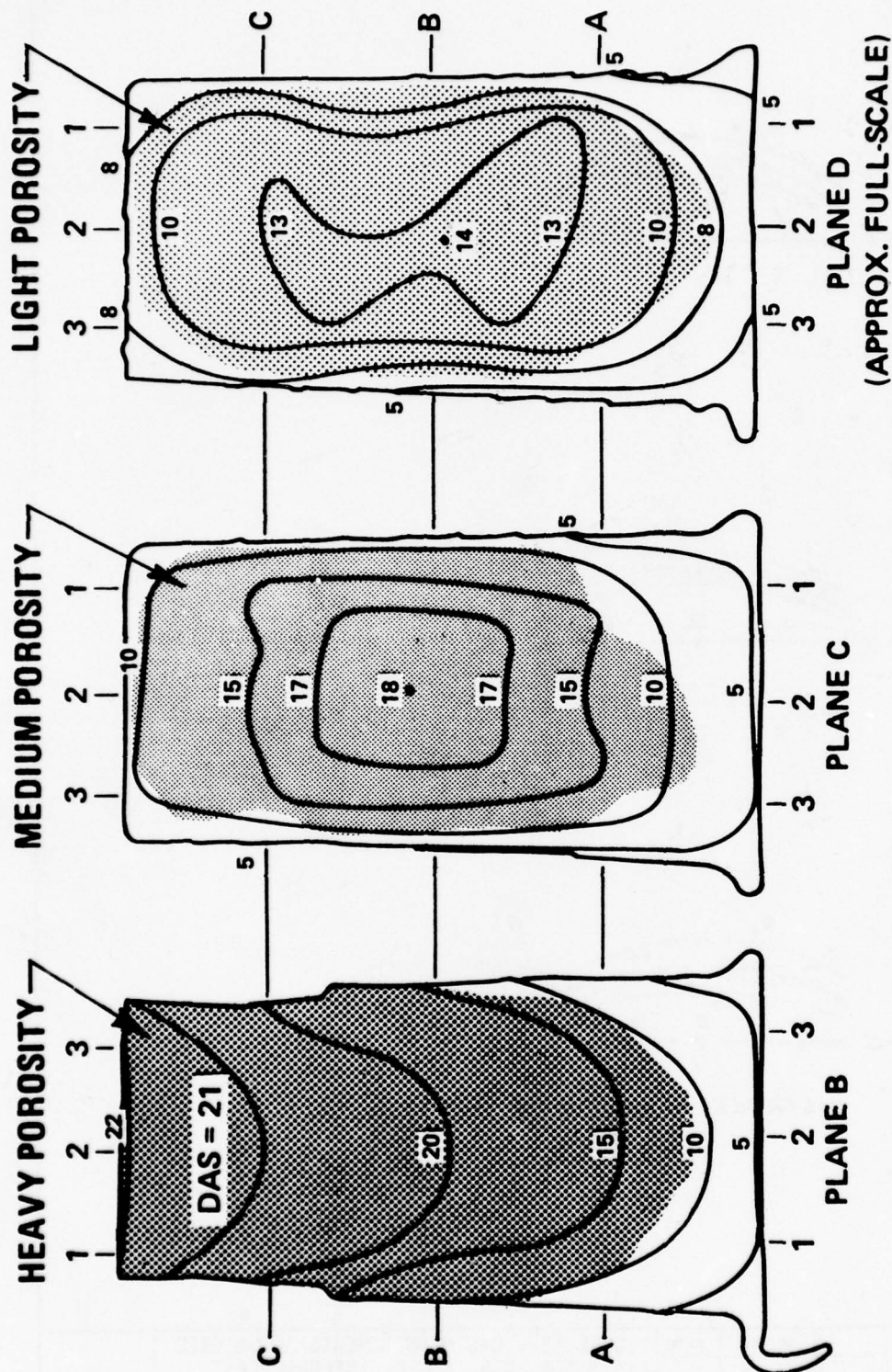
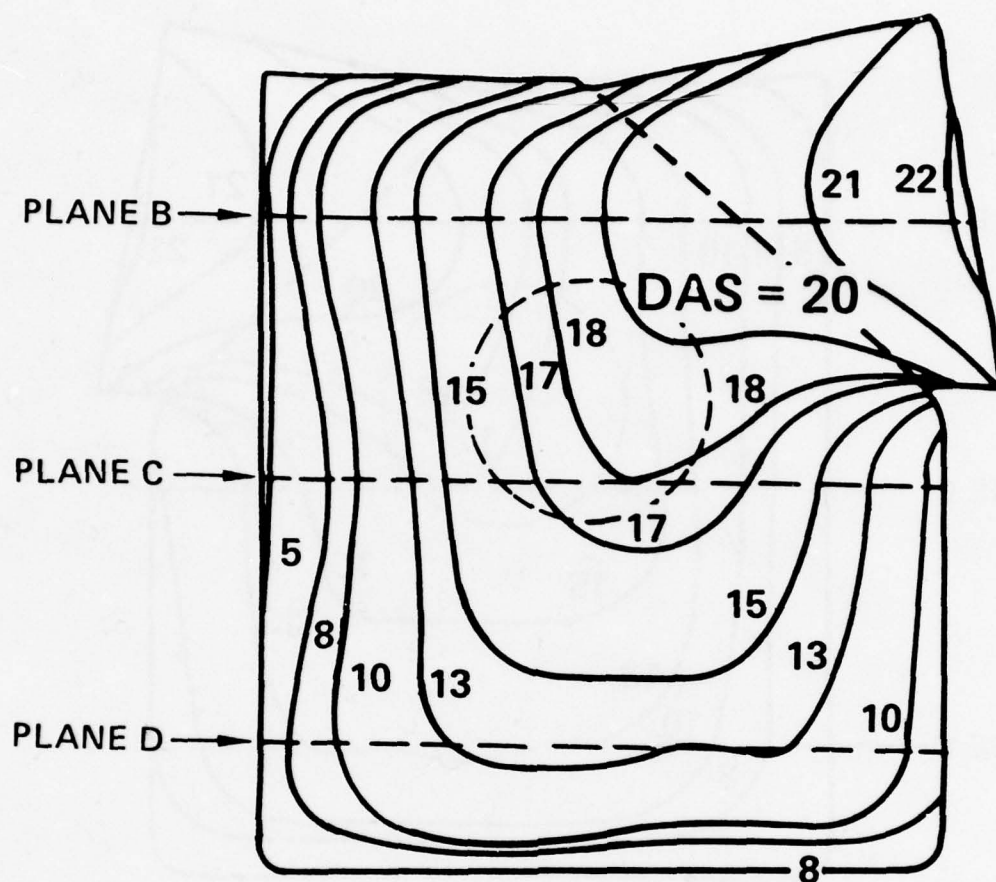
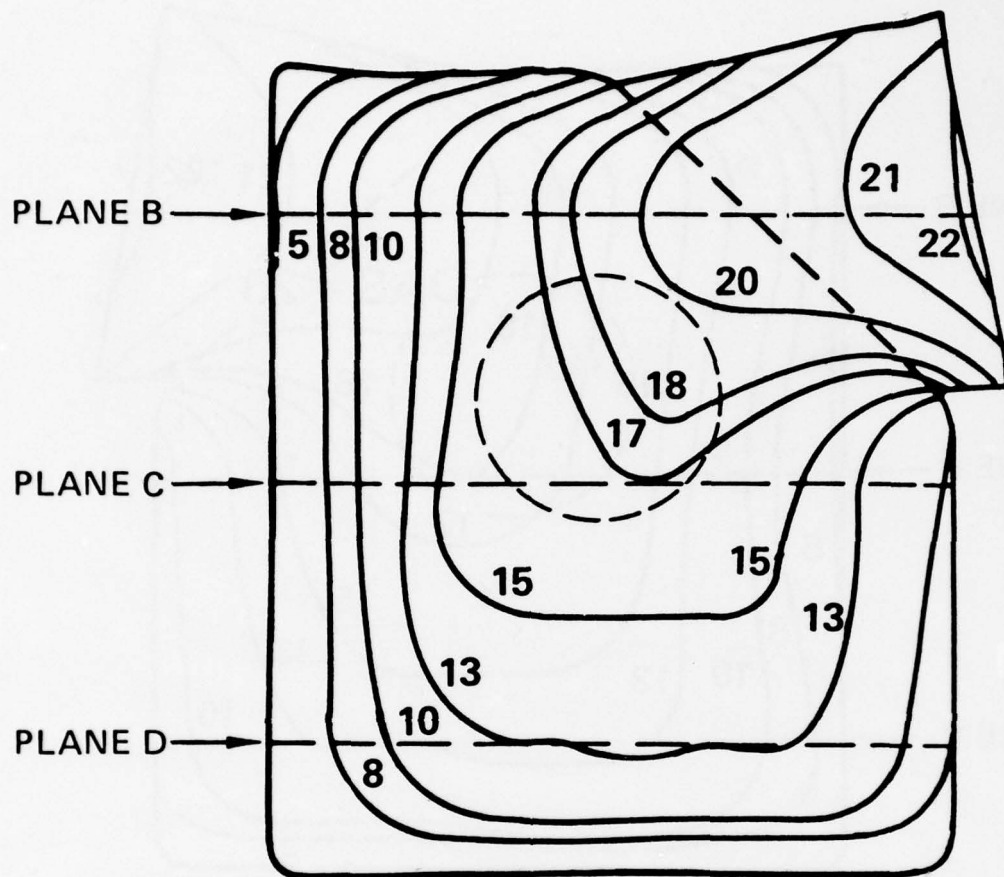


FIGURE 128. LINES OF CONSTANT AVERAGE DAS & EXTENT OF VISUAL POROSITY IN PLANES B, C, & D; INTEGRAL-CAST LUG FROM BOEING CASTING S/N 578.



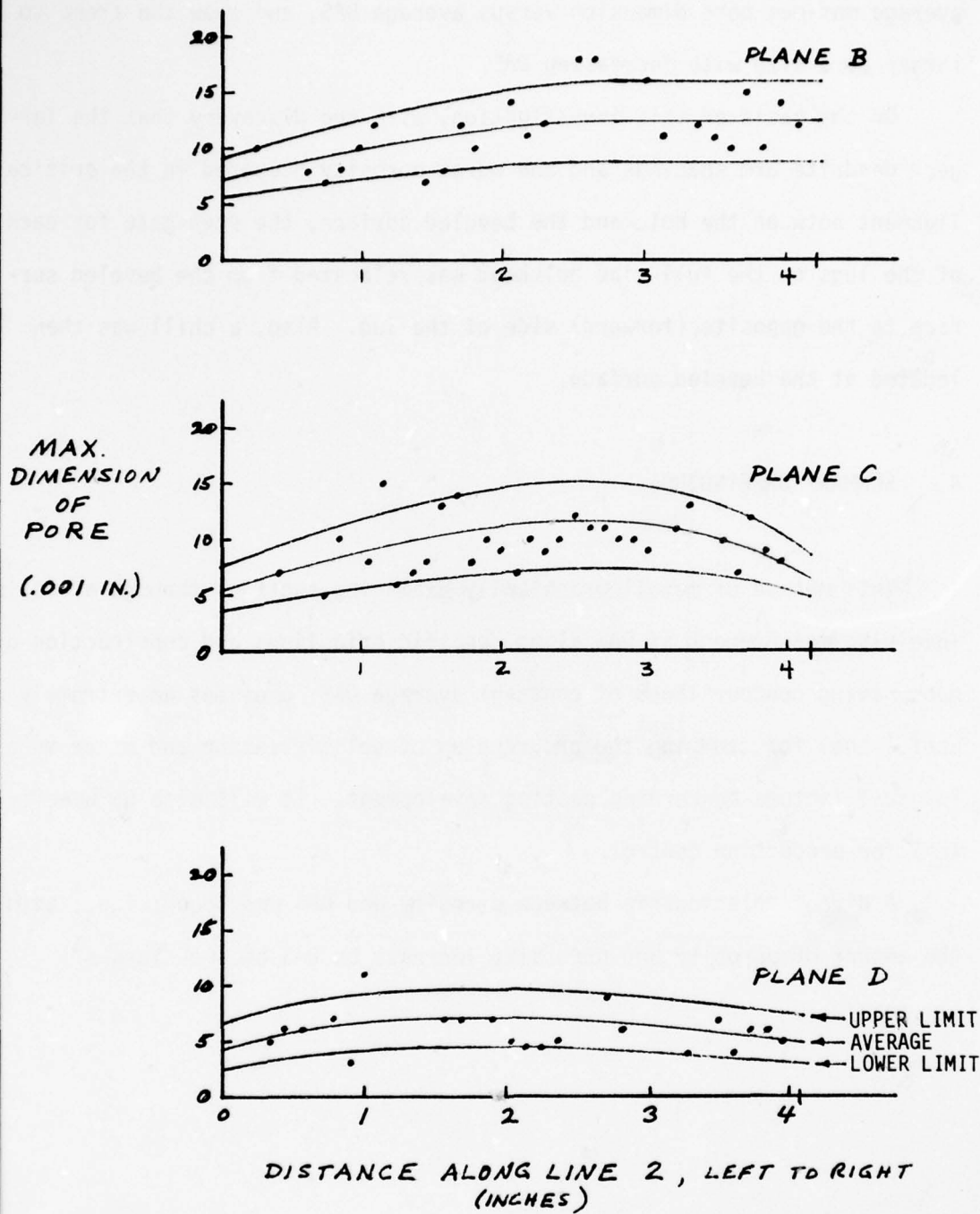
(APPROX. FULL-SCALE)

FIGURE 129. LINES OF CONSTANT AVERAGE DAS IN PLANE E;
INTEGRAL CAST LUG FROM BOEING CASTING
S/N 578.



(APPROX. FULL-SCALE)

FIGURE 130. LINES OF CONSTANT AVERAGE DAS IN PLANE F;
INTEGRAL CAST LUG FROM BOEING CASTING
S/N 578.



DATE		REVISED	DATE	FIGURE 131, MAXIMUM PORE DIMENSIONS ALONG GRID LINE 2-2 IN PLANES B, C, & D; INTEGRAL CAST LUG FROM BOEING CASTING S/N 578.	
DATE					
DATE					
DATE					
				THE BOEING COMPANY	PAGE 253

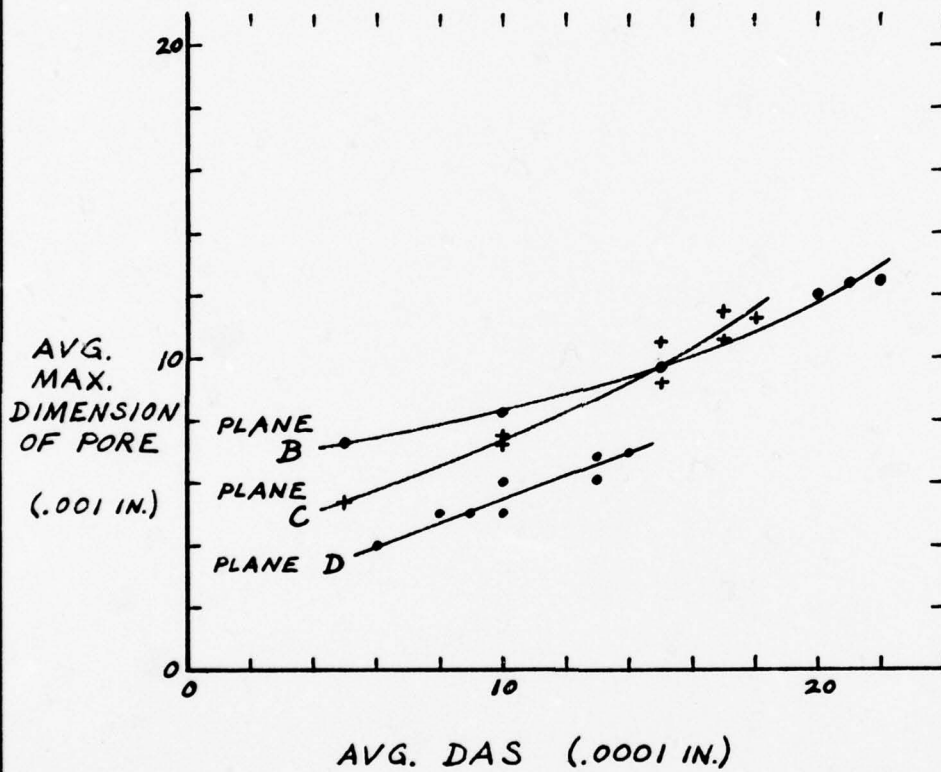
Data taken from Figures 128 and 131 are plotted in Figure 132 as average maximum pore dimension versus average DAS, and show the trend to larger pore size with increasing DAS.

On the basis of this investigation, with the discovery that the largest dendrite arm spacings and the worst porosity occurred in the critical ligament between the hole and the beveled surface, the step-gate for each of the lugs on the full-size bulkhead was relocated from the beveled surface to the opposite (forward) side of the lug. Also, a chill was then located at the beveled surface.

4. SUMMARY OF FINDINGS

This method of metallographically examining sections through a casting, involving measurement of DAS along specific grid lines and construction of maps having contour lines of constant average DAS, provides an extremely useful tool for studying the progression of solidification and other metallurgical factors concerning casting development. It will also be beneficial for production control.

A direct relationship between porosity and DAS was found; i.e., both the amount of porosity and pore size increase as DAS becomes larger.



CALC			REVISED	DATE	FIGURE 132. AVERAGE MAXIMUM PORE DIMENSION VERSUS AVERAGE DAS; INTEGRAL CAST LUG FROM BOEING CASTING S/N 578.	
CHECK						
APR						
APR						
					THE BOEING COMPANY	PAGE 255

SECTION XV

MANUFACTURING PLAN

At the conclusion of this phase, a manufacturing process plan was prepared for the fabrication of the YC-14 station 170 body bulkhead. The manufacturing concepts used in this plan were based on the results of the work conducted during this phase. The process plan includes the manufacturing concepts and major tool requirements needed to cast the bulkhead. It will be used by the foundry in Phase IV to fabricate the bulkhead castings.

SECTION XVI

FOUNDRY CONTROL PROCEDURES

Castings have failed to achieve widespread use in primary structural airframe applications. This has been due mainly to lack of designer confidence in the casting process control, mechanical property reproducibility, and quality assurance techniques. This lack of confidence has resulted in either complete elimination from consideration during the aircraft design phase or the imposition of a casting factor that results in a significant weight penalty.

In order to extend the use of aluminum castings to large primary airframe structures, close control of the foundry process must be exercised. The purpose of this section is to outline an approach to foundry process control that will assure the consistent, reproducible fabrication of large primary airframe structural castings. Foundry process control is divided into four categories: personnel qualification, critical operations within the casting process, process plans, and record keeping.

These Foundry Control Procedures are intended to be used for the casting of large primary airframe structural aluminum castings.

1. PERSONNEL QUALIFICATIONS AND CRITICAL SKILLS

The use of properly trained people for a specific operation is vital to achieve consistency in the foundry process. Since the production of castings is a very labor-intensive process, the skill level of the foundry

personnel will determine the quality of castings produced. Personnel should have experience in their specific job descriptions. This experience, depending on the sophistication of the job and employee, may be a short, on-the-job training program or an intensive apprentice program.

During this phase of the program, several operations in the foundry process were identified as requiring the attention of skilled personnel. The foundry operations judged critical and level of personnel qualification required are described below:

- o Metal Preparation -- This operation includes metal melting and alloying, degassing, checking the gas content, and preparing the pouring ladles for use. Metal preparation is a very important step in the casting process, since the metal quality depends on the degree of care taken in preparing the metal. The personnel responsible for this task should be familiar with the operation of the furnace equipment. They should be able to demonstrate their ability to precisely control the temperature of a melt. Knowledge of the problems associated with superheated metal should be understood. Persons responsible for metal preparation should be able to interpret spectrographic results and adjust the chemistry of the metal as required. The degassing operation is a critical step in the casting operation. If it is not done properly, the casting could be scrapped. The degassing operator should be able to demonstrate his knowledge of the effects that various degassing media have on the hydrogen content of the metal and their impact on metal chemistry. The effect of degassing time and flow rate must also be known.

- o Pouring -- Metal pouring is an operation normally left to the experienced foundryman. For obvious reasons, if the pouring operation is not conducted properly, the part will be rejected. The person responsible for pouring should have an understanding of the importance of maintaining a choke on the sprue and/or pouring basin and the correct ladle-to-pouring basin distance. He should be able to demonstrate his working knowledge of these points.
- o Mold and Core Making -- This is probably the most important step in the successful casting of a part. The mold and core making operations are ones that require a high degree of skill and knowledge of the foundry process. During these operations, personnel must be able to foresee problems that, if not corrected in time, may cause casting defects. Personnel involved in the mold and core making must be experienced foundrymen capable of demonstrating their skills. The level of an individual's skill should determine the degree of responsibility given him.
- o Heat Treat and Straightening -- Mechanical properties, to some extent, can be manipulated with heat treatment. Personnel responsible for heat treatment should have a basic understanding of heat-treat principles, including the effect of solution time and temperature, quench delay, and natural and artificial aging, on the resultant mechanical properties of aluminum casting alloys. A knowledge of straightening characteristics is necessary to assure that the casting will meet the dimensional tolerances specified on the casting drawing. To accomplish this task, personnel responsible for straightening must have a working

knowledge of the straightening characteristics of the metal. In addition, they must be proficient in the use of appropriate straightening tools and aids. Personnel should demonstrate their proven ability to straighten parts per a casting drawing.

Other foundry operations require semi-skilled labor. No prior foundry experience is necessary. However, it is the responsibility of every foundry supervisor or foundry engineer that all foundry personnel understand their job functions as they relate to the overall casting process. If these steps in the foundry personnel qualification procedures are practiced, consistency of the casting process will follow.

2. CRITICAL OPERATIONS

Critical operations are those steps of the casting process that, if done improperly, will cause rejection of the casting. Large primary airframe structural castings are generally complex in nature and costly to produce. The rejection of one casting, due to an oversight, can be very costly. To keep costs down and to ensure consistent, reproducible castings, control over the critical operations is mandatory. As a result of the work conducted during this phase, the following operations were judged as being critical to the casting process:

Metal Preparation

- o Chemical analysis
- o Hydrogen content of the melt
- o Pouring temperature

Mold Fabrication

- o Sand fineness and type
- o Binder quantity and type
- o Chill/insulation locations
- o Riser locations
- o Core alignment
- o Mold alignment

Heat Treatment/Straightening

- o Fixturing techniques
- o Dimensional accuracy after straightening

Each of the above operations should be approved by the foundry supervisor, engineer, or inspector prior to the start of the next sequential operation. If this procedure is meticulously followed, the result will be a reproducible casting process.

3. PROCESS PLANS

Each primary airframe structural casting should have a manufacturing plan that includes the manufacturing steps and major tool requirements necessary to fabricate a particular casting. The purpose of this plan is to provide the foundry personnel with detailed instructions on how to fabricate the casting in question. This plan should be initially formulated using the information contained in this report. Substituting the trial and error method of foundry tool design with a scientific approach will reduce the number of tool tryout castings and provide for a more consistent casting process. Constant updating of the plan must be accomplished, as required, during fabrication of the tool tryout castings. When the casting process

has been perfected, the plan is then released to the foundry for the production phase of the casting process.

In addition to the manufacturing plan, each specific job should have supplemental shop aids. These aids should describe in detail the specific tasks to be performed and provide a checklist to assure completion of the task. Supplemental shop aids would typically include instructions to the metal preparation personnel outlining what metal to use, chemistry limits, degassing media and time, pouring temperature, etc. The mold and core making personnel require diagrams specifying the chill/insulation and riser locations, and instruction sheets outlining sand type and fineness, binder type, and quantity required. Heat-treat personnel need to have instructions on how to fixture the part and sketches showing locations where straightening will be required.

These are just a few examples of what supplemental shop aids should contain. Their use will provide foundry personnel with descriptions of their task assignments so that no costly misunderstandings may occur.

4. RECORD KEEPING

An important aspect of the casting process is what was done in the past. Record keeping is necessary to be assured of a repeatable process. If the foundryman does not know what he did in the past, he will not know what to do in the future. An unrecorded casting process will provide for inconsistent and nonreproducible results.

Detailed records should be kept on all aspects of the casting process. Typical record forms are shown in Figures 133-141. The use of photographs to record what has been done is a useful technique. The information must be recorded as soon as it is available so it will not be lost in the confusion of generating more data. It should be the responsibility of every foundry supervisor or engineer to record all pertinent data and be responsible for its retention.

Widespread use of castings for primary airframe structures will only come about when foundry control procedures, like those outlined above, are followed. It is the use of control procedures that will assist in regaining designers' confidence in the use of castings without a casting factor.

PAGE 1 OF 3

CHEMICAL ANALYSES

INGOT SUPPLIER _____ INGOT HEAT NO. _____

FOUNDRY TEMPERATURE _____ FOUNDRY HUMIDITY _____

PART WEIGHT _____

FURNACE NO. _____ INGOT HEAT NO. _____ WEIGHT OF CHARGE _____

MAX. MELT TEMPERATURE _____ TIME MELT IS IN MOLTEN STATE _____

HOLDING TEMPERATURE _____ POURING TEMPERATURE (EACH LADLE) _____

NO OF LADLES USED _____

FLUXING MEDIUM _____ AMOUNT OF FLOW RATE _____

FLUXING TIME _____ MEANS OF MEASURING GAS CONTENT _____

GAS CONTENT BEFORE FLUXING _____ GAS CONTENT AFTER FLUXING _____

TIME BETWEEN FLUXING & POURING _____

[illegible]

TYPE _____ AMOUNT _____ HEAT NO. _____

TYPE _____ AMOUNT _____ HEAT NO. _____

COMMENTS:

264

CASTING PARAMETERS - CAST PROGRAM

PAGE 2 OF 3

CASTING SERIAL NO. _____ DATE _____
 PART NAME _____ PART NO. _____
 ENGINEER _____

MOLDS

SAND TYPE _____
 SIEVE SIZE _____
 AMOUNT OF SAND _____
 SODIUM SILICATE TYPE _____
 SODIUM SILICATE AMOUNT _____
 ADDITIONS TO SODIUM SILICATE _____
 MULLING TIME _____
 MULLING SPEED _____
 MOISTURE CONTENT _____
 PERMEABILITY, GREEN _____
 PERMEABILITY, HARDENED _____
 HARDNESS _____
 CO₂ GASSING FLOW RATE _____
 CO₂ GASSING TIME _____

CORES

SAND TYPE _____
 SIEVE SIZE _____
 AMOUNT OF SAND _____
 SODIUM SILICATE TYPE _____
 SODIUM SILICATE AMOUNT _____
 ADDITIONS TO SODIUM SILICATE _____
 MULLING TIME _____
 MULLING SPEED _____
 MOISTURE CONTENT _____
 PERMEABILITY, GREEN _____
 PERMEABILITY, HARDENED _____
 HARDNESS _____
 CO₂ GASSING FLOW RATE _____
 CO₂ GASSING TIME _____

GATING SYSTEM (SEE ATTACHED POURING SYSTEM SKETCH)

PATTERN NO. _____ SPRUE AREA: RUNNER AREA: GATE AREA RATIO _____
 NO. OF SPRUES _____ SPRUE CONFIGURATION _____

COMMENTS

FIGURE 134 TYPICAL CASTING RECORD FORM

CASTING PARAMETERS - CAST PROGRAM

PAGE 3 OF 3

CASTING SERIAL NO. _____ DATE _____
PART NAME _____ PART NO. _____
ENGINEER _____

RISERS (SEE ATTACHED POURING SYSTEM SKETCH)

NO. OF RISERS _____ TYPE _____

CHILLS (SEE ATTACHED POURING SYSTEM SKETCH)

NO. OF CHILLS _____ TYPE _____

HEAT TREATMENT

	SOLUTION TREATMENT	NATURAL AGING (-T4)	ARTIFICIAL AGING
FURNACE NO.		_____	
LOAD NO.		_____	
TEMPERATURE		_____	
HEAT-UP TIME		_____	
TIME AT TEMPERATURE		_____	
QUENCH MEDIUM		_____	_____
QUENCH MEDIUM TEMPERATURE		_____	_____
QUENCH DELAY TIME		_____	_____
TIME			
TEMPERATURE (AMBIENT)			

COMMENTS _____

FIGURE 135 TYPICAL CASTING RECORD FORM

AD-A060 339

BOEING AEROSPACE CO SEATTLE WASH
CAST ALUMINUM STRUCTURES TECHNOLOGY (CAST) MANUFACTURING METHOD--ETC(U)
MAY 78 R G CHRISTNER, D D GOEHLER

F/G 11/6

F33615-76-C-3111

UNCLASSIFIED

D180-24610-1

AFFDL-TR-78-62

NL

4 OF 4
AD
A060339



END
DATE
FILMED
12-78

DDC

POURING SYSTEM -- CAST PROGRAM

CASTING SERIAL NO. _____ PART NO. _____ DATE _____

<p>LEGEND:</p>	<p>SKETCH OF PART WITH POURING SYSTEM</p>
----------------	---

FIGURE 136 TYPICAL CASTING RECORD FORM

CASTING SERIAL NO. _____ DATE _____
PART NAME _____ PART NO. _____
ENGINEER _____

[illegible]

☐ X-RAY

☐ PENETRANT

☐ DAS/DCS

FIGURE 137 TYPICAL CASTING RECORD FORM

TEST SPECIMEN LOCATIONS - CAST PROGRAM

CASTING SERIAL NO. _____	PART NO. _____	DATE _____
<div data-bbox="430 1501 451 1585">LEGEND:</div> <div data-bbox="430 766 451 1228">SKETCH OF PART WITH SPECIMEN LOCATIONS</div>		

FIGURE 138 TYPICAL CASTING RECORD FORM

CASTING APPROVAL RECORD *

Casting Part Number	Casting Name	Weight Trimmed	Wgt. Not Trimmed	Alloy	Class	APPROVALS		
						Approved By	Date	
Tooling Coordination (Discussion of gates, risers, chills, cores, etc.) Notes **						Foundry		
						Pattern Shop		
						Engineering		
Pattern Inspection (Conformance to pattern drawing) Notes **						Inspection		
Pouring Temperature (°F)						Foundry		
First - Casting Inspection Notes **						Foundry		
						X-Ray		
						Penetrant		
						Dimensional		
Photographic Record of Set-up Notes **						Foundry		
Final Approval (Required before production run) Comment:						Inspection		
						Manufacturing		
						Engineering		

* File - Manufacturing, Inspection and Engineering.
 ** Enter applicable report numbers. Attach sketches, photos or references. Record Photograph numbers.

FIGURE 139 TYPICAL CASTING RECORD FORM

APPENDIX A

WELD CORRECTION OF IMPERFECTIONS; PROCEDURES FOR A357 ALUMINUM SAND CASTINGS

1. APPLICATION NOTE

The information contained herein is intended to provide a general guideline for shop personnel performing weld correction of typical aluminum sand casting imperfections. However, in practice, each casting imperfection must be evaluated separately and the detail welding procedures altered to suit the specific application.

In addition, the practicality of restoring any given casting by weld correction requires the careful consideration of such factors as the number, size, and location of individual imperfections, working access, distortion produced by weld shrinkage, weld restraint conditions, and the rework and inspection costs associated with weld correction.

In general, the welding procedures and techniques required to perform weld correction of A357 aluminum sand castings are identical to those commonly employed for weldable wrought alloys. Experience has demonstrated that high-quality weld corrections can be consistently produced by employing reasonable care and standard industry practices (Figure 142).

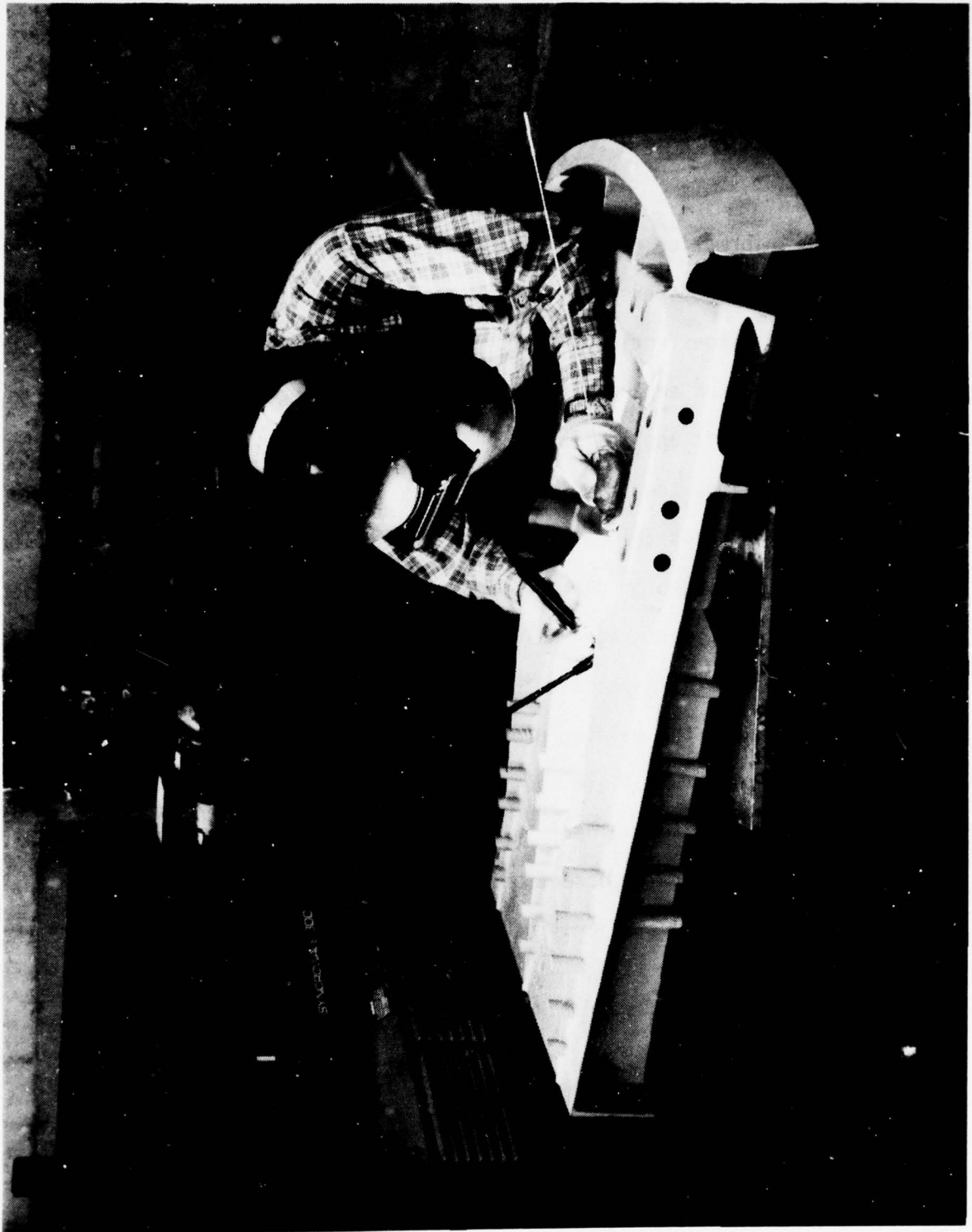


FIGURE 142 WELD CORRECTION OF CAST TEST PART

2. TYPICAL CASTING IMPERFECTIONS

a. Surface Imperfections

Typical surface imperfections include porosity, voids, tears, cold shuts, and sand entrapment. To correct surface imperfections, it is usually advisable to mechanically remove the imperfection and a minimal amount of surrounding material to produce a smooth, shallow cavity in sound base metal. The cavity is subsequently filled with A357 filler metal during a follow-on welding operation.

b. Internal Imperfections

Internal casting imperfections, such as porosity, voids, and inclusions, are usually detected by radiographic and/or ultrasonic inspection methods. The area containing the imperfection is usually denoted on the part or the X-ray film by the Quality Control technician. Internal imperfections are corrected by mechanically removing the imperfection and enough surrounding material to provide adequate welding access and a groove configuration that will produce adequate sidewall fusion. In some cases, it may be advisable to accomplish the correction from both sides of the part. The welding groove configuration, produced in one or both sides of the part, is filled with A357 filler material in one or more passes during a subsequent welding operation.

c. Misruns

Misruns usually appear as holes or voids completely through the part. These imperfections may occur at a part edge inside the part periphery. Correction of a misrun is accomplished by backing up the void area with a copper plate and filling the void area with A357 filler metal during a subsequent welding operation. The edges of the weld deposit are usually remelted from the reverse side of the part to complete the correction.

d. Cracks

Cracks, detected by penetrant, radiographic, or ultrasonic inspection methods, are also correctable casting imperfections. The corrective procedure usually involves drilling a small "crack stopper" hole through the part at each end of the crack, grooving the part from one side, and filling with A357 weld filler metal. The part is subsequently grooved from the reverse side into sound weld metal and welded again with the addition of A357 filler material.

3. PREWELD PREPARATION

a. Equipment

Preweld preparation for weld correction is usually accomplished using manually held, air-driven equipment. Although both are used, the in-line type of air grinder is smaller, lighter, and more maneuverable than a pistol-grip-type drill motor. The air grinder rotational speed is also better suited to the cutters used for preweld metal removal. With either type, exercise care so that lubricating oil from the motor geartrain or air exhaust does not contaminate the weld area.

b. Cutters

A multi-toothed, full radius, Woodruff keyseat cutter is best suited for removal of casting imperfections prior to weld correction. Cutter sizes from 1 to 1-1/2 inches in diameter and widths of 3/16 and 1/4 inch are the most useful for general-purpose work. For best results, use only sharp cutters.

For cutter sharpening or regrinding, specify the following information:

Land width - 0.015 inch

Positive rake angle - 3 degrees

Clearance angle - 8 degrees

c. Groove Preparation

Carefully examine the area to be prepared for weld correction and the X-ray film. Correct orientation and alignment of the X-ray film is especially important. Be particularly cautious if the imperfection is not visible on the surface.

Select a sharp cutter suited to the size and location of the area containing the imperfection. Use a shallow, conventional cut to rough out the cavity. This technique provides good control and minimizes the chance of cutter skidding. Work slowly and carefully. Never remove more material than is necessary to remove the imperfection.

To prevent the adherence and build-up of aluminum material on the face of the cutter teeth, pass the cutter lightly across a block of clean paraffin prior to making the cut. Experience has demonstrated that no weld apparent contamination results if the paraffin is used very sparingly.

The ends and sides of the cavity must be sloped outwards to prevent premature melt-down during welding. From a line perpendicular to the part surface, the cavity walls should slope approximately 15 degrees; the cavity ends should slope at least 45 degrees, Figure 143.

To complete the cavity and provide a suitable surface finish for welding, use a light, climb cut with the drive motor firmly held. The cavity smoothness should be from 32 to 64 RHR with no sharp ridges or tool marks evident.

Cavity depth should be limited to approximately 50% of the part thickness. If the imperfection extends into the lower half of the material thickness, groove out and weld from one side and then turn the part over and repeat the operations on the opposite side. When preparing the second side, remove sufficient material so that the bottom of the cavity is located in sound weld metal.

4. PREWELD CLEANING

The quality of weld corrections is largely dependent upon the cleanliness of the area of the part to be welded. The part surfaces to be melted and the adjacent base metal must be free of inclusions, entrapped sand, dirt, oil, grease and other contaminants, if high-quality weld corrections are to be produced consistently.

Solvent cleaning with acetone or methyl ethyl ketone (MEK) is an effective means of removing oily surface contaminants prior to welding. Tilt the part to promote drainage and flush the weld area with a small quantity of either solvent, preferably dispensed from a squirt bottle.

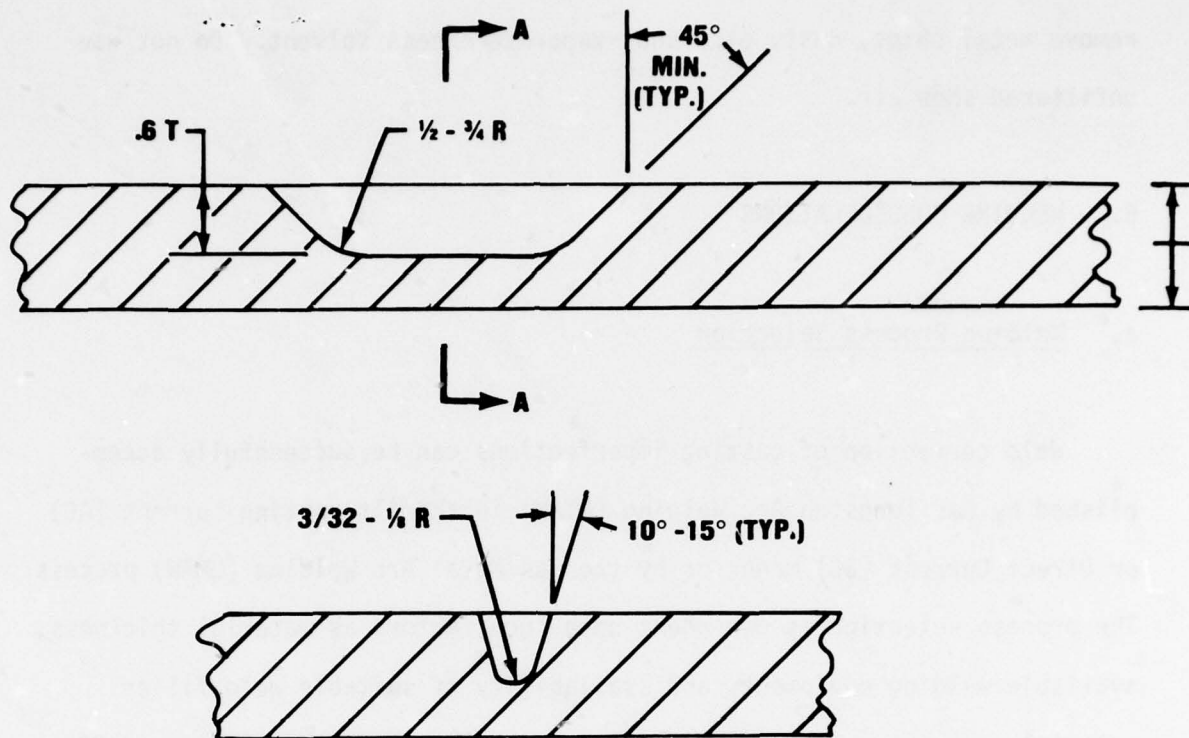


FIGURE 143 TYPICAL GROOVE CONFIGURATION FOR WELD CORRECTION

Unless absolutely necessary, avoid wiping the weld area after solvent cleaning. The roughness of the casting surface may cause fuzz, lint, or other particles from the wiper to be deposited in the weld area.

Blow off the weld area with clean, dry filtered air or inert gas to remove metal chips, dust, etc. and evaporate excess solvent. Do not use unfiltered shop air.

5. WELDING CONSIDERATIONS

a. Welding Process Selection

Weld correction of casting imperfections can be successfully accomplished by Gas Tungsten Arc Welding (GTAW) in the Alternating Current (AC) or Direct Current (DC) modes or by the Gas Metal Arc Welding (GMAW) process. The process selection is dependent upon such factors as material thickness, available welding equipment, and availability of suitable weld filler material. However, for general usage, the GTAW process in the AC and DC modes is recommended.

GTAW-AC is usually used for single-side corrections in materials up to 1/8 inch thick without a prepared weld cavity and up to 1/4 inch with a cavity. Thicknesses up to 3/8 inch can be welded successfully using GTAW-AC by grooving and welding both sides. The GTAW-AC mode provides excellent cathodic surface cleaning and good visibility due to the high arc intensity. However, the weld penetration tends to be wide and shallow.

The GTAW-DC mode is used for heavier material sections and produces deep, narrow weld penetration. Because the DC mode produces a small, concentrated arc, the welding visibility is limited and further restricted by the presence of soot-like surface deposits commonly encountered when using helium-rich gas mixtures.

b. Welding Equipment

Although many conventional, commercially available, manual AC/DC GTAW power sources can be used to produce acceptable quality weld corrections, consistently better results can be obtained using solid state, square wave, variable polarity duty cycle equipment, such as the Syncrowave 300, built by the Miller Electric Company, Appleton, WI.

During test welding in the AC mode, such a power source completely eliminated the problem of tungsten spitting and produced a substantial reduction in the incidence of porosity in the weld deposit. This equipment also performed well in the DC mode, providing excellent arc stability and smooth weld tailouts.

The power source was operated in the maximum unbalanced polarity duty cycle condition which provided approximately 70% of the time in the straight polarity (electrode negative) mode. This mode promotes increased weld penetration while retaining the AC cathodic cleaning benefits.

c. Preheating

Preheating the casting prior to performing a weld correction is sometimes used to minimize the local thermal gradients and thermal stresses produced by welding. This technique is also used to minimize the effect of different material thicknesses and locally thickened areas such as pad-ups, busses, stiffeners, etc. However, since A357 does not appear to be a crack-prone material, preheating will probably not be required, except under unusual circumstances.

If employed, preheat the casting as uniformly as possible using a heat source that does not contaminate the weld area. Oven heating is the most desirable method because the whole part becomes uniformly heated; however, some parts may be too large for available ovens.

Flame heating is an acceptable preheating method, providing that a soot-free flame is used and the heat is not concentrated in a small local area. Although hydrocarbon fuel gases can be used, a more efficient and contaminant-free heat source is provided by an oxy-hydrogen flame.

Regardless of the heating method employed, the casting should be preheated in the range of 250-300°F, to prevent moisture condensation. The casting temperature can be checked with a contact pyrometer, temperature-indicating crayon, or other suitable means.

Under normal circumstances, controlled or artificial cooling of weld-corrected A357 castings is not required. Natural cooling in still air is usually adequate. Cooling of the base metal between multiple weld passes is not usually required unless the base metal temperature exceeds 500°F.

d. Shielding Gases

The tungsten electrode, weld puddle, and adjacent base metal are protected from atmospheric contamination during and immediately after welding by providing a uniform flow of high-purity inert gas through the welding torch. Where space permits, the welding torch should be equipped with a gas lens accessory to collimate the gas flow and minimize turbulence. Underbead shielding of welds in A357 aluminum castings is not required.

For GTAW-AC welding of A357 aluminum, inert gas mixtures containing 10-15 cfh argon + 4-5 cfh helium provide adequate shielding and arc stabilization. GTA welding in the DC mode is done using pure helium gas at 40-60 cfh.

e. Tungsten Electrodes

Two percent thoriated tungsten electrodes are recommended for GTAW-DC welding. GTAW-AC welding can be accomplished with either 2% thoriated or zirconium tungsten. For general-purpose use, a 3/32-inch-diameter electrode is preferred. If a stable, molten ball cannot be maintained on the electrode tip during AC welding because the current is too low, taper the electrode tip over a 1/2-inch length to 3/4 of its original diameter and reform the ball. For GTAW-DC welding, grind the electrode tip to a smooth, uniform, 20-30° included-angle taper.

f. Filler Material

Only A357 aluminum filler metal should be used for weld correction of A357 sand castings. For general-purpose use, 3/32-inch-diameter filler rod produces the best results.

Prior to each weld pass, cut approximately 1/4 inch from the end of the filler wire to be introduced into the weld puddle. During welding, exercise care to keep the tip of the filler metal rod within the inert gas envelope at all times. This will prevent the formation of oxides on the heated portion of the rod.

If impurities appear in or on top of the weld puddle after the addition of filler metal, the filler rod may be contaminated. Occasionally, laps, folds, inclusions, and other discontinuities are produced in the filler metal rods during manufacturing. If the contaminants are on or near the surface of the wire, pickling the wire in acid solutions used for deoxidizing aluminum prior to welding may eliminate the contamination.

g. Edge Wetting and Laps

Exercise care during welding to ensure that the edges of the weld deposit are fused to the walls of the weld groove and not just cast in against them. Avoid an excessively large weld puddle. Deposit the weld in multiple passes if necessary, to keep the size of each weld pass in a controllable range.

Torch manipulation and thorough melting of each portion of filler rod added to the puddle will minimize premature sidewall melting and eliminate the occurrence of laps and folds.

h. Interpass Cleaning

In multiple-pass welding, it may be necessary to clean the surface of the weld deposit between passes to improve visibility. Although not usually required when welding in the AC mode, interpass cleaning is particularly necessary when welding in the DC mode with helium shielding gas. Although the soot-like "smut" that occurs on the surface of the weld bead and adjacent weld metal is not detrimental to weld quality, it obscures the weld area and particularly the edges of the deposit.

For interpass cleaning, use a hand held wire brush having 0.010-0.013-inch-diameter AISI 300 series stainless steel bristles. Use only light pressure when brushing the completed weld to prevent smearing the metal surface and interfering with subsequent penetrant inspection.

i. Tailouts

Tailout areas are frequent sources of defects in aluminum welds. The rapid solidification rate of aluminum requires that the size of the puddle be minimized when the arc is extinguished to minimize shrinkage pipes and prevent crater cracks.

Frequently, defective or maladjusted foot controls prevent the welder from reducing the welding current to a sufficiently low level to prevent craters. If such a condition exists, refer the problem to qualified welding equipment maintenance personnel for correction.

With many GTAW power sources, the current waveform becomes very distorted at low current levels, increasing puddle rectification and arc reignition problems and producing a very erratic arc. The solid state, square wave, variable polarity duty cycle equipment discussed in Section 5b provides good arc stability and minimizes tailout problems.

As a general multipass welding technique, carefully remelt the tailout area of the previous pass before adding more filler metal and tailing out the current pass. For the final pass, add excessive filler metal after the metal deposit is completed to build up a beehive-shaped cone well above the top surface of the weld reinforcement. Reduce the current to minimize the puddle size while holding the torch stationary above the top of the cone. Surface contaminants that may have floated along on the puddle will usually become entrapped in the cone and can be removed. Also, if the welding arc becomes extinguished prematurely, the resultant weld crater and/or cracks should be restricted to the area of the cone. The cone, along with any tailout weld imperfections, will be removed during a subsequent bead shaving operation.

6. WELD BEAD REINFORCEMENT REMOVAL

a. Weld Bead Shaving

The engineering drawing or other controlling documentation may require the removal of weld bead face and/or root reinforcement after weld correction. The most efficient means of weld reinforcement removal is by bead shaving. Other methods can be used, but care must be exercised to prevent metal smearing that will interfere with subsequent penetrant inspection operations.

b. Bead Shaving Equipment

Bead shaving can be accomplished satisfactorily using hand-held, air-driven equipment. Suitable bead shaving equipment may be purchased commercially from manufacturers such as Zephyr Manufacturing Co., Inglewood, Calif. or can be built by the user, Figure 144.

c. Bead Shaving Techniques

It is mandatory that the bead shaver cutters be sharp to prevent metal smearing. Use light, smooth strokes to produce a uniform surface. To prevent the adherence of aluminum to the face of the cutter teeth, carefully pass a bar of clean paraffin lightly across the cutter prior to shaving.

In confined areas that do not have sufficient access for a bead shaver, a sharp, fine-toothed rotary file can be used for weld bead reinforcement removal, Figure 145. A climb cut with a firmly held tool and light, smooth strokes will produce the best results. Paraffin can also be used to minimize aluminum pickup with this technique.



FIGURE 144 BEAD SHAVING EQUIPMENT FOR CLEANING CORRECTED AREA AFTER WELDING



FIGURE 145 USE OF A FINE TOOTH ROTARY FILE FOR WELD BEAD REINFORCEMENT REMOVAL

7. WELD CORRECTION PROCEDURES

a. Weld Correction of Surface Imperfections

Use the following sequence of operations for correcting typical surface imperfections on A357 aluminum sand castings:

1. Determine the location and extent of the imperfections.
2. Determine the type of metal removal equipment and cutters to be used.
3. Remove the surface imperfections to sound base metal using the equipment and techniques described in Section 3.
4. If necessary, solvent clean the weld area as described in Section 4.
5. Weld the prepared area using the equipment and techniques described in Section 5. Add A357 filler rod as required to fill the weld cavity and build-up the weld reinforcement at least 1/16 inch above the surface. Tailout carefully on a cone-shaped build-up.
6. Remove the weld bead reinforcement as required to meet the engineering drawing or weld correction instructions using the equipment and techniques described in Section 6.
7. Submit casting for nondestructive inspection.
8. As required, correct by welding any rejectable imperfections occurring in the corrected area. Process such weld imperfections in the same manner as casting imperfections.

b. Weld Correction of Internal Imperfections

Use the following sequence of operations for correcting typical internal imperfections in A357 aluminum sand castings:

1. Determine the location and extent of the imperfections.
2. Exercise particular care when locating imperfection detected by radiography. Make sure that the X-ray film and casting bear the same X-ray reference number and that the view markers are identical.
3. Inspect the X-ray film in a viewer to verify the location and extent of the imperfections marked on the X-ray film.
4. Carefully transfer the location of the imperfection from the film to the part, using dividers or other suitable means to ensure accuracy. Mark the area to be corrected with a red marking pencil, General No. 1818, or equivalent. Do not use a common graphite (lead) pencil, felt-tipped pen, or layout fluid because these materials leave a residue which may contaminate the weld.
5. Prepare a weld cavity just large enough to remove the imperfection using the equipment and techniques described in Section 3.
6. If necessary, solvent clean the weld area as described in Section 4.
7. Weld the prepared area using the equipment and techniques described in Section 5. Add A357 filler rod during welding to fill the weld cavity and build-up the weld reinforcement at least 1/16 inch above the casting surface. Tailout carefully on a cone-shaped build-up.

8. If the imperfection extended into the lower half of the original casting thickness, repeat steps 4 through 7 on the reverse side of the part. Make sure that the second side cavity extends into sound weld metal.
9. Remove the weld bead reinforcement as required to meet the engineering drawing requirements or weld correction instructions, using the equipment and techniques described in Section 6.
10. Submit the casting for nondestructive inspection.
11. As required, correct by welding any rejectable imperfections occurring in the corrected area. Process such weld imperfections in the same manner as casting imperfections.

c. Weld Correction of Misruns

Use the following sequence of operations for correcting typical misruns in A357 aluminum sand castings:

1. Closely examine the misrun area for surface contamination, sand entrapment, laps and folds, etc., and rework as required. If the edges of the misrun area are smooth, preweld preparation is usually not required.
2. If necessary, solvent clean the weld area as described in Section 4.
3. Prior to welding, clamp a 1/4-inch-thick copper backup plate underneath the misrun area. Although not required, the copper plate should be chrome plated to minimize the chance of copper pickup in the weld and improve the durability of the copper plate. The copper plate must be clean and free of contaminants that could produce imperfections in the weld.

4. Weld the misrun area using the equipment and techniques described in Section 5. Since misruns more commonly occur in material thicknesses of 1/2 inch and less, GTAW-AC is the preferred welding mode. Add A357 filler rod during welding to fill the misrun area. Weld around the periphery of the misrun, exercising care to ensure good fusion with the base metal at the edges of the weld deposit. Fill the misrun area in a uniform thickness layer from the outside toward the center in a continuous pass, casting the weld metal against the copper backup plate. Add sufficient filler rod to buildup the weld reinforcement at least 1/16 inch above the casting surface. Tailout carefully on a cone-shaped buildup.
5. Turn the casting over and closely examine the reverse side of the misrun area. If only shallow surface imperfections are visible in the weld, remelt the surface in those areas, adding a minimal amount of filler material. If deep crevices, laps, or folds are present, remove them to sound metal using the equipment and techniques described in Section 3, and fill with weld metal.
6. Remove the weld bead reinforcement as required to meet the engineering drawing requirements or weld correction instructions, using the equipment and techniques described in Section 6.
7. Submit the casting for nondestructive inspection.
8. As required, correct by welding any rejectable imperfections occurring in the corrected area. Process such weld imperfections in the same manner as casting imperfections.

d. Weld Correction of Cracks

Use the following sequence of operations for correcting cracks in A357 aluminum sand castings:

1. Determine the location and extent of the imperfections.
2. Exercise particular care when locating imperfections detected by radiography. Make sure that the X-ray film and casting bear the same X-ray reference number and that the view markers are identical.
3. Inspect the X-ray film in a viewer to verify the location and extent of the imperfections marked on the X-ray film.
4. Carefully transfer the location of the imperfection from the film to the part, using dividers or other suitable means to ensure accuracy. Mark the area to be corrected with a red marking pencil, General No. 1818, or equivalent. Do not use a common graphite (lead) pencil, felt-tipped pen, or layout fluid because these materials leave a residue that may contaminate the weld.
5. Drill a 1/8- to 3/16-inch-diameter "crack stopper" hole at each end of the crack to prevent propagation during welding. The holes should pass through the part, if possible.
6. Prepare a weld cavity just large enough to remove the imperfection using the equipment and techniques described in Section 3.
7. Weld the prepared area using the equipment and techniques described in Section 5, exercising particular care to fill the holes. Add A357 filler rod during welding to fill the weld cavity and build up the weld reinforcement at least 1/16 inch above the casting surface. Tailout carefully on a cone-shaped buildup.

8. Turn the part over and repeat steps 4 through 7 on the reverse side of the part. Make sure that the second side cavity extends into sound weld metal.
9. Remove the weld bead reinforcement as required to meet the engineering drawing requirements or weld correction instructions, using the equipment and techniques described in Section 6.
10. Submit the casting for nondestructive inspection.
11. As required, correct by welding any rejectable imperfections occurring in the corrected area. Process such weld imperfections in the same manner as casting imperfections.